

THE PYROLYSIS AND PHOTOLYSIS OF  
SOME OLIGOSILANES

Thesis submitted for the degree of

Doctor of Philosophy

at the University of Leicester

by

Terence Simpson B.Sc.(Hons.)

Department of Chemistry

University of Leicester

September 1991

UMI Number: U041611

All rights reserved

INFORMATION TO ALL USERS

The quality of this reproduction is dependent upon the quality of the copy submitted.

In the unlikely event that the author did not send a complete manuscript and there are missing pages, these will be noted. Also, if material had to be removed, a note will indicate the deletion.



UMI U041611

Published by ProQuest LLC 2015. Copyright in the Dissertation held by the Author.  
Microform Edition © ProQuest LLC.

All rights reserved. This work is protected against  
unauthorized copying under Title 17, United States Code.



ProQuest LLC  
789 East Eisenhower Parkway  
P.O. Box 1346  
Ann Arbor, MI 48106-1346



8259601057

X751945462

## T. Simpson: The Pyrolysis and Photolysis of some Oligosilanes

### Abstract

The thermolysis of octamethyltrisilane yields trimethylsilane as the major product. Other prominent products are cyclic carbosilanes; evidence is presented that one of these is formed in a novel cyclisation/elimination reaction.

The thermolysis of n-decamethyltetrasilane and i-decamethyltetrasilane also yield trimethylsilane as the major product. Other major products include cyclic carbosilanes and high molecular weight multiple ring disilacyclobutane compounds.

Kinetic and trapping experiments show that all these pyrolysis mechanisms are predominantly radical in nature; there is also a notable contribution from silylenes, silenes and disilenes. The difference in product composition between the high and low sample pressure reactions is rationalised in terms of the relative importance of uni- and bimolecular reactions in the pyrolysis mechanisms.

The main silicon containing product in the pyrolysis of 2,2-diethyl-hexamethyltrisilane apart from trimethylsilane was vinyltrimethylsilane. Unlike the pyrolyses of the permethylated oligosilanes cyclic carbosilanes were found to be minor products. Mechanistic suggestions, of relevance to polysilane laser photoablation, explain this difference.

Computer modelling by numerical integration, using the KINAL and ACUCHEM packages, was used to validate the pyrolysis mechanisms of octamethyltrisilane and 2,2-diethyl-hexamethyltrisilane.

Three primary photochemical pathways have been identified in the irradiation of three oligosilanes at 254 and 228 nm. These pathways include a reductive elimination not previously observed in oligosilanes but analogous to a chain scission process that occurs in polysilanes.



### Statement

The work described in this thesis was carried out in the Department of Chemistry of the University of Leicester during the period between October 1988 and September 1991 and at the Department of Chemistry of the University of Texas between April 1990 and June 1990.

All the work recorded in this thesis is original unless otherwise acknowledged in the text or by references. None of the work has been submitted for another degree in this or any other University

Signed T. Simpson

Date 28/9/91

### Acknowledgments

I would like to thank my supervisor, Prof. I.M.T. Davidson, for his advice and encouragement over the past three years.

I am indebted to all the members of the Chemistry Department Workshop and to Mr. P. Acton for keeping the electronics in working order. Thanks also to Mr. G.H. Morgan for writing the G.C. data manipulation program used in the kinetic experiments.

I am particularly grateful to Drs. R. Taylor and B.N. Bortolin for the synthesis of the oligosilanes.

I wish to thank Prof. J. Michl for my visit to the University of Texas at Austin which was both rewarding and enjoyable.

I would like to thank the S.E.R.C. for financial support and both the S.E.R.C. and the U.S. Air Force Office of Scientific Research for financial support during my stay in Texas.

Finally, I would like to thank my parents for their faith and support, without which none of this work would have been possible.

**To Mum and Dad**

## Contents

### Chapter 1: Introduction

(I)	Silyl Radicals ( $R_3Si\cdot$ )	1
(II)	Silylenes ( $R_2Si:$ )	3
(III)	Silenes ( $R_2Si=CH_2$ )	5
(IV)	Disilenes ( $R_2Si=SiR_2$ )	7
(V)	Oligo and Polysilanes: Structure and Properties	8
(VI)	Photoresists	10
(VII)	Oligosilane Photochemistry	12
(VIII)	Oligosilane Thermal Chemistry	14
(IX)	References	21

### Chapter 2: Experimental

(I)	Kinetic Measurements Using The Stirred Flow Reactor (SFR) Apparatus	25
(II)	Product Identification Using the Gas Chromatograph/Mass Spectrometer-Stirred Flow Reactor Apparatus	28
(III)	The Q8-Mass Spectrometer/Sealed Tube Pyrolysis Technique for the Detection of Hydrogen and Methane	30
(IV)	Preparative Experiments Using the Preparative Gas Chromatograph-Stirred flow Reactor Apparatus	31
(V)	Photolysis Experiments	32
(VI)	References	33

### Chapter 3: The Pyrolysis of Octamethyltrisilane

(I)	Introduction	35
(II)	GC/MS-SFR Results	36
(III)	Kinetic-SFR Results	44
(IV)	Q8/MS-Sealed Tube Pyrolysis Results	49
(V)	Discussion	51
(VI)	Summary	61

(VII) Acknowledgements	62
(VIII) References	62

#### **Chapter 4: The Pyrolysis of n-Decamethyltetrasilane**

(I) Introduction	64
(II) GC/MS-SFR Results	65
(III) Kinetic-SFR Results	72
(IV) Q8/MS-Sealed Tube Pyrolysis Results	77
(V) Discussion	79
(VI) Summary	86
(VII) Acknowledgement	87
(VIII) References	87

#### **Chapter 5: The Pyrolysis of iso-Decamethyltetrasilane**

(I) Introduction	89
(II) GC/MS-SFR Results	90
(III) Kinetic-SFR Results	96
(IV) Q8/MS-Sealed Tube Pyrolysis Results	101
(V) Discussion	102
(VI) Summary	106
(VII) Acknowledgements	108
(VIII) References	108

#### **Chapter 6: The Pyrolysis of 2,2-Diethylhexamethyltrisilane**

(I) Introduction	110
(II) GC/MS-SFR Results	111
(III) Kinetic-SFR Results	115
(IV) Q8/MS-SFR Results	120
(V) Discussion	122
(VI) Summary	128
(VII) The Potential of Methylated versus Ethylated Polysilanes as Self-Developing Photoresists in Laser Photoablation	129
(VIII) Acknowledgements	130
(IX) References	131

## **Chapter 7: The Photochemistry of Some Permethyloligosilanes**

(I)	Introduction	132
(II)	Results	134
(III)	Discussion	149
(IV)	Summary	154
(V)	Acknowledgements	156
(VI)	References	156

## **Appendix 1: The Pyrolysis of Carbosilanes [A] and [B]**

(I)	Introduction	157
(II)	GC/MS-SFR Results for [A]	158
(III)	Kinetic-SFR Results for [A]	159
(IV)	GC/MS-SFR Results for [B]	161
(V)	Summary	162
(VI)	Acknowledgement	164

## **Appendix 2: Numerical Integration**

(I)	Introduction	165
(II)	The Pyrolysis of Octamethyltrisilane	166
(III)	The Pyrolysis of 2,2-Diethylhexamethyl- trisilane	171
(IV)	Acknowledgement	177
(V)	References	178

## List of Tables

### Chapter 1

Table 1.1	Heats of formation for hexamethyldisilane, tetramethylsilane and dimethylsilylene	18
Table 1.2	Some physical constants for the series of straight chained permethyloligosilanes	20

### Chapter 3

Table 3.1	Chemical shifts for OMTS, products [18], [24] and [25]	40
Table 3.2	Products from the pyrolysis of OMTS	41
Table 3.3	Kinetic results from the OMTS experiments	45
Table 3.4	Kinetic results from the OMTS/butadiene experiments	47
Table 3.5	Kinetic results from the OMTS/toluene experiments	48
Table 3.6	Experimental and Calculated Arrhenius parameters for the pyrolysis of OMTS	58

### Chapter 4

Table 4.1	Products from the pyrolysis of n-DMTS	69
Table 4.2	Kinetic results from the n-DMTS experiments	73
Table 4.3	Kinetic results from the n-DMTS/2,3-dimethyl-1,3-butadiene experiments	74
Table 4.4	Kinetic results from the n-DMTS/toluene experiments	76

### Chapter 5

Table 5.1	Products from the pyrolysis of i-DMTS	93
Table 5.2	Kinetic results for the formation of trimethylsilane from i-DMTS	96
Table 5.3	Kinetic results from the i-DMTS/2,3-dimethyl-1,3-butadiene experiments	98

Table 5.4	Kinetic results from the i-DMTS/toluene experiments	99
-----------	---	----

## Chapter 6

Table 6.1	Products from the pyrolysis of DEHMTS	112
Table 6.2	Kinetic results from the DEHMTS experiments	116
Table 6.3	Kinetic results from the DEHMTS/2,3-dimethyl-1,3-butadiene experiments	118
Table 6.4	Kinetic results from the DEHMTS/toluene experiments	119
Table 6.5	Experimental and Calculated Arrhenius parameters for the pyrolysis of DEHMTS	127

## Chapter 7

Table 7.1	UV absorption characteristics for oligosilanes (i)-(v)	133
Table 7.2	Relative yields for the products of BTMS-OMTS irradiation	138
Table 7.3	Relative yields for the products of i-DMTS irradiation	141
Table 7.4	Relative yields for the products of n-DMTS irradiation	143
Table 7.5	Relative yields for the products of DEHMTS irradiation	146
Table 7.6	Relative yields for the products of OMTS irradiation	148

## Appendix 1

Table A1.1	Arrhenius parameters for the formation of 3MS, CYCLO 3 and CYCLO [A]	159
Table A1.2	Arrhenius parameters for the formation of CYCLO [B]	162



## Appendix 2

Table A2.1	Experimental and Calculated Arrhenius parameters for the pyrolysis of OMTS	169
Table A2.2	Experimental and Calculated Arrhenius parameters for the pyrolysis of DEHMTS	175

## List of figures

### Chapter 1

Figure 1.1	Schematic representation of the effect increasing chain length on $\lambda_{\text{max}}$ for a typical di-alkylpolysilane	10
Figure 1.2	Schematic representation of photolithography	11
Figure 1.3	Structure of the most persistent radical	14
Figure 1.4	Graphs A & B showing the enthalpy and activation energy changes favourable for either silyl radical or silylene formation	15

### Chapter 2

Figure 2.1	Schematic representation of the SFR apparatus	26
Figure 2.2	A stirred flow reactor	26
Figure 2.3	Diagrams of quartz photolysis cells	33

### Chapter 3

Figure 3.1	Mass spectrum of product [23]	38
Figure 3.2	Mass spectrum of product [24]	38
Figure 3.3	Gas chromatogram for the pyrolysis of OMTS at 648°C	45
Figure 3.4	Arrhenius plot for the formation of CYCLO 2 from OMTS between 586-654°C	46
Figure 3.5	Order plot for the formation of CYCLO 2	46
Figure 3.6	Gas chromatogram for the pyrolysis of OMTS/butadiene at 612°C	47
Figure 3.7	Arrhenius plot for the formation of CYCLO 3 (in the presence of butadiene) between 564-636°C	48
Figure 3.8	Gas chromatogram for the pyrolysis of OMTS/toluene at 645°C	49
Figure 3.9	Arrhenius plot for the formation of	

	CYCLO 3 (in the presence of toluene) between 608-683°C	49
Figure 3.10	Mass spectrum of H <sub>2</sub> and CH <sub>4</sub> from the sealed tube pyrolysis of OMTS at 550°C	50

## Chapter 4

Figure 4.1	Gas chromatogram for the pyrolysis of n-DMTS at 626°C	73
Figure 4.2	Arrhenius plot for the formation of 3MS	74
Figure 4.3	Gas chromatogram for the pyrolysis of n-DMTS/2,3-dimethyl-1,3-butadiene at 645°C	75
Figure 4.4	Arrhenius plot for the formation of 1,1,3,4-tetramethyl-1-silacyclopent- 3,4-ene	75
Figure 4.5	Gas chromatogram for the pyrolysis of n-DMTS/toluene at 639°C	76
Figure 4.6	Arrhenius plot for the formation of benzyltrimethylsilane	77
Figure 4.7	Mass spectrum of H <sub>2</sub> & CH <sub>4</sub> from the sealed tube pyrolysis of n-DMTS at 400°C	78

## Chapter 5

Figure 5.1	Gas chromatogram for the pyrolysis of i-DMTS at 607°C	97
Figure 5.2	Arrhenius plot for the formation of 3MS	97
Figure 5.3	Gas chromatogram for the pyrolysis of i-DMTS/2,3-dimethyl-1,3-butadiene at 626°C	98
Figure 5.4	Arrhenius plot for the formation of 1,1,3,4-tetramethyl-1-silacyclopent- 3,4-ene	99
Figure 5.5.	Gas chromatogram for the pyrolysis of i-DMTS/toluene at 595°C	100
Figure 5.6	Arrhenius plot for the formation of 3MS in the presence of toluene	100

Figure 5.7	Mass spectrum of $H_2$ & $CH_4$ from the sealed tube pyrolysis of i-DMTS at 550°C	101
------------	---	-----

## Chapter 6

Figure 6.1	Order plot for the formation of ethene	116
Figure 6.2	Gas chromatogram for the pyrolysis of DEHMTS at 616°C	117
Figure 6.3	Arrhenius plot for the formation of ethene between 570-630°C	117
Figure 6.4	Gas chromatogram for the pyrolysis of DEHMTS/2,3-dimethyl-1,3-butadiene at 579°C	118
Figure 6.5	Arrhenius plot for the formation of ethene (in the presence of 2,3-dimethyl-1,3-butadiene) between 570-630°C	119
Figure 6.6	Gas Chromatogram for the pyrolysis of DEHMTS/toluene at 630°C	120
Figure 6.7	Arrhenius plot for the formation of ethene (in the presence of toluene) at 570-630°C	120
Figure 6.8	Mass spectrum of $H_2$ , $CH_4$ and ethene from the sealed tube pyrolysis of DEHMTS at 400°C	121

## Chapter 7

Figure 7.1	Graph showing the increase in trapping product formation with increasing TES concentration	137
Figure 7.2	Progress curve for the irradiation of BTMS-OMTS at 254 nm.	137
Figure 7.3	Progress curve for the irradiation of BTMS-OMTS at 228 nm	138
Figure 7.4	Progress curve for the irradiation of i-DMTS at 254 nm	140
Figure 7.5	Progress curve for the irradiation of n-DMTS at 254 nm	143
Figure 7.6	Progress curve for the irradiation of DEHMTS at 228 nm	145

Figure 7.7	Progress curve for the irradiation of OMTS at 228 nm	146
------------	--	-----

## Appendix 1

Figure A1.1	Gas chromatogram for the pyrolysis of [A] at 630°C	160
Figure A1.2	Arrhenius plot for the formation of CYCLO 3	160
Figure A1.3	Mass spectrum of H <sub>2</sub> & CH <sub>4</sub> from the sealed tube pyrolysis of [A]	161

## Appendix 2

Figure A2.1	Order plot for the formation of CYCLO 3 (from calculated rate constants)	169
Figure A2.2	Experimental Arrhenius plot for the formation of HMDS between 570-650°C	170
Figure A2.3	Calculated Arrhenius plot for the formation of HMDS between 570-650°C	170
Figure A2.4	Order plot for the formation of ethene (from calculated rate constants)	175
Figure A2.5	Experimental Arrhenius plot for the formation of ethene between 570-630°C	176
Figure A2.6	Calculated Arrhenius plot for the formation of ethene between 570-630°C	176

## Chapter 1

### Introduction

Polysilanes are of current interest because of their industrial potential as photoresists and precursors to silicon carbide fibres<sup>1</sup>. This thesis reports on the gas phase pyrolysis of some permethylated oligosilanes. The kinetic and mechanistic studies reported may act as models for polysilane thermal chemistry and therefore help to understand their industrial use.

Photolysis experiments were carried out on a series of branched and chained oligosilanes to expand and update earlier mechanistic studies<sup>2</sup>. It is known that the results of oligosilane photochemistry are readily transferable to polysilanes<sup>3</sup>.

The use of oligosilanes instead of polysilanes in thermal and photochemical studies is desirable as these simpler molecules allow easier product identification, reveal the intermediates involved and the relative importance of separate intermediates in each process. The inherent simplicity of studying molecules in the gas phase also favours using volatile oligosilanes. The common intermediates in organosilicon chemistry are silyl radicals, silylenes, silenes and disilenes; a brief summary of their chemistry is given below. The structure and physical properties of oligo and polysilanes are also summarised, followed by a description of polysilanes as photoresists and oligosilane photo and thermal chemistry.

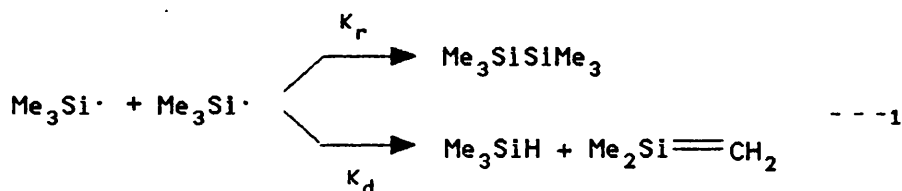
### (II) Silyl Radicals ( $R_3Si\cdot$ )

Silyl radical chemistry has been reviewed by Davidson<sup>4</sup>, Sakurai<sup>5</sup> and Arthur *et. al.*<sup>6</sup>. The primary source of silyl radicals is the pyrolysis of permethylated oligosilanes<sup>7</sup>, providing the oligosilane does not contain any Silicon-Hydrogen (Si-H), Silicon-Halogen (Si-Hal) or Silicon-Alkoxy (usually Si-OMe) bonds; in these cases silylene formation would dominate<sup>8</sup>. Silyl radicals may also be

produced via direct photolysis of oligosilanes containing aryl groups<sup>9</sup> or mercury photosensitisation of silicon hydrides e.g. mercury photosensitisation of trimethylsilane yields trimethylsilyl radicals<sup>10</sup>. Trimethylsilyl radicals will also be generated by the isomerisation of  $\alpha$ -silylmethyl radicals e.g.  $\text{HMe}_2\text{SiCH}_2\cdot \rightarrow \text{Me}_3\text{Si}\cdot$  and when methyl radicals attack trimethylsilane<sup>10</sup>.

Theoretical calculations and experimental evidence predict that silyl radicals will be pyramidal in structure<sup>11</sup>. The reactions of silyl radicals are similar to those of alkyl radicals. Silyl radicals undergo disproportionation, radical recombination, abstraction and addition reactions<sup>5,6</sup>. However there are some fundamental differences in reactivity as silicon is a larger and more electropositive atom<sup>10</sup>. Silicon forms stronger bonds to oxygen, nitrogen and the halogens than carbon, but, silicon forms weaker bonds to carbon and hydrogen than carbon.

The disproportionation of silyl radicals is known to play a role in the disappearance of these species. The ratio of recombination to disproportionation is 10:1 for trimethylsilyl radicals in the gas phase<sup>12</sup>:



$$\text{and } K_d/K_r = 0.1$$

The silaethene (silene) formed by the disproportionation of trimethylsilyl radicals is highly unstable due to the reactive silicon-carbon  $\pi$ -bond. Silyl radicals add rapidly to silenes to form linear carbosilanes with a new silicon centred radical. Unlike alkyl radicals, recombination reactions of silyl radicals are not affected by the substitution of bulky pendant groups (due to the large size of the silicon atom)<sup>10</sup>.

The irreversible abstraction of chlorine from alkyl halides by silyl radicals has led to the use of methyl chloride as a radical transfer agent in silyl radical chemistry<sup>13</sup>. Useful thermodynamic data such as bond dissociation energies and enthalpies of formation are readily accessible from the generation of silyl radicals as they are less disposed to being radical chain carriers than alkyl radicals<sup>14</sup>. However,

chain reactions involving silyl radicals are not unknown.

## (II) Silylenes ( $R_2Si:$ )

These neutral divalent species are the silicon analogues of carbenes. Silylene chemistry has been reviewed by Gaspar<sup>15</sup> and Davidson<sup>4</sup>. Unlike silyl and alkyl radicals, silylenes show major differences in structure and reactivity to carbenes e.g. silylenes are known to have a singlet ground state whereas carbenes have a triplet ground state.

Silylenes may be generated by pyrolysing disilanes containing Si-H, Si-Hal or Si-OMe bonds<sup>16</sup>. Kinetic data led to the conclusion that the transition state involves a penta-coordinated  $sp^3d$  hybridised silicon atom<sup>15</sup>.

The photolysis of linear and cyclic oligosilanes containing three or more silicon atoms generates silylenes in high yields. The ease of generation of silylenes by both these methods allows these species to be generated bearing a wide variety of substituents. Other methods of generation include hydridomonosilane pyrolysis and recoiling silicon atom reactions<sup>15</sup>.

The singlet to triplet energy gap in  $H_2Si:$  is large, but different substituents are calculated to affect the ordering of states. Bulky substituent groups may be able to lower the triplet to the ground state by increasing the bond angle to  $129^\circ$ <sup>17</sup>. However, *ab initio* calculations on di-tertiary butyl silylene show that the singlet state is still the ground state lying  $42 \text{ kJmol}^{-1}$  below the triplet<sup>18</sup>.

Highly electronegative substituents are known to stabilise the singlet state while electropositive atoms destabilise it<sup>15</sup>. The singlet to triplet promotional energy for the series  $H_2Si:$ ,  $Me_2Si:$ ,  $F_2Si:$  and  $Li_2Si:$  are calculated to be 73.6, 95.8, 310 and  $-43.1 \text{ kJmol}^{-1}$  respectively<sup>19</sup>. Therefore in the case of  $Li_2Si:$  the triplet manifold is the ground state, although this species has no experimental precedent.

Silylenes can insert into  $\sigma$ -bonds, add to carbon-carbon and carbon-oxygen double bonds, dimerise and undergo rearrangement reactions.  $\sigma$ -bond insertion reactions are believed to be concerted for singlet silylenes. The insertion of  $H_2Si:$  into  $H_2$  is thought to proceed via a two step process with the  $\sigma$ -



bonding electrons donated to the empty p-orbital of the silylene and the lone pair donated to the  $\sigma$ -anti-bonding orbital of the substrate<sup>20</sup>. Insertion reactions may be *inter-* or *intra-*molecular and silylenes are known to insert into Si-H, Si-Hal, Si-OMe and O-H bonds. Compounds containing these bonds may be utilised as silylene traps. *Inter-*molecular silylene reactions also include C-H and Si-C  $\sigma$ -bond insertions as well as the insertions mentioned above<sup>15</sup>.

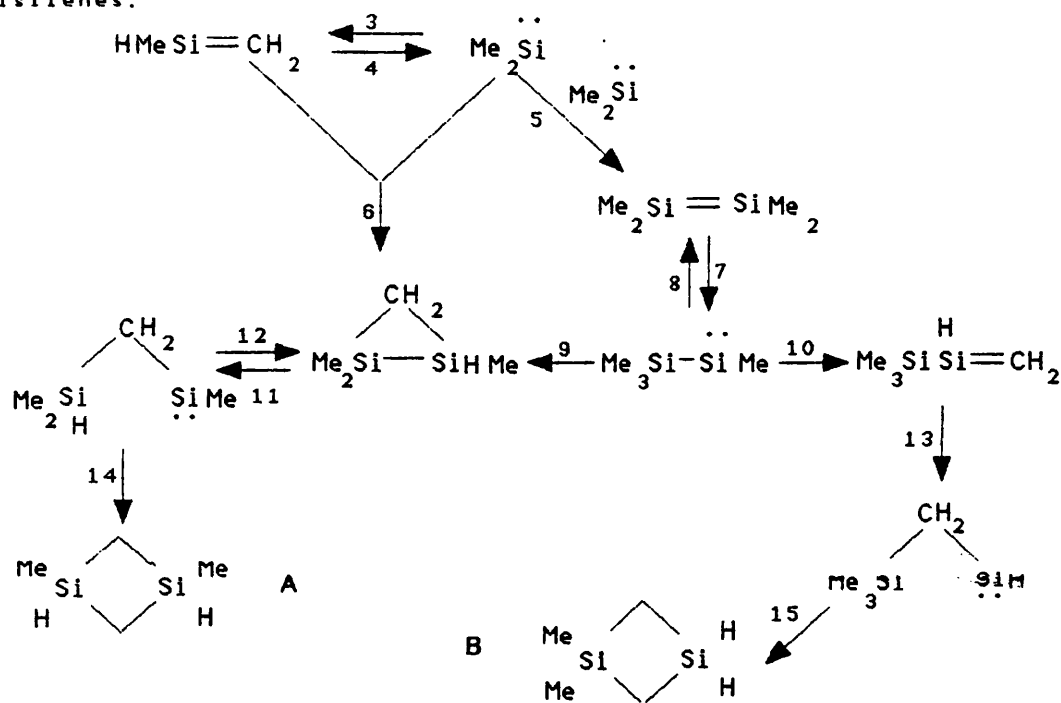
Silylenes add to carbon-carbon double bonds in a concerted fashion involving an electrophilic and nucleophilic stage<sup>21</sup> yielding a silacyclopropane. The addition of silylenes to carbon-double bonds is of use for silylene trapping reactions as they form stable adducts with conjugated 1,3 butadienes. The reaction is formally a 1,4 cycloaddition reaction but it is thought to proceed via a 1,2 addition to one double bond followed by rearrangement<sup>22</sup>.

Silylenes may isomerise to silenes via 1,2- hydrogen, methyl or silyl shifts<sup>23,24</sup>. The isomerisation of dimethylsilylene to 1-methyl silene is thought to be a thermoneutral reaction with a barrier of 120 kJmol<sup>-1</sup>. *ab initio* calculations predict the 1-methylsilene is slightly more stable than dimethylsilylene by 14 kJmol<sup>-1</sup> <sup>25</sup>.

Silylsilylenes may isomerise to disilenes and experimental evidence shows that when a disilene is generated by pyrolysis in the presence of butadiene the corresponding silylsilylene is also be trapped<sup>26</sup>. Disilene-silylsilylene interconversions are thought to be approximately thermoneutral with the disilene calculated to be more stable by 48 kJmol<sup>-1</sup> <sup>19</sup>. Addition of electronegative groups increasingly stabilise the silylsilylene and the ground state energy of Cl<sub>2</sub>Si=SiClH is calculated to be 1.6 kJmol<sup>-1</sup> above that of its silylsilylene isomer<sup>4</sup>.

Barton and his co-workers first suggested *intra-*molecular silylene insertion reactions and silylene-silylene interconversions<sup>26</sup>, helping to rationalise many organosilicon pyrolysis and photolysis reactions. The common isomerisation and rearrangement reactions of dimethylsilylene and related silenes, disilenes and silylenes may be summarised in scheme 1.1.

Scheme 1.1: Reaction scheme demonstrating isomerisation, dimerisation and rearrangement reactions of some related silylenes, silenes and disilenes.



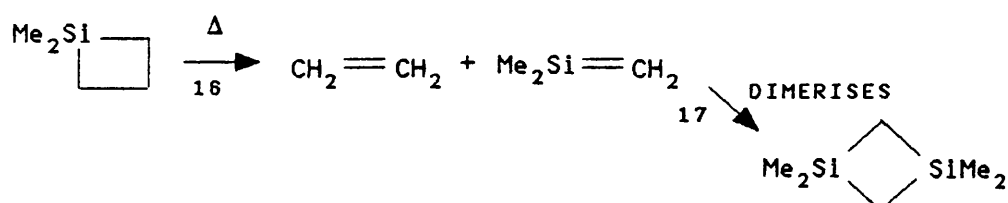
Reaction 4 is the isomerisation of 1-hydrosilene to dimethylsilylene via a 1,2 H-shift from Si to C. Dimethylsilylene can undergo the reverse reaction (3), dimerise to form tetramethyldisilene (5) or insert into the Si=C bond to form a disilacyclopropane (6). The disilacyclopropane can isomerise via a 1,2 H-shift to form a  $\beta$ -dimethylsilylmethylsilylene (11). This silylene can isomerise back to the disilacyclopropane (12) or undergo *intra*-molecular Si-H insertion to form product A (14). Tetramethyldisilene can isomerise to trimethylsilylmethylsilylene via a 1,2-methyl shift (7). Trimethylsilylmethylsilylene can isomerise back to the disilene (8), undergo *intra*-molecular C-H insertion to form a disilacyclopropane (9) or form trimethylsilylsilene via a 1,2 H-shift from the C to Si (10). A 1,2-silyl shift yields a disilacyclopropane (13) which can undergo *intra*-molecular C-H insertion to form product B (15).

### (III) Silenes ( $\text{R}_2\text{Si}=\text{CH}_2$ )

Silenes have been reviewed by Davidson<sup>4</sup> and Raabe and Michl<sup>27</sup>. They are silicon-carbon  $\pi$ -bonded species which are highly reactive. The Si=C bond is polar i.e.  $\delta^+\text{Si}=\text{C}\delta^-$  with the dipole moment calculated at  $0.84\text{D}^{28}$ , corresponding to a

-0.6|e| charge on C and a + 0.5|e| charge on Si. Silenes were thought of as intermediates only, until the first stable silene was prepared in 1981<sup>29</sup>. The Si=C bond was protected using bulky substituent groups to suppress dimerisation, other similarly substituted stable silenes have also been prepared<sup>30</sup>.

Silenes may be generated by a variety of thermal and photochemical methods e.g. the thermolysis of 1,1-dimethylsilacyclobutane yields ethene and dimethylsilene (16), which can be thought of as a 2+2 cycloreversion reaction<sup>31</sup>. The dimethylsilene once formed undergoes head to tail dimerisation (17).



The dimerisation is thermally forbidden but it takes place due to the polarity of the Si=C bond. In the case of  $\text{H}_2\text{Si}=\text{CH}_2$  the barrier to dimerisation is  $52 \text{ kJmol}^{-1}$ , the reaction being exothermic by  $319 \text{ kJmol}^{-1}$ . Other thermal generations include retro-Diels Alder reactions and silyl radical disproportionation.

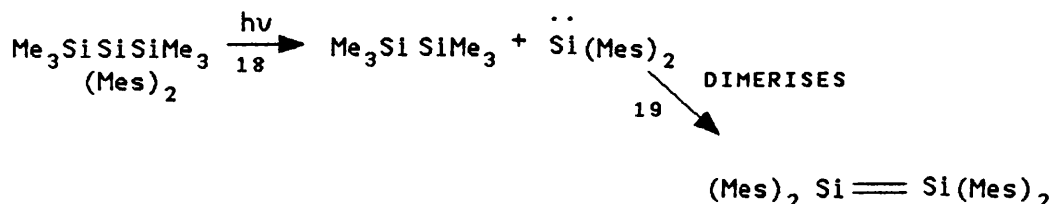
Silenes have a singlet ground state and are planar about the Si=C bond<sup>33</sup>. The Si=C bond length is calculated to be  $170 \text{ pm}^{27}$ , in good agreement with X-ray crystallography measurements on the least sterically hindered stable silene ( $170.2 \text{ pm}$ )<sup>34</sup>. The bond length is consistent with double bonding, being shorter than the Si-C bond. The high polarity of the Si=C bond is not affected by substituents such as hydrogen or carbon, but addition of electronegative substituents such as fluorine may increase the natural polarity of the bond if bonded to carbon, or reverse the polarity of the bond if bonded to silicon<sup>35</sup>; in the latter case the reactivity of the silene is reduced.

Silenes are known to dimerise, undergo Diels Alder cycloaddition reactions and radical addition reactions. The reaction of silenes with 1,3-butadiene yields 3,4-dimethyl-3-silylcyclohexene, a stable adduct, therefore pyrolysis in the presence of butadiene can be used as a test of silene intermediacy<sup>24</sup>.

Their isomerisation reactions to silylenes (*vide supra*) are not mirrored in carbon chemistry where the carbene is much higher in energy than the alkene.

(IV) Disilenes ( $R_2Si=SiR_2$ )

These silicon-silicon  $\pi$ -bonded species were first proposed as reactive intermediates by Roarke and Peddle when they pyrolysed disilabicyclo [2.2.2.] octadiene to generate tetramethyldisilene<sup>36</sup>. The first stable disilene was prepared in 1981 by West, Michl *et. al.* when they photochemically generated dimesitylsilylene which dimerised to tetramesityldisilene, an orange crystalline compound stable to 160°C in the absence of air and moisture<sup>37</sup>.



The primary source of disilenes in solution is the photolysis of trisilanes followed by silylene dimerisation. Disilene chemistry has been reviewed by Davidson<sup>4</sup>, West<sup>38</sup> and Michl and Raabe<sup>27</sup>.

The Si=Si bond for stable disilenes are nearly planar with bond lengths of between 214-216 pm depending on the substituents bonded to the disilene<sup>39</sup>. These bond lengths are shorter than the Si-Si bond in accordance with double bonding. The  $\pi$ -bond energy has been found experimentally to be 120 kJmol<sup>-1</sup> by monitoring cis-trans isomerisation reactions<sup>27</sup> although theory predicts this value to be 92 kJmol<sup>-1</sup> <sup>40</sup>.

Disilenes, like alkenes, are known to undergo addition with chlorine, oxygen and HCl, however, unlike alkenes, ethanol can also add across the double bond<sup>27</sup>. It is their isomerisation to silylsilylenes that is of most interest in the gas phase (*vide supra*)<sup>26</sup>.

## (V) Oligo and Polysilanes: Structure and Properties

Oligo and polysilanes are catenates of silicon which possess different chemical and physical properties to alkanes, their carbon counterparts. Oligosilanes with Si-H or Si-Cl bonds are very reactive and are unstable to moisture and air<sup>41</sup>, however, peralkylated oligosilanes are stable and can be prepared in polymeric form. Oligo and polysilanes possess characteristic absorptions in the near-UV, suggesting extensive delocalisation<sup>42,43</sup>. Polysilane chemistry has been reviewed by West<sup>1</sup>, Michl<sup>3</sup> and Hengge<sup>41</sup>.

The first polysilanes were prepared by Kipping in 1924 by the condensation of  $\text{Me}_2\text{SiCl}_2$  with sodium in the presence of an inert organic solvent<sup>44</sup>. The permethylated polymer formed was a brittle, insoluble solid. The modern era of polysilane chemistry began in 1980 when the first soluble polymers were prepared and it was found that these polymers could be cast as high quality films<sup>45</sup>. The behaviour of these polymers is largely affected by the nature of their pendant substituent groups. The UV absorption maxima ( $\lambda_{\text{max}}$ ) of polysilanes with pendant alkyl groups are between 300-325 nm, large alkyl groups cause a red shift in  $\lambda_{\text{max}}$  compared to small alkyl groups.  $\lambda_{\text{max}}$  for polysilanes with directly substituted aryl groups are red shifted by 25-35 nm<sup>42</sup>.

Spectroscopic evidence suggests the backbone conformation of decamethyltetrasilane is more stable in the trans form than the gauche by  $\approx 2 \text{ kJmol}^{-1}$ . The barrier between both forms is thought to be small. The backbone conformation of polysilanes is believed to mirror that of oligosilanes<sup>3</sup>.

The ground state electronic structure for oligosilanes and polysilanes may be explained in terms of LCBO theory<sup>3</sup>. Calculations show that there is no d-orbital contribution in the silicon-silicon bonding. Considering the all trans conformer, each silicon atom will have four  $\text{sp}^3$  orbitals, the silicon backbone will have a resonance integral between two  $\text{sp}^3$  orbitals on adjacent silicon atoms ( $\beta_{\text{vic}}$ ). This resonance integral is responsible for sigma bond formation giving rise to strongly bonding and antibonding sigma orbitals ( $\sigma$  and  $\sigma^*$ ). A secondary interaction of smaller magnitude between two sigma orbitals on the same silicon atom gives rise to a second resonance integral ( $\beta_{\text{gem}}$ ).

These two resonance integrals are the primary source of delocalisation in the silicon backbone. The degree of delocalisation is a function of  $\beta_{\text{gem}}/\beta_{\text{vic}}$ , the ratio being 0.87 for oligosilanes and 0.76 for alkanes. The most stable molecular orbital will have no nodes at bond midpoints or at each silicon atom; the least stable bonding orbital, the HOMO, will have no nodes at each bond midpoint but a node at each silicon atom. The LUMO will therefore have a node at each bond midpoint but no nodes across each silicon atom<sup>3</sup>.

Perfect delocalisation is brought about by non-nearest neighbour resonance integrals and the interactions of substituent groups with the silicon backbone. Substituents such as hydrogen or methyl groups will form  $\sigma$  and  $\sigma^*$  antibonding orbitals with the two remaining silicon  $\text{sp}^3$  orbitals. The local symmetry of these orbitals may be  $\sigma$  or  $\pi$  in nature and they interact with the molecular orbitals of the silicon backbone.

Non-nearest neighbour interactions are responsible for the conformational effects along the silicon chain. These 1,4 orbital interactions are affected by the angle of twist in the silicon chain and are largest when the silicon backbone is trans and planar.

Although there is net stabilisation of the  $\sigma$ -bonding orbitals in the silicon chain by substituent effects and non-nearest neighbour resonance integrals, these interactions act to destabilise the HOMO and stabilise the LUMO. Therefore there is a red shift in the absorption maxima upon substitution of bulky groups i.e. enforcing planarity on the silicon backbone.

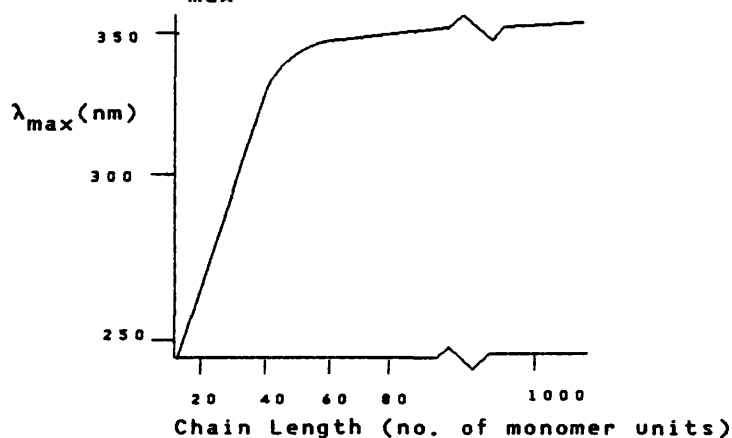
This simple molecular orbital picture of the bonding in oligosilanes helps explain the extensive delocalisation in the silicon chain, characterised by the UV absorptions exhibited by all oligo and polysilanes.

Photophysical studies suggest that oligo and polysilanes are made up of chains of mutually interacting chromophores of differing lengths separated by gauche links<sup>46</sup>. The UV absorptions of polysilanes are broad and featureless (typically 25-35 nm wide) and have large extinction coefficients<sup>47</sup>.

$\lambda_{\text{max}}$  and  $\epsilon_{\text{max}}$  increase rapidly with molecular weight but reach a limiting value at 40-50 monomer units long suggesting

a limiting value for the length of chromophore in the silicon chain (fig. 1.1)<sup>48</sup>.

Figure 1.1: Schematic representation of the effect of increasing chain length on  $\lambda_{\max}$  for a typical di-alkylpolysilane.



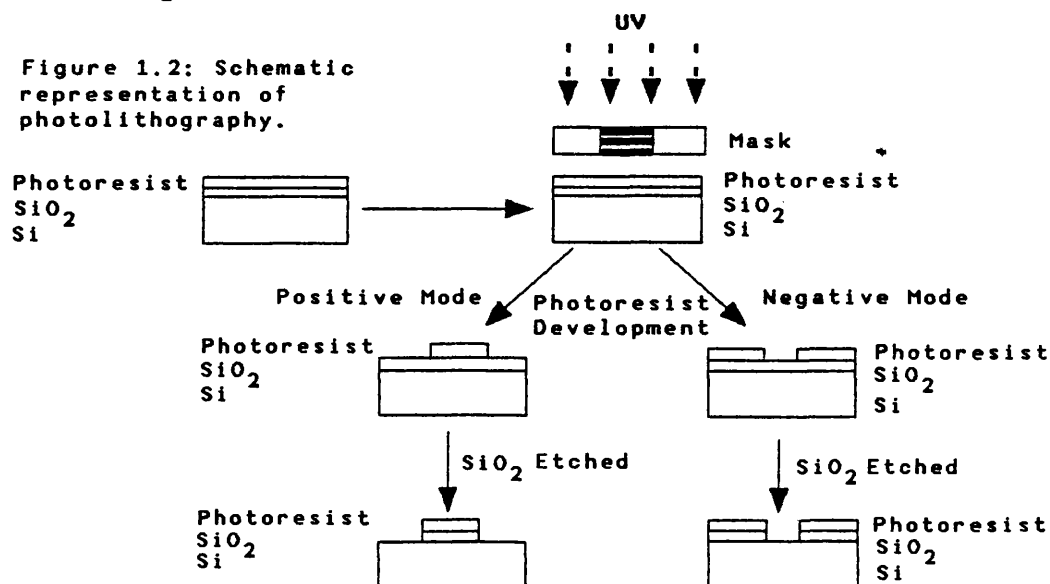
The UV transition is between the  $\sigma$  and  $\sigma^*$  molecular orbitals of the silicon backbone<sup>48</sup>. Emission studies show that the first excited state is also delocalised, while fluorescence quantum yield studies confirm that the chain is a statistical distribution of chromophores by exciting either long or short chromophores depending on the wavelength of irradiation<sup>48</sup>. The maximum number of monomer units in a single chromophore in solution is believed to be 20 from fluorescence polarisation studies<sup>46</sup>.

## (VI) Photoresists

Photolithography is the method used in the electronics industry to place microcircuitry onto silicon chips. The role of photoresists in the lithographic process is to transpose a template of the circuitry onto the silicon substrate. Photoresists may behave in a positive or negative fashion (fig. 1.2)<sup>49</sup>.

Photoresists are commonly spun coated onto a silicon wafer to achieve uniform thickness. The resist is then irradiated through a mask with the desired relief pattern. Depending on whether the resist is positive or negative the irradiated portion becomes more or less soluble. Wet development of the resist is followed by etching the  $\text{SiO}_2$  layer. Dopants or metallic contacts may now be deposited onto the silicon wafer. Positive photoresists are known to give higher resolution than negative resists and it is in this area that polysilanes are

of most interest<sup>50</sup>. With any photoresist there is always some lateral development due to solvent effects, as a result there is a move towards multilayer resist systems<sup>51</sup> using a thin top layer of photoresist which will undergo less lateral development<sup>52</sup>. The image can be transferred using all dry development techniques such as oxygen reactive ion etching ( $O_2$ -RIE) which is an all anisotropic technique which, however, places stringent demands on the resist<sup>50</sup>.



Polysilanes are now available as high quality films and seem ideal candidates for positive acting photoresists in bilayer applications having bleachable UV absorption maxima and being stable to  $O_2$ -RIE. The role of polysilanes as photoresists has been reviewed by Miller<sup>50</sup>. The three main uses for polysilanes in this area are:

- (i) Bilayer photoresists.
- (ii) Contrast Enhanced Photolithography (CEL).
- (iii) Laser Photoablation.

#### (i) Bilayer Photoresists<sup>51, 53</sup>

The first layer applied to the substrate is a thick planarising layer that will cover any existing topography. A thin layer of polysilane is then applied and developed as usual. The exposed planarising layer is then developed using  $O_2$ -RIE to produce line widths of 0.75  $\mu$ m.



### (ii) Contrast Enhanced Lithography<sup>1,54</sup>

This bilayer process utilises the ability of the polysilane film to bleach rapidly and then transmit light to a photoresist layer below i.e. effectively placing a new mask in contact with the lower resist layer. An in-contact mask minimises diffraction effects at the edges of the incident light. The contrast is improved at the edges of the exposed resist where light of lower intensity is incident. Only light of high enough intensity will bleach the polysilane film, light below the required intensity will not be transmitted. Line widths of 0.5  $\mu\text{m}$  are achievable using CEL.

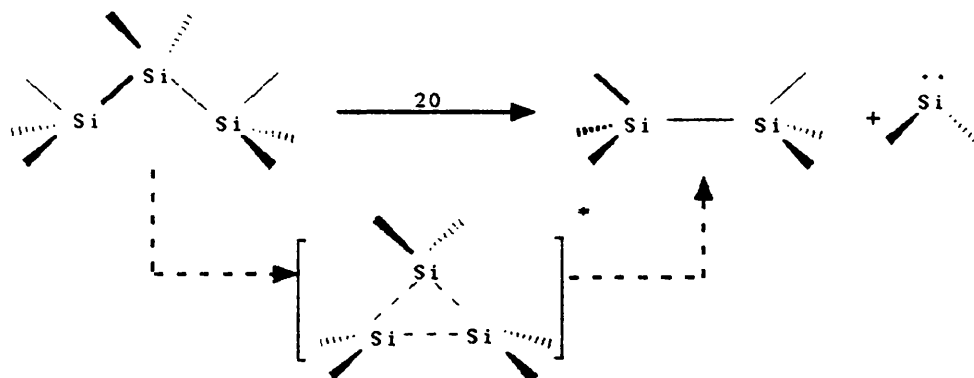
### (iii) Laser Photoablation<sup>55,56</sup>

Sub-micron features can be produced using a XeCl laser emitting light of 300 nm wavelength on a polysilane bilayer system. No wet development is required after initial exposure, the image is transferred using the  $\text{O}_2$ -RIE technique.

The three processes above utilise the photochemical (i) and (ii) and thermal (iii) properties of polysilanes. The thermal and photochemical properties of the related oligosilanes may prove useful in establishing the processes which occur in these techniques.

## (VII) Oligosilane Photochemistry

Oligosilanes are known to undergo photochemical degradation upon direct photolysis and the photochemistry of these compounds has been reviewed by Kumada<sup>2,57</sup>. The two processes that occur are silylene elimination and Si-Si bond cleavage. Kumada *et. al.* irradiated a number of straight chain<sup>58</sup>, cyclic<sup>59</sup> and branched<sup>60</sup> permethylated oligosilanes in hexane using incident radiation of 254 nm. Silylene elimination was found to be the major process, occurring via an extrusion reaction formally represented below:



It is believed the photochemistry of polysilanes is similar to that of oligosilanes<sup>3</sup>. It is known  $\lambda_{\max}$  and  $\epsilon_{\max}$  depend on molecular weight and that upon photolysis  $\lambda_{\max}$  and  $\epsilon_{\max}$  are reduced (photochemical bleaching). Processes which reduce molecular weight, similar to those in oligosilanes, are thought to be occurring.

Initial photochemical experiments on polysilanes showed that silylene elimination and silicon bond homolysis were taking place; it was suggested that these processes may be linked,<sup>50</sup> but later investigations proved that this was not the case<sup>3</sup>. Indeed it was proved that silylene formation was wavelength dependant, above 300 nm irradiation no silylenes were formed. Silylene formation is the minor photochemical process in polysilanes following on from the fact that in oligosilane photochemistry silicon bond homolysis increases with increasing chain length<sup>53</sup>. Silicon bond homolysis, the major photochemical breakdown route, is wavelength independent. This wavelength independence can be rationalised as follows.

Irradiation above 300 nm leads to excitation of long chained chromophores which undergo Si-Si bond homolysis to yield silyl radicals. Upon irradiation at short wavelengths, short chained chromophores are excited leading to silylene extrusion. However, an excited short chained chromophore can also undergo energy transfer to a longer chained chromophore, the longer chained chromophore can then undergo Si-Si bond homolysis. Silylene extrusion in oligosilanes is the major reaction upon photolysis as there are no long chained chromophores to be excited and energy transfer from excited short chained chromophores is therefore impossible.

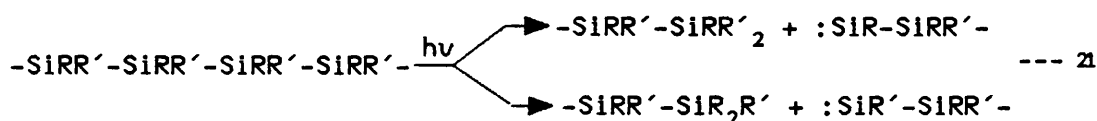
A novel photochemical breakdown mechanism has been suggested to account for 10 % of polysilane photolysis products, trialkyl terminated oligosilanes. Evidence for this

mechanism is backed by the separate observation that the most persistent radical has a unique structure and is thought to be formed via the same photochemical breakdown route as the trialkylated oligosilanes (fig. 1.3)<sup>61</sup>.

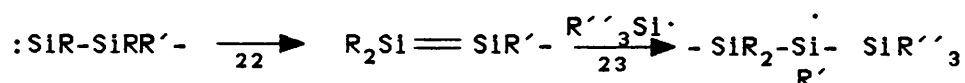


Figure 1.3: The structure of the most persistent radical

Radical A is not formed by the loss of an alkyl group since no alkanes or alkenes were isolated. The mechanism to account for both these observations is termed chain 'cleavage by reductive elimination'.



The first step of this mechanism is the formation of silylene terminated polysilane chain and the simultaneous formation of a trialkylated oligosilane (10% of products). The second step leading to the formation of the most persistent radical, is thought to be the rearrangement of the silylene to a disilene.



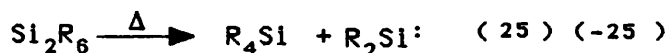
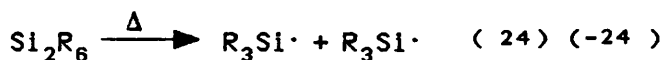
The disilene would be consumed rapidly under these reaction conditions by radical addition to yield the most persistent radical, as observed by ESR and ENDOR spectroscopy. There is no precedent for this mechanism in oligosilane photochemistry. However, hexamethyldisilane undergoes the first step of the 'reductive elimination' reaction (0.4%) upon direct photolysis in the gas phase (206 nm)<sup>62</sup>.

Silyl radicals are formed via the first triplet excited state as shown by quenching experiments and the fact that the triplet excited state only has a very weak phosphorescence, the transition energy being in the same order as the Si-Si bond strength<sup>46</sup>. Silylene formation is believed to arise from the doubly excited singlet state<sup>3</sup>.

### (VIII) Oligosilane Thermal Chemistry

Substituents affect the formation of silylenes or silyl radicals upon oligosilane pyrolysis<sup>16</sup>. For example for disilanes containing Si-H, Si-Hal or Si-OMe bonds, silylene

formation will be dominant<sup>16</sup>. However, for disilanes containing only Si-C (alkyl or aryl) bonds, silyl radical formation will take precedence<sup>7</sup>.



Silylene elimination is the thermodynamically favoured process<sup>8</sup>. However, it is the activation energy of the reverse reaction (-25) i.e. the insertion of a silylene into a silicon substituent bond, which mainly determines whether silyl radicals or silylenes are formed. Activation energies for *inter*-molecular silylene insertions into Si-H, Si-Hal and Si-OMe bonds are known to be low but are high for insertions into Si-C or C-C bonds. Figure 1.4 shows the energy profiles of the two competing processes, silylene formation being favoured in graph A and silyl radical formation being favoured in graph B.

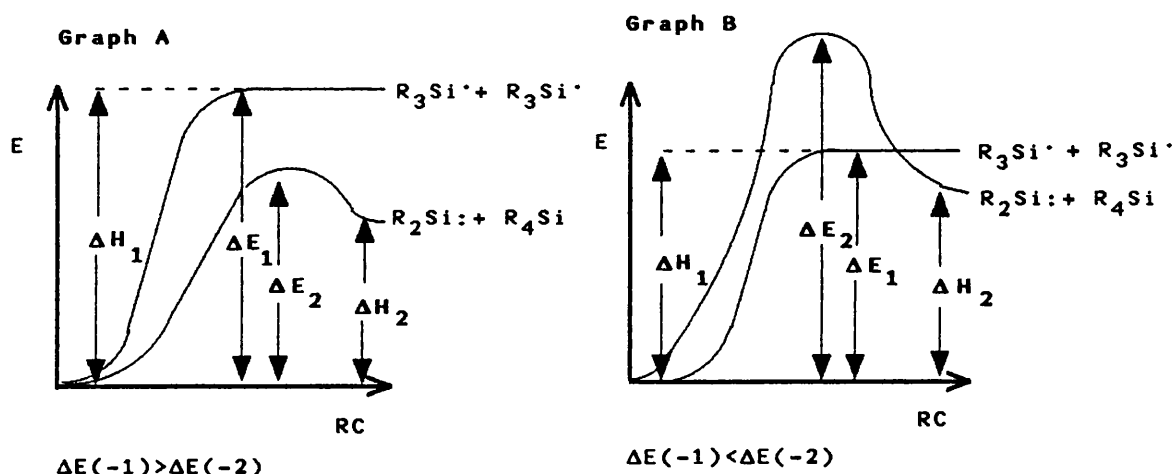
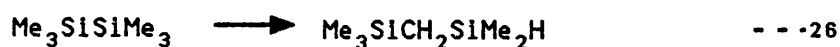


Figure 1.4: Graph A; Shows enthalpy (ΔH) and activation energy (ΔE) changes favourable to silylene formation.  
Graph B; Shows enthalpy (ΔH) and activation energy (ΔE) changes favourable to silyl radical formation.

Because silylene elimination proceeds via a tight three membered transition state, the A-factor (usually represented as logA) for a silylene elimination will always be smaller than the A-factor for a radical dissociation. Therefore, it is not only the activation energy (usually represented as E<sub>a</sub>) that dictates whether silyl radicals or silylenes are formed upon pyrolysis, but also the A-factors. Where the activation energy for silylene elimination is only slightly less than the activation energy for radical dissociation, the larger A-factor for the latter will facilitate this process.

The role gas phase kinetics has played in elucidating complex organosilicon reaction mechanisms is neatly demonstrated by the pyrolysis of hexamethyldisilane (HMDS)<sup>7,63</sup>. A simple but effective way of determining reaction kinetics is by the stirred flow technique (SFR)<sup>64</sup>. The SFR technique enables kinetic parameters to be measured over a range of temperatures, so orders, rate constants and Arrhenius parameters can be calculated (see chapter 2).

High pressure pyrolyses of HMDS carried out in sealed tubes<sup>65</sup> or continuous flow apparatus<sup>66</sup> gave the isomer trimethylsilyl (dimethylsilyl)methane (ISO) as the major product.



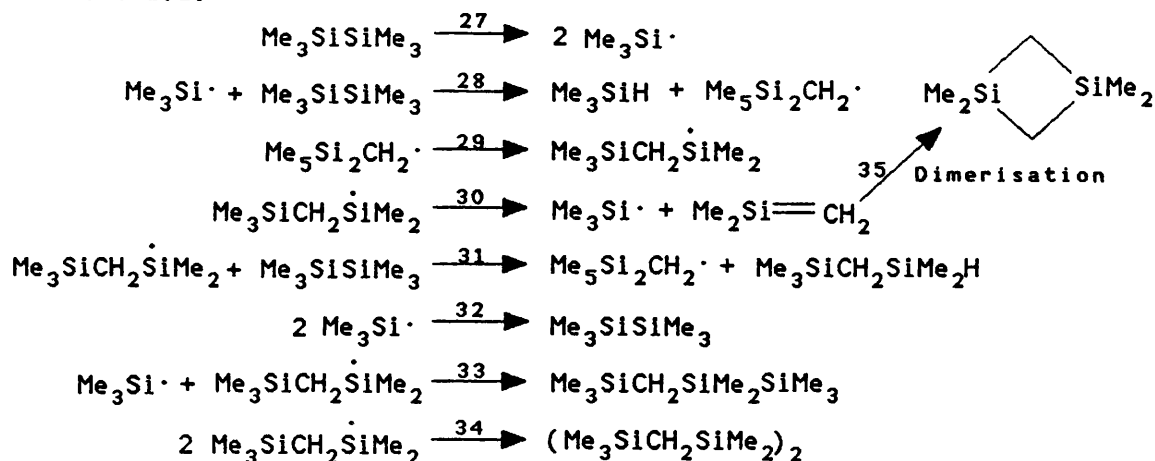
Addition of m-xylene, a known radical trap, reduced the rate of formation of ISO, indicating that a radical chain mechanism may be responsible for its formation. Kinetic experiments in a static system between 444-507°C showed three halves order for the formation of ISO<sup>67</sup>.

Low pressure pyrolysis of HMDS, on the other hand, yielded trimethylsilane (3MS) as the major product along with smaller amounts of ISO, tetramethylsilane (4MS) and 1,1,2,2-tetramethyl-1,2-disilacyclo-butane (TMDSCB).

The apparent inconsistency in product composition between the high and low pressure experiments was solved by the SFR technique. HMDS was pyrolysed between 497-600°C giving 3MS as the major product with smaller amounts of ISO, TMDSCB and 4MS. The orders of formation of all the products, except 4MS, were complex ranging between 1 and 2. The formation of 4MS was first order while 3MS and TMDSCB followed the same rate equation suggesting a common route to their formation.

Scheme 1.2 shows the series of reactions which account for the pressure dependence of this pyrolysis.

Scheme 1.2:

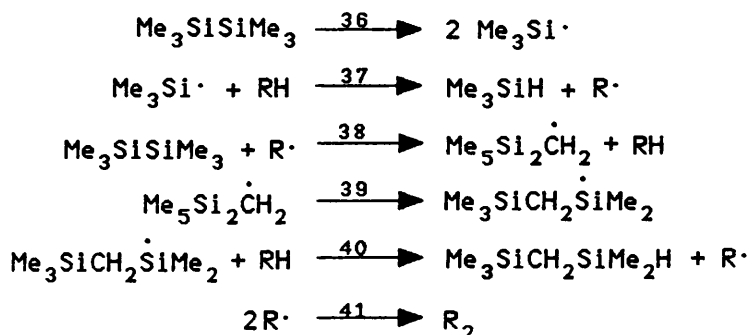


At high pressures reaction 31 is much faster than 30, leading to ISO being the major product along with a small amount of 3MS. The major radical termination step is 34 as the ISO radical is in the highest concentration, leading to three halves order for the formation of ISO.

At low pressure reaction 30 will compete with 31 leading to the formation of TMDSCB (via reaction 35) and larger quantities of 3MS. Radical termination reactions 32, 33 as well as 34 also occur, leading to fractional orders for the formation 3MS, ISO and TMDSCB.

When HMDS is pyrolysed in the presence of excess m-xylene using the SFR technique the major product is ISO with smaller amounts of 3MS and 4MS, no TMDSCB being formed. The formation of ISO follows three halves order kinetics, while 3MS is formed at a reduced rate following first order kinetics. There is no effect on the rate of formation of 4MS (first order). The reactions to account for these observations are shown in scheme 1.3.

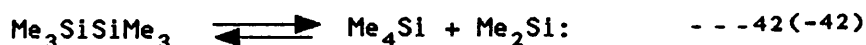
Scheme 1.3:



TMDSCB is not formed because reaction 40 is much faster than reaction 30 (scheme 1.2). The single radical termination step (41) ensures three halves order for the formation of ISO. 3MS is not produced by a radical chain mechanism, the rate determining step being the dissociation of the Si-Si bond

(36). The Arrhenius parameters for the formation of 3MS are  $E_a = 337 \pm 4 \text{ kJmol}^{-1}$  and  $\log A = 17.2 \pm 0.3 \text{ s}^{-1}$ ; this  $E_a$  is believed to be the best measurement of the Si-Si bond dissociation energy<sup>14</sup>.

The formation of 4MS is first order throughout all pyrolysis experiments and is believed to result from the unimolecular elimination of dimethylsilylene from HMDS.



The Arrhenius parameters for this elimination are  $E_a = 282 \pm 12 \text{ kJmol}^{-1}$  and  $\log A = 13.7 \pm 0.7$ . The activation energy for the insertion of dimethylsilylene into a Si-C bond of 4MS is related to the enthalpy change of reaction by<sup>68</sup>:

$$\Delta H_{42,-42} = E_{a42} - E_{a-42} \quad ---\{1.1\}$$

The molecular heats of formation for HMDS, 4MS and dimethylsilylene are given in table 1.1.

Table 1.1:

	$\Delta H_f^\circ (\text{kJmol}^{-1})$
$\text{Me}_3\text{SiSiMe}_3$	-361
$\text{Me}_4\text{Si}$	-233
$\text{Me}_2\text{Si:}$	109

Therefore by Hess's law:

$$\Delta H_{42,-42} = ( \Delta H_{f(4ms)} + \Delta H_{f(\text{Me}_2\text{Si:})} ) - \Delta H_{f(\text{HMDS})} \quad ---\{2\}$$

$$\begin{aligned} \Delta H_{42,-42} &= ( -233 + 109 ) - ( -361 ) \\ &= 237 \text{ kJmol}^{-1} \end{aligned}$$

From equation 1  $E_{a-42}$  can be calculated:

$$E_{a-42} = E_{a42} - \Delta H_{42,-42}$$

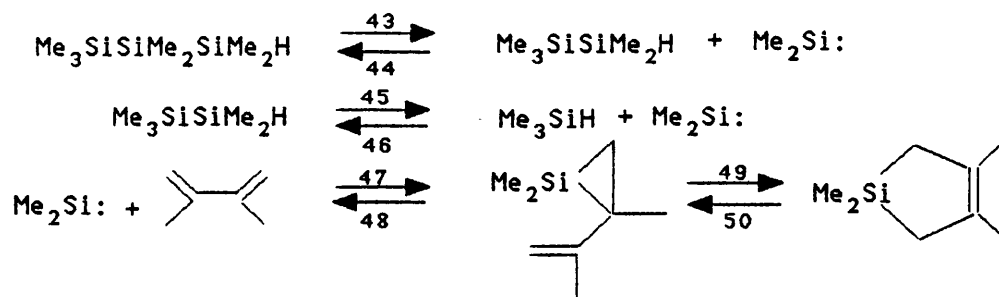
$$\begin{aligned} E_{a-42} &= 282 - 237 \\ &= 45 \text{ kJmol}^{-1} \end{aligned}$$

demonstrating that silylene insertions into Si-C bonds have high activation energies whereas it is known that silylene insertions into Si-H bonds have activation energies of 0  $\text{kJmol}^{-1}$ .

When heptamethyltrisilane is pyrolysed between 390-450°C using the SFR technique it dissociates into dimethylsilylene and pentamethyldisilane (PMDS)<sup>69</sup>. Dimethylsilylene may be trapped using 2,3-dimethylbuta-1,3-diene. PMDS will dissociate at these high temperatures into dimethylsilylene

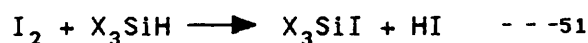
and trimethylsilane. The mechanism of trapping is complex involving the initial formation of a silacyclopropane (Scheme 1.4)<sup>70</sup>.

Scheme 1.4:

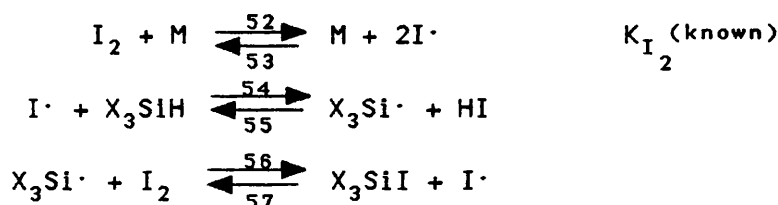


The Arrhenius parameters for reaction 43 are  $E_a = 175 \pm 5$   $\text{kJmol}^{-1}$  and  $\log(A/\text{s}^{-1}) = 11.8 \pm 0.4$ , clearly showing a major reduction in  $E_a$  for silylene elimination when compared to the Si-Si bond dissociation energy.

Other experimental techniques may be used for gas kinetic studies. Walsh reacted iodine with a series of silanes in the gas phase<sup>14</sup>, a method first introduced by Benson<sup>71</sup>, to access bond dissociation energies. The technique involves the reaction of iodine with molecules containing Si-H bonds.



The reaction mechanism in the majority of cases of silicon hydrides is simple:



As mentioned, silyl radicals are less likely to undergo chain reactions than alkyl radicals, thus simplifying the kinetic measurements using this technique. The reverse reaction (57) is unimportant due to the strength of the Si-I bond, therefore the rate of disappearance of  $\text{I}_2$  is given by:

$$- \frac{d[\text{I}_2]}{dt} = k_{52} K_{\text{I}_2}^{1/2} [\text{I}_2]^{1/2} [\text{X}_3\text{SiH}] \quad - - - (1.3)$$

$-d[\text{I}_2]/dt$  can be measured to yield  $k_{54}$ , whose temperature dependence gives the activation energy. As  $E_{a53}$  is small and does not vary with the nature of X,  $E_{a54}$  provides a good approximation of  $\Delta H_{54,55}$  ( $=E_{a54} - E_{a55}$ ). The enthalpy change at room temperature can be calculated using standard thermodynamic equations. The enthalpy change ( $\Delta H^\circ_{54,55}$ ) is



related to the bond dissociation energies thus:

$$\Delta H_{54,55}^{\circ} = D(\text{Si-H}) - D(\text{H-I}) \quad \dots \{1.4\}$$

As  $D(\text{H-I})$  is known  $D(\text{Si-H})$  can be calculated. The Si-H bond strengths in the series  $\text{H}_3\text{Si-H}$ ,  $\text{H}_2\text{MeSi-H}$ ,  $\text{HMe}_2\text{Si-H}$  and  $\text{Me}_3\text{Si-H}$  are 378, 375, 374 and 378  $\text{kJmol}^{-1}$  respectively. The effect of increasing methyl substitution does not significantly alter the Si-H bond strength, unlike the same series for increasing methyl substitution of methane. Methyl groups, therefore, do not weaken the Si-H bond (i.e. stabilise the resultant silyl radical).

Consecutive bond dissociation energies calculated from Walsh's experimental data on  $\text{SiH}_4$  show a decrease in the second bond dissociation energy; for the series  $\text{H}_3\text{Si-H}$ ,  $\text{H}_2\text{Si-H}$ ,  $\text{HSi-H}$  and  $\text{Si-H}$  the bond dissociation energies are 378, 268, 352 and 294  $\text{kJmol}^{-1}$  respectively. The lower value for second bond dissociation energy is thought to be a consequence of the group IV inert pair effect, the difference between the first and second bond dissociation energies giving a lone-pair stabilisation energy of 109  $\text{kJmol}^{-1}$  for  $\text{H}_2\text{Si}:$ .

Recent investigations into laser photoablation of polysilanes revealed the major intermediates involved were silyl radicals. Cyclic carbosilanes were also formed but these were poorly characterised<sup>72</sup>.

The physical property of primary importance is the volatility of the oligosilane under investigation in this gas phase study. Table 1.2 gives some common physical constants for a series of straight chained permethyloligosilanes<sup>73</sup>.

Table 1.2: Some Physical Constants for the Series of Straight Chained Permethyloligosilanes.

COMPOUND	Masses (m/u)*	Melting Point ( $^{\circ}\text{C}$ )	Boiling Point ( $^{\circ}\text{C}$ )
$\text{Me}_8\text{Si}_3$	204	-52	175-176
$\text{Me}_{10}\text{Si}_4$	262	-14	112-113
$\text{Me}_{12}\text{Si}_5$	321	-34	135-136
$\text{Me}_{14}\text{Si}_6$	379	28	165
$\text{Me}_{16}\text{Si}_7$	438	20	194

$1\text{u} = 1.66 \times 10^{-27} \text{ kg}$ ;  $m = M_r \text{u}$

The increasing involatility of these compounds with increasing chain length led to the development of the liquid

injection SFR technique (see Chapter 2).

#### (IX) References

- (1) R. West, *J. Organomet. Chem.*, 1986, 300, 327.
- (2) M. Ishikawa, M. Kumada, *Rev. Silicon, Germanium, Tin and Lead Compd.*, 1979, 4, 7.
- (3) R.D. Miller, J. Michl, *Chem. Rev.*, 1989, 89, 1359.
- (4) I.M.T. Davidson, *Roy. Soc. Chem., Ann. Rep. C.*, 1985, 47.
- (5) H. Sakuri, in '*Free Radicals*', Ed. J.K. Kochi, Wiley, New York, 1973, 741.
- (6) N.L. Arthur, T.N. Bell, *Rev. Chem. Intermed.*, 1978, 2, 37.
- (7) I.M.T. Davidson, A.V. Howard, *J. Chem. Soc., Faraday Trans I*, 1975, 71, 69.
- (8) I.M.T. Davidson, *J. Organomet. Chem.*, 1970, 24, 97.
- (9) P.P. Gaspar, J. Wilking, in '*Frontiers of Organosilicon Chemistry*', Ed. A.R. Bassindale & P.P. Gaspar, 1991, in press.
- (10) I.M.T. Davidson, *Chem. Soc., Quart. Rev.*, 1971, XXV, 111.
- (11) R.L. Morehouse, J.J. Christiansen, W. Gordy, *J. Phys. Chem.*, 1966, 45, 1751.
- (12) Th. Brix, U. Paul, P. Potzinger, B. Reimann, *J. Photochem. Photobiol., A: Chem.*, 1990, 54, 19.
- (13) T.J. Barton, S.A. Burns, I.M.T. Davidson, S. Ijadi-Maghsoodi, I.T. Wood, *J. Am. Chem. Soc.*, 1984, 106, 6367.
- (14) R. Walsh, *Acc. Chem. Res.*, 1981, 84, 246.
- (15) P.P. Gaspar, '*Reactive Intermediates*', Eds. M. Jones, R.A. Moss, Wiley, New York; 1978, 1, 229; 1981, 2, 335; 1985, 3, 333.
- (16) I.M.T. Davidson, K.S. Hughes, S. Ijadi-Maghsoodi, *Organometallics*, 1987, 6, 639.
- (17) M.S. Gordon, *Chem. Phys. Lett.*, 1985, 124, 348.
- (18) M.S. Gordon, M.W. Schmidt, *Chem. Phys. Lett.*, 1986, 132, 294.
- (19) K. Krogh-Jespersen, *J. Am. Chem. Soc.*, 1984, 107, 537.
- (20) M.S. Gordon, D.R. Gano, *J. Am. Chem. Soc.*, 1984, 106,

5421.

- (21) F. Anwari, M.S. Gordon, *Isr. J. Chem.*, 1983, 23, 129.
- (22) M.P. Clarke, I.M.T. Davidson, M.P. Dillon, *J. Chem. Soc., Chem. Commun.*, 1988, 1251.
- (23) I.M.T. Davidson, R.J. Scampton, *J. Organomet. Chem.*, 1984, 271, 249.
- (24) I.M.T. Davidson, K.J. Hughes, R.J. Scampton, *J. Organomet. Chem.*, 1984, 272, 11.
- (25) T.N. Bell, A.F. Kierran, K.A. Perkins, P.G. Perkins, *J. Phys. Chem.*, 1984, 88, 1334.
- (26) W.D. Wulff, W.F. Goure, T.J. Barton, *J. Am. Chem. Soc.*, 1978, 100, 6636.
- (27) G. Raabe, J. Michl, *Chem. Rev.*, 1985, 85, 419.
- (28) G. Trinquier, J-P. Malrieu, *J. Am. Chem. Soc.*, 1981, 103, 6313.
- (29) A.G. Brook, F. Abdesaken, B. Gutekunst, G. Gutekunst, R.K.M. Kallury, *J. Chem. Soc., Chem. Commun.* 1981, 191.
- (30) A.G. Brook, F. Nyburg, F. Abdesaken, B. Gutekunst, G. Gutekunst, R.K.M. Kallury, Y.C. Poon, Y.M. Chang, N.W. Wang, *J. Am. Chem. Soc.*, 1982, 104, 5667.
- (31) L.E. Gusel'nikov, M.C. Flowers, *J. Chem. Soc., Chem. Commun.*, 1967, 864; *J. Chem. Soc. B*, 1968, 419, 1396.
- (32) G. Bertrand, G. Trinquier, S. Mazerolles, *J. Organomet. Chem. Libr.*, 1981, 12, 1.
- (33) R. Ahlrichs, R. Heinzmann, *J. Am. Chem. Soc.*, 1977, 99, 7452; D.M. Hood, H.F. Schaefer, *J. Phys. Chem.*, 1978, 68, 2985.
- (34) N. Wiberg, G. Wagner, G. Muller, *Angew Chem. Int. Ed. Engl.*, 1985, 24, 229.
- (35) Y. Apeloig, M. Karni, *J. Chem. Soc., Chem. Commun.*, 1984, 768.
- (36) D.N. Roark, G.J.D. Peddle, *J. Am. Chem. Soc.*, 1971, 94, 5837.
- (37) R. West, M.J. Fink, J. Michl, *Science*, 1981, 214, 1343.
- (38) R. West, *Pure & Appl. Chem.*, 1984, 56, 163.
- (39) R. West, J. Michl, M.J. Fink, *Organometallics*, 1984, 3, 793.
- (40) G. Olibrich, P. Potzinger, B. Reimann, R. Walsh, *Organometallics*, 1984, 3, 1267.
- (41) B.J. Hengge, in 'Silicon Chemistry' Eds. J.Y. Corey, E.R. Corey, P.P. Gaspar, IUPAC, 1988, Chapter 23, p

237.

- (42) P. Trefonas III, R. West, R.D. Miller, D. Hofer, J. *Polymer. Sci., Polymer Lett. Ed.* 1983, 21, 823.
- (43) H. Gilman, W.H. Atwell, G.L. Schweke, J. *Organomet. Chem.* 1964, 2, 369.
- (44) F.S. Kipping, J. *Chem. Soc.*, 1924, 125, 229.
- (45) J.P. Wesson, T.C. Williams, *Polym. Sci.; Polym. Chem. Ed.*, 1980, 18, 959.; R. West, L.D. David, P.I. Djurovich, K.L. Stearley, K.S.V. Srinivasen, H. Yu, J. *Am. Chem. Soc.*, 1981, 103, 7352.
- (46) J. Michl, *Pure & Appl. Chem.*, 1990, 60, 959.
- (47) R.D. Miller, D. Hofer, J. Rabolt, G.N. Fickes, J. *Am. chem. Soc.*, 1985, 107, 2172.
- (48) K.A. Klingensmith, J.W. Downing, R.D. Miller, J. Michl, J. *Am. Chem. Soc.*, 1986, 108, 7438.
- (49) D.J. Elliott, '*Integrated Circuit Fabrication Technology*', McGraw-Hill, New York, 1982.
- (50) R.D. Miller, in '*Silicon Chemistry*' Eds. J.Y. Corey, E.R. Corey, P.P. Gaspar, IUPAC, 1988, Chapter 35, p377.
- (51) J.R. Havas, *Electrochem. Soc., extended abstracts.*, 1976, 76, 734.
- (52) B.J. Lin, *Am. Chem. Soc. Symposium Series.*, No. 219, A.C.S. Washington D.C., 1980, Chapter 6.
- (53) D.C. Hofer, R.D. Miller, C.G. Willson, *Proc. Spie.*, *Adv. in Resist Technology*, 1984, 469, 109.
- (54) D.C. Hofer, R.D. Miller, C.G. Willson, *Proc. Spie.*, *Adv. in Resist Technology*, 1984, 469, 16.
- (55) R.D. Miller, D. Hofer, *I.B.M. Disclos. Bull.*, 1984, 26, 5683.
- (56) R.D. Miller, D. Hofer, *Polym. Eng. Sci.*, 1986, 26, 1129.
- (57) M. Ishikawa, M. Kumada, *Adv. Organomet. Chem.*, 1986, 6, 19.
- (58) M. Ishikawa, T. Takaoka, M. Kumada, J. *Organomet. chem.*, 1972, 42, 333.
- (59) M. Ishikawa, M. Kumada, J. *Organomet. Chem.*, 1972, 42, 325.
- (60) M. Ishikawa, M. Kumada, J. *Chem. Soc., Chem. Commun.*, 1971, 489.
- (61) A.J. McKinley, T. Karatsu, G.M. Wallraff, R.D. Miller,

- R. Sooriyakumaran, J. Michl, *Organometallics*, 1988, 7, 2567.
- (62) Th. Brix, E. Bastian, P. Potzinger, *J. Photochem. Photobiol., A*, 1989, 49, 287.
- (63) I.M.T. Davidson, *J. Organomet. Chem.*, 1988, 341, 255.
- (64) I.M.T. Davidson, G. Eaton, K.J. Hughes, *J. Organomet. Chem.*, 1988, 347, 17.
- (65) H. Sakurai, A. Hosomi, M. Kumada, *J. Chem. Soc., Chem. Commun.*, 1968, 930.
- (66) K. Shiina, M. Kumada, *J. Org. Chem.*, 1958, 23, 139.
- (67) I.M.T. Davidson, C. Eaborn, J.M. Simmie, *J. Chem. Soc., Faraday Trans. I*, 1974, 70, 249.
- (68) R. Walsh, in 'Silicon Chemistry' Eds. J.Y. Corey, E.R. Corey, P.P. Gaspar, IUPAC, 1988, Chapter 5, p371.
- (69) M.P. Clarke, I.M.T. Davidson, M.P. Dillon, *J. Chem. Soc., Chem. Commun.*, 1988, 1251.
- (70) D. Lei, R-J. Hwang, P.P. Gaspar, *J. Organomet. Chem.*, 1984, 271, 1; D. Lei, P.P. Gaspar, *J. Chem. Soc., Chem. Commun.*, 1985, 1149.
- (71) D.M. Golden, S.W. Benson, *Chem. Rev.*, 1969, 69, 125.
- (72) T.F. Magnera, V. Balaji, J. Michl, R.D. Miller, R. Sooriyakumaran, *Macromolecules*, 1989, 22, 1624.
- (73) M. Kumada, M. Ishikawa, *J. Organomet. Chem.*, 1963, 1, 157.

## Chapter 2

### Experimental

#### (I) Kinetic Measurements Using The Stirred Flow Reactor (SFR) Apparatus

The SFR technique is a continuous flow method enabling kinetic measurements to be carried out over a range of temperatures; orders, rate constants and Arrhenius parameters can be calculated using this method<sup>1</sup>. The conventional SFR technique allows a steady stream of reactant vapour to be carried by an inert carrier gas into a specially designed reactor. The reactor design ensures perfect mixing so reactant concentration is constant throughout<sup>2</sup>. The extent of pyrolysis is dependant upon the temperature and 'residence time' in the reactor (where the 'residence time' = reactor volume divided by volumetric flow rate). Simple kinetic equations can be derived for product formation by considering the mass balance in a continuous flow reactor.

For a first order reaction  $A \rightarrow B$  with a rate constant  $k_1$ , consider the mass balance for product B:

$$\text{Formation} - \text{Loss} = 0 \quad \text{---}\{2.1\}$$

$$k_1 \nu [A] - \nu [B] = 0 \quad \text{---}\{2.2\}$$

where  $\nu$  = volume of reactor,  $\nu$  = volumetric flow rate,  
and  $[]$  = molar concentration in the reactor.

$$\text{Hence, } k_1 = [B]/[A]\tau \quad \text{---}\{2.3\}$$

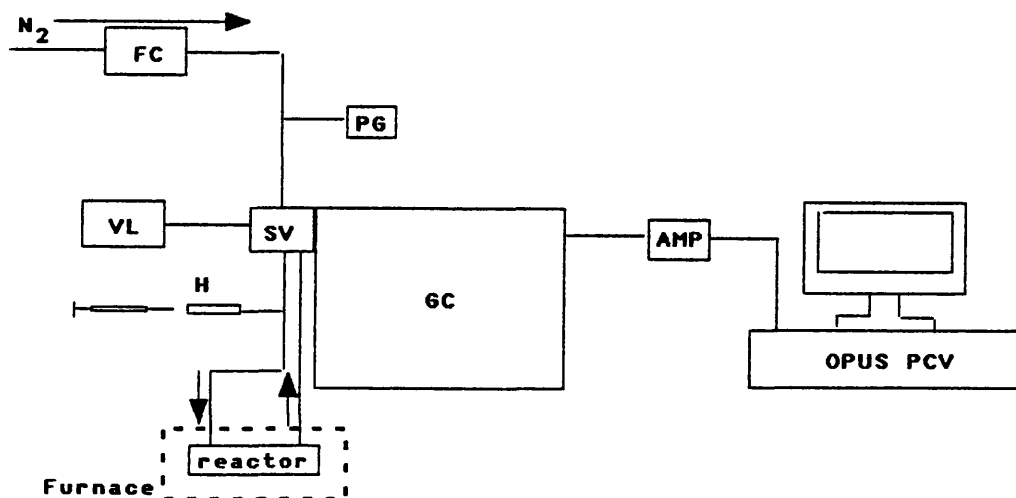
$$\text{where } \tau = \nu/\nu, \text{ is the 'residence time'} \quad \text{---}\{2.4\}$$

Rate constants for product formation can be calculated using equation {2.3} as long as  $\nu$ ,  $\nu$  and the concentrations of reactant and product are known. Continuous flow methods use large quantities of reactant and problems arise in achieving a uniform flow rate and knowing exact reactant and product concentrations in the reactor. The batch SFR technique

developed by Davidson overcomes these problems<sup>3,4</sup>.

The basic experimental apparatus consists of a gas chromatograph (GC) with an attached gas sample valve (Fig. 2.1).

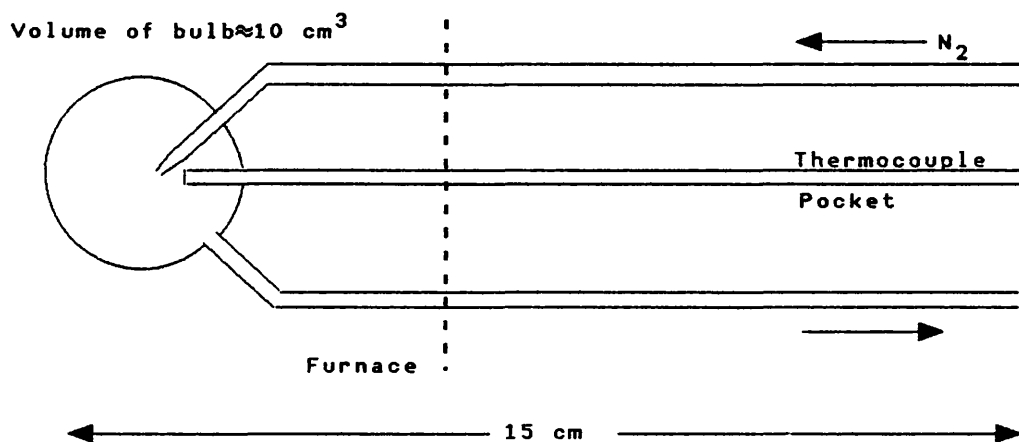
Figure 2.1: Schematic diagram of the Stirred Flow Reactor Apparatus.



FC= Flow Controller, PG= inlet pressure Gauge, SV= Sample Valve, VL= Vacuum Line, H= Liquid Injector Heater, AMP= 0-5V amplifier.

Inserted between the gas sample valve and GC is a miniature quartz stirred flow reactor of a similar design to that used by Mulcahy and Williams<sup>2</sup> (Fig. 2.2). The stirred flow reactor differs from the original design in two ways; the reactor is of smaller volume (10 cm<sup>3</sup>) and instead of a perforated bulb being at the reactor inlet, a nozzle ensures perfect mixing.

Figure 2.2: A Stirred Flow Reactor



The reactor is placed in an electrically heated tubular furnace, the reactor temperature being measured by a thermocouple inserted into a pocket at the centre of the bulb. An attached vacuum line allows reactant vapour to fill the gas

sample valve. The vacuum line is used for storage and manipulation of volatile reactants and is fitted with Youngs greaseless taps throughout; sample pressure is measured by a Baratron pressure gauge.

Reactants of low vapour pressures, such as high molecular weight oligosilanes, may be injected into the carrier gas by a syringe placed in a heated injection port. The injector is electrically heated (250°C) and contains a quartz wool plug to ensure a large surface area for rapid vaporisation. Involatile oligosilanes are stored under nitrogen in V-Vials fitted with ptfa septa.

The nitrogen carrier gas is dried (by passing through molecular sieves) and deoxygenated (by passing through an oxytrap). The flow rate of the carrier gas is controlled by a solid state flow controller (ASM).

An 'analytical sized' pulse of reactant vapour is injected into the carrier gas stream by the gas sample valve (Pye Unicam) or a syringe. The reactant pulse is mixed by stirred flow and partially pyrolysed. Products and unpyrolysed reactant flow out of the reactor and into the GC (Pye Unicam G.C.D. Gas Chromatograph), where reactant and products are separated on a packed column (3.5 m/3% SE-30). Gaseous products can be separated by cooling the GC oven to 0°C with dry ice.

The separated peaks are detected by a flame ionisation detector (FID), data being recorded and used to construct a visual display on a dedicated microcomputer (OPUS PCV). The FID supplies a 0-1V signal which is amplified to 0-5V for the AD converter card inserted in the OPUS PCV. The GC is calibrated for various reactants and products for calculation of their final molar concentrations.

In the batch SFR method, as the sweeping out of the reactor is a first order process with a rate constant  $\tau^{-1}$ , equation {2.3} is still valid for a first order reaction and independent of the percentage breakdown of reactant<sup>3</sup>. The validity of equation {2.3} is dependant upon; (i) the volume of the pulse being small compared to the volume of the reactor, (ii) perfect mixing and (iii) perfect pulse behaviour i.e. the concentration of the pulse at the reactor inlet becomes zero upon injection. First order rate constants can be calculated over a range of temperatures and concentrations



allowing a full kinetic investigation to be carried out on relatively small amount of reactant. Specially written software allows easy calculation of rate constants and Arrhenius parameters. From equation {2.3} the volumetric flow rate must be calculated at the reactor temperature ( $v_r$ ):

$$v_r = \frac{v_a P_a T_r}{P_r T_a} \quad \text{--- (2.5)}$$

$$\text{therefore } \tau = \frac{P_r T_a v}{v_a P_a T_r} \quad \text{--- (2.6)}$$

If the percentage conversion of reactant is small, rate constants for reactions of orders greater than one can be calculated, the change in concentration of reactant relative to  $\tau$  is insignificant<sup>3</sup>. If reaction  $A \rightarrow B$  has an order of  $n$  then the rate constant  $k$  may be calculated thus:

$$k = \frac{[B] v^{(n-1)}_n}{[A]^n \tau} \quad \text{--- (2.7)}$$

$$\text{therefore } [B] = [A]^n \left\{ \frac{k \tau}{v^{(n-1)}_n} \right\} \quad \text{--- (2.8)}$$

A plot of  $\log[B]$  versus  $\log[A]$  will have a slope =  $n$ , the order of the reaction.

Product identification using the kinetic apparatus can be achieved by comparative retention time experiments using authentic samples, although some degree of uncertainty will remain using this method.

## (II) Product Identification Using the Gas Chromatograph/Mass Spectrometer-Stirred Flow Reactor Apparatus (GC/MS-SFR)

The problem of product identification is overcome by attaching an SFR to a Hewlett-Packard HP5995C GC/MS, controlled by a series 300 Chemstation. The SFR apparatus is similar to that in fig. 2.1 but modified slightly to accommodate the inherent differences in using a capillary GC/MS<sup>5</sup>. A quadrupole mass spectrometer is used to record mass spectra and detect peaks eluting from the GC by measuring the total ion current (TIC). Capillary columns (50 and 12m polysiloxane SCOT) are used for more efficient separation, leading to two differences between the kinetic and GC/MS-SFR

(*vide infra*). Dried, deoxygenated helium carrier gas is used, reactor residence times being altered by a solid state flow controller. The gas sample valve is of unconventional design to prevent helium carrier gas leakage<sup>5</sup>.

The mass spectrometer has a mass range of between 10-800 atomic mass units (amu). Tuning of the mass spectrometer is software controlled and is achieved by focusing on the known fragmentation peaks of perfluorotributylamine (pftba). The GC/MS may operate in two modes; scan mode, recording mass spectra over a preset range, or single ion monitoring (SIM) mode where individual ions are monitored.

The use of high resolution capillary columns results in two differences in the GC/MS-SFR apparatus. The first is the necessity to use a liquid nitrogen cold trap between the exit of the reactor and the injection port of the GC/MS<sup>4</sup>. The sweeping out of the reactor is a first order process ( $\tau^{-1}$ ), at time  $5\tau$  99% of the sample has left the reactor. Short retention times for volatile samples in a capillary column result in a broad, diffuse peaks if a cold trap is not used. A time scale of  $5\tau$  is too long for a capillary column, retention times should be at least  $10\tau$  for good separation (a condition met by the packed column without the use of a cold trap). The liquid nitrogen cold trap condenses the sample if kept in place for a suitable length of time ( $>5\tau$ ). The reactant and products are then volatilised using hot water at approximately 90°C. Concentrated reactant and product peaks result, giving satisfactory resolution. Methane and other samples which exert a vapour pressure at liquid nitrogen temperatures are not condensed.

A packed column has the capacity to separate all the reaction mixture, however, the reduced capacity of a capillary column and the differences in flows between the reactor (25ml/min) and the column flow entering the mass spectrometer (1ml/min) means a nondiscriminatory splitter must be used<sup>5</sup>.

The injection port of the GC/MS has been modified to suit gas phase injections. The carrier gas is diverted through the injection port ending just above the splitter (as in a normal syringe injection), thus avoiding indiscriminate loss of products and reactant via the septum purge<sup>5</sup>.

The series 300 Chemstation's macro-driven software allows easy data manipulation, the recorded mass spectra of the

separated peaks being used for product identification. Therefore the GC/MS-SFR apparatus is a powerful tool in establishing organosilicon pyrolysis mechanisms.

### (III) The Q8/MS-Sealed Tube Pyrolysis Technique for the Detection of Hydrogen and Methane

The lowest mass the HP5995-C mass spectrometer can detect is 10 amu, therefore it cannot detect hydrogen. To detect hydrogen a V.G. Q8 quadrupole mass spectrometer is used (mass range 0-300 amu). The Q8/MS has an attached vacuum line fitted throughout with Youngs greaseless stopcocks. Gaseous samples enter the ion source via a leak between the vacuum line and the Q8/MS.

A sealed tube pyrolysis is carried out on a known volume/sample pressure of oligosilane; the pyrolysis cell being a standard gas sample vessel. A rough time scale for 50% pyrolysis ( $t_{1/2}$ ) is calculated from the Arrhenius parameters for the formation of a major product e.g. the production of trimethylsilane from iso-decamethyltetrasilane gave the Arrhenius parameters  $E_a = 294 \text{ kJmol}^{-1}$  and  $\log (A/s^{-1}) = 16.4$  (see Chapter 5):

$$k = A e^{-(E_a/RT)} \quad \text{---(2.9)}$$

The half-life of a first order reaction is given by:

$$t_{1/2} = (1/k) \ln 2 \quad \text{---(2.10)}$$

$$\text{At } 620^\circ\text{C: } k = 0.252 \text{ s}^{-1} \text{ and } t_{1/2} = 2.75 \text{ s}$$

$$\text{At } 550^\circ\text{C: } k = 5.25 \times 10^{-3} \text{ s}^{-1} \text{ and } t_{1/2} = 3.00 \text{ mins}$$

$$\text{At } 500^\circ\text{C: } k = 3.35 \times 10^{-4} \text{ s}^{-1} \text{ and } t_{1/2} = 35 \text{ mins}$$

A time scale of approximately 5 minutes is desirable. The mixture is pyrolysed in a tubular furnace for the calculated length of time. The sample vessel containing the pyrolysed mixture is then attached to the Q8/MS vacuum line.

Heterogeneous reactions with the sample vessel walls lead to the formation of more products in a sealed tube pyrolysis than a SFR pyrolysis. To simplify the mass spectra of the pyrolysed mixture the sample vessel is kept under liquid nitrogen. The only products having vapour pressures at liquid nitrogen temperatures will be hydrogen and methane, the mass spectra of both these gases are easily recognisable.

Therefore if hydrogen and methane are pyrolysis products they will be detected using this method.

#### (IV) Preparative Experiments Using The Preparative Gas Chromatograph Stirred Flow Reactor Apparatus (GC-PREP/SFR)

There can be some uncertainty in product identification using GC/MS alone unless there are authentic samples of products to compare retention times and mass spectra. Therefore, products were isolated for NMR analysis by attaching a large scale SFR apparatus to a Pye-Unicam 105 Mark 2 Preparative Gas Chromatograph. The differences to the apparatus shown in fig. 2.1 are; (i) a 25 cm<sup>3</sup> volume reactor with a perforated bulb at the inlet is used, (ii) no sample valve (and therefore no vacuum line) is required as all injections are liquid and (iii) an acetone-dry ice cold trap is used to concentrate reactant and product peaks (the larger reactor size leading to longer residence times)<sup>4</sup>. Monosilanes are not condensed as they exert a vapour pressure at -78°C.

Typically 10 mls of reactant is introduced into the nitrogen carrier gas (dry/deoxygenated) via a syringe injection and mixed by stirred flow in the reactor. This process is repeated up to five times to ensure a collectable quantity of product is condensed in the cold trap (the quantity of product not being large enough to result in poor peak separation).

The condensed reactant and products are then volatilised using water at 90°C. All reactant and products flow onto the preparative packed GC column (20% SE-30). The exit end of the column is fitted with a 100:1 splitter; the majority of the carrier gas flows out of the GC and into super-efficient cold traps in an acetone/'dry-ice' slush bath. The minority of the carrier gas flows to the flame ionisation detector, the FID output being recorded on a chart recorder. Separated products can therefore be collected in different super-efficient cold traps. High nitrogen carrier gas flow rates (75-100 mls/min) ensures sharp, well resolved peaks.

When enough product is isolated, each cold trap is washed out with 250 mls of deuterated chloroform. The purity of each product being tested by GC/MS (HP5995C). Three sets of

NMR spectra were run on each sample; proton, carbon 13 and DEPT. All NMR spectra were recorded on a Bruker AM 300 NMR spectrometer operating at 300.133 MHz for proton and 75.469 MHz for carbon 13/DEPT NMR.

#### (V) Photolysis Experiments<sup>6</sup>

The simple photolysis apparatus consists of a quartz photolysis cell and an ultra-violet (UV) light source. A sample of an oligosilane solution is placed in a photolysis cell and degassed on a vacuum line. The degassed solution is then placed a known distance from a light source (typically 0.5 cm) and irradiated for a timed period. Product identification of irradiated samples is by GC/MS (HP5995C); the sample being injected directly onto a 50 or 12 m capillary column (polysiloxane SCOT). Product identification is followed by progress curve construction to gain more quantitative mechanistic information.

A sample of irradiated oligosilane solution is taken at each timed period, GC/MS analysis providing reactant and product peak areas. The oligosilane solution contains a known standard (n-Decane) to normalise peak areas and a plot of normalised product peak area versus time indicates whether a product is formed via a primary or secondary photochemical pathway.

The relative photochemical yield of an exhaustive photolysis experiment is then measured by first performing a preparative photolysis and isolating the products by GC/PREP. GC calibration for each product is followed by GC analysis of a photolysed solution; product peak areas being converted into molar amounts from which relative photochemical yields can be calculated.

UV absorption spectra of all oligosilane solutions were recorded on a Cary 2300 UV/VIS/NIR absorption spectrophotometer. The photolysis cells used were of two different designs (Fig. 2.3); cell A was used for normal mechanistic studies and cell B was used for monitoring photolysis reactions by UV-Spectrophotometry.

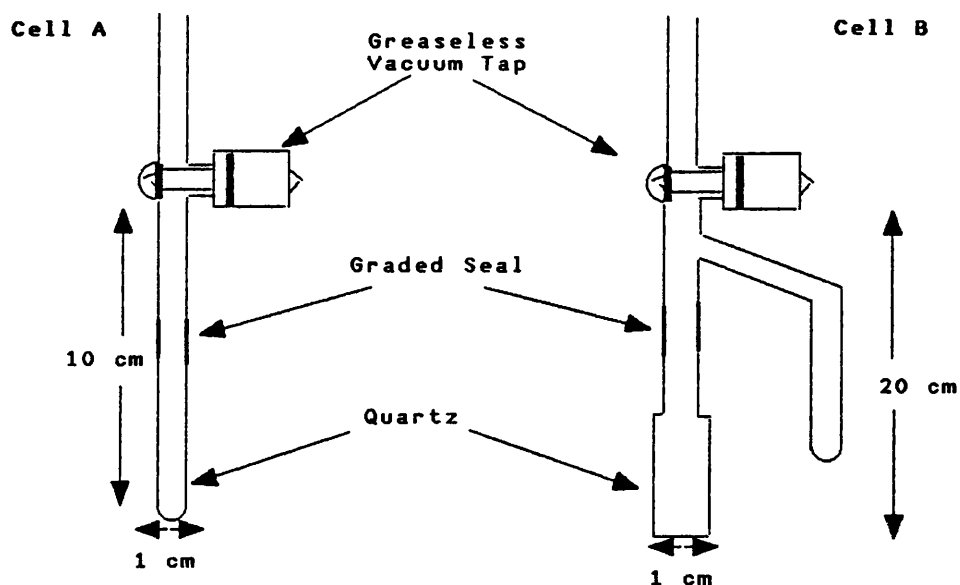


Figure 2.3: Diagram of Quartz Photolysis Cells.

The oligosilanes used were dissolved in highly purified hexane (Fluka Chemicals-52750 puriss. standard for GC >99.7%) or pentane (Fluka Chemicals-76870 puriss. standard for GC >99.8%). Trapping experiments were performed in triethylsilane (>99%). The light sources used were a 228 nm quartz cadmium lamp (Phillips Spectral Lamp-Cd Typ 93107E E27); powered by a lab discharge lamp transformer (Phillip Harris P41254/0) and a 254 nm low pressure/high intensity mercury lamp (Mineralight UVGL-58).

Products which could not be identified by GC/MS alone were isolated by GC/Prep and NMR spectra were taken. All NMR spectra were run on a Bruker AM300 spectrometer; proton run at 300.133 HZ and carbon 13/DEPT run at 75.469Hz.

GC analyses were performed on a Pye Unicam G.C.D. Gas Chromatograph; the data was recorded and displayed on a dedicated OPUS V microcomputer. GC/Prep experiments were performed on a Pye-Unicam 105 Mark 2 Preparative Gas Chromatograph.

## (VI) References

- (1) W.C. Herndon, *J. Chem. Educ.*, 1964, 41, 425.
- (2) M.F.R. Mulcahy, D.J. Williams, *Austral. J. Chem.*, 1961, 14, 535.
- (3) A.C. Baldwin, I.M.T. Davidson, A.V. Howard, *J. Chem. Soc., Faraday Trans. I*, 1975, 71, 972.

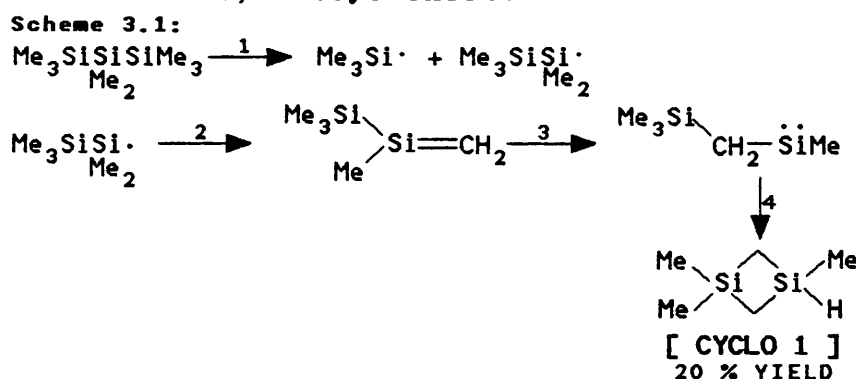
- (4) I.M.T. Davidson, G. Eaton, K.J. Hughes, *J. Organomet. Chem.*, 1988, 347, 17.
- (5) M.P. Clarke, PhD. Thesis, Leicester, 1989. .
- (6) M. Ishikawa, T. Takaoka, M. Kumada, *J. Organomet. Chem.*, 1972, 42, 333.

## Chapter 3

### The Pyrolysis of Octamethyltrisilane

#### (I) Introduction

The first study on the gas phase pyrolysis of octamethyltrisilane (OMTS) was by Barton and co-workers<sup>1</sup>. Their flash vacuum experiment (860°C/10<sup>-3</sup> Torr) gave 1-methyl-3,3-dimethyl-1,3-disilacyclobutane (CYCLO 1) as the major product. Scheme 3.1 shows the mechanism Barton proposed to explain the formation of CYCLO 1. Reactions (1) (bond homolysis), (2) (disproportionation) and (4) (cyclisation by C-H bond insertion) all had precedents in organosilicon chemistry, but reaction 3 was a novel silene-to-silylene rearrangement via a 1,2-silyl shift.



It is well known that the pyrolysis mechanism of HMDS shows an intriguing pressure dependence, rationalised by the relative importance of unimolecular and bimolecular reactions<sup>2</sup>. This pressure dependence would be expected to be mirrored in pyrolysis of OMTS<sup>3</sup>. Thus the pyrolysis mechanism of OMTS using the SFR apparatus would be expected to give different results from those in Barton's low pressure experiments, the mechanism probably involving silyl radicals, silylenes, silenes and disilenes simultaneously.

The mechanism of the pyrolysis of OMTS was therefore investigated using the GC/MS-SFR apparatus<sup>4</sup>. To test for the intermediacy of silylenes, silenes, disilenes and silyl radicals, trapping experiments were performed. Preparative experiments were carried out using the GC-PREP/SFR followed by <sup>1</sup>H, <sup>13</sup>C and DEPT NMR for complete product identification.

Using the kinetic-SFR apparatus, experiments were performed

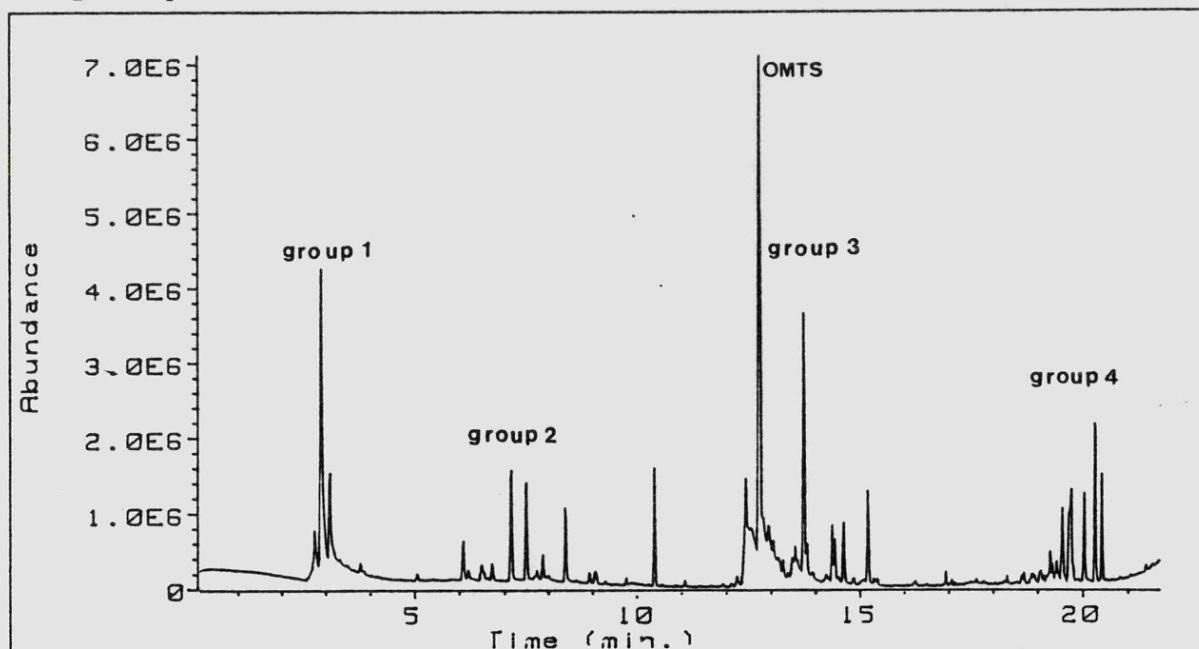


to measure first order rate constants for the formation of the major products and trapped species. The pyrolysis experiments were performed over a temperature range to enable the calculation of Arrhenius parameters.

## (II) GC/MS-SFR Results

### (i) OMTS pyrolysis experiments

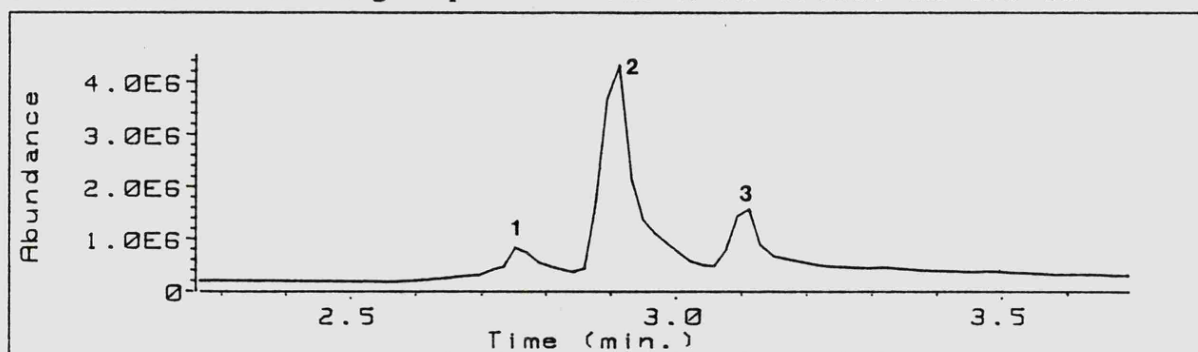
OMTS was pyrolysed between 570-650°C at sample pressures ranging between 0.2-1.5 Torr. TIC 1 shows the groups of products formed in a typical mid temperature/sample pressure range experiment.



TIC 1: Group 1- monosilanes; Group 2- disilicon compounds; Group3- trisilicon compounds; Group4- tetrasilicon compounds.

Temperature= 631°C; Sample Pressure= 1.0 Torr

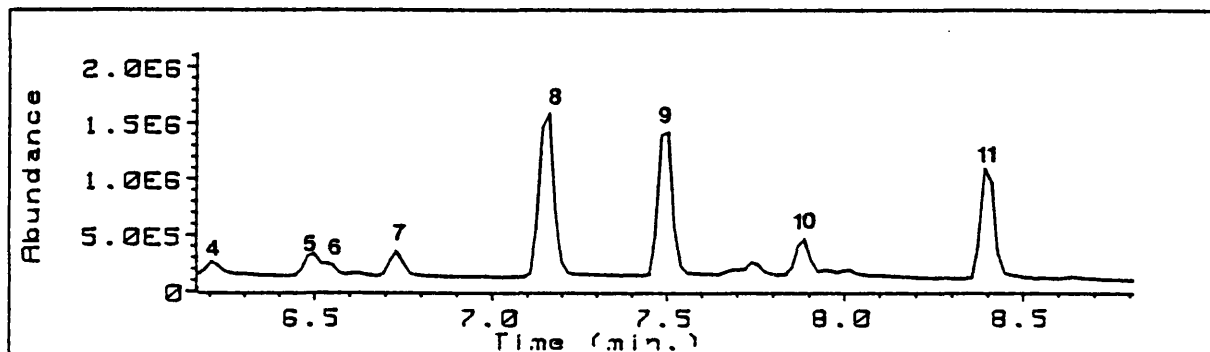
The monosilanes in group 1 are shown in detail in TIC 1a.



TIC 1a: Group 1:- [1]  $\text{Me}_2\text{SiH}_2$ , [2]  $\text{Me}_3\text{SiH}$ , [3]  $\text{Me}_4\text{Si}$

Group 1 contains the major product of the pyrolysis, trimethylsilane [2] (3MS). Smaller amounts of dimethylsilane [1] (2MS) and tetramethylsilane [3] (4MS) are also produced.

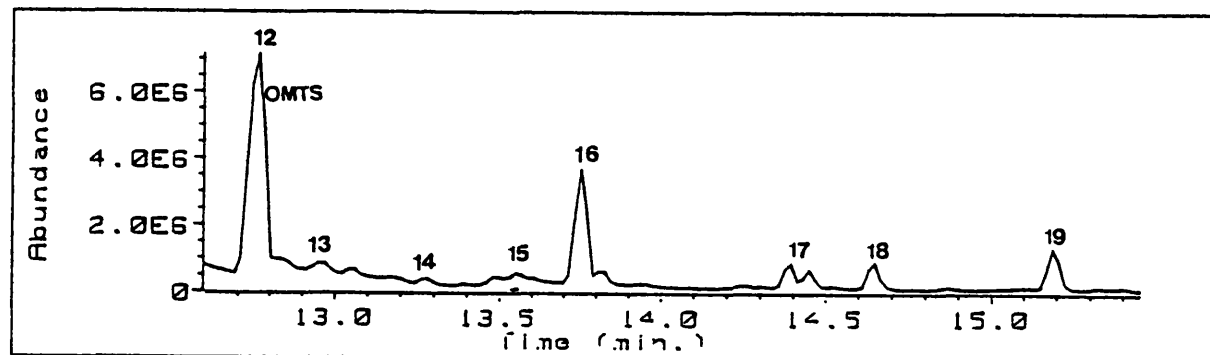
TIC 1b shows group 2, the products corresponding to di-silicon compounds.



TIC 1b: Group 2:- [4]  $\text{Me}_2\text{Si}-\text{SiH}_2$ , [5]  $\text{MeHSi}-\text{SiMeH}$ , [6]  $\text{Me}_2\text{Si}-\text{SiMe}_2$ , [7]  $\text{Me}_3\text{SiSiMe}_2\text{H}$ , [8]  $\text{Me}_3\text{SiSiMe}_3$ , [9]  $\text{Me}_2\text{Si}-\text{SiMeH}$ , [10]  $\text{Me}_3\text{Si}-\text{SiMe}_2$ , [11]  $\text{Me}_2\text{Si}-\text{SiMe}_2$ .

A number of prominent products are contained in group 2; including HMDS [8], CYCLO 1 [9], and 1,1,3,3-tetramethyl-1,3-disilacyclobutane [11] (CYCLO 2).

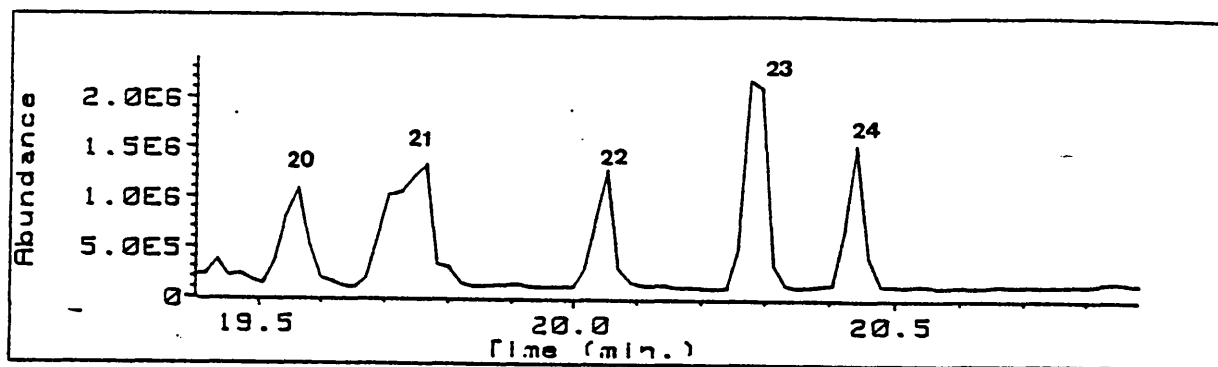
TIC 1c shows the products in group 3 plus the reactant OMTS.



TIC 1c: Group 3:- [12]  $\text{Me}_8\text{Si}_3$ , [13]  $\text{Me}_3\text{SiSi}-\text{SiMe}_2$ , [14]  $\text{Me}_2\text{Si}-\text{SiMe}_2$ , [15]  $\text{Me}_2\text{Si}-\text{SiMe}_3$ , [16]  $\text{Me}_2\text{Si}-\text{SiMe}_2$ , [17]  $\text{Me}_2\text{Si}-\text{SiMe}_2$ , [18]  $\text{MeHSi}-\text{Si}-\text{SiMe}_2$ , [19]  $\text{Me}_2\text{Si}-\text{Si}-\text{SiMe}_2$ .

The major product in group 3 is 1,1,3,3,4,4-hexamethyl-1,3,4-trisilacyclopentane [16] (CYCLO 3). Other products in the group are minor by comparison, including [13], pentamethyldisilyl(dimethylsilyl)methane.

Mass spectral data was insufficient to fully characterise the products in group 4 (TIC 1d).



Figures 3.1 and 3.2 show the mass spectra of compounds [23] (containing Si-H bond) and [24] (no Si-H bonds):

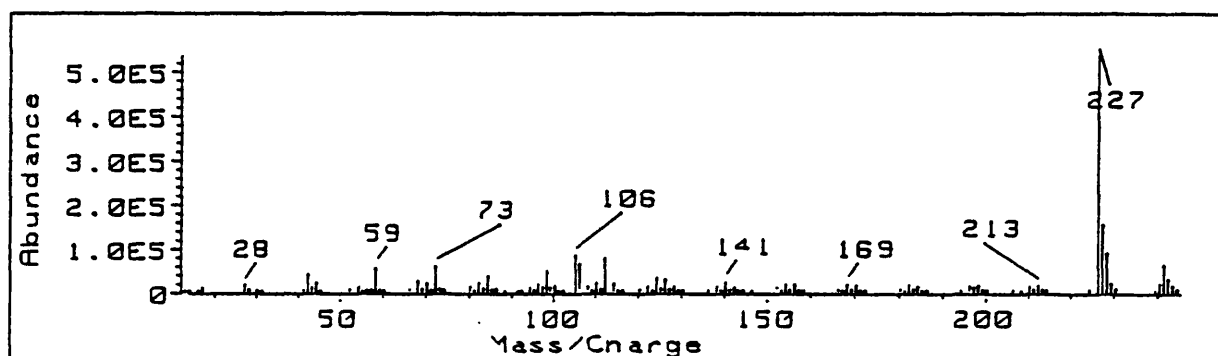


Figure 3.1: mass spectrum of [23] (contains Si-H bonds).

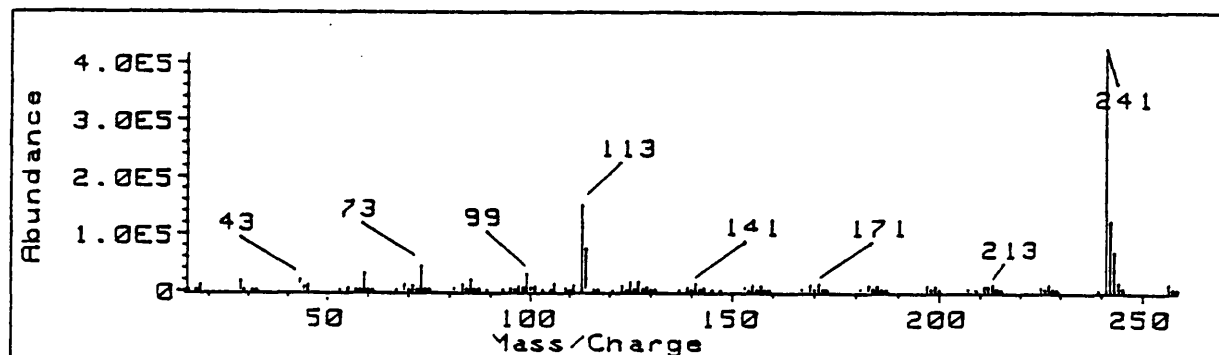
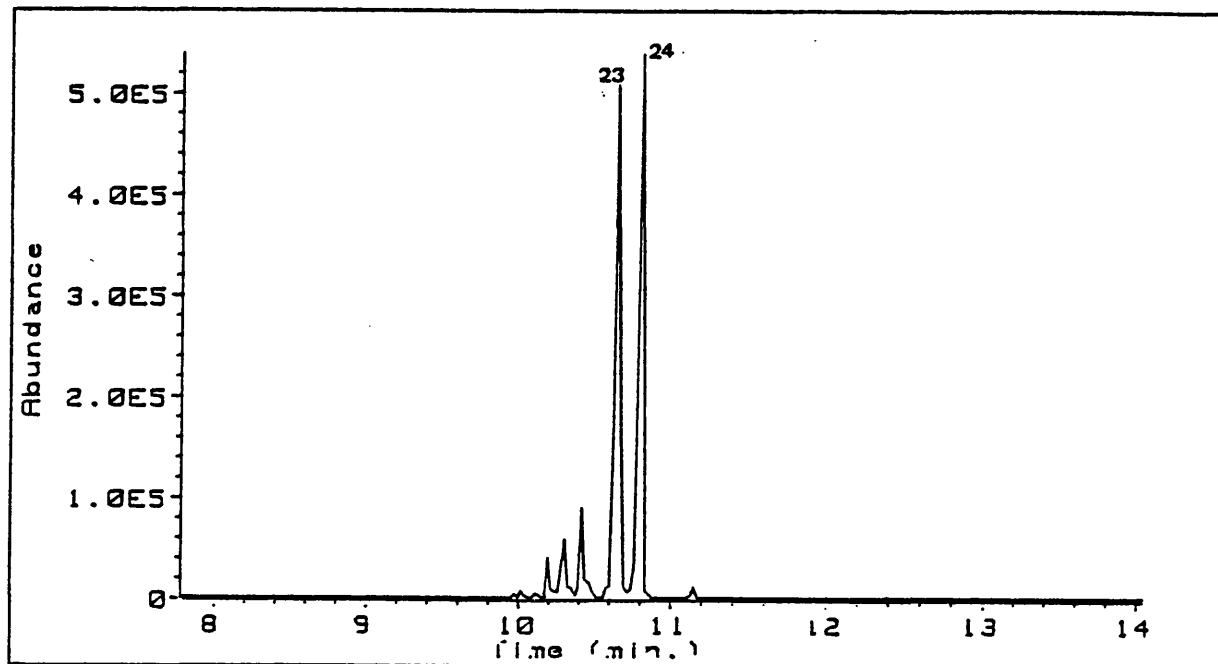


Figure 3.2: mass spectrum of [24] (NO Si-H bonds)

From the mass spectra of these compounds it was deduced that they are all 4 silicon containing cyclic carbosilanes and it was possible to assign two types of structure to each peak; (i) carbosilanes containing Si-C=C-Si linkages or (ii) cyclic carbosilanes containing Si-C-Si and/or Si-C-C-Si linkages.

A series of preparative experiments were carried out using the GC/PREP-SFR apparatus (650°C). After a GC/MS purity test,  $^1\text{H}$ ,  $^{13}\text{C}$  and DEPT NMR spectra were run on each sample. Simple analysis of NMR spectra can readily distinguish signals arising from HC=CH bonds from those of  $\text{CH}_2$  and  $\text{CH}_3$  groups. Isolation of single products proved difficult using a preparative column but through comparison of GC peak areas

with NMR peak intensities, some assignments may be made. TIC 2 shows a purity test carried out on the sample containing products [23] & [24]:



TIC 2: sample from preparative experiments containing products [23] and [24].

Table 3.1 shows the chemical shifts in the  $^1\text{H}$ ,  $^{13}\text{C}$  and DEPT NMR spectra for products [23] and [24]. The chemical shifts for OMTS and CYCLO 3 are also given to help characterisation. The absence of any CH groups in the DEPT NMR spectra plus the lack of low field signals in the  $^1\text{H}$  and  $^{13}\text{C}$  spectra proved that [23] and [24] do not contain Si-C=C-Si linkages. The absence of characteristic hyperfine coupling of the A'A-B'B type suggests -Si-CH<sub>2</sub>-CH<sub>2</sub>-Si linkages are not present. The NMR spectra show only CH<sub>3</sub>-Si and Si-CH<sub>2</sub>-Si to be present.

The other high molecular weight products ([20]-[22]) were in poorly isolated samples but NMR spectra again revealed that there were no C=C bonds in any of the molecules, only Si-CH<sub>2</sub>-Si and CH<sub>3</sub>-Si groups. Therefore from the mass spectral and NMR information products [20]-[24] could only be of the type:

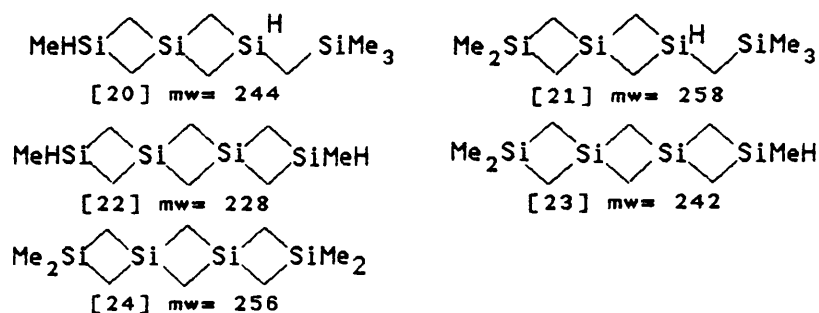


Table 3.1: Chemical shifts for OMTS , [18], [23] and [24].

Product	<sup>1</sup> H NMR	<sup>13</sup> C NMR	DEPT NMR	
OMTS	-0.068	-1.4	CH <sub>3</sub>	SiMe <sub>3</sub> × 2
	-0.078	-7.2	CH <sub>3</sub>	SiMe <sub>2</sub>
No. 18	-0.018	2.965	CH <sub>3</sub>	SiMe <sub>2</sub> × 2
	-0.087	1.9	CH <sub>3</sub>	SiMe <sub>2</sub>
	-0.415	-1.2	CH <sub>2</sub>	CH <sub>2</sub> × 2
No. 23 & 24	0.142	6.1	CH <sub>3</sub>	
	0.1180	5.4	CH <sub>3</sub>	
	0.1680	5.1	CH <sub>2</sub>	
	0.1904	5.0	CH <sub>2</sub>	
	-0.1166	4.8	CH <sub>3</sub>	
	-0.2380	3.5	CH <sub>3</sub>	
		2.3	CH <sub>3</sub>	
		2.1	CH <sub>3</sub>	
		1.8	CH <sub>3</sub>	
		-1.5	CH <sub>2</sub>	

When low sample pressures of OMTS are pyrolysed it is noticed that the higher molecular weight products (groups 3 & 4) are reduced in yield.

To summarise, a substantial amount of the products from the pyrolysis of OMTS are cyclic carbosilanes; table 3.2 shows the products identified from the straight pyrolysis of OMTS:

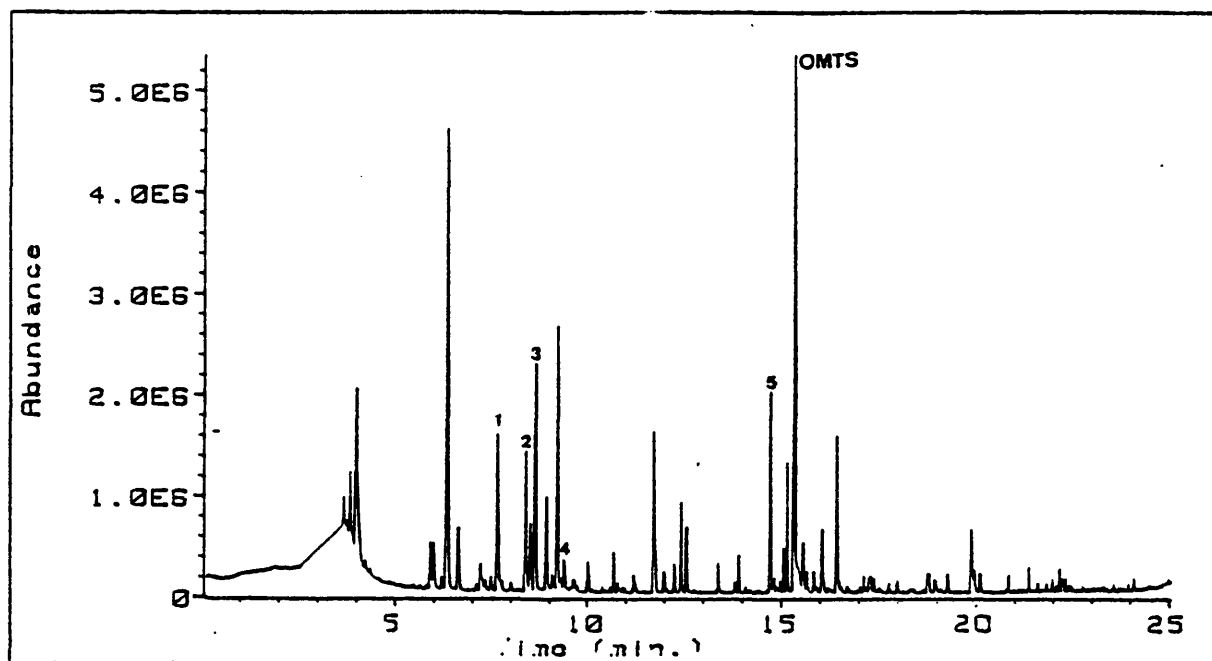
Table 3.2:

Major Products	
$\text{Me}_3\text{SiH}$ [2]	$\text{Me}_3\text{SiSiMe}_3$ [8]
$\text{Me}_2\text{Si} \begin{array}{c} \diagup \text{H} \\ \diagdown \text{Me} \end{array}$ [9]	$\text{Me}_2\text{Si} \begin{array}{c} \diagup \\ \diagdown \end{array} \text{SiMe}_2$ [11]
$\text{Me}_2\text{Si} \begin{array}{c} \diagup \\ \diagdown \end{array} \text{SiMe}_2$ [16]	
Minor products	
$\text{H}_2^* \text{CH}_4^*$ [1]	$\text{Me}_2\text{SiH}_2$ [3]
$\text{MeHSi} \begin{array}{c} \diagup \\ \diagdown \end{array} \text{SiMeH}$ [5]	$\text{Me}_2\text{Si} \begin{array}{c} \diagup \text{H} \\ \diagdown \text{SiMe}_2 \end{array}$ [6]
$\text{Me}_3\text{SiSi} \begin{array}{c} \diagup \text{Me} \\ \diagdown \text{SiMe}_2\text{H} \end{array}$ [13]	$\text{Me}_2\text{Si} \begin{array}{c} \diagup \text{Me} \\ \diagdown \text{SiMe}_2 \end{array}$ [14]
$\text{Me}_2\text{Si} \begin{array}{c} \diagup \\ \diagdown \end{array} \text{SiMeH}$ [17]	$\text{Me}_2\text{Si} \begin{array}{c} \diagup \text{H} \\ \diagdown \text{SiMe}_3 \end{array}$ [15]
$\text{MeHSi} \begin{array}{c} \diagup \\ \diagdown \end{array} \text{Si} \begin{array}{c} \diagup \text{H} \\ \diagdown \text{SiMe}_3 \end{array}$ [20]	$\text{Me}_2\text{Si} \begin{array}{c} \diagup \\ \diagdown \end{array} \text{Si} \begin{array}{c} \diagup \text{H} \\ \diagdown \text{SiMe}_3 \end{array}$ [21]
$\text{MeHSi} \begin{array}{c} \diagup \\ \diagdown \end{array} \text{Si} \begin{array}{c} \diagup \\ \diagdown \end{array} \text{Si} \begin{array}{c} \diagup \\ \diagdown \end{array} \text{SiMeH}$ [22]	$\text{Me}_2\text{Si} \begin{array}{c} \diagup \\ \diagdown \end{array} \text{Si} \begin{array}{c} \diagup \\ \diagdown \end{array} \text{Si} \begin{array}{c} \diagup \\ \diagdown \end{array} \text{SiMeH}$ [23]
$\text{Me}_2\text{Si} \begin{array}{c} \diagup \\ \diagdown \end{array} \text{Si} \begin{array}{c} \diagup \\ \diagdown \end{array} \text{Si} \begin{array}{c} \diagup \\ \diagdown \end{array} \text{SiMe}_2$ [24]	

\*see section (IV); Q8/MS-Sealed tube results

(ii) Butadiene/OMTS pyrolysis experiments

OMTS was pyrolysed in a 10 fold excess of butadiene (570–640°C). End product analysis showed major product formation was reduced but not suppressed. However, the formation of the tetra-silicon compounds was completely suppressed. The major trapping products are identified in TIC 3.

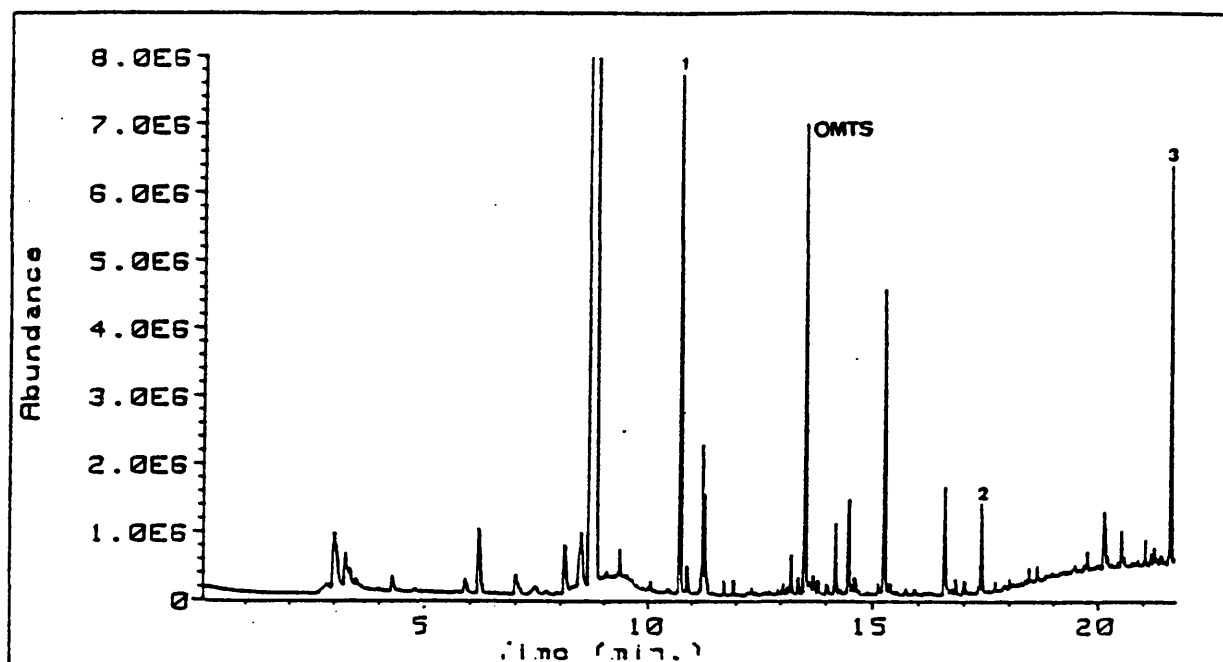


TIC 3: [1] Me2Si-C6H5, [2] Me2Si-C6H10, [3] Me2Si-C6H7,  
 [4] Me2Si-CH2-C6H5, [5] Me2Si-SiMe2-C6H5 Temperature = 637°C.

Therefore the major intermediates trapped in the butadiene pyrolysis experiments were Me2Si: and Me2Si=SiMe2. A small amount of Me2Si=CH2 was also trapped. Other peaks present in TIC 4, along with the products the straight pyrolysis, were non-silicon containing compounds such as benzene, resulting from the radical induced reactions of butadiene.

### (iii) Toluene/OMTS pyrolysis experiments.

OMTS was pyrolysed in a ten fold excess of toluene between 570-650°C. Major product formation was reduced, the formation of tetra-silicon compounds being completely suppressed. Products unique to this experiment were ethylbenzene, benzyltrimethylsilane and 1,2-dibenzylethane (shown in TIC 4):

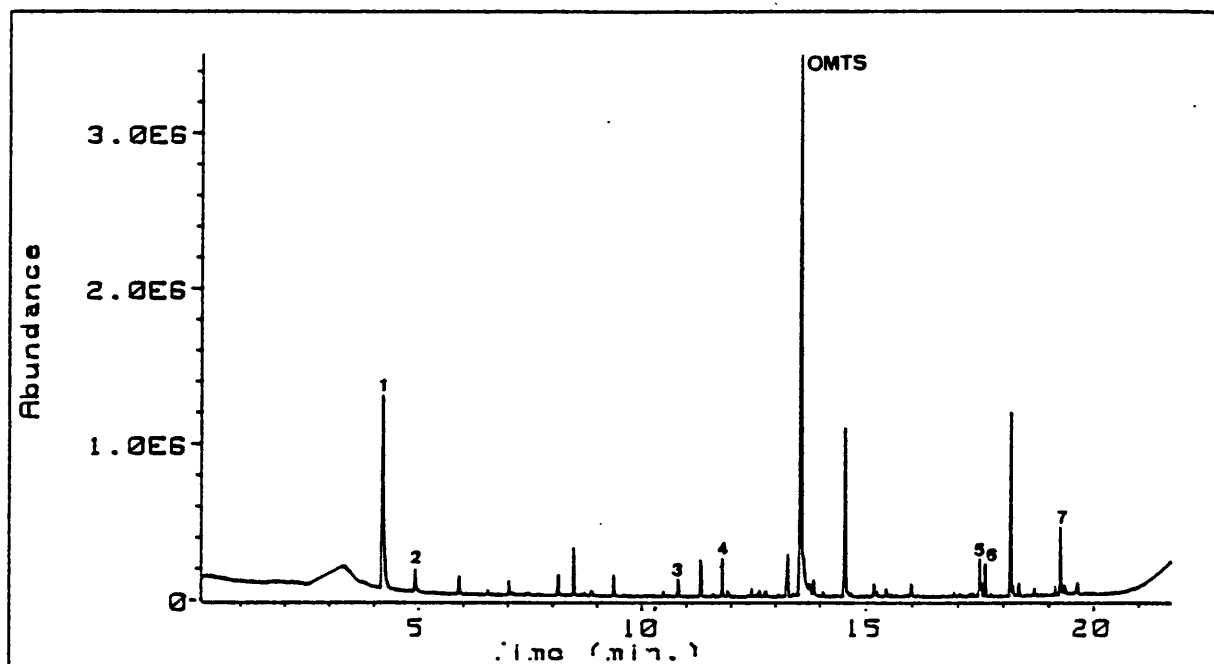


TIC 4: Where 1 is ethylbenzene and 2 is benzyltrimethylsilane, 3 is 1,2-dibenzylethane. Temperature= 637°C

#### (iv) Methylchloride/OMTS pyrolysis experiments

OMTS was pyrolysed in a five fold excess of methylchloride between 570-650°C. End product analysis showed there to be a reduction in all product yields, the formation of tetra-silicon compounds being completely suppressed. Methylchloride acts as a radical transfer agent and isolates as chlorosilanes the main silicon containing radicals involved in the pyrolysis. The products unique to this pyrolysis are shown in TIC 5.





TIC 5: Where 1 is  $\text{Me}_3\text{SiCl}$ , 2 is  $\text{Me}_2\text{SiCl}_2$ , 3 is  $\text{Me}_2\text{Si}(\text{H})(\text{Cl})\text{SiMe}_2$ ,  
 4 is  $\text{Me}_2\text{Si}(\text{Cl})(\text{H})\text{SiMe}_3$ , 5 is  $\text{Me}_2\text{Si}(\text{H})(\text{Cl})\text{Si}(\text{Me})(\text{Cl})\text{SiMe}_3$ , 6 is  
 $\text{Me}_2\text{Si}(\text{H})(\text{H})\text{Si}(\text{Me})(\text{H})\text{SiMe}_2\text{Cl}$ , 7 is  $\text{Me}_2\text{Si}(\text{H})(\text{H})\text{Si}(\text{H})(\text{H})\text{SiMeCl}_2$ . Temp = 624°C.



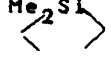
The major product was trimethylchlorosilane with smaller amounts of products [2] to [7] also formed.

### (III) Kinetic-SFR Results

#### (i) Straight pyrolysis kinetic results

OMTS was pyrolysed between 570-650°C with sample pressures ranging between 0.2-1.0 Torr. Figure 3.3 shows a typical gas chromatogram for a mid-temperature range pyrolysis experiment. First order rate constants were measured for the peaks shown in figure 3.3. The Arrhenius parameters for the formation of these products are shown in table 3.3.

Table 3.3: Kinetic results for major products of the straight pyrolysis of OMTS.

Product	$\log(A/s^{-1})$	$E_a$ (kJmol <sup>-1</sup> )	$k(620^\circ C)$
Me <sub>3</sub> SiH	14.6 ± 0.6	268.5 ± 11.8	0.0783
Me <sub>3</sub> SiSiMe <sub>3</sub>	8.9 ± 0.2	186.4 ± 4.2	9.9 × 10 <sup>-3</sup>
	10.0 ± 0.6	198.4 ± 10.1	0.0248
	13.6 ± 0.3	269.1 ± 5.4	7.2 × 10 <sup>-3</sup>
	5.2 ± 0.4	123.2 ± 6.1	9.8 × 10 <sup>-3</sup>

A typical Arrhenius plot is shown in figure 3.4, in this case for the formation of cyclo 2. The products measured had various orders of formation between 1 and 1.5, varying with temperature, for simplicity, first order rate constants were calculated. Figure 3.5 shows a typical order plot for the formation of CYCLO 2 at high and low temperatures.

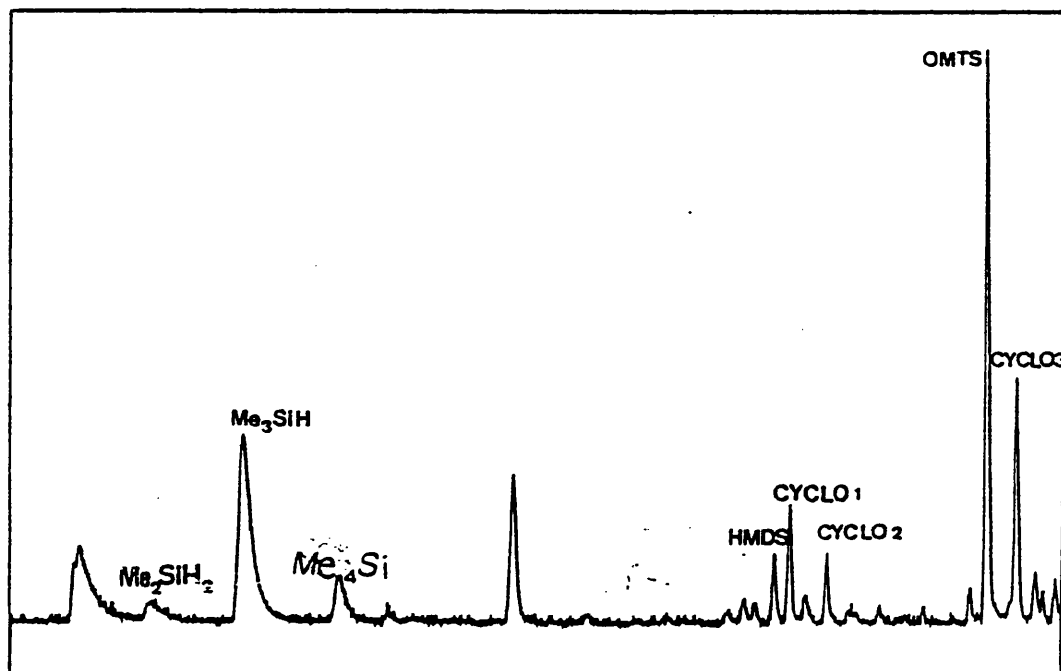


Figure 3.3: Gas Chromatogram for the pyrolysis of OMTS at 648°C.

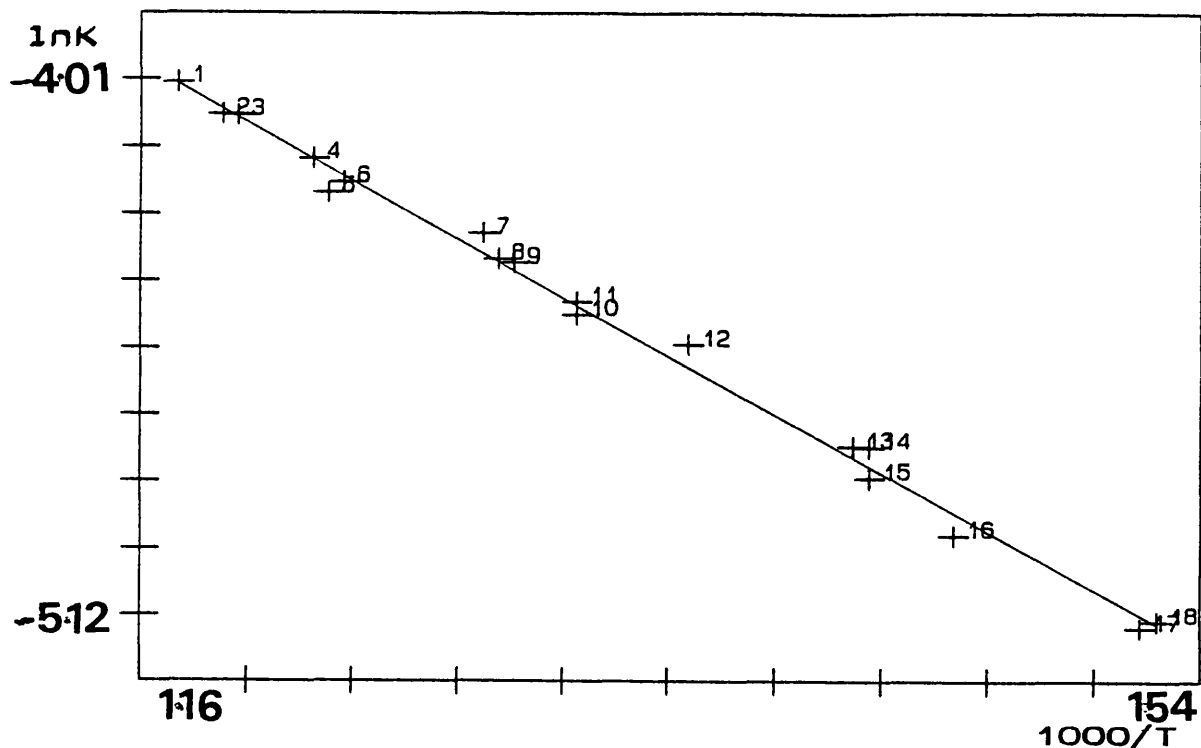
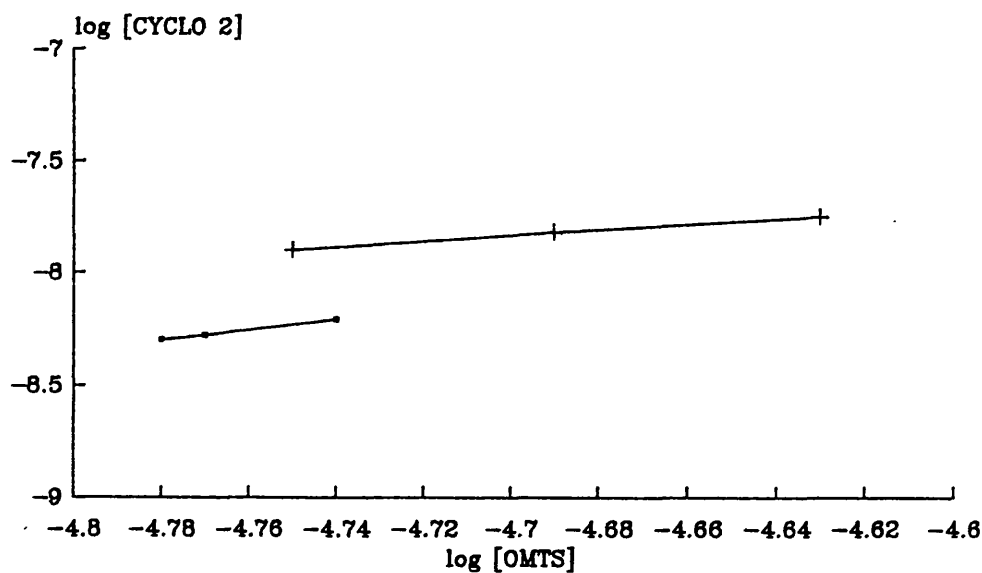


Figure 3.4: Arrhenius plot for the formation of cyclo 2 from OMTS between 586-654°C.



—•— ORDER = 1.3 (883 K)    —+— ORDER = 1.0 (924 K)

Figure 3.5: Order Plot for the formation of CYCLO 2 at 883 K (= 1.3 ± 0.1) and 924 K (= 1.0 ± 0.2).

### (ii) Butadiene/OMTS kinetic results

OMTS was pyrolysed in a ten fold excess of butadiene between 570-650°C. Figure 3.6 shows a typical gas chromatogram for a mid-temperature range pyrolysis. First order rate constants were measured for the peaks shown in figure 3.6. The Arrhenius parameters for the formation of

Table 3.4: Kinetic results for butadiene/OMTS  
pyrolysis experiments

Product	$\log(A/s^{-1})$	$E_a$ (kJmol <sup>-1</sup> )	$k(620^\circ\text{C})$
<chem>Me3SiSiMe3</chem>	$14.7 \pm 2.3$	$282.0 \pm 39.3$	0.016
<chem>Me2Si-CH2-CH2-SiMe2</chem>	$9.3 \pm 0.9$	$192.8 \pm 6.6$	0.105
<chem>Me2Si-CH=CH-SiMe2</chem>	$15.8 \pm 2.0$	$300.3 \pm 34.0$	0.017
<chem>Me2Si-CH2-CH=CH-SiMe2</chem>	$13.9 \pm 2.8$	$277.3 \pm 46.9$	$4.8 \times 10^{-3}$

Figure 3.7 shows a typical Arrhenius plot for the formation of cyclo 3. Kinetic measurements were difficult to make because the number of products in the pyrolysed mixture from the secondary reactions of butadiene.

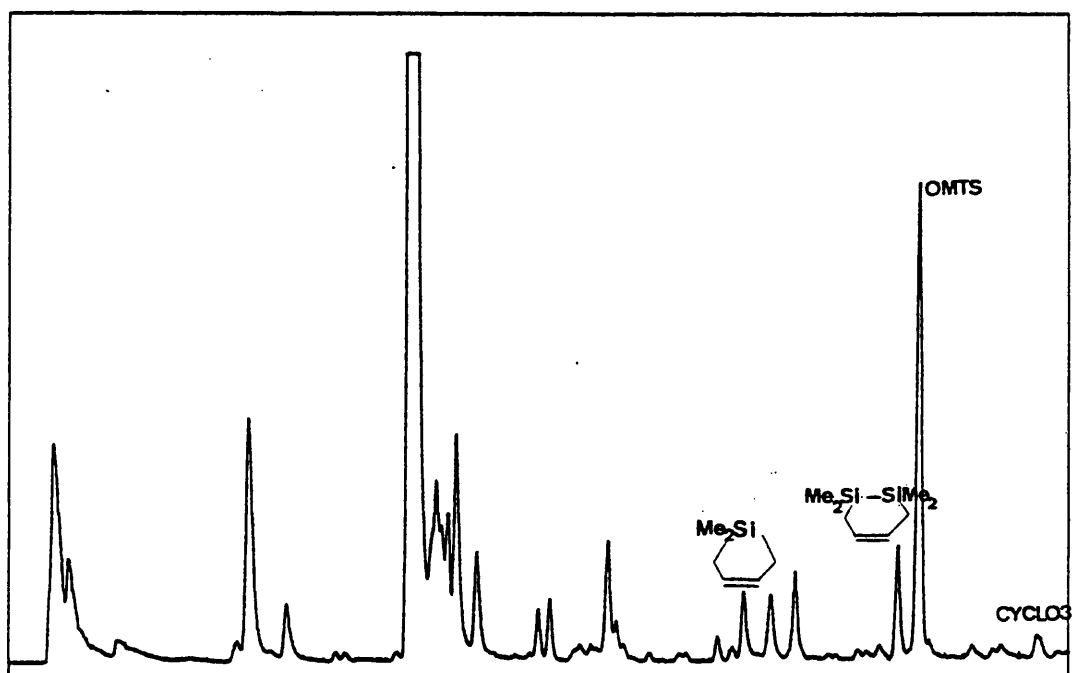


Figure 3.6: Gas Chromatogram for the pyrolysis of OMTS/butadiene at 612°C.

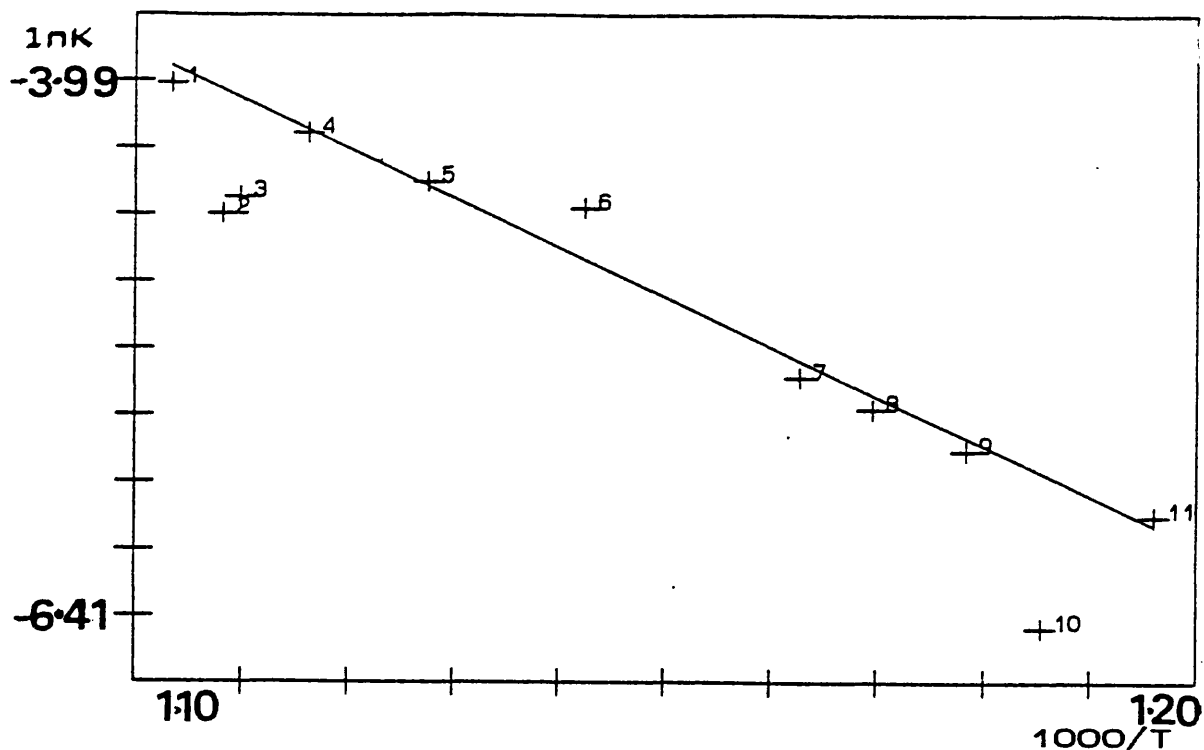


Figure 3.7: Arrhenius plot for the formation of cyclo 3 from OMTS (in the presence of butadiene) between 564-636°C.

### (iii) Toluene/OMTS kinetic results

OMTS was pyrolysed in a 10 fold excess of toluene between 570-650°C. Figure 3.8 shows a gas chromatogram for a mid-temperature range experiment. First order rate constants were measured for the products shown in figure 3.8. The Arrhenius parameters for the formation of these products are given in table 3.5.

Table 3.5: Kinetic results for toluene/OMTS experiments.

Product	$\log(A/s^{-1})$	$E_a$ (kJmol $^{-1}$ )	$k(620^\circ C)$
Me <sub>3</sub> SiH	$14.5 \pm 0.5$	$271.8 \pm 9.4$	0.0400
Me <sub>3</sub> SiSiMe <sub>3</sub>	$9.8 \pm 0.4$	$195.4 \pm 11.8$	0.0234
$  \begin{array}{c}  \text{Me}_2\text{Si} \\  \diagup \quad \diagdown \\  \text{---} \quad \text{---} \\  \diagdown \quad \diagup \\  \text{Me}_2\text{Si} \text{---} \text{SiMe}_2  \end{array}  $	$9.6 \pm 0.2$	$203.2 \pm 3.3$	$5.2 \times 10^{-3}$
$  \text{CH}_3 \text{---} \text{C}_6\text{H}_5  $	$17.9 \pm 0.4$	$347.8 \pm 6.7$	$3.6 \times 10^{-3}$

The Arrhenius plot for the formation of cyclo 3 is shown in figure 3.9.

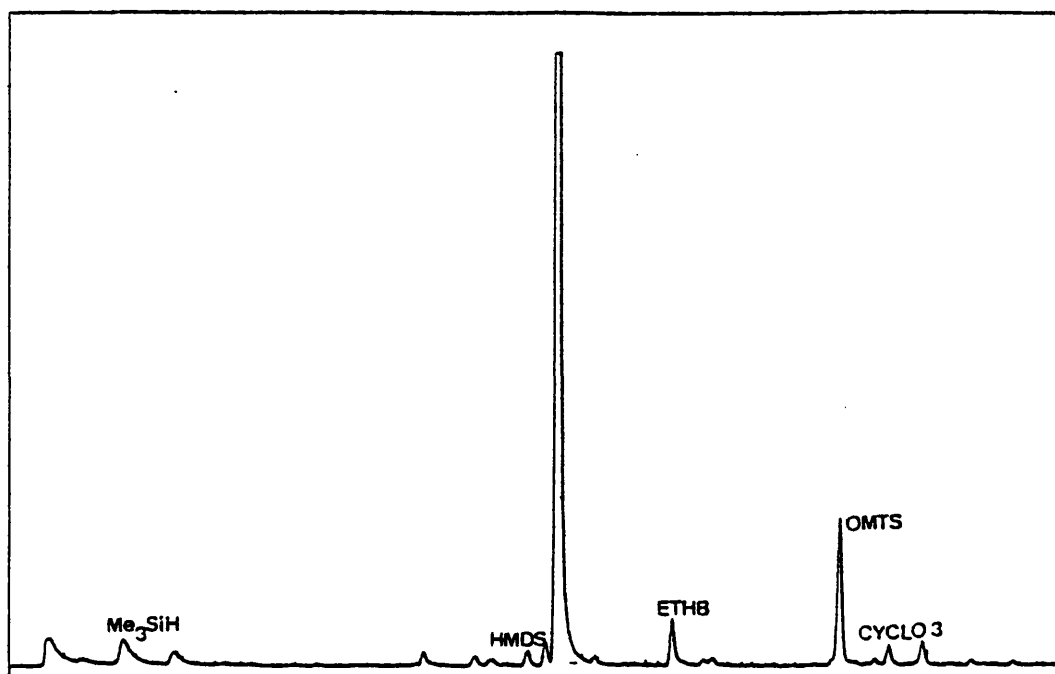


Figure 3.8: Gas Chromatogram for the pyrolysis of OMTS/toluene at 645°C.

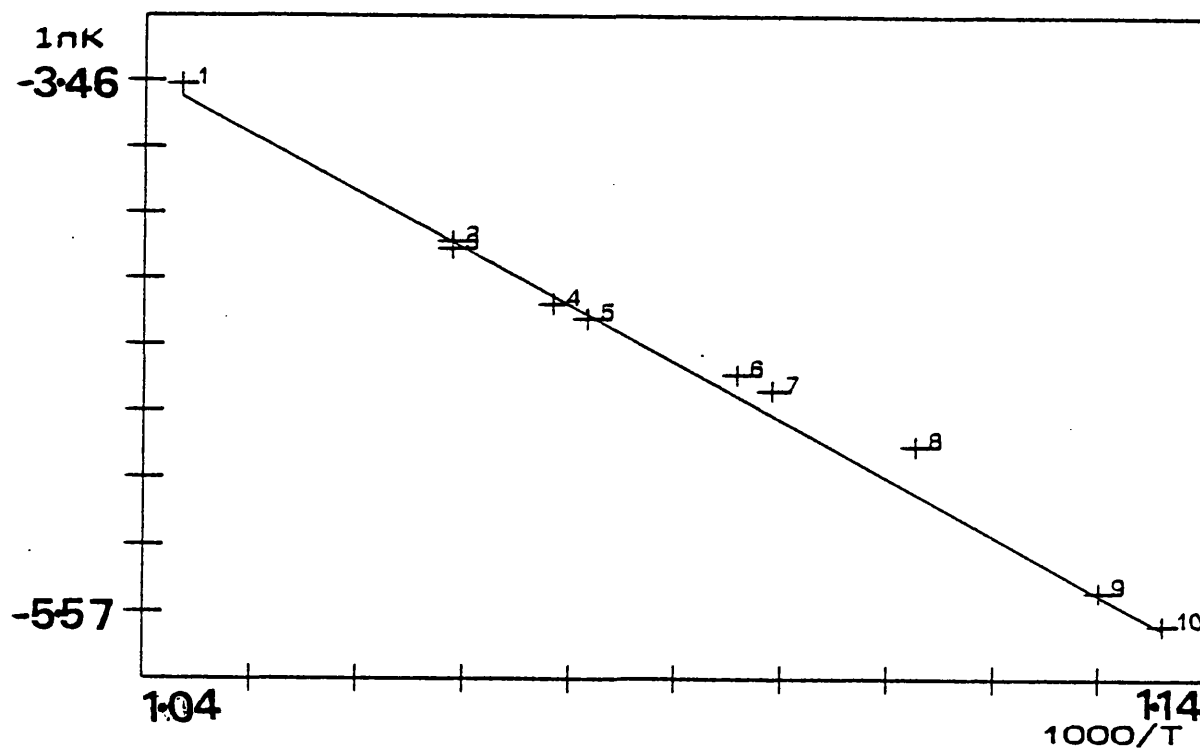


Figure 3.9: Arrhenius plot for the formation of cyclo 3 from OMTS (in the presence of toluene) between 608-683°C.

#### (VI) Q8/MS-Sealed Tube Pyrolysis Results

OMTS was pyrolysed in a sealed sample vessel at 550°C. The time scale for the pyrolysis was calculated from the Arrhenius parameters for 3MS formation given by the kinetic-SFR experiments:

At 620°C  $k = 0.0783 \text{ (s}^{-1}\text{)}$ ,  $t_{1/2} = 8.85 \text{ s}$ .

At 550°C  $k = 3.61 \times 10^{-3} \text{ (s}^{-1}\text{)}$ ,  $t_{1/2} = 3.2 \text{ mins}$ .

The Q8/MS revealed that large quantities of hydrogen were produced in the pyrolysis of OMTS (Fig 3.10). A small amount of methane was also detected.

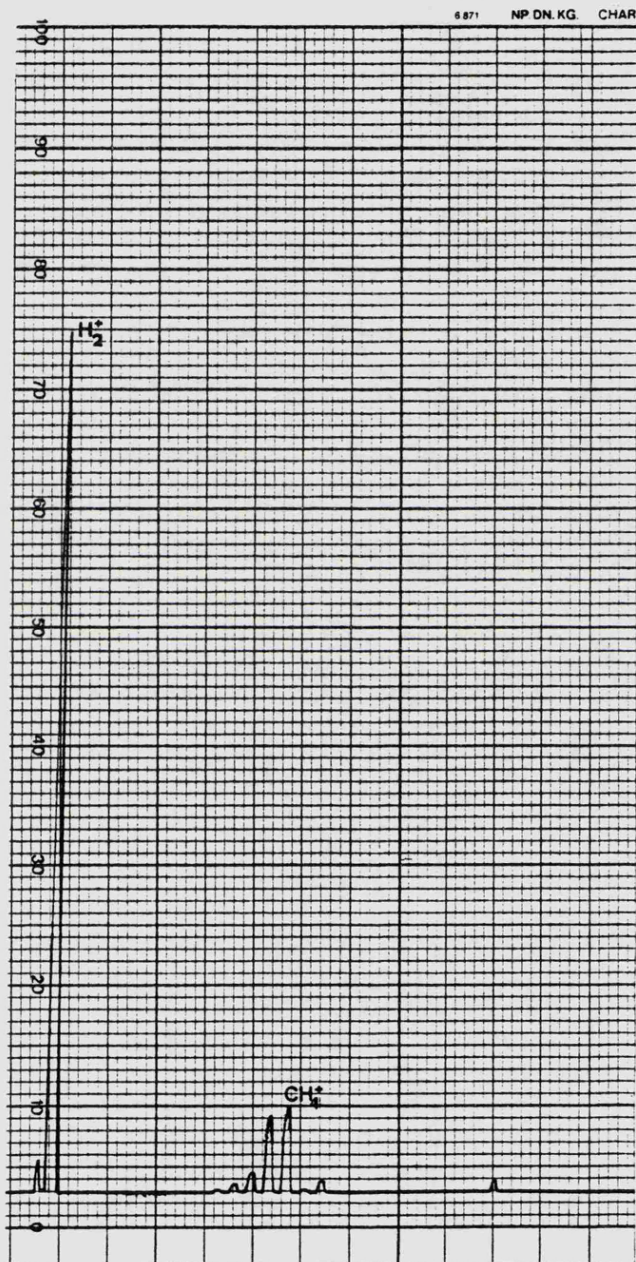
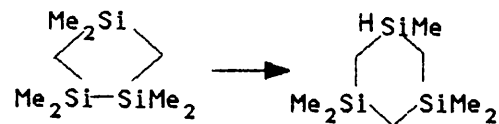



Figure 3.10: Mass Spectrum of  $\text{H}_2$  and  $\text{CH}_4$  from the sealed tube pyrolysis of OMTS at 550°C.

## (V) Discussion



The relative yields of the major products, trimethylsilane (3MS), 1,1,3-trimethyl-1,3-disilacyclobutane (CYCLO1), 1,1,3,3,4,4-hexamethyl-1,3,4-trisilacyclopentane (CYCLO 3), hexamethyldisilane (HMDS) and 1,1,3,3-tetramethyl-1,3-disilacyclobutane (CYCLO 2) were 10:3.3:2:2:1 respectively over the pyrolysis temperature range. Kinetic measurements revealed that it is unlikely that any of the major products arose from first order unimolecular reactions or from a sequence of reactions with a rate limiting step that is first order. It is concluded, therefore, that radical chain mechanisms lead to major product formation. There is also a possibility that there may be more than one route to the formation of each major product. The accuracy of the kinetic measurements may be affected by the secondary decompositions of some the di-silicon compounds and it is known that at these elevated temperatures HMDS, CYCLO 2 and CYCLO 3 have appreciable decomposition rate constants<sup>2,5,6</sup>:

	<u>Log (A/s<sup>-1</sup>)</u>	<u>E<sub>a</sub> (kJmol<sup>-1</sup>)</u>	<u>K<sub>(620 °C)</sub>(s<sup>-1</sup>)</u>
	16.1 ± 0.6	316 ± 11	4.12 × 10 <sup>-3</sup>
	14.4 ± 0.2	296 ± 3	1.21 × 10 <sup>-3</sup>

Co-pyrolysis in the presence of butadiene revealed that dimethylsilylene (Me<sub>2</sub>Si:), tetramethyldisilene (Me<sub>2</sub>Si=SiMe<sub>2</sub>) and dimethylsilene (Me<sub>2</sub>Si=CH<sub>2</sub>) were formed during the pyrolysis. Pyrolysis in the presence of methylchloride or toluene showed that trimethylsilyl radicals (Me<sub>3</sub>Si·) were the most abundant intermediates. Co-pyrolysis in toluene also revealed that there was also a substantial concentration of methyl radicals (CH<sub>3</sub>·). Pyrolysis in the presence of butadiene or toluene did not suppress the Arrhenius parameters for major product formation (although these Arrhenius parameters are subject to large error limits). Kinetic measurements on trapping product formation showed that most of the intermediates are not formed via first order reactions. Therefore, it seems reasonable to assume that they are formed by radical chain mechanisms and may arise from more than one



source. The trapping products will again have appreciable decomposition rate constants at these high temperatures e.g.<sup>7</sup>

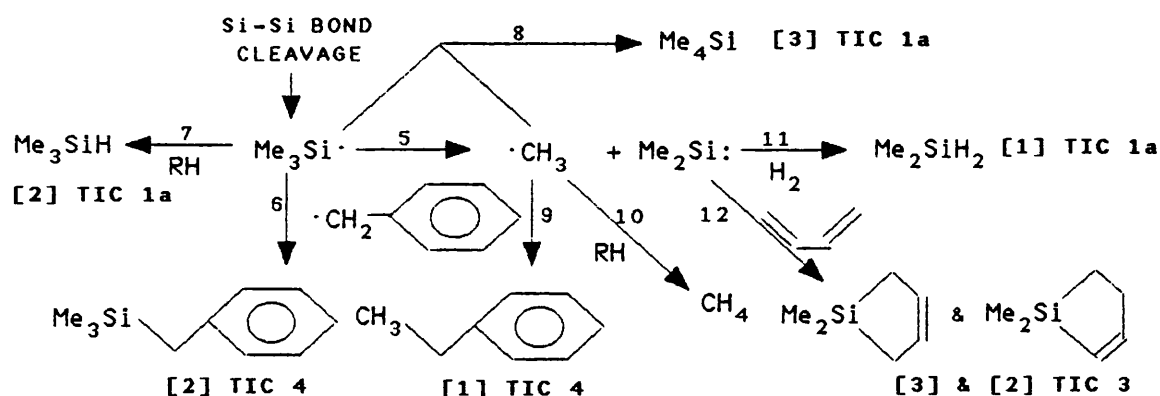
	$\log(A/s^{-1})$	$E_a(kJmol^{-1})$	$k(620^\circ C)(s^{-1})$
	$12.3 \pm 0.2$	$251 \pm 9$	$4.15 \times 10^{-3}$
	$11.9 \pm 0.2$	$230 \pm 4$	0.0279

Ethylbenzene is formed by a first order process with Arrhenius parameters in the order of Si-Si bond dissociation energy. Benzyltrimethylsilane gave a curved Arrhenius plot.

The complexity of the kinetic results can be related to:-  
(i) the difficulty in accurate product area measurement because of the number of products formed, (ii) product decomposition, (iii) there being more than one mechanism to form some of the major products and intermediates. However, the measurements do give some insight into the mechanism of major product and intermediate formation.

The formation of the products in group 1 can be explained by the reactions in scheme 3.2:

Scheme 3.2:



Following Si-Si bond cleavage trimethylsilyl radicals ( $Me_3Si\cdot$ ) can either abstract hydrogen to give 3MS (7) or they can dissociate to form methyl radicals ( $\cdot CH_3$ ) and dimethylsilylene ( $Me_2Si:$ ) (5). The combination of  $\cdot CH_3$  and  $Me_3Si\cdot$  radicals leads to the formation of 4MS [4] (8).

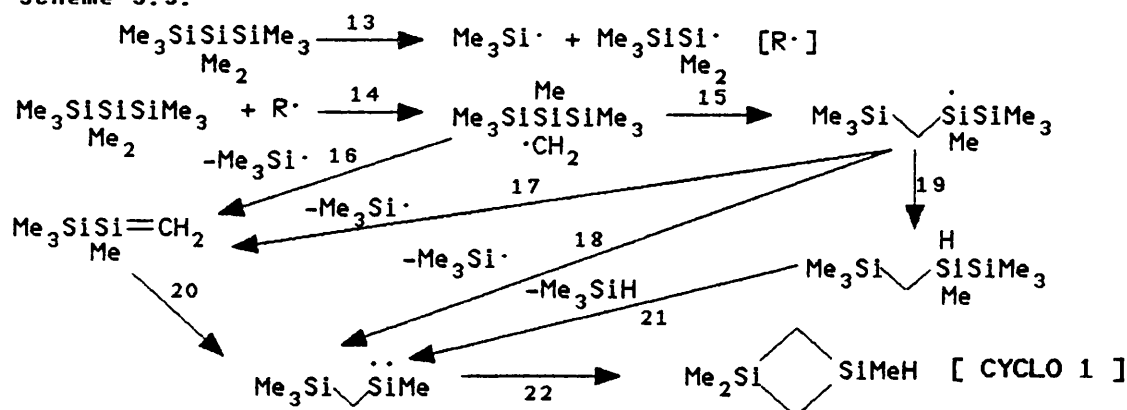
The Q8/MS-Sealed tube experiments revealed that hydrogen and methane were produced in the pyrolysis of OMTS. Hydrogen could arise from two sources; (i) hydrogen radical H-abstraction reactions or (ii) cyclisation with elimination of hydrogen (*vide infra*). Methane will have two possible sources; (i) methyl radical H-abstraction reactions (10) or (ii) methyl and hydrogen radical combination.  $Me_2Si:$  produced via the dissociation of  $Me_3Si\cdot$  radicals can insert into the  $H_2$

$\sigma$ -bond to yield 2MS [1] (11).

Evidence for scheme 3.2 comes from kinetic measurements on the formation of 1,1-dimethyl-1-silacyclo-3,4-pentene in the 1,3-butadiene/OMTS experiments ([2] & [3] TIC 3) and the formation of ethylbenzene in the toluene/OMTS experiments ([1] TIC 4). Both these trapped species give Arrhenius parameters in the order of the Si-Si bond dissociation energy. The rate of  $\cdot\text{CH}_3$  and  $\text{Me}_2\text{Si}:$  production depends on the formation of  $\text{Me}_3\text{Si}\cdot$  radicals whose rate limiting step is Si-Si bond cleavage, explaining the values for the Arrhenius parameters<sup>2</sup>. The toluene/OMTS experiments also produce TMSB ([2] TIC 4) by the combination of benzyl and  $\text{Me}_3\text{Si}\cdot$  radicals (6).

The formation of CYCLO 1 can be rationalised by using the mechanistic ideas first introduced by Barton (scheme 3.3)<sup>1</sup>:

Scheme 3.3:



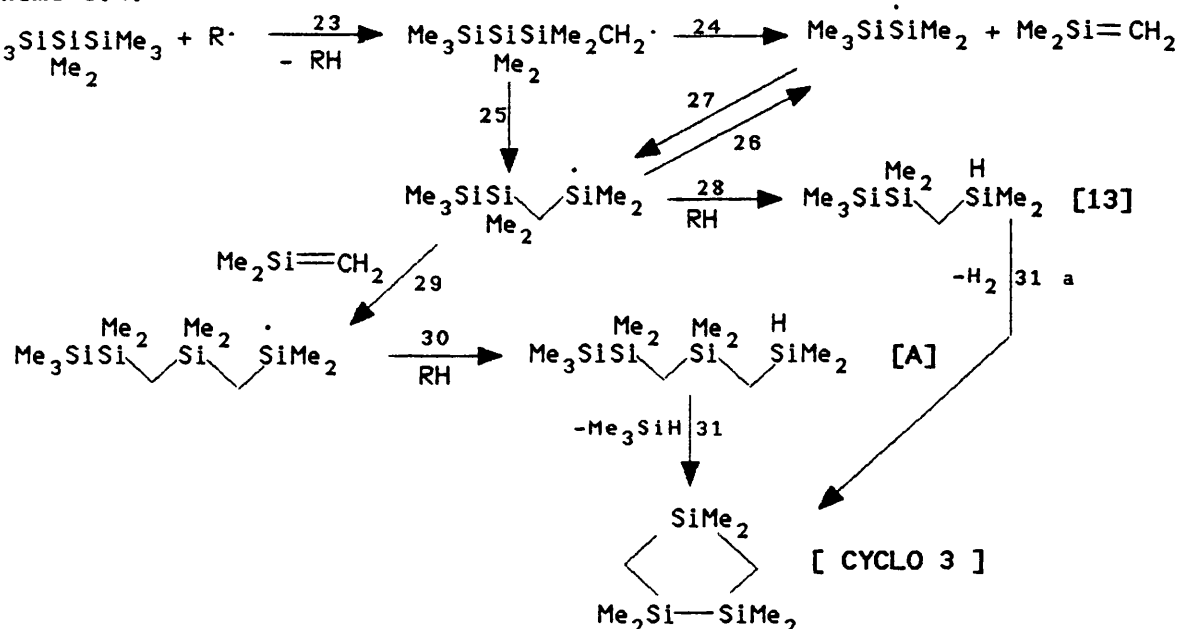
In scheme 3.3 initial Si-Si bond cleavage (13) is followed by hydrogen abstraction from a central methyl group on OMTS (14). The carbon centred radical formed will either undergo isomerisation to form a new silicon centred radical (15)<sup>2,8</sup> or dissociate to form  $\text{Me}_3\text{Si}\cdot$  and trimethylsilyl(methyl)silene (silene 1)(16). The silicon centred radical formed via reaction (15) can then undergo three reactions:- (i) dissociation into a  $\text{Me}_3\text{Si}\cdot$  radical and silene 1 (17), (ii) dissociation into a  $\text{Me}_3\text{Si}\cdot$  radical and  $\alpha$ -trimethylsilyl-(methyl)silylene (silylene 1)(18), (iii) hydrogen abstraction to form an isomer of OMTS (19). At the high temperatures of reaction, the isomer of OMTS would rapidly eliminate 3MS to form silylene 1 (21)<sup>9</sup>. Silylene 1 may also be formed by the rearrangement of silene 1 via a trimethylsilyl shift (20)<sup>1</sup>. Once formed silylene 1 will rapidly cyclise by C-H bond insertion to form CYCLO 1 (22)<sup>10</sup>.

The kinetics of formation of CYCLO 1 appear to support a complex mechanism of formation and all the reactions given in

scheme 3.3 have strong precedents in organosilicon chemistry.

The formation of CYCLO 3 is thought to be by a quite different route. As there are no Si-H bonds in the molecule, conventional cyclisation reactions are ruled out. Scheme 3.4 shows the series of reactions believed to lead to CYCLO 3.

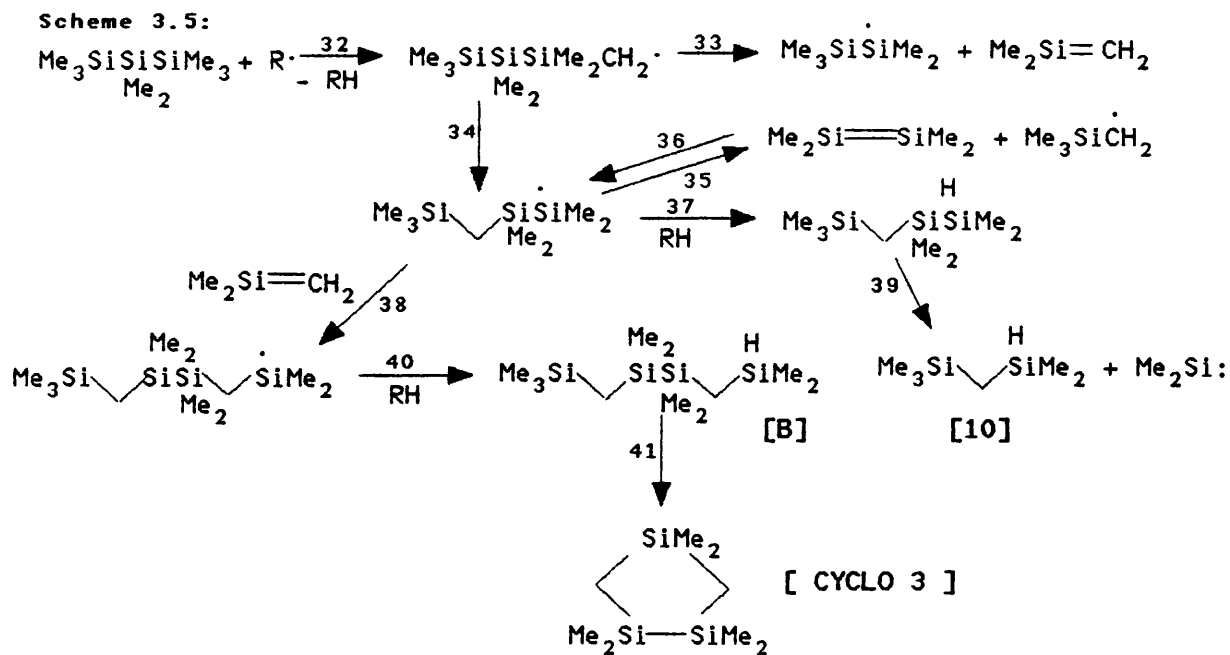
Scheme 3.4:



Hydrogen abstraction from a terminal methyl group will yield a carbon centred radical (23). This radical will either dissociate to form a pentamethyldisilyl radical and dimethylsilene (24) or isomerise to form a new silicon centred radical (25)<sup>2,8</sup>. The new silicon centred radical can undergo three reactions:- (i) dissociation to form a pentamethyldisilyl radical and dimethylsilene (26) (recombination gives the reverse reaction (27)), (ii) abstract hydrogen to yield product [13] (28), (iii) undergo dimethylsilene addition to yield a new silicon centred radical (29). Reaction (29) is feasible as the addition of silenes to radicals is known to be fast<sup>11</sup>. The silicon centred radical produced via reaction (29) can abstract hydrogen to yield compound [A]. [A] is thought to undergo a novel cyclisation reaction with elimination of 3MS to form CYCLO 3. This novel elimination reaction may be thought to be akin to the elimination of trimethylsilane from pentamethyldisilane, a well characterised reaction in organosilicon chemistry. Another possible cyclisation reaction is (31 a) where [13] eliminates hydrogen to yield CYCLO 3 (see Appendix 1).

The isomerisation reaction (25) is a 1,2-shift but a 1,3-shift can also take place generating an isomeric silicon

centred radical (Scheme 3.5):



The radical formed via reaction (34) may undergo three reactions:- (i) dissociation to form tetramethyldisilene and trimethylsilylmethyl radical (35) (recombination leads to the reverse reaction (36)), (ii) hydrogen abstraction to yield a hydridosilane (37) which at these temperatures will dissociate to form dimethylsilylene and product [10] (39), (iii) addition of dimethylsilene to yield a new silicon centred radical (38). This radical can then abstract hydrogen to form compound [B] (40). [B] is also thought to cyclise, eliminating 3MS to yield CYCLO 3 (41).

To test this novel elimination reaction, compounds [A] and [B] were synthesised (see Appendix 1). [A] was pyrolysed at low sample pressures and same temperatures as OMTS and CYCLO 3 was indeed found to be the major product. Arrhenius parameters measured for the production of 3MS were  $\log A = 11.7 \pm 1.3 \text{ s}^{-1}$ ,  $E_a = 220 \pm 23 \text{ kJmol}^{-1}$  and for the production of CYCLO 3 were  $\log A = 11.5 \pm 0.8 \text{ s}^{-1}$ ,  $E_a = 215 \pm 13.6 \text{ kJmol}^{-1}$ . These parameters are consistent with a ring closure reaction with a similar mechanism to the formation of 3MS from pentamethyldisilane.

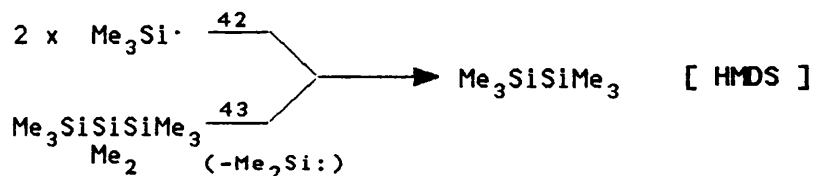
The major products of the pyrolysis of [B] were CYCLO 1, CYCLO 2 and CYCLO 3. Characteristic products of both [A] and [B] were cyclic carbosilanes formed by the cyclisation with the elimination of hydrogen, giving support to reaction (31 a).

The reactions in scheme 3.5 may indeed take place but with the balance tilted towards dissociation and hydrogen abstraction<sup>2</sup> instead of silene addition to the silicon centred radical. The formation of product [10] and the trapping of tetramethyldisilene support this argument ([5] TIC 3). The explanation for this may lie in the fact that this silicon centred radical is attached to an adjacent silicon atom, which opens pathways of dissociation not available for the radical formed by reaction (25) (c.f. scheme 3.3 where dissociation and hydrogen abstraction are also favoured by a silicon centred radical with an adjacent silicon atom). The radical formed by reaction (25) does not have an adjacent silicon atom which explains why product [13] is the only isomer of OMTS detected and why this radical may be more susceptible to silene addition or H-abstraction followed by cyclisation with elimination of hydrogen rather than dissociation.

This argument may be extended to the elimination reactions (31) and (41); the former takes place with the constituents of 3MS being bonded to silicon centred groups only, which is not the case for (41), therefore, CYCLO 3 is the major product of the pyrolysis of [A] but not [B]. It can be concluded that the differing local environments for radicals produced by the isomerisation reactions (15), (25) and (34) dictate whether dissociation or silene addition are favoured (H-abstraction is probably the same for all these radicals).

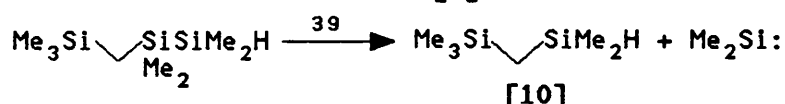
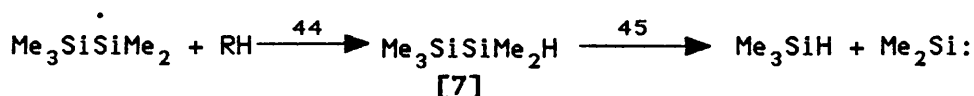
The kinetic measurements on CYCLO 3 appear to support a complicated mechanism of formation such as scheme 3.4, which would give very low Arrhenius parameters.

HMDS may be formed via two separate mechanisms,  $\text{Me}_3\text{Si}\cdot$  radical combination or the unimolecular elimination of  $\text{Me}_2\text{Si:}$  from OMTS. The unimolecular elimination reaction could be more important in the pyrolysis of OMTS than it is in HMDS<sup>2</sup> as it is known that silylene insertions into Si-Si bonds require a lower activation energy than insertions into Si-C bonds<sup>13</sup>:

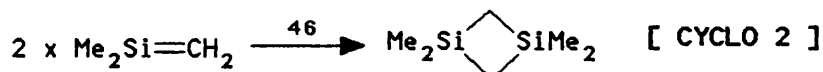


The Arrhenius parameters for the formation of HMDS favour the radical combination reaction as the major contributor. Therefore reaction (42) is favoured, as there are many sources

for  $\text{Me}_3\text{Si}\cdot$  radicals (e.g. 13, 16 & 17). The kinetics of formation of dimethylsilacyclopent-3,4-ene<sup>14</sup> also suggests that the source of dimethylsilylene is not only OMTS, in fact the indications are that OMTS is a minor source, the primary sources being the dissociation of  $\text{Me}_3\text{Si}\cdot$  (5) radicals with minor contributions from secondary decomposition reactions such as 39 and 45<sup>9</sup>:



CYCLO 2 is probably formed by the head to tail dimerisation of dimethylsilene<sup>15</sup>:



The major source of dimethylsilene is reaction (24). A minor source may be the disproportionation of  $\text{Me}_3\text{Si}\cdot$  radicals (the ratio of combination to disproportionation being 10:1)<sup>12</sup>:



Only a small quantity of dimethylsilene was trapped in the presence of butadiene but it is known that the rate of formation of the cyclic adduct is low when compared to radical addition or dimerisation<sup>16</sup>. The kinetics of formation for CYCLO 2 reflect the number of different sources for  $\text{Me}_2\text{Si}=\text{CH}_2$ , the values not being consistent with a unimolecular reaction or a sequence of reactions with a first order rate limiting step.

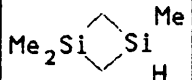
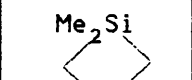

The major product, 3MS, arises from a number of different sources:- (i) the abstraction of hydrogen by  $\text{Me}_3\text{Si}\cdot$  radicals, (ii) elimination from compound [A] in the cyclisation reaction, (iii) from the dissociation of pentamethyldisilane and (iv)  $\text{Me}_3\text{Si}\cdot$  radical disproportionation.

Therefore it would be expected that 3MS would give Arrhenius parameters in accordance with a complex mechanism of formation even in the presence of toluene.

Schemes 3.2, 3.3, 3.4 and 3.5 were modelled by numerical integration using the KINAL and ACUCHEM packages (see Appendix 2)<sup>17</sup>. Arrhenius parameters were calculated over the experimental temperature range. Table 3.6 gives the

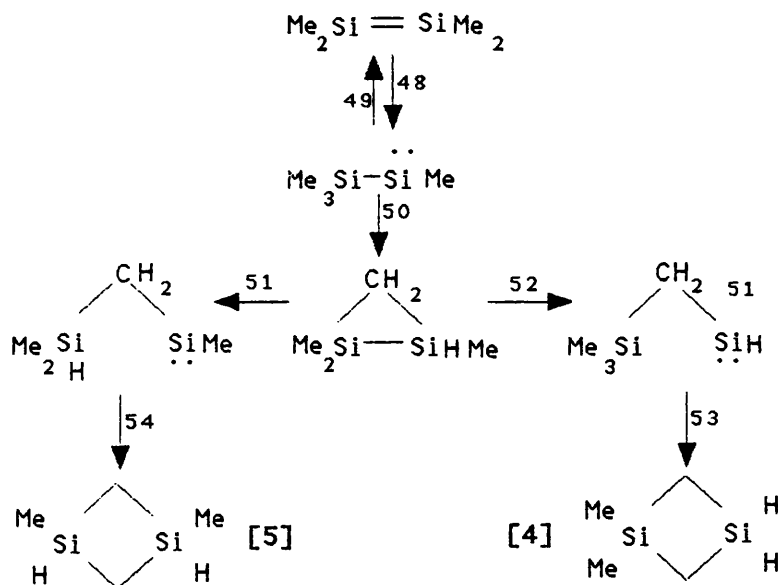
experimental and calculated Arrhenius parameters for the major products. In view of the complexity of the mechanisms for major product formation the agreement is reasonable.

Table 3.6:

Product	Experimental		Calculated	
	$\log(A/s^{-1})$	$E_a$ (kJmol $^{-1}$ )	$\log(A/s^{-1})$	$E_a$ (kJmol $^{-1}$ )
Me <sub>3</sub> SiH	14.6 ± 0.6	268 ± 11	12.1 ± 0.9	216 ± 13
	10.0 ± 0.6	198 ± 10	10.6 ± 0.9	204 ± 17
	5.2 ± 0.3	123 ± 6	7.1 ± 0.2	138 ± 4
Me <sub>3</sub> SiSiMe <sub>3</sub>	8.9 ± 0.2	186 ± 4	9.1 ± 0.9	188 ± 15
	13.6 ± 0.4	269 ± 5	13.8 ± 1.1	264 ± 18

A route to products [4] and [5] could be via the isomerisation of Me<sub>2</sub>Si=SiMe<sub>2</sub>:

Scheme 3.6:



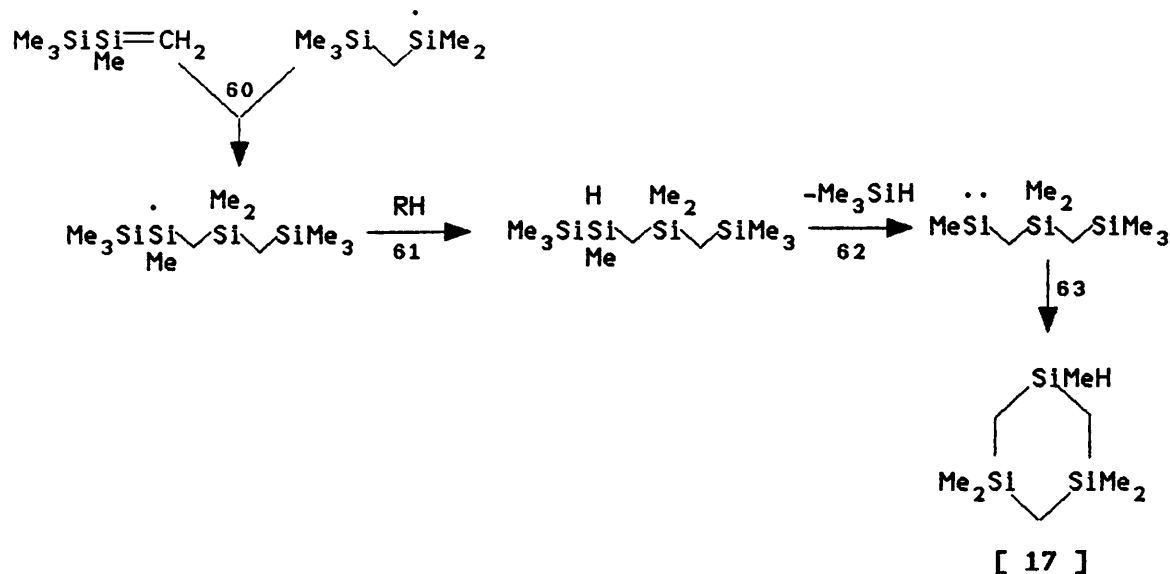
Me<sub>2</sub>Si=SiMe<sub>2</sub> is known to isomerise to trimethylsilyl(methyl)silylene. Once formed this silylene may undergo an intramolecular C-H insertion reaction to yield a disilirane, a reaction first suggested by Barton<sup>18</sup>. The disilirane will then undergo competing ring opening reactions to yield two isomeric β-silylsilylenes via 1,2 methyl or hydrogen shifts. Intramolecular C-H insertions give [4] and [5].

Product [6] is thought to be formed via a radical





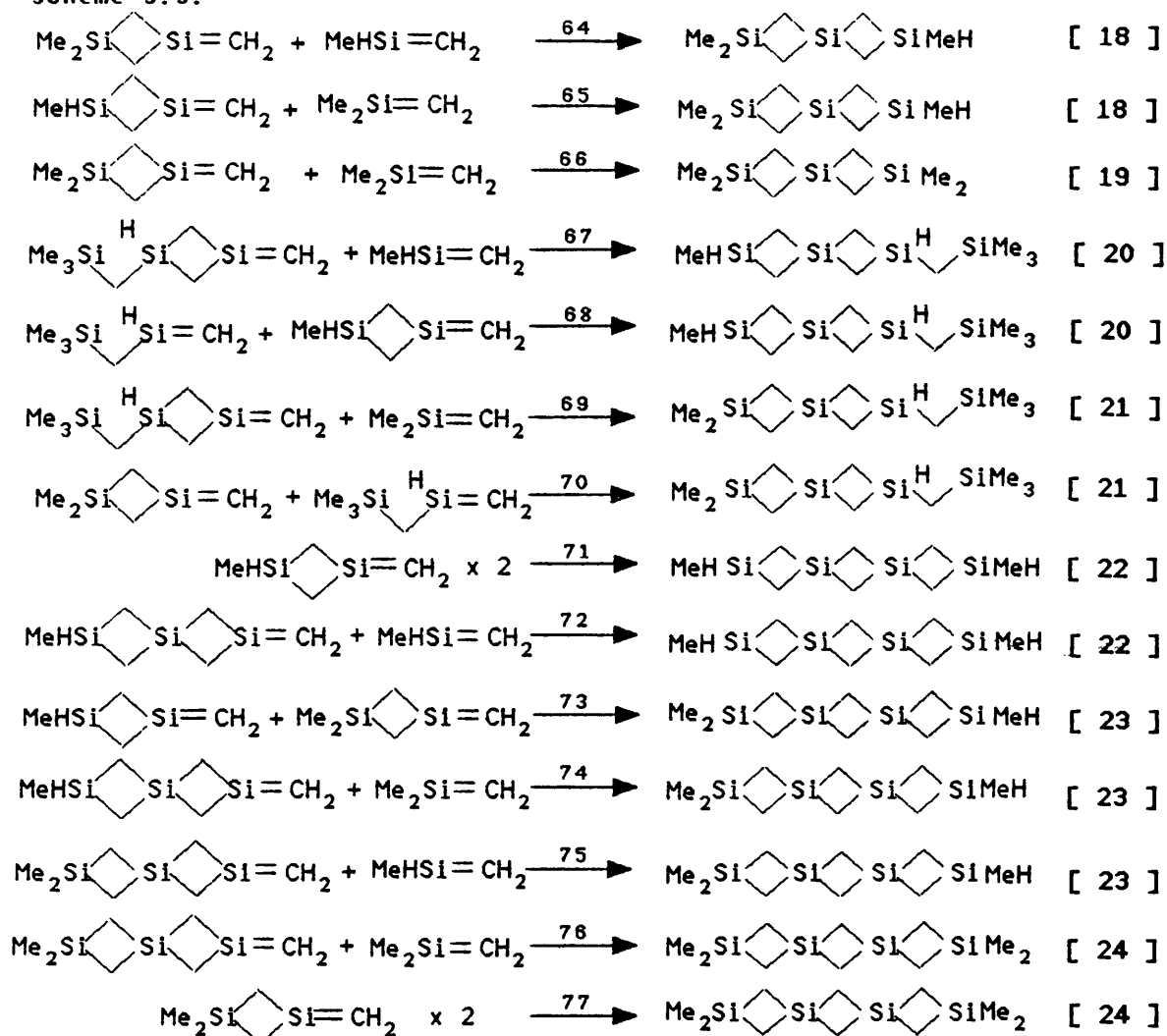
Scheme 3.8:



Reactions (16 & 17) lead to the formation of trimethylsilyl(methyl)silene whilst the secondary decomposition of HMDS<sup>2</sup> yields trimethylsilyl(dimethylsilyl)methane radical. At high sample pressures, the addition of these two species will be fast<sup>11</sup>(60). Hydrogen abstraction (61) is followed by the elimination of 3MS and the formation of a silylene (62). This silylene will then cyclise by an internal C-H insertion to yield [17].

Products [18]-[24] have a similar disilacyclobutane-multiple ring backbone. These products are greatly affected by sample pressure and trapping agents, suggesting they arise from bimolecular reactions. One simple explanation for the formation of these products could be the head to tail dimerisation of silenes bearing different substituents:

Scheme 3.9:



Small quantities of  $\text{Me}_2\text{Si}=\text{CH}_2$  and trace amounts of  $\text{MeHSi}=\text{CH}_2$  were trapped when OMTS was pyrolysed in the presence of butadiene but no trapping products corresponding to the other silenes in scheme 3.9 were detected. However the formation of these silenes from OMTS would involve a complex series of reactions, the intermediates and, therefore, products being formed a long way down the reaction pathway. Co-pyrolysis in the presence of butadiene, toluene and  $\text{MeCl}$  suppressed the formation of these products indicating that complex bimolecular reactions are involved in their formation.

## (VI) Summary

The pyrolysis mechanism of OMTS shows a marked difference from that of HMDS. However, the pressure dependent nature for the formation of the major products of OMTS bears a similar relationship to that of HMDS, the pressure dependence being

rationalised by the balance of unimolecular and bimolecular reactions. The major product in Barton's low pressure experiments was CYCLO 1 but the SFR technique at high pressure leads to the formation of CYCLO 3 as well as CYCLO 1, CYCLO 3 being formed via bimolecular reactions, CYCLO 1 being formed via a unimolecular dissociation.

The most significant difference between the two pyrolyses is the formation of CYCLO 3 by the elimination of 3MS and hydrogen, reactions not observed in the pyrolysis of HMDS. Two of the three linear isomers of OMTS were not detected due to their rapid decomposition at these temperatures (21 & 39); the other linear isomer may cyclise to CYCLO 3 with the elimination of hydrogen (31 a). Therefore the linear isomers of OMTS are not prominent products.

The unimolecular elimination of  $\text{Me}_2\text{Si:}$  from OMTS is not a major breakdown pathway, the pyrolysis mechanisms being predominantly radical in nature.

#### (VII) Acknowledgements

I would like to thank Dr. P. Lo of Dow Corning for the generous gift of octamethyltrisilane. Thanks also to Denis Lancaster, Deborah Wild and Geraint Morgan for help with the pyrolysis experiments. I am most grateful to Dr. Ross Markwell for obtaining NMR spectra on less than ideal samples.

#### (VIII) References

- (1) T.J. Barton, G.T. Burns, S.A. Burns, *Organometallics*, 1982, 1, 210.
- (2) I.M.T. Davidson, A.V. Howard, *J. Chem. Soc., Faraday Trans. I*, 1975, 71, 69.
- (3) I.M.T. Davidson, *J. Organomet. Chem.*, 1988, 341, 255.
- (4) B.N. Bortolin, I.M.T. Davidson, D. Lancaster, T. Simpson, D.A. Wild, *Organometallics*, 1990, 9, 281.
- (5) I.M.T. Davidson, G. Fritz, F.T. Lawrence, A.E. Matern, *Organometallics*, 1982, 1, 1453.
- (6) N. Auner, I.M.T. Davidson, S. Ijadi-Maghsoodi, F.T. Lawrence, *Organometallics*, 1986, 5, 431.

- (7) M.P. Clarke, I.M.T. Davidson, G. Eaton, *Organometallics*, 1988, 7, 2076.
- (8) I.M.T. Davidson, P. Potzinger, B. Reimann, *Ber. Bunsen. Phys. Chem.*, 1982, 86, 13.
- (9) I.M.T. Davidson, K.J. Hughes, S. Ijadi-Maghsoodi, *Organometallics*, 1987, 6, 639.
- (10) T.J. Barton, S.A. Jacobi, *J. Am. Chem. Soc.*, 1980, 102, 7979.
- (11) E. Bastian, P. Potzinger, A. Ritter, H.-P. Schuchmann, C. von Sonntag, G. Weddle, *Ber. Bunsen. Phys. Chem.*, 1980, 84, 56.
- (12) Th. Brix, U. Paul, P. Potzinger, B. Reimann, *J. Photochem. Photobiol., A: Chem.*, 1990, 54, 19.
- (13) H. Sakurai, T. Kobayachi, Y. Nakadaira, *J. Organomet. Chem.*, 1978, 162, C43.
- (14) M.P. Clarke, I.M.T. Davidson, M.P. Dillon, *J. Chem. Soc., Chem. Commun.*, 1988, 1251.
- (15) L.E. Gusel'nikov, M.C. Flowers, *J. Chem. Soc., Chem. Commun.*, 1967, 864.
- (16) I.M.T. Davidson, R.J. Scampton, *J. Organomet. Chem.*, 1984, 271, 249.
- (17) T. Turanyi, V.S. Berces, S. Vajada, *Int. J. Chem. Kinetics*, 1989, 21, 83; T. Turanyi, *J. Mathematical Chem.*, 1990, 5, 203; W. Braun, J.T. Herron, D.K. Kahaner, *Int. J. Chem. Kinetics*, 1988, 20, 51.
- (18) W.D. Wulff, W.F. Goure, T.J. Barton, *J. Am. Chem. Soc.*, 1978, 100, 6236.

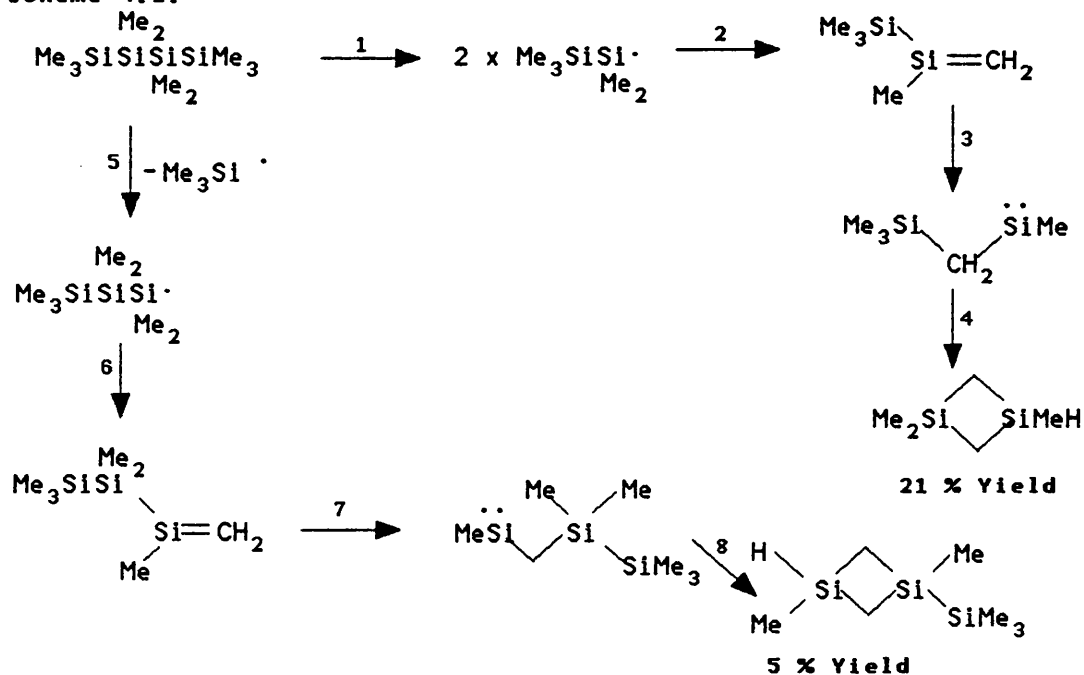
## Chapter 4

### The Pyrolysis of n-Decamethyltetrasilane

#### (I) Introduction

Barton *et. al.* first studied the pyrolysis mechanism of n-decamethyltetrasilane (n-DMTS)<sup>1</sup>. Their low pressure flash vacuum experiments gave 1,1,3-trimethyl-1,3-disilacyclobutane (CYCLO 1- 21%) and 1,3-dimethyl-1-(trimethylsilyl)-1,3-disilacyclobutane (CYCLO 2- 5%) as the major volatile products. Scheme 4.1 shows the mechanism Barton invoked to explain their formation:

Scheme 4.1:



These products were formed via either initial central (CYCLO 1) or terminal Si-Si bond cleavage (CYCLO 2).

If n-DMTS is pyrolysed using the SFR technique the results would be expected to be different from Barton's low pressure experiments. As in the pyrolysis of hexamethyldisilane (HMDS)<sup>2</sup> and octamethyltrisilane (OMTS)<sup>3</sup> product formation will be expected to depend on the balance between bimolecular and unimolecular reactions. The pyrolysis mechanism will be expected to be complex, involving silyl radicals, silylenes, silenes and disilenes.

The pyrolysis mechanism of n-DMTS was studied using the GC/MS-SFR apparatus<sup>4</sup>. Trapping experiments were performed to

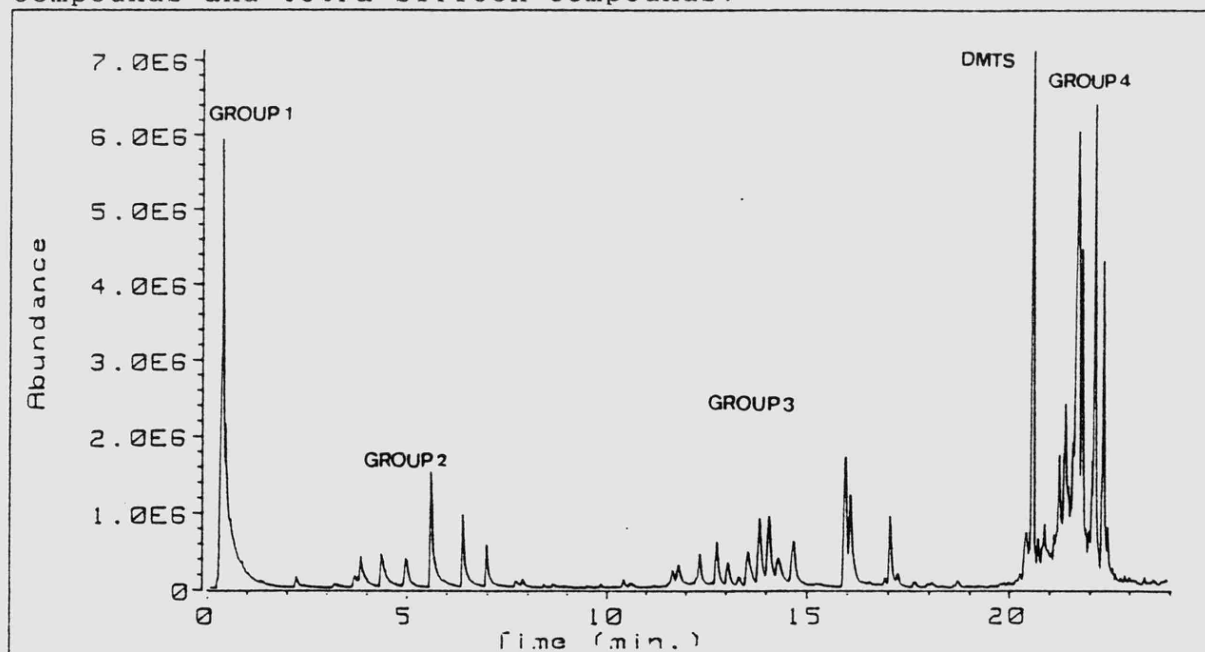
test for the different intermediates involved. GC/MS product identification was supplemented by comparative retention time tests and mass spectral analysis on authentic samples.

Kinetic measurements were performed using the kinetic-SFR apparatus to further elucidate the pyrolysis breakdown mechanism. First order rate constants were measured for major and trapping products over a range of temperatures to allow the calculation of Arrhenius parameters.

## (II) GC/MS-SFR Results

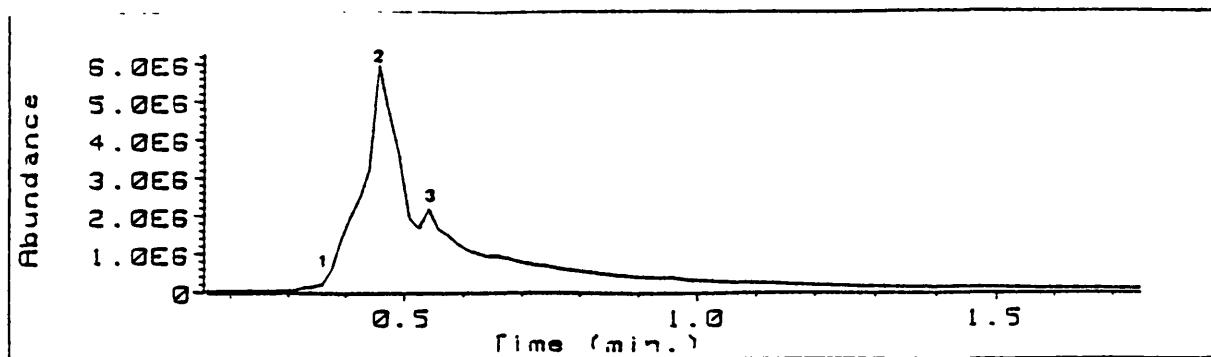
### (i) n-DMTS pyrolysis experiments

n-DMTS, being an involatile liquid, was pyrolysed using the syringe injection technique. Reactant volumes varied from 0.01 to 0.10  $\mu$ l, while the experimental temperature range was 570-650°C. TIC 1 shows the range of products formed in a high sample pressure experiment, the products being sub-divided into groups of monosilanes, di-silicon compounds, tri-silicon compounds and tetra-silicon compounds:



TIC 1: Group 1- monosilanes, Group 2- disilicon compounds, Group 3- tri-silicon compounds, Group 4- tetrasilicon compounds.

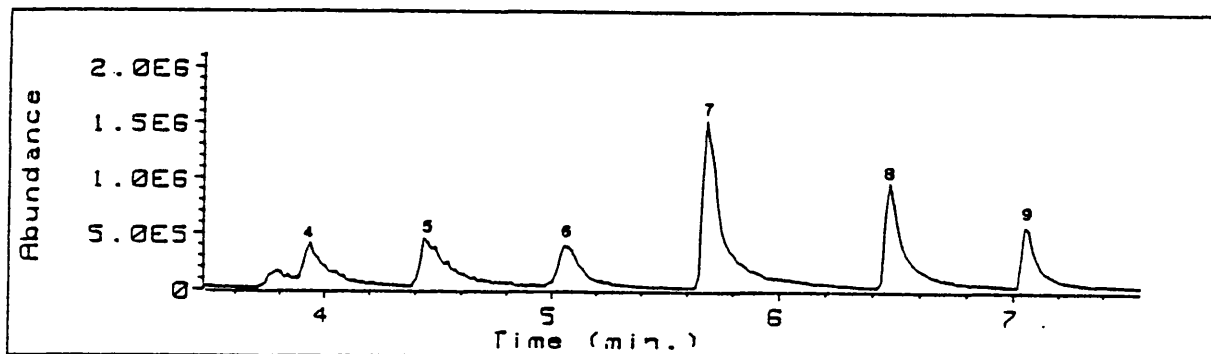
TIC 1a shows the products in group 1:



TIC 1a: [1]  $\text{Me}_2\text{SiH}_2$ , [2]  $\text{Me}_3\text{SiH}$ , [4]  $\text{Me}_4\text{Si}$ .

Group 1 contains the major product of the pyrolysis is trimethylsilane (3MS); other prominent products are dimethylsilane (2MS) and tetramethylsilane (4MS).

TIC 1b shows the products corresponding to the di-silicon compounds in group 2:

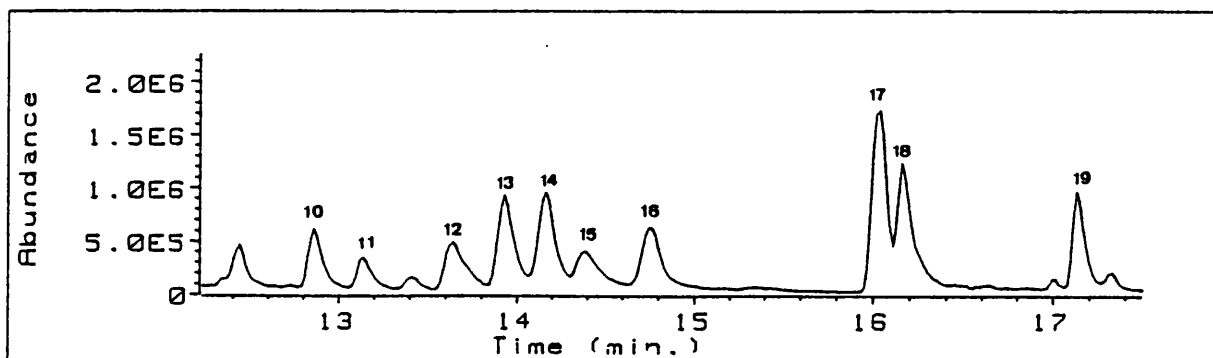


TIC 1b: [4]  $\text{Me}_2\text{HSi}\diagdown\text{SiMe}_2\text{H}$ , [5]  $\text{Me}_3\text{Si}\diagdown\text{SiMe}_2\text{H}$ , [6]  $\text{Me}_3\text{SiSiMe}_3$ ,

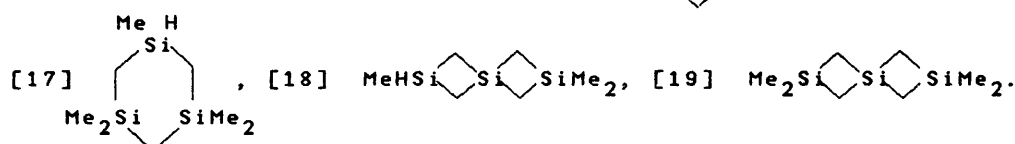
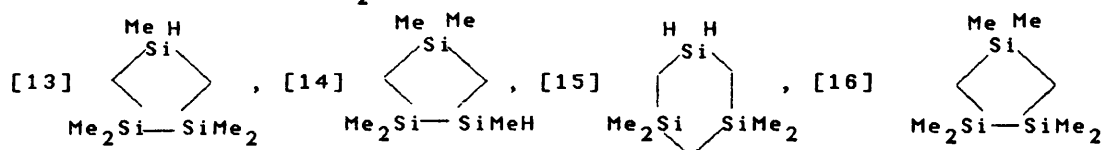
[7]  $\text{Me}_2\text{Si}\diagup\text{SiMeH}$ , [8]  $\text{Me}_3\text{Si}\diagdown\text{SiMe}_2\text{H}$ , [9]  $\text{Me}_2\text{Si}\diagup\text{SiMe}_2$ .

Prominent products in this group include HMDS [6], CYCLO 1 [7], ISO-HMDS [8] and 1,1,3,3-tetramethyl-1,3-disilacyclobutane [9].

TIC 1c shows the tri-silicon compounds in group 3:

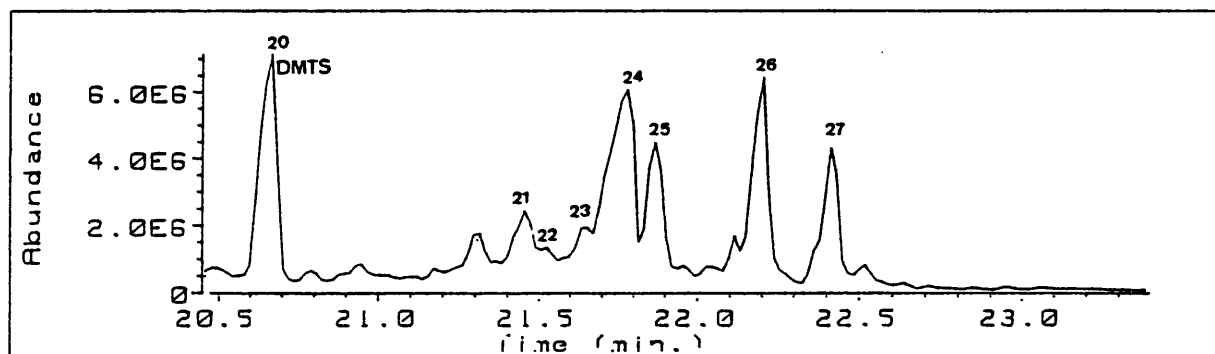


TIC 1c: [10]  $\text{Me}_3\text{SiSiSiMe}_3$ , [11]  $\text{Me}_2\text{Si}-\text{Si}^{\text{H}}-\text{SiMe}_2\text{H}$ , [12]  $\text{MeHSi}-\text{Si}^{\text{H}}-\text{SiMe}_3$ ,

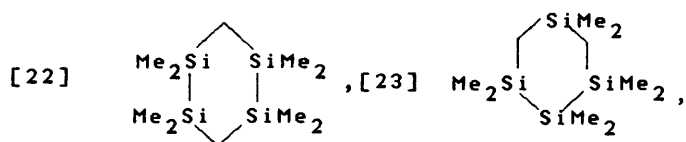


All but one of the products in group 3 are cyclic carbo-silanes, with 1,3,3,5,5-pentamethyl-1,3,5-trisilacyclohexane [17] being the most prominent.

TIC 1d contains the tetra-silicon compounds in group 4 and the reactant n-DMTS:



TIC 1d: [20] n- $\text{Me}_{10}\text{Si}_4$ , [21]  $\text{MeHSi}-\text{Si}-\text{Si}^{\text{H}}-\text{SiMe}_3$ ,



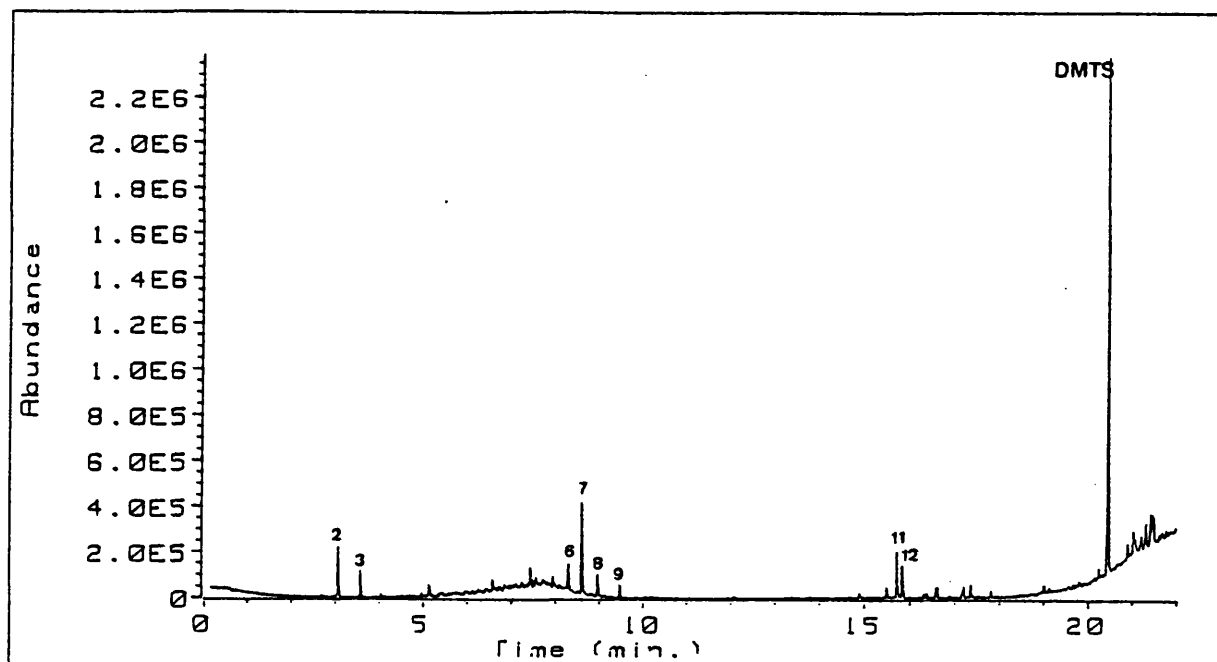
[24]  $\text{Me}_2\text{Si}-\text{Si}-\text{Si}^{\text{H}}-\text{SiMe}_3$ , [25]  $\text{MeHSi}-\text{Si}-\text{Si}-\text{SiMeH}$

[26]  $\text{Me}_2\text{Si}-\text{Si}-\text{Si}-\text{SiMeH}$ , [27]  $\text{Me}_2\text{Si}-\text{Si}-\text{Si}-\text{SiMe}_2$

Therefore product composition at high sample pressures comprised mainly 3MS, 2MS, 4MS and  $\text{CH}_4$  with smaller amounts of di-, tri- and tetra-silicon cyclic carbosilanes. At low



sample pressures product composition is simplified. TIC 2 shows the products from a low pressure pyrolysis, using the numbers of the corresponding products in TIC 1:



TIC 2: [2]  $\text{Me}_3\text{SiH}$ , [3]  $\text{Me}_2\text{SiH}_2$ , [6]  $\text{Me}_3\text{SiSiMe}_3$ , [7]  $\text{Me}_2\text{Si} \begin{array}{c} \diagup \diagdown \\ \diagdown \diagup \end{array} \text{SiMeH}$ ,  
 [8]  $\text{Me}_3\text{Si} \begin{array}{c} \diagup \diagdown \\ \diagdown \diagup \end{array} \text{SiMe}_2\text{H}$ , [9]  $\text{Me}_2\text{Si} \begin{array}{c} \diagup \diagdown \\ \diagdown \diagup \end{array} \text{SiMe}_2$ , [11]  $\text{Me}_2\text{Si} \begin{array}{c} \diagup \diagdown \\ \diagdown \diagup \end{array} \text{Si}^{\text{H}} \begin{array}{c} \diagup \diagdown \\ \diagdown \diagup \end{array} \text{SiMe}_2\text{H}$ ,  
 [12]  $\text{MeHSi} \begin{array}{c} \diagup \diagdown \\ \diagdown \diagup \end{array} \text{Si}^{\text{H}} \begin{array}{c} \diagup \diagdown \\ \diagdown \diagup \end{array} \text{SiMe}_3$ .

There is a marked suppression of the higher molecular weight carbosilanes in groups 3 and 4 suggesting that these may arise from bimolecular reactions.

Table 4.1 gives the products identified from the pyrolysis of n-DMTS:

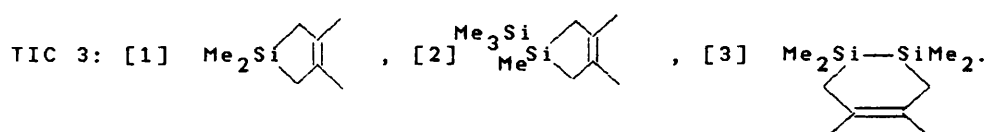
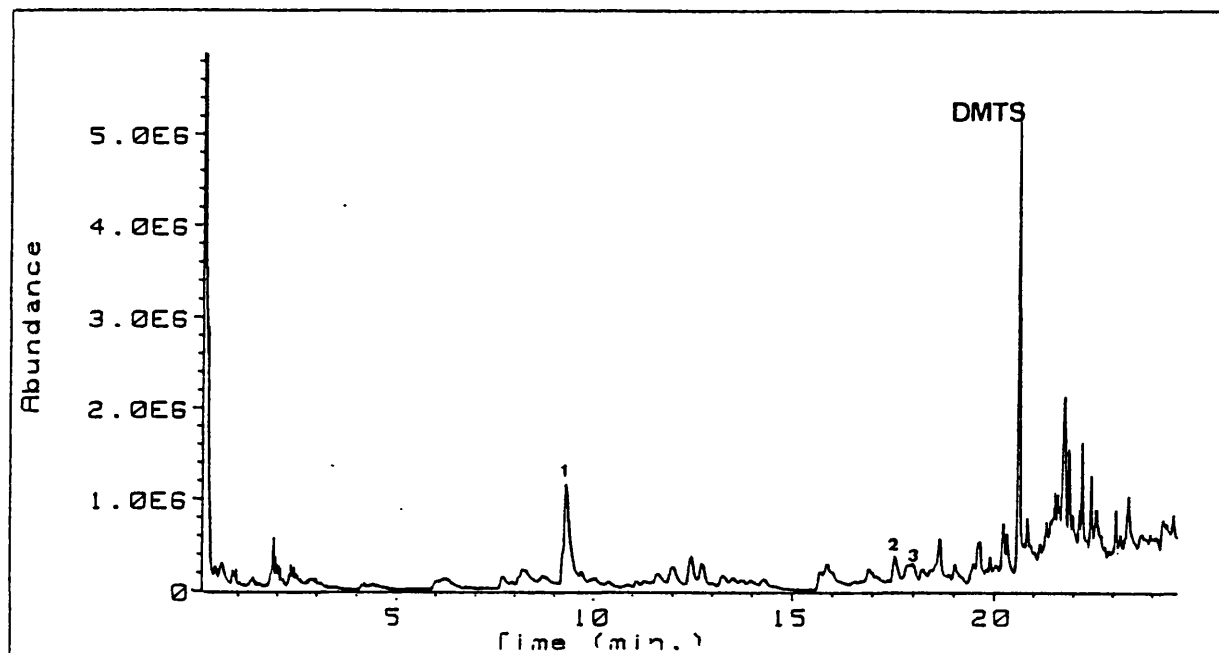
Table 4.1:

Group 1				
$H_2^*$	$CH_4^*$	$Me_2SiH_2$ [1]	$Me_3SiH$ [2]	$Me_4Si$ [3]
Group 2				
$Me_2SiH-CH_2-SiMe_2H$ [4]	$Me_3Si-CH_2-SiMe_2H$ [5]	$Me_3SiSiMe_3$ [6]	$Me_2Si-CH_2-SiMe_2H$ [7]	
$Me_3Si-CH_2-SiMe_2H$ [8]	$Me_2Si-CH_2-SiMe_2H$ [9]			
Group 3				
$Me_3SiSiSiMe_3$ [10]	$Me_2Si-CH_2-SiMe_2H$ [11]	$Me_2Si-CH_2-SiMe_2H$ [12]		
$Me_2Si-CH_2-SiMe_2H$ [13]	$Me_2Si-CH_2-SiMe_2H$ [14]	$Me_2Si-CH_2-SiMe_2H$ [15]	$Me_2Si-CH_2-SiMe_2H$ [16]	
$Me_2Si-CH_2-SiMe_2H$ [17]	$Me_2Si-CH_2-SiMe_2H$ [18]	$Me_2Si-CH_2-SiMe_2H$ [19]		
Group 4				
$MeHSi-CH_2-Si-CH_2-SiMe_3$ [21]	$Me_2Si-CH_2-SiMe_2H$ [22]	$Me_2Si-CH_2-SiMe_2H$ [23]		
$Me_2Si-CH_2-SiMe_2H$ [24]	$MeHSi-CH_2-Si-CH_2-SiMeH$ [25]			
$Me_2Si-CH_2-SiMe_2H$ [26]	$Me_2Si-CH_2-SiMe_2H$ [27]			

\*see section (IV)-Q8/MS-Sealed tube experiments

### (ii) 2,3-dimethyl-1,3-butadiene/n-DMTS pyrolysis experiments

A 10:1 mixture of 2,3-dimethyl-1,3-butadiene and n-DMTS was pyrolysed using the liquid injection technique. The pyrolysis temperature range was 570-650°C. High pressure experiments had little effect on product yield or composition. The complexity of end product composition increased due to the secondary reactions of butadiene. Low pressure experiments reduced but did not suppress product formation. The products unique to this pyrolysis are shown in TIC 3:

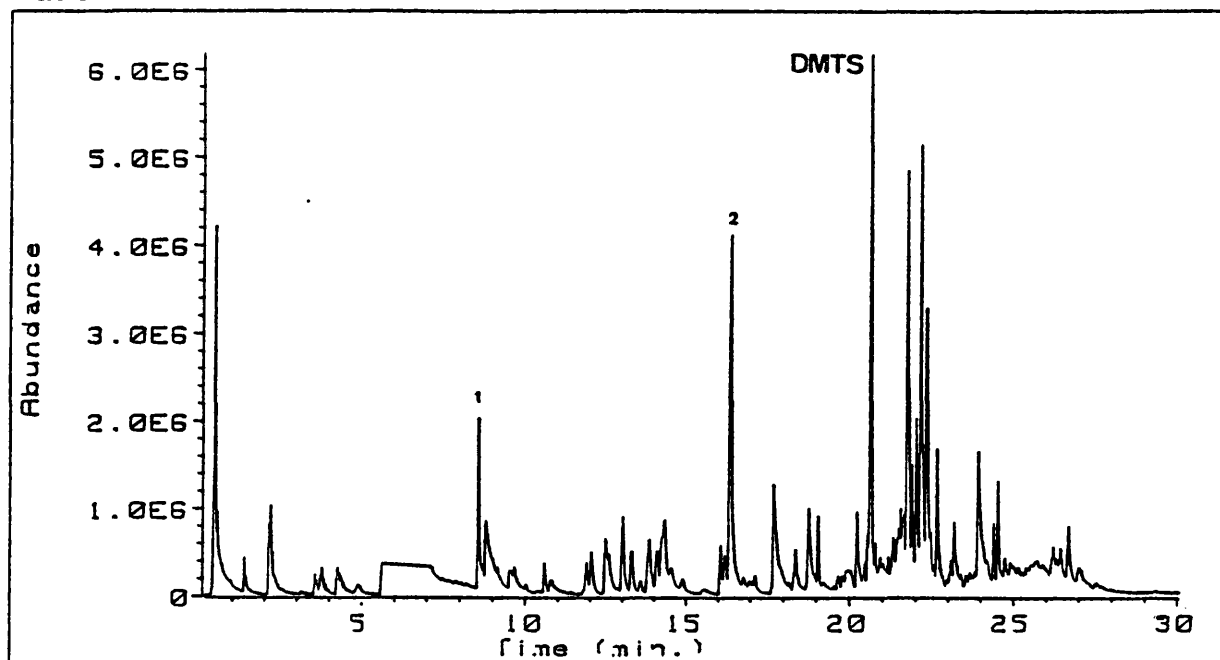


The most abundant intermediate trapped in this pyrolyses was dimethylsilylene ( $\text{Me}_2\text{Si}:$ ) with smaller amounts of trimethylsilyl(methyl)silylene ( $\text{Me}_3\text{Si}(\text{Me})\text{Si}:$ ) and tetramethyldisilene ( $\text{Me}_2\text{Si}=\text{SiMe}_2$ ). Trace amounts of dimethylsilene were also trapped.

### (iii) Toluene/n-DMTS pyrolysis experiments

A 10:1 toluene:n-DMTS mixture was pyrolysed between 570-650°C using the liquid injection technique. Product composition was not affected but yields were slightly reduced by the presence of toluene. Products unique to this pyrolysis

are shown in TIC 4:

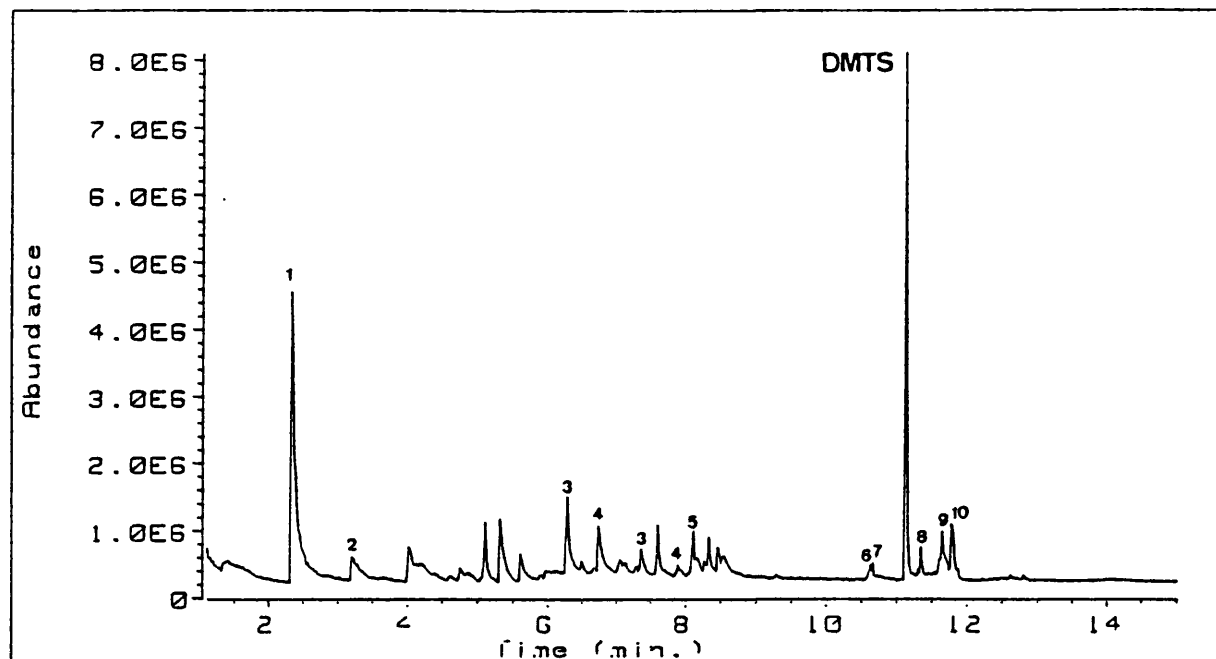


TIC 4: [1] ethylbenzene (ETHB) and [2] benzyltrimethylsilane (TMSB).

The major products were benzyltrimethylsilane (TMSB) and ethylbenzene (ETHB).

#### (iv) Methylchloride/n-DMTS pyrolysis experiments

n-DMTS was pyrolysed in an excess of methylchloride (MeCl) between 570-650°C. The n-DMTS was introduced via the liquid injection technique while the MeCl was injected via the gas sample valve. The high pressure products were suppressed but the yields of the low pressure products remained unchanged. TIC 5 shows the products unique to this pyrolysis:



TIC 5: [1]  $\text{Me}_3\text{SiCl}$ , [2]  $\text{Me}_2\text{SiCl}_2$ , [3]  $\text{Me}_3\text{SiSiMe}_2\text{Cl}$ ,  
 [4]  $\text{Me}_2\text{Si} \begin{array}{c} \diagup \diagdown \\ \text{Si} \end{array} \text{SiMeCl}$ , [5]  $\text{Me}_2\text{Si} \begin{array}{c} \text{H} \\ | \\ \text{Si} \end{array} \begin{array}{c} \text{Cl} \\ | \\ \text{SiMe}_2 \end{array}$ , [6]  $\text{Me}_3\text{Si} \begin{array}{c} \text{Cl} \\ | \\ \text{SiMeH} \end{array}$   
 [7]  $\text{Me}_3\text{Si} \begin{array}{c} \diagup \diagdown \\ \text{Si} \end{array} \text{SiCl}_2\text{H}$ , [8]  $\text{Me}_2\text{Si} \begin{array}{c} \text{Me} \\ | \\ \text{Si} \end{array} \begin{array}{c} \diagup \diagdown \\ \text{Si} \end{array} \text{SiMeCl}_2$   
 [9]  $\text{Me}_3\text{Si} \begin{array}{c} \diagup \diagdown \\ \text{Si} \end{array} \begin{array}{c} \text{SiMe}_3 \\ | \\ \text{SiMe} \end{array}$ , [10]  $\text{Me}_3\text{Si} \begin{array}{c} \text{Me} \\ | \\ \text{Si} \end{array} \begin{array}{c} \text{Me} \\ | \\ \text{Si} \end{array} \begin{array}{c} \diagup \diagdown \\ \text{Si} \end{array} \text{SiMe}$

The major product from this pyrolysis was trimethylchlorosilane, arising from the abstraction of chlorine by  $\text{Me}_3\text{Si}\cdot$  radicals; another prominent product arises from abstraction of chlorine by pentamethyldisilyl radicals. Two interesting products are [9] and [10], which do not contain chlorine and are not present in the straight pyrolysis of n-DMTS.

### (III) Kinetic-SFR Results

#### (i) n-DMTS kinetic experiments

n-DMTS was pyrolysed using the liquid injection technique between 570-650°C. Volumes of n-DMTS varied between 0.04-0.14  $\mu\text{l}$ . Figure 4.1 shows a typical gas chromatogram for a mid-temperature range pyrolyses. First order rate constants were calculated for the products shown in figure 4.1. Table 4.2 gives the Arrhenius parameters for the formation of these products.

Table 4.2: Kinetic results for n-DMTS pyrolysis experiments.

Product	$\log (A/s^{-1})$	$E_a$ (kJmol <sup>-1</sup> )	$k_{(620^\circ C)}(s^{-1})$
Me <sub>3</sub> SiH	$16.6 \pm 0.5$	$294.5 \pm 8$	0.252
CH <sub>4</sub>	$22.9 \pm 0.2$	$406.7 \pm 3$	0.140
Me <sub>2</sub> SiH <sub>2</sub>	$16.3 \pm 0.9$	$299.7 \pm 16$	0.064
Me <sub>4</sub> Si	$18.0 \pm 0.8$	$333.3 \pm 14$	0.033

Figure 4.2 shows the Arrhenius plot for the formation of 3MS.

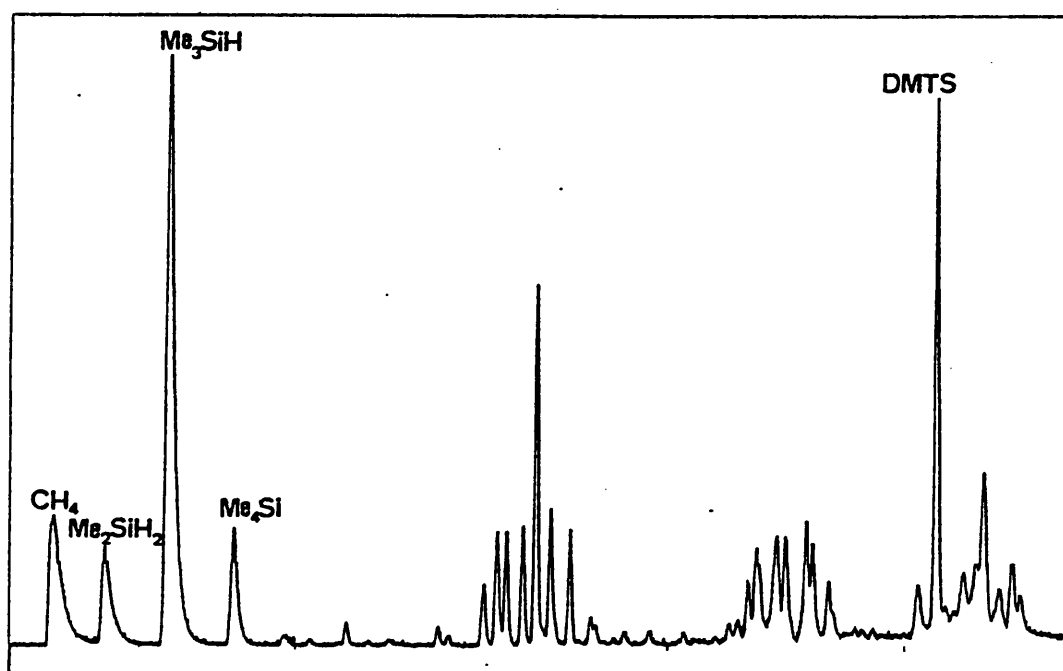


Figure 4.1: Gas Chromatogram for the pyrolysis of n-DMTS at 626°C.

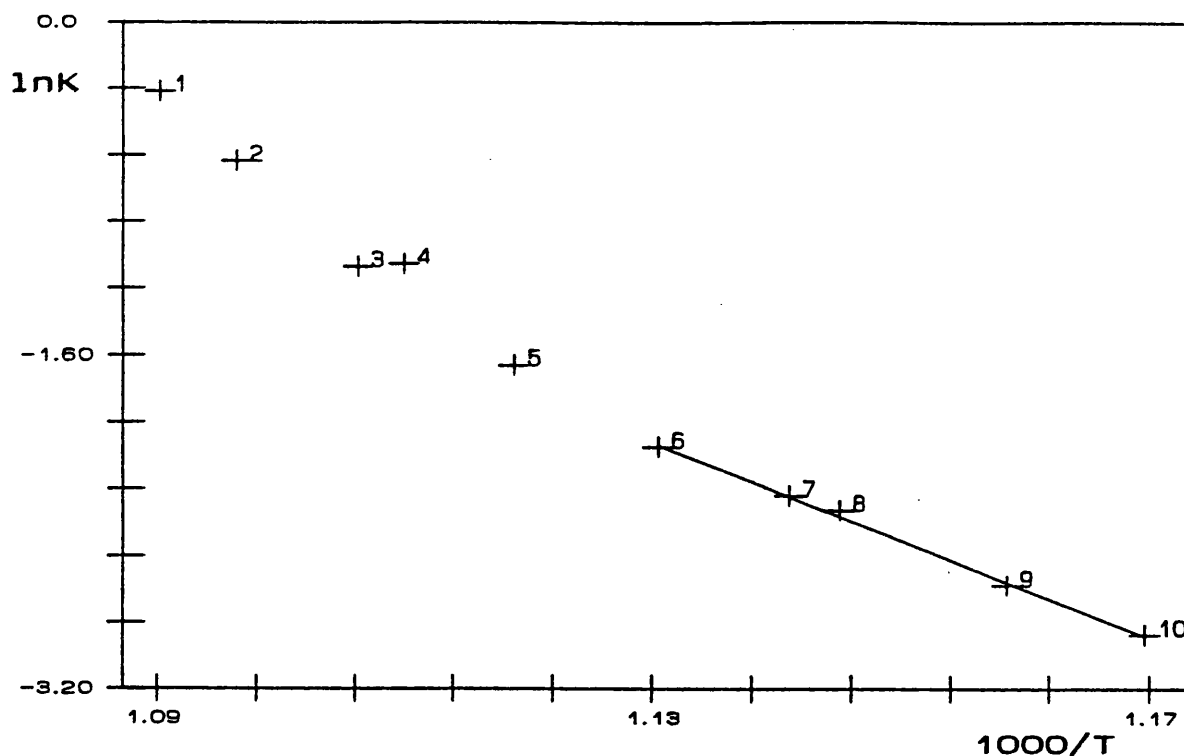


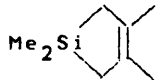
Figure 4.2: Arrhenius plot for the formation of trimethylsilane.

Figure 4.2 shows a curved Arrhenius plot, but, if the low to mid temperature range points are considered the values in table 4.2 result.

(ii) 2,3-dimethyl-1,3-butadiene/n-DMTS kinetic experiments

A 5:1 mixture of 2,3-dimethyl-1,3-butadiene and n-DMTS was pyrolysed using the liquid injection technique. The experimental temperature range was 570–650°C. Rate constants proved difficult to measure because of the complexity of the pyrolysed mixture. First order rate constants were measured for the formation of the  $\text{Me}_2\text{Si}$ : adduct, 1,1,3,4-tetramethyl-1-silacyclopent-3,4-ene (Fig 4.3). The Arrhenius parameters for the formation of the adduct are given in table 4.3:

Table 4.3: Kinetic results for 2,3-dimethyl-1,3-butadiene/n-DMTS experiments.

Product	$\log (A/s^{-1})$	$E_a \text{ (kJmol}^{-1}\text{)}$	$k_{(620^\circ\text{C})}(s^{-1})$
	$16.0 \pm 1.2$	$305.4 \pm 21$	0.014

The Arrhenius plot for the formation of this product is shown in figure 4.4.

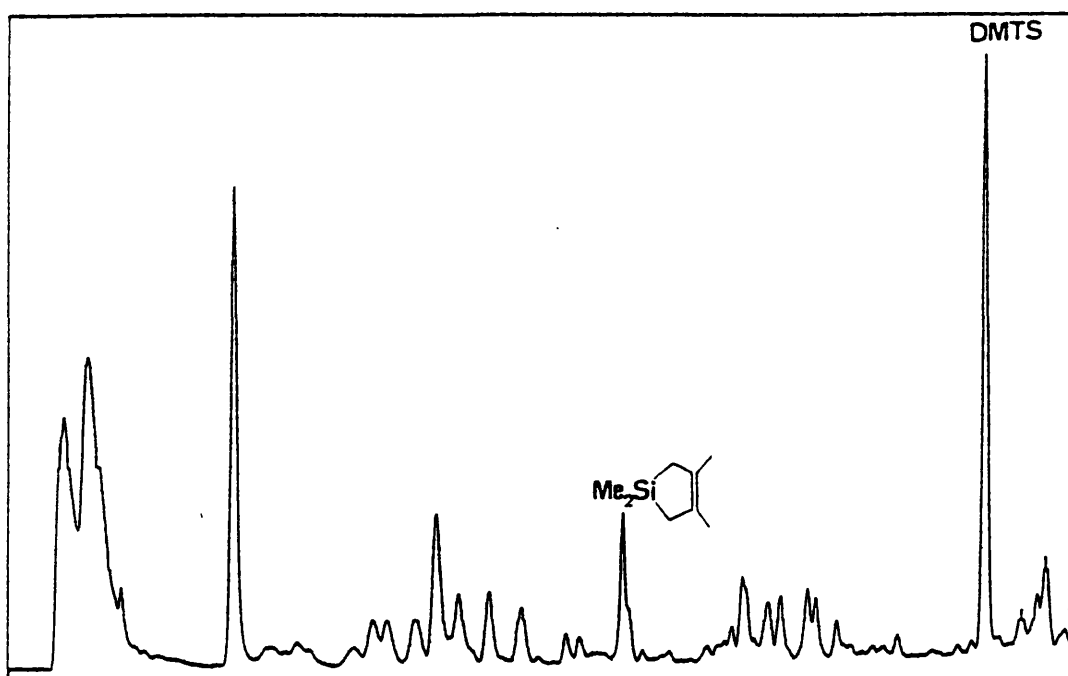


Figure 4.3: Gas Chromatogram for the pyrolysis of n-DMTS/ 2,3-dimethyl-1,3-butadiene at 645°C.

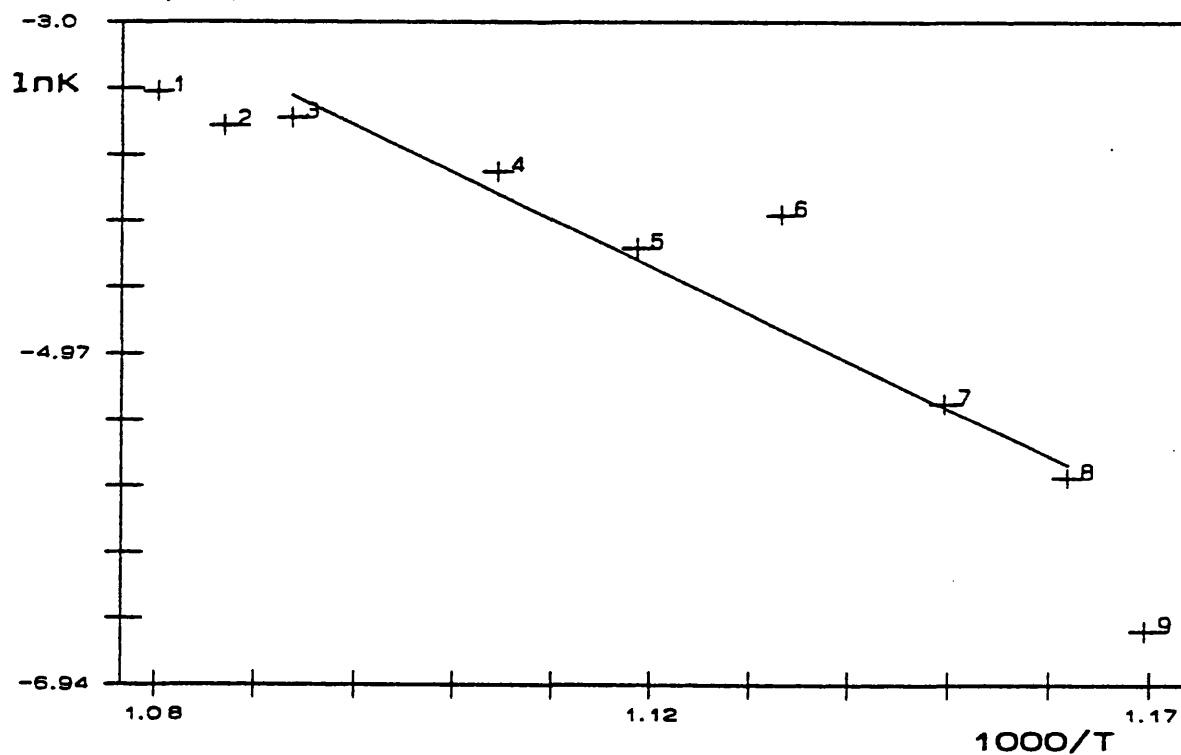


Figure 4.4: Arrhenius plot for the formation of 1,1,3,4-tetramethyl-1-silacyclopent-3,4-ene.



The Arrhenius parameters are subject to large error limits due to the difficulty in measuring correct reactant and product areas.



(iii) Toluene/n-DMTS kinetic experiments

A 10:1 mixture of toluene:n-DMTS mixture was pyrolysed using the liquid injection technique. The mixture was pyrolysed between 570-650°C. Figure 4.5 shows a gas chromatogram for a typical mid-temperature range experiment. First order rate constants were measured for the peaks identified in figure 4.5. The Arrhenius parameters for the formation of these products are given in table 4.4:

Table 4.4: Kinetic results for toluene/n-DMTS experiments.

Product	$\log (A/s^{-1})$	$E_a$ (kJmol <sup>-1</sup> )	$k_{(620^\circ C)}(s^{-1})$
Me <sub>3</sub> SiH	15.0 ± 0.5	278.1 ± 8	0.0710
Me <sub>2</sub> SiH <sub>2</sub>	17.3 ± 0.8	325.4 ± 10	0.0184
Me <sub>4</sub> Si	16.1 ± 0.9	305.9 ± 14	0.0160
Me <sub>3</sub> Si- 	15.8 ± 0.14	294.4 ± 9	0.0380
CH <sub>4</sub>	17.4 ± 0.6	321.9 ± 10	0.0371
CH <sub>3</sub> - 	16.3 ± 0.4	316.7 ± 6	5.9 × 10 <sup>-3</sup>

The Arrhenius plot for the formation of benzyltrimethylsilane is shown in figure 4.6.

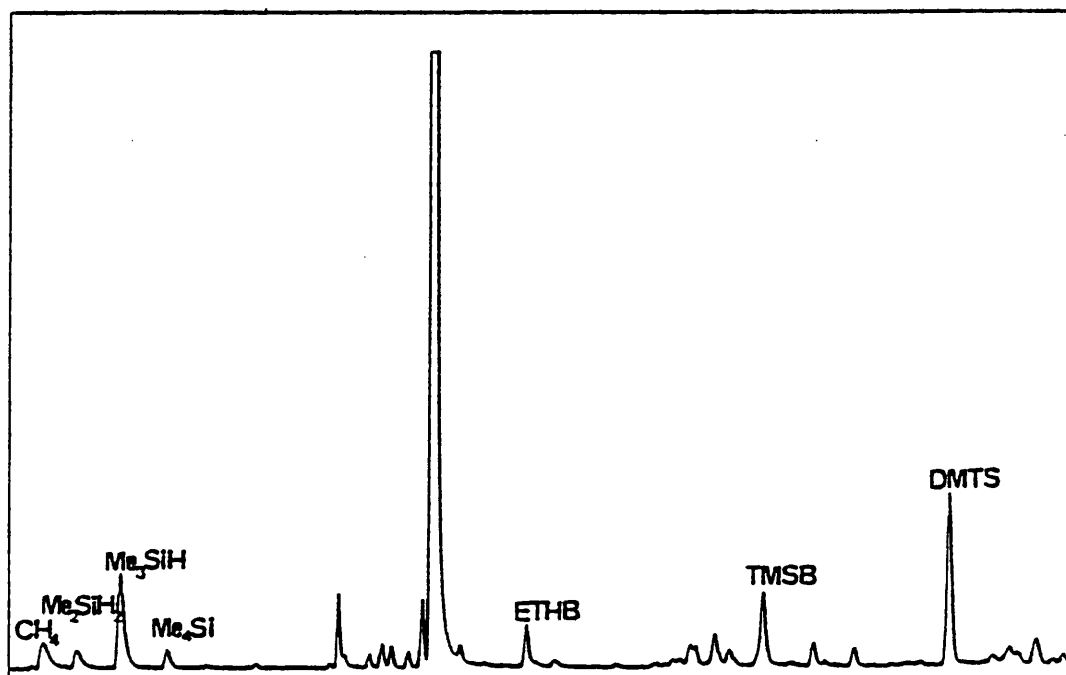


Figure 4.5: Gas Chromatogram for the pyrolysis of n-DMTS/toluene at 639°C.

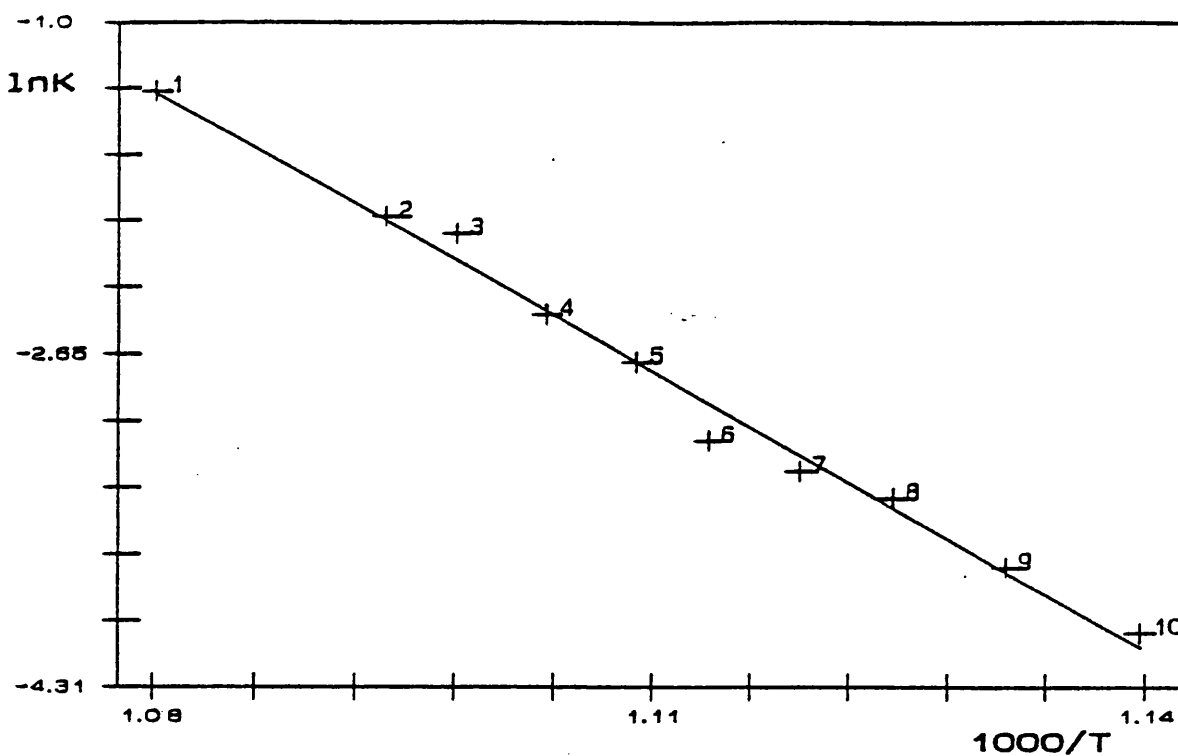


Figure 4.6: Arrhenius plot for the formation of benzyltrimethylsilane.

#### (IV) Q8/MS-Sealed Tube Pyrolysis Results

n-DMTS was pyrolysed at 550°C in a sealed sample vessel for 2.00 minutes. The time scale of the pyrolysis was calculated from the Arrhenius parameters for the formation of 3MS given in the kinetic-SFR results.

At 550°C:  $k = 8.09 \times 10^{-3} \text{ (s}^{-1}\text{)}$ ,  $t_{1/2} = 2.00 \text{ mins.}$

The Q8/MS revealed large amount of hydrogen were produced (fig. 4.7). A smaller amount of methane was also formed.

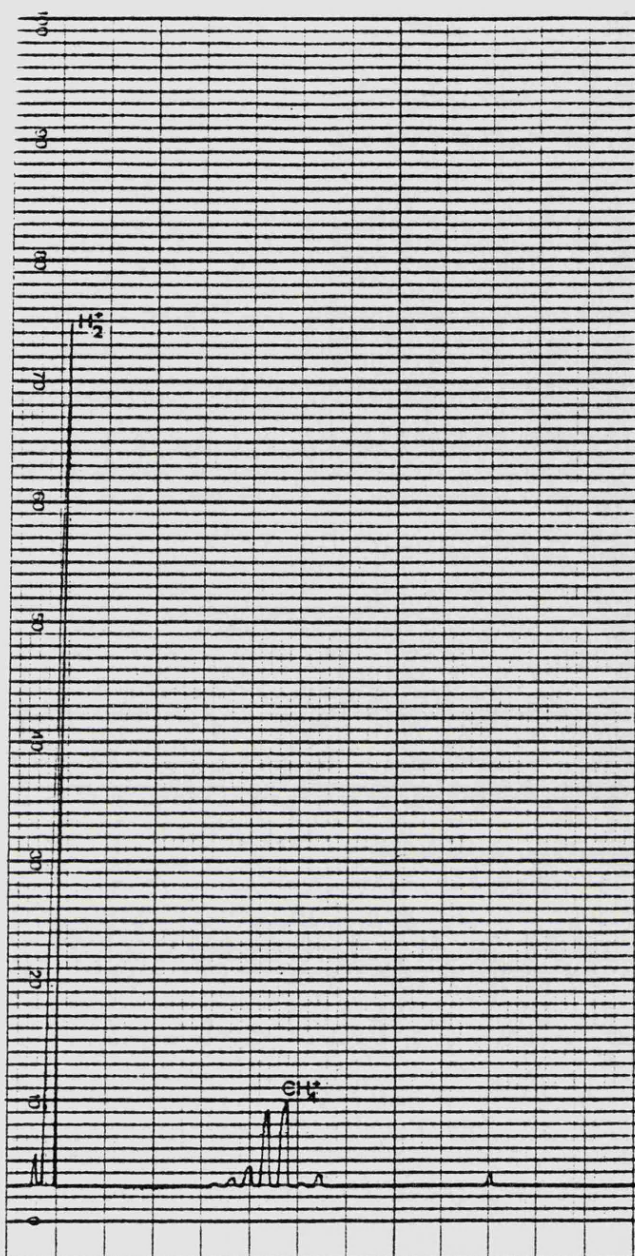


Figure 4.7: Mass Spectrum of  $H_2$  and  $CH_4$  from the sealed tube pyrolysis of n-DMTS at  $400^\circ C$ .

## (V) Discussion

The Arrhenius parameters for the formation of trimethylsilane in the low temperature range are in the order of the Si-Si bond dissociation energy (BDE)<sup>2</sup>. These Arrhenius parameters suggest that the primary source for 3MS is Si-Si bond cleavage, however, the Arrhenius plot for the formation of 3MS is curved emphasising the importance of secondary reactions at high temperatures. Pyrolysis in the presence of toluene reduces the number of secondary reactions and the Arrhenius parameters for the formation of 3MS and benzyltrimethylsilane (TMSB) are both in the order of the Si-Si BDE over a wide temperature range. Therefore the major source of 3MS is  $\text{Me}_3\text{Si}\cdot$  radicals produced by the cleavage of a terminal n-DMTS Si-Si bond. The combination of  $\text{Me}_3\text{Si}\cdot$  and benzyl radicals leads to the formation of TMSB, the rate limiting step for its formation being the cleavage of a Si-Si bond.

Pyrolysis in the presence of 2,3-dimethyl-1,3-butadiene yielded 1,1,3,4-tetramethyl-1-silacyclopent-3,4-ene (ADD1), the adduct of  $\text{Me}_2\text{Si:}$ , as a major product<sup>5</sup>. The Arrhenius parameters for the formation of ADD 1 were in the order of the Si-Si BDE. Also the kinetics of formation of methane and ethylbenzene (ETHB) in the toluene/n-DMTS experiments are consistent with the Si-Si BDE. Methane being formed via the hydrogen abstraction by  $\cdot\text{CH}_3$  radicals and ETHB being formed by the combination of benzyl and  $\cdot\text{CH}_3$  radicals. Therefore, the source of both  $\cdot\text{CH}_3$  radicals and  $\text{Me}_2\text{Si:}$  could be the unimolecular dissociation of  $\text{Me}_3\text{Si}\cdot$  radicals, the rate limiting step for the formation of  $\cdot\text{CH}_3$  radicals and  $\text{Me}_2\text{Si:}$  being the formation of  $\text{Me}_3\text{Si}\cdot$  radicals. The Arrhenius parameters for the formation of methane in absence of toluene are very high, revealing the increasing importance of secondary reactions in methane formation. The Arrhenius parameters for the formation of 4MS in the presence and absence of toluene are in the order of the Si-Si BDE. The combination of  $\text{Me}_3\text{Si}\cdot$  and  $\cdot\text{CH}_3$  radicals leads to its formation, the rate limiting step for the production of both these species being the cleavage of the Si-Si bond.

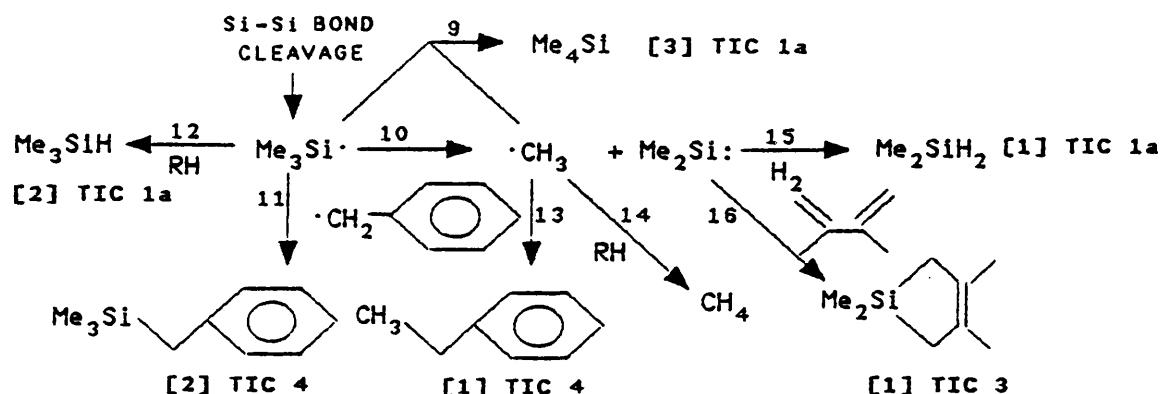
The Q8/MS experiments revealed that hydrogen and methane are formed when n-DMTS is pyrolysed. The source of methane is

methyl radical H-abstraction (*vide supra*) or hydrogen and methyl radical combination. Hydrogen is formed by either hydrogen radical H-abstraction, hydrogen radical combination or the cyclisation with elimination of hydrogen reaction (*vide infra*).

The Arrhenius parameters for the formation of 2MS in the straight and toluene pyrolyses are in the order of the Si-Si BDE.  $\text{Me}_2\text{Si:}$  formed by the dissociation of  $\text{Me}_3\text{Si}\cdot$  radicals is thought to insert into the hydrogen  $\sigma$ -bond to yield 2MS (15)<sup>6</sup>.

The mechanism of formation for methane, 2MS, 3MS, 4MS, ETHB, TMSB and ADD1 is summarised by the reactions in scheme 4.2:

Scheme 4.2:



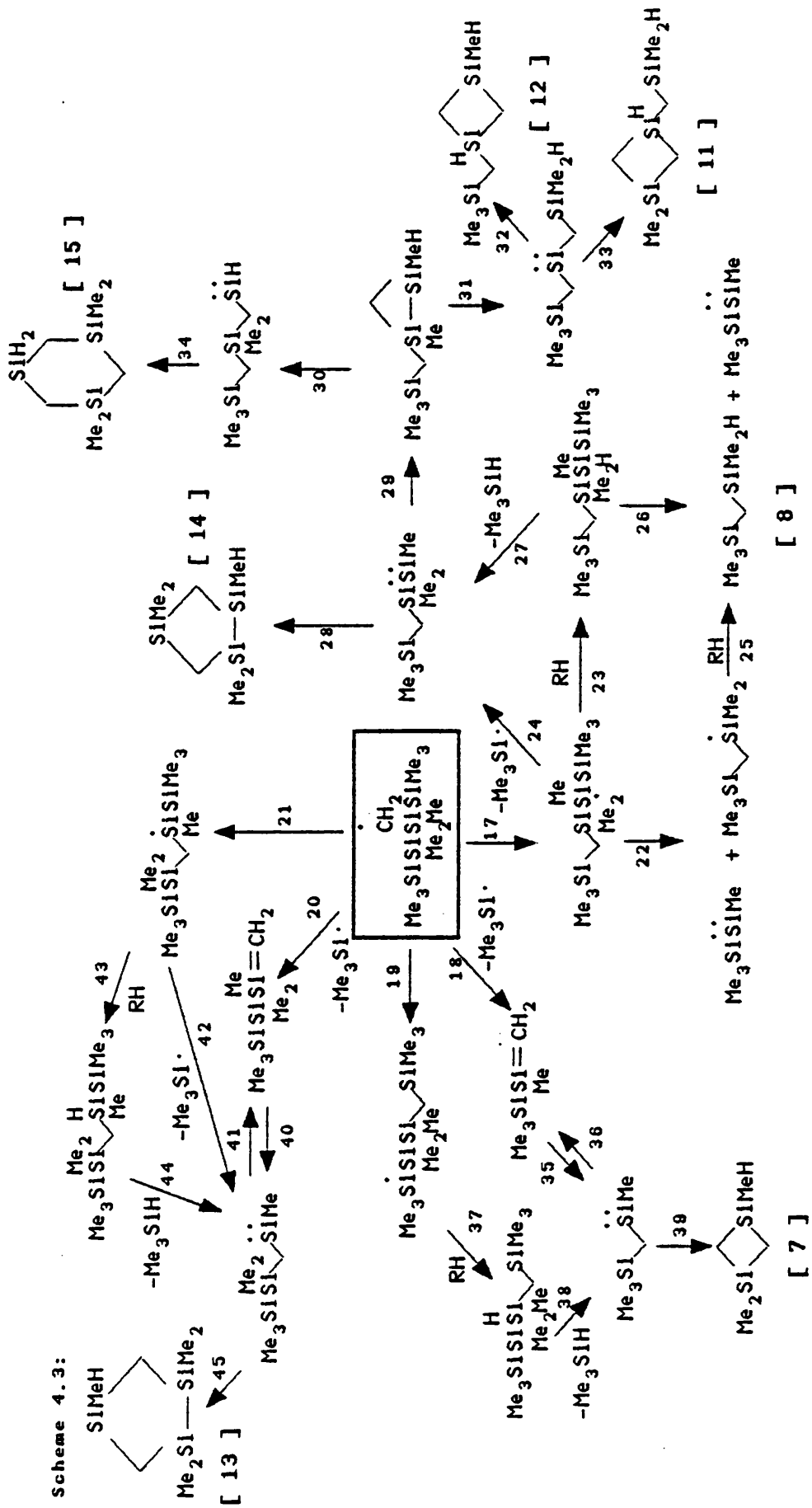
The di- and tri-silicon cyclic carbosilanes in groups 2 and 3 are believed to be formed via more complex mechanisms. Most of these compounds are more prominent in the low pressure experiments. Scheme 4.3 shows a set of unimolecular reactions leading to some of the products in groups 2 and 3.

The reactions in scheme 4.3 all have precedents in organo-silicon chemistry and being unimolecular in nature offer a reason why these products are less affected by lower sample pressures, toluene and methylchloride experiments.

There are 6 general types of reaction taking place in scheme 4.3:- (i) radical dissociation reactions (18, 20, 22, 24, 42), (ii) isomerisation reactions via 1,2- (19, 21) or 1,3- shifts (22), (iii) hydrogen abstraction reactions (23, 25, 37, 43), (iv) silylene elimination via 1,2 hydrogen shifts (26, 27, 38, 44), (v) cyclisation via internal C-H silylene insertion (28, 29, 30, 32, 33, 39, 45) and (vi) silylene-silylene isomerisation via disilirane intermediates (29-31)<sup>7,8</sup>.

The silylene produced in reactions 22 and 23 can be trapped in the presence of 2,3-dimethyl-1,3-butadiene yielding product

### Scheme 4.3:



### [2]-TIC 3.

Hydrogen abstraction from a terminal methyl group leads to the reactions shown in scheme 4.4.

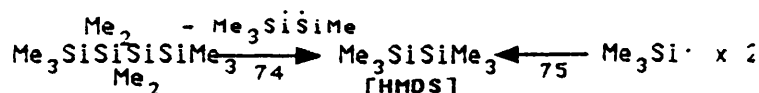
The majority of products in scheme 4.4 are linear carbosilanes. The reactions in scheme 4.4 can be grouped into:- (i) radical dissociation reactions (46, 50, 58), (ii) isomerisation reactions via 1,2- (49), 1,3- (47) or 1,4 shifts (48), (iii) hydrogen abstraction reactions (51, 53, 55, 57, 62, 65, 68), (iv) silylene elimination via 1,2 hydrogen shifts (52, 60, 61, 69). The isolation of the chlorosilane [5] (TIC 5) gives evidence for reaction (66) leading to product [4]. Evidence for reaction (58) comes from the isolation of the  $\text{Me}_2\text{Si}=\text{SiMe}_2$  adduct (product [3] TIC 3). Most reactions are unimolecular in both schemes 3 and 4, but, the formation of [16] is believed to involve the bimolecular addition of dimethylsilene, explaining its suppression in low sample pressures. The formation of the radical in reaction (50) is thought to be an analogous reaction to the unimolecular dissociation of  $\text{Me}_3\text{Si}\cdot$  radicals. The cyclisation/elimination reaction leads to the formation of [16]<sup>3</sup>. The remainder of the products in group 3 are formed in high yields at high sample pressures. Product [17] is believed to arise by the same reactions shown in scheme 3.8, chapter 3. [17] is suppressed in low pressure pyrolyses, because the bimolecular silene/radical addition (70) reaction is suppressed<sup>9</sup>. The silene is produced in reaction (18) and the radical is produced in reactions (22) and (58). Evidence for scheme 3.8, Chapter 3 comes from the MeCl experiments. The silene produced in reaction 18 can undergo head to tail dimerisation to form product [9] TIC 5 (*vide infra*). The MeCl experiments suppress the bimolecular silene/radical addition, thus the silene-silene addition is possible.

The kinetics of formation of the di- and tri-silicon compounds were not measured because of:- (i) the difficulty in measuring correct peak areas, (ii) the importance of secondary decomposition reactions of these compounds<sup>2,10,11</sup> and (iii) the complexity of their formation. Therefore little could be learned from measuring first order rate constants.

Hexamethyldisilane can be formed by the combination of  $\text{Me}_3\text{Si}\cdot$  radicals or the unimolecular elimination of trimethylsilyl(methyl)silylene via an internal 1,2 methyl shift<sup>12</sup>.

[illegible]

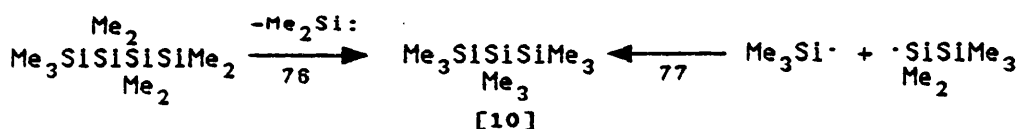




The abundance of  $\text{Me}_3\text{Si}\cdot$  is demonstrated in the MeCl and toluene trapping experiments; also there was only a small amount of trimethylsilyl(methyl)silylene trapped in the butadiene experiments. Therefore, the primary source of HMDS is  $\text{Me}_3\text{Si}\cdot$  radical combination (75).

1,1,3,3-tetramethyl-1,3-disilacyclobutane is thought to be formed by the head to tail dimerisation of dimethylsilene ( $\text{Me}_2\text{Si}=\text{CH}_2$ ) (see reaction (46) Chapter 3). The major source for dimethylsilene is reaction (46) although some may arise from the disproportionation of  $\text{Me}_3\text{Si}\cdot$  radicals (reaction (47) Chapter 3).

Octamethyltrisilane (OMTS) can be formed by two routes; the unimolecular elimination of  $\text{Me}_2\text{Si:}$  from n-DMTS or the combination of  $\text{Me}_3\text{Si}\cdot$  and  $\text{Me}_3\text{Si}(\text{Me}_2)\text{Si}\cdot$  radicals:

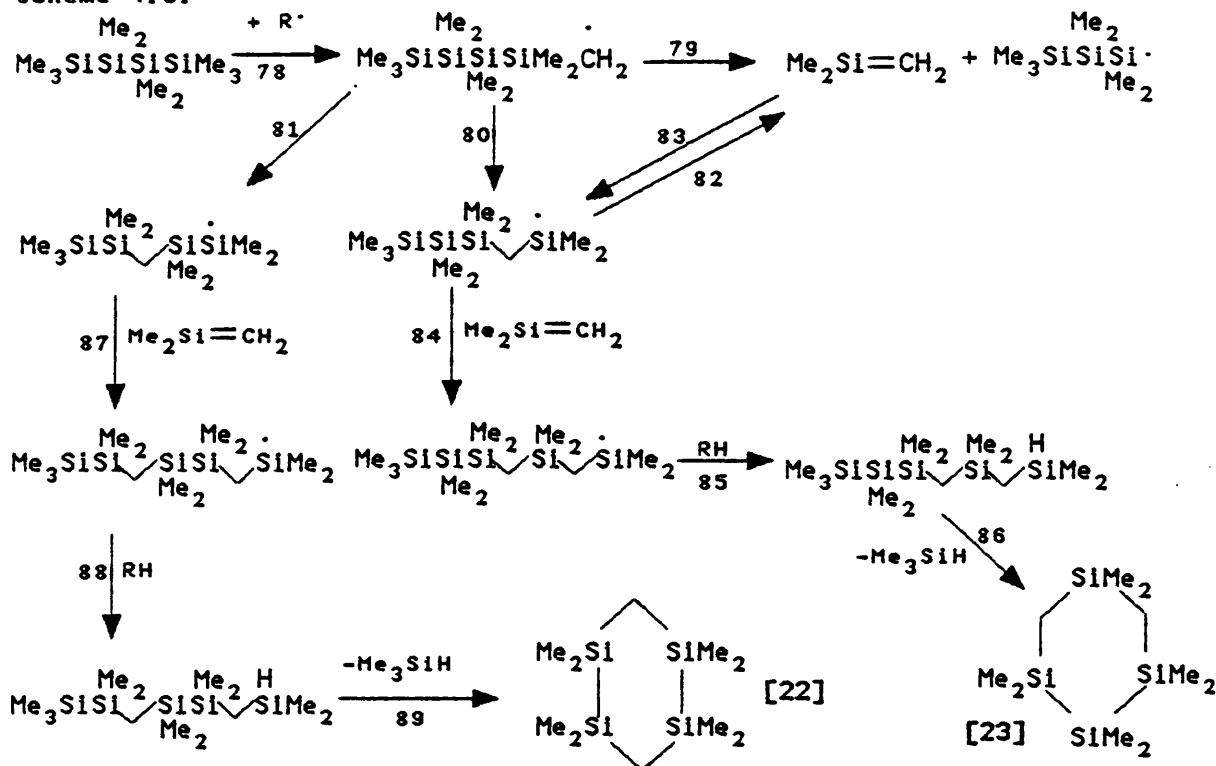


From the MeCl and toluene experiments it is clear that there are substantial quantities of  $\text{Me}_3\text{Si}\cdot$  and  $\cdot\text{Si}(\text{Me}_2)\text{SiMe}_3$  radicals. The Arrhenius parameters for the formation of the  $\text{Me}_2\text{Si:}$  adduct, ADD1, are not consistent with a unimolecular elimination involving a three membered transition state<sup>14</sup>. Therefore the radical combination reaction is thought to be the major source of OMTS (79).

The isolation of the chlorosilane [6] in TIC 5 suggests that product [5] (TIC 1b) may be formed via a radical mechanism. Product [5] may also arise from the insertion of the silylene formed by reactions 35 and 38 inserting into hydrogen.

The majority of products [18]–[27] are cyclic carbosilanes with multiple ring disilacyclobutane backbones. The exception to these structures are compounds [22] and [23]. These products are thought to be formed via cyclisation/ elimination reactions. Scheme 4.5 shows a possible sequence of reactions leading to products [22] and [23]:

Scheme 4.5:

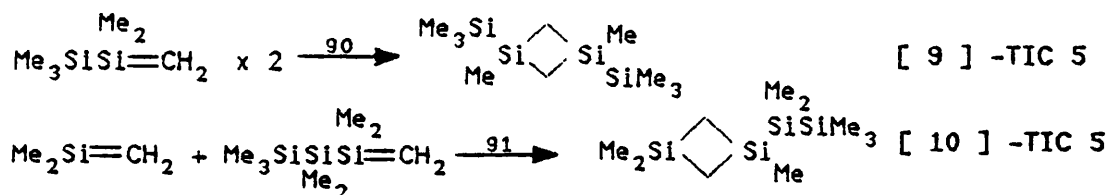


Hydrogen abstraction from a terminal methyl group leads to a carbon centred radical (78). This radical may dissociate to form  $\text{Me}_2\text{Si}=\text{CH}_2$  and a heptamethyltrisilyl radical (79) or isomerise via a 1,2 (80) or 1,3 shift (81). The silicon centred radicals formed can then undergo silene addition to generate new silicon centred radicals (84 & 87). Hydrogen abstraction by these new silicon centred radicals lead to the formation of two isomeric carbosilanes (85 & 88). These carbosilanes may cyclise and eliminate 3MS to form products [22] & [23] (86 & 89).

The radicals produced by reactions (80) and (81) may abstract hydrogen and undergo cyclisation with elimination of hydrogen, giving another route to products [22] and [23].

These products are minor in comparison with the multiple disilacyclobutane compounds. Head to tail dimerisation of differently substituted silenes could lead to the formation of these multiple ring compounds (see scheme 4.9, Chapter 3). The suppression of these products at low sample pressures and in the MeCl experiments suggests a complex route to their formation. The formation of these silenes would indeed be complex, being formed a long way down the reaction pathway, explaining why they are not trapped in the 2,3-di-methyl-1,3-butadiene experiments.

Two interesting products are formed in the MeCl experiments were [9] and [10] (TIC 5). These can be formed by the dimerisation of the silenes produced in reactions (18, 20 & 46):



[9] & [10] (TIC 5) are not noticed in the straight pyrolysis. The formation of these silenes is via the decomposition of the carbon centred radicals formed in the first steps of schemes 4.3 & 4.4. Under the complex reaction conditions of the straight pyrolysis silenes would not be expected to survive long enough to dimerise, however, under the less complex conditions of the MeCl experiments, dimerisation is possible. Low pressure products of the straight pyrolysis are not suppressed in the presence of MeCl, supporting the idea that MeCl reduces the number of bimolecular secondary reactions.

#### (VI) Summary

There is a general consistency in the pyrolysis mechanisms of HMDS, OMTS and n-DMTS. The mechanisms are all predominantly radical in nature and product formation is linked to the balance between bimolecular (high pressure) and unimolecular reactions (low pressure).

The major difference between HMDS and the other two oligomers is the lack of cyclic carbosilanes products; the major product in the high pressure pyrolysis of HMDS is the isomer, a linear carbosilane<sup>2,15</sup>. Linear carbosilane isomers of OMTS and n-DMTS are not prominent products in either pyrolyses because of their rapid secondary decomposition reactions. The products containing more than one silicon atom in the pyrolyses of OMTS and n-DMTS are predominantly cyclic carbosilanes.

The low pressure products for OMTS and n-DMTS can be explained by known reactions in organosilicon chemistry. However, the high pressure reactions of OMTS and n-DMTS differ, the cyclisation/elimination reactions being prominent

in the pyrolysis of OMTS and the formation of multiple disilacyclobutane compounds being more important for n-DMTS. The cyclisation/elimination reactions do take place in n-DMTS but are minor in comparison to the formation of the multiple ring compounds. This may be because the cyclisation/ elimination reactions are less favourable for n-DMTS e.g. the precursors for reactions (88), (91) may be too large for ring closure to be rapid. Thus the multiple rings may be formed with no competition from the cyclisation/elimination mechanism.

The kinetics of formation of 3MS support this argument; in the case of OMTS, 3MS formation gives Arrhenius parameters lower than the expected value for Si-Si bond cleavage, even in the presence of toluene, because the elimination of 3MS/ cyclisation reaction is more important. The Arrhenius parameters for the formation of 3MS from n-DMTS, however, are in the order of the Si-Si BDE. Therefore, 3MS formation is mostly via Si-Si bond cleavage, the elimination of 3MS/ cyclisation reaction being less important in this case.

There is an absence of the second most prominent product in Barton's low pressure experiments [CYCLO 2]. This can be attributed to the differing reaction conditions between the SFR and the flash vacuum pyrolysis technique.

#### (VII) Acknowledgement

I would like to thank Dr. Richard Taylor of Dow Corning for preparing the n-Decamethyltetrasilane.

#### (VIII) References

- (1) T.J. Barton, G.T. Burns, S.A. Burns, *Organometallics*, 1982, 1, 210.
- (2) I.M.T. Davidson, A.V. Howard, *J. Chem. Soc., Faraday Trans. I*, 1975, 71, 69.
- (3) B.N. Bortolin, I.M.T. Davidson, D. Lancaster, T. Simpson, D.A. Wild, *Organometallics*, 1990, 9, 281.
- (4) I.M.T. Davidson, T. Simpson, R. Taylor in '*Frontiers of Organosilicon Chemistry*' Eds. A.R. Bassindale & P.P. Gaspar,, 1991, Section II, p 89.

- (5) M.P. Clarke, I.M.T. Davidson, M.P. Dillon, *J. Chem. Soc., Chem. Commun.*, 1988, 1251.
- (6) P. John, J.H. Purnell, *J. Chem. Soc., Faraday Trans. I*, 1973, 69, 1455.
- (7) I.M.T. Davidson, *J. Organomet. Chem.*, 1988, 341, 255.
- (8) T.J. Barton, S.A. Jacobi, *J. Am. Chem. Soc.*, 1980, 102, 7979.
- (9) E. Bastian, P. Potzinger, A. Ritter, H.-P. Schuchmann, C. von Sonntag, G. Weddle, *Ber. Bunsen. Phys. Chem.*, 1980, 84, 56.
- (10) I.M.T. Davidson, G. Fritz, F.T. Lawrence, A.E. Matern, *Organometallics*, 1982, 1, 1453.
- (11) N. Auner, I.M.T. Davidson, S. Ijadi-Maghsoodi, F.T. Lawrence, *Organometallics*, 1986, 5, 431.
- (12) P.P. Gaspar, '*Reactive Intermediates*', Eds. M. Jones, R.A. Moss, Wiley, New York; 1978, 1, 229; 1981, 2, 335; 1985, 3, 333.
- (13) L.E. Gusel'nikov, M.C. Flowers, *J. Chem. Soc., Chem. Commun.*, 1967, 864.
- (14) I.M.T. Davidson, K.J. Hughes, S. Ijadi-Maghsoodi, *Organometallics*, 1987, 6, 639.
- (15) I.M.T. Davidson, C. Eaborn, J.M. Simmie, *J. Chem. Soc., Faraday Trans. I*, 1975, 71, 69.

## Chapter 5

### The Pyrolysis of iso-Decamethyltetrasilane

#### (I) Introduction

The pyrolysis of iso-decamethyltetrasilane (i-DMTS) has not been previously studied. A knowledge of the pyrolysis mechanisms of hexamethyldisilane (HMDS)<sup>1</sup>, octamethyltrisilane (OMTS)<sup>2</sup> and n-decamethyltetrasilane (n-DMTS)<sup>3</sup> should help elucidate the thermal breakdown mechanism of i-DMTS. i-DMTS is an interesting oligosilane to study as it can be thought of as a trisilane with a central trimethylsilyl group or as a tetrasilane. The low pressure reactions of the compounds studied so far have been explained by familiar organosilicon chemistry<sup>4</sup>, but, their high pressure reactions show remarkable differences. Therefore, it is an aim of this study to see if the cyclisation/elimination reactions (c.f. OMTS) or the formation of multiple disilacyclobutane ring compounds (c.f. n-DMTS) will dominate. The pyrolysis mechanism of i-DMTS will be expected to be as complex as the others studied with the simultaneous involvement of silyl radicals, silylenes, silenes and disilenes.

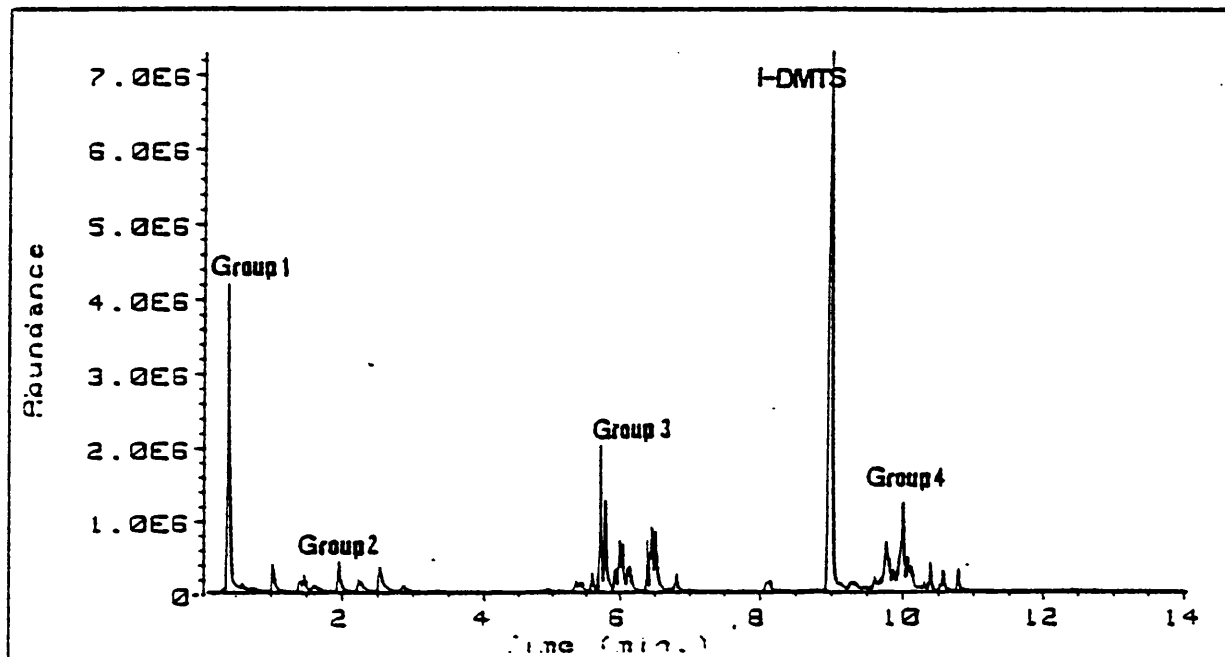
The pyrolysis mechanism of i-DMTS was investigated using the GC/MS-SFR apparatus for product identification. Trapping experiments were performed to test for the presence of different intermediates. GC/MS product identification was supplemented with comparative retention time tests and mass spectra analysis of known samples<sup>3</sup>.

Kinetic experiments were performed to further elucidate the thermal breakdown mechanism. First order rate constants were measured over a range of temperatures to enable the calculation of Arrhenius parameters.

## (II) GC/MS-SFR Results

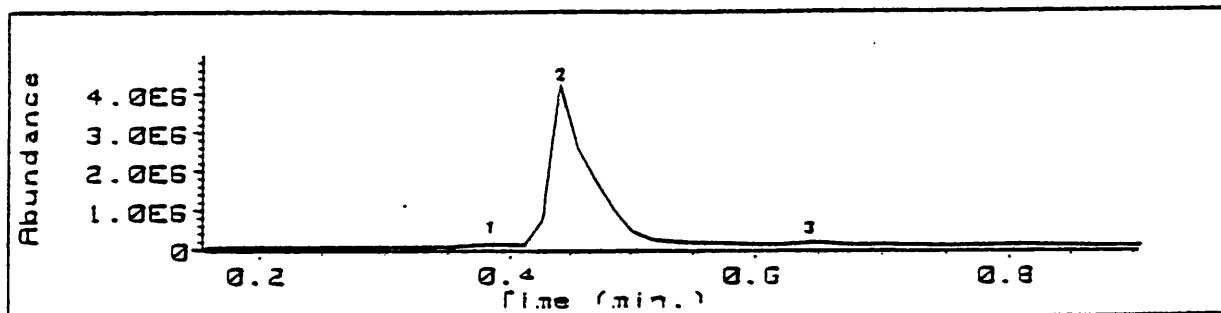
### (i) i-DMTS pyrolysis experiments

i-DMTS was pyrolysed between 570-650°C using the liquid injection technique. The reactant volumes varied between 0.02-0.10 µl. TIC 1 shows the range of products formed from a typical high pressure experiment. The products are grouped into monosilanes, di-, tri- and tetra-silicon compounds:



TIC 1: Group 1 contains monosilanes, Group 2 contains di-silicon compounds, Group 3 contains tri-silicon compounds and Group 4 contains tetra-silicon compounds.

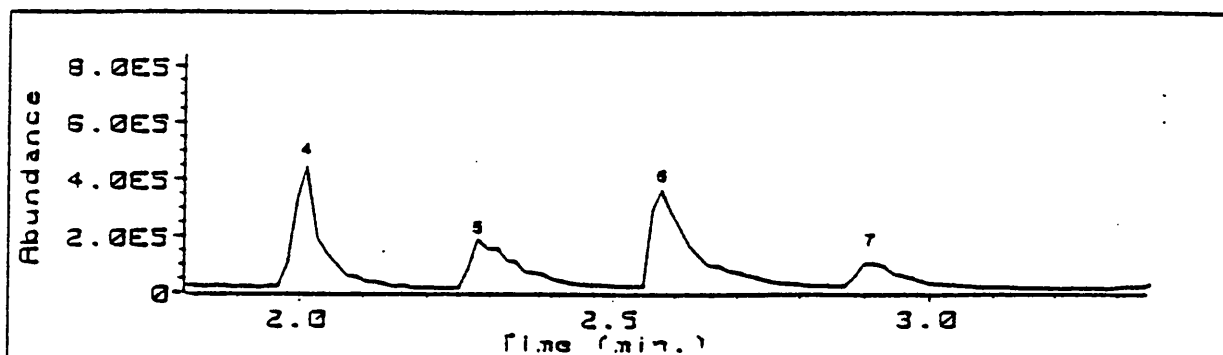
The monosilanes in group 1 are shown in TIC 1a:



TIC 1a: [1]  $\text{Me}_2\text{SiH}_2$ , [2]  $\text{Me}_3\text{SiH}$ , [3]  $\text{Me}_4\text{Si}$ .

This group contains the major product of the pyrolysis trimethylsilane (3MS) with smaller amounts of dimethylsilane (2MS) and tetramethylsilane (4MS).

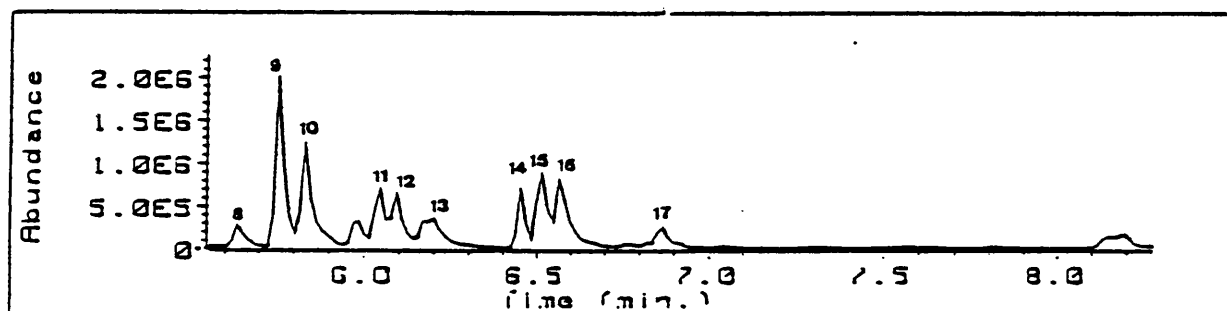
TIC 1b shows the di-silicon compounds in group 2:



TIC 1b: [4]  $\text{Me}_3\text{SiSiMe}_3$ , [5]  $\text{Me}_2\text{Si} \begin{array}{c} \diagup \diagdown \\ \text{SiMeH} \end{array}$ , [6]  $\text{Me}_3\text{Si} \begin{array}{c} \diagup \diagdown \\ \text{SiMe}_2 \end{array}$ ,  
[7]  $\text{Me}_2\text{Si} \begin{array}{c} \diagup \diagdown \\ \text{SiMe}_2 \end{array}$ .

This group contains HMDS, 1,1,3-trimethyl-1,3-silacyclobutane, trimethylsilyl(dimethylsilyl)methane (ISO-HMDS) and 1,1,3,3-teramethyl-1,3-disilacyclobutane.

TIC 1c shows the tri-silicon compounds in group 3:



TIC 1c: [8]  $\text{Me}_3\text{SiSiSiMe}_3$ , [9]  $\text{Me}_2\text{Si} \begin{array}{c} \diagup \diagdown \\ \text{Si}^{\text{H}} \text{SiMe}_2 \end{array}$ , [10]  $\text{MeHSi} \begin{array}{c} \diagup \diagdown \\ \text{Si}^{\text{H}} \text{SiMe}_3 \end{array}$ ,

[11]  $\text{Me}_2\text{Si} \begin{array}{c} \diagup \diagdown \\ \text{Si}^{\text{H}} \text{SiMeH} \end{array}$ , [12]  $\text{MeHSi} \begin{array}{c} \diagup \diagdown \\ \text{Si}^{\text{H}} \text{SiMe}_2 \end{array}$ , [13]  $\text{Me}_2\text{Si} \begin{array}{c} \diagup \diagdown \\ \text{Si}^{\text{H}} \text{SiMe}_2 \end{array}$ ,

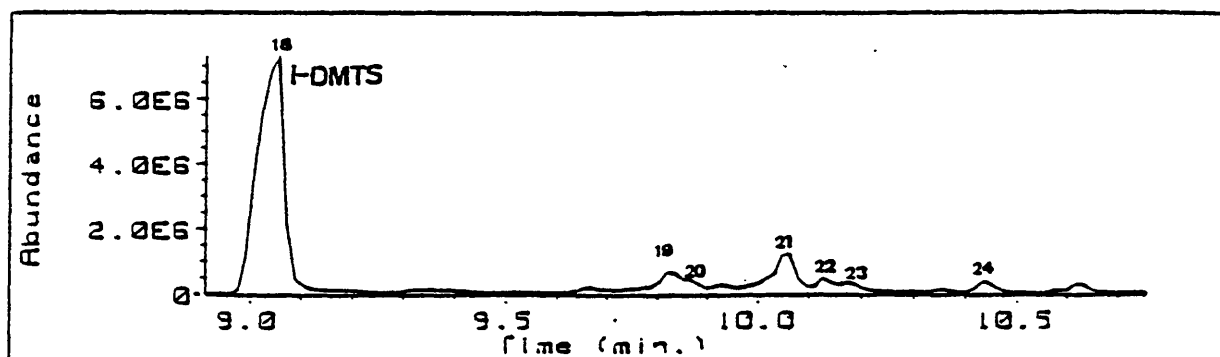
[14]  $\text{MeHSi} \begin{array}{c} \diagup \diagdown \\ \text{Si}^{\text{H}} \text{SiMe}_2 \end{array}$ , [15]  $\text{Me}_2\text{Si} \begin{array}{c} \diagup \diagdown \\ \text{Si}^{\text{H}} \text{SiMeH} \end{array}$ , [16]  $\text{Me}_2\text{Si} \begin{array}{c} \diagup \diagdown \\ \text{Si}^{\text{H}} \text{SiMe}_2 \end{array}$ ,

[17]  $\text{Me}_2\text{Si} \begin{array}{c} \diagup \diagdown \\ \text{Si}^{\text{H}} \text{SiMe}_3 \end{array}$ .

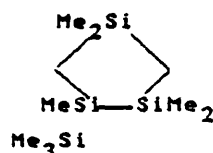
The majority of the products in group 3 are isomeric cyclic carbosilanes.

TIC 1d shows the reactant and the tetra-silicon compounds in group 4:





TIC 1d: [18] i-DMTS, [19]

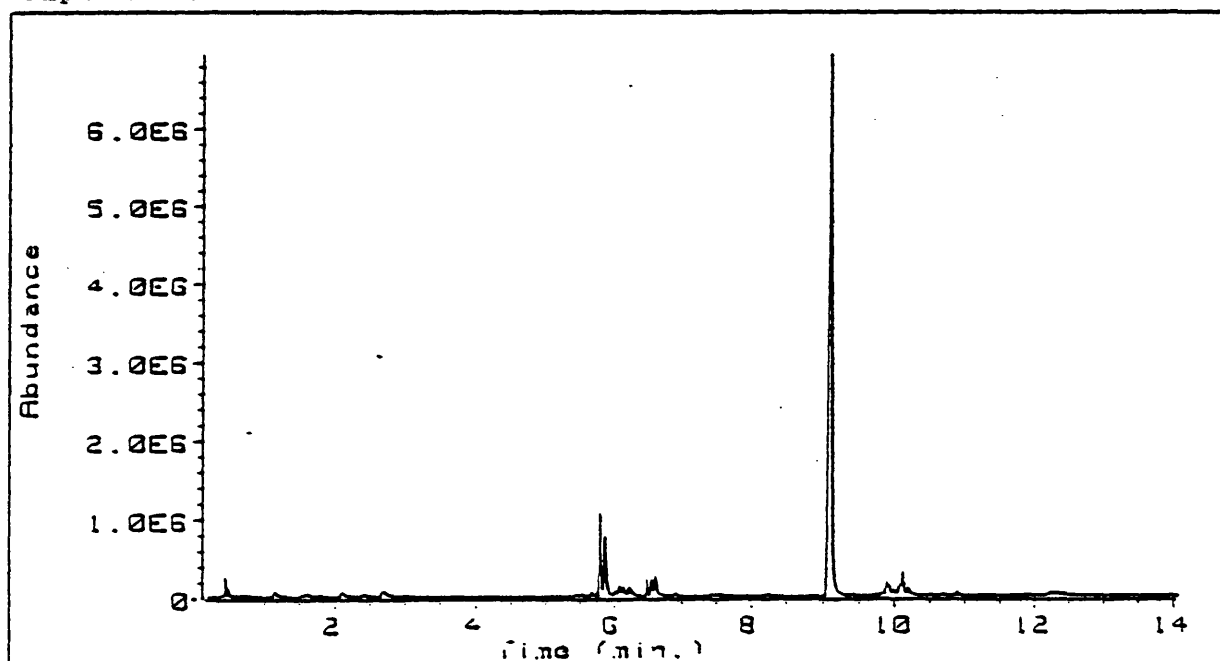


, [20]  $\text{MeHSi}-\text{Si}-\text{SiH}-\text{SiMe}_3$

[21]  $\text{Me}_2\text{Si}-\text{Si}-\text{SiH}-\text{SiMe}_3$ , [22]  $\text{MeHSi}-\text{Si}-\text{Si}-\text{SiMeH}$ ,

[23]  $\text{MeHSi}-\text{Si}-\text{Si}-\text{SiMe}_2$ , [24]  $\text{Me}_2\text{Si}-\text{Si}-\text{Si}-\text{SiMe}_2$ .

Low pressure experiments had a large affect on some of the tri-silicon ([14], [15] & [16]) and all of the tetrasilicon compounds ([18]-[24]). TIC 2 shows a typical low pressure experiment:



TIC 2: Low sample pressure pyrolysis (587°C/0.02μl);  
products [9] & [10] (TIC 1c) are still prominent.

The yield of 3MS is also reduced.

The products identified from the pyrolysis of i-DMTS are given in table 5.1:

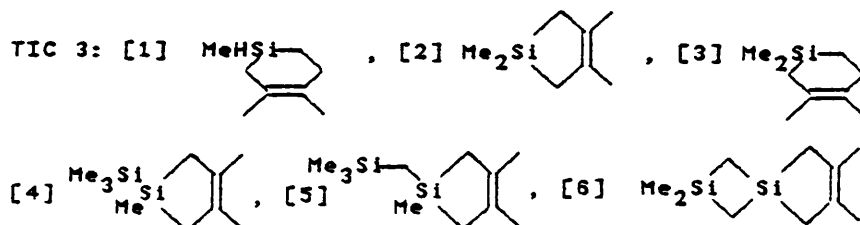
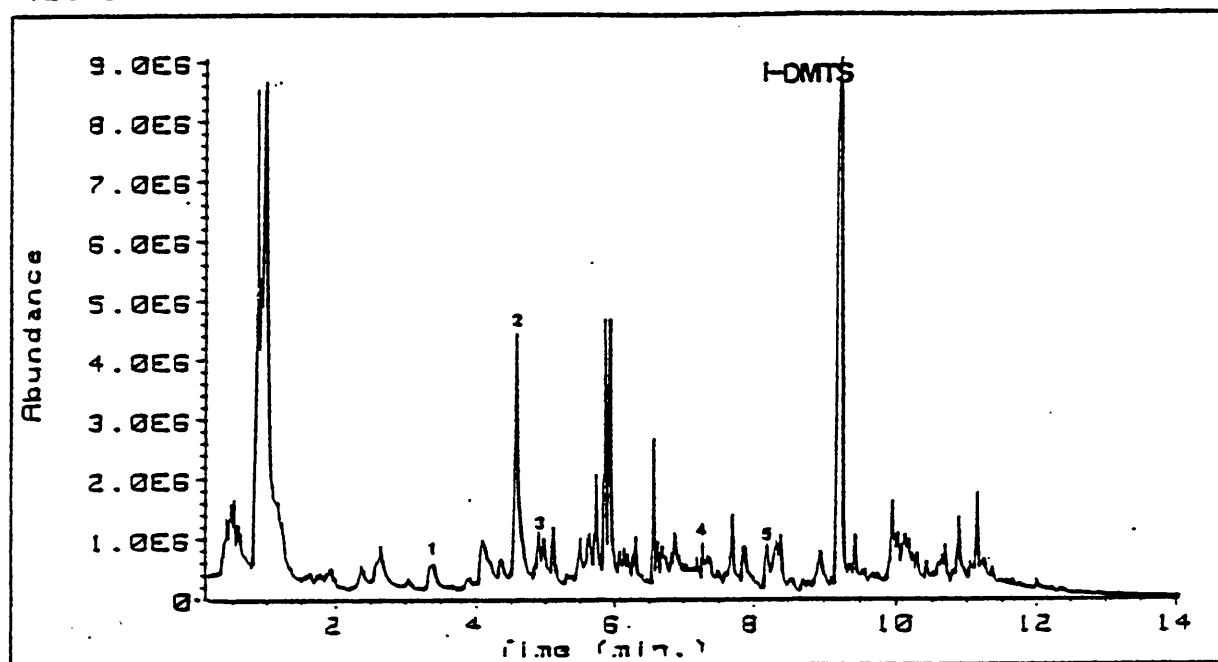
Table 5.1:

Group 1				
$H_2^*$	$CH_4^*$	$Me_2SiH_2$ [1]	$Me_3SiH$ [2]	$Me_4Si$ [3]
Group 2				
$Me_3SiSiMe_3$ [4]	$Me_2Si \begin{array}{c} \diagup \diagdown \\ \diagdown \diagup \end{array} SiHMe$ [5]	$Me_3Si \begin{array}{c} \diagup \diagdown \\ \diagdown \diagup \end{array} SiHMe_2$ [6]	$Me_2Si \begin{array}{c} \diagup \diagdown \\ \diagdown \diagup \end{array} SiMe_2$ [7]	
Group 3				
$Me_3SiSiSiSiMe_3$ [8]	$Me_2Si \begin{array}{c} \diagup \diagdown \\ \diagdown \diagup \end{array} SiHMe_2$ [9]	$Me_2Si \begin{array}{c} \diagup \diagdown \\ \diagdown \diagup \end{array} SiHMe_2$ [10]		
$Me_2Si \begin{array}{c} \diagup \diagdown \\ \diagdown \diagup \end{array} SiHMe_2$ [11]	$Me_2Si \begin{array}{c} \diagup \diagdown \\ \diagdown \diagup \end{array} SiHMe_2$ [12]	$Me_2Si \begin{array}{c} \diagup \diagdown \\ \diagdown \diagup \end{array} SiHMe_2$ [13]		
$Me_2Si \begin{array}{c} \diagup \diagdown \\ \diagdown \diagup \end{array} SiHMe_2$ [14]	$Me_2Si \begin{array}{c} \diagup \diagdown \\ \diagdown \diagup \end{array} SiHMe_2$ [15]	$Me_2Si \begin{array}{c} \diagup \diagdown \\ \diagdown \diagup \end{array} SiHMe_2$ [16]		
Group 4				
$Me_2Si \begin{array}{c} \diagup \diagdown \\ \diagdown \diagup \end{array} SiHMe_2$ [19]	$MeHSi \begin{array}{c} \diagup \diagdown \\ \diagdown \diagup \end{array} Si \begin{array}{c} \diagup \diagdown \\ \diagdown \diagup \end{array} SiHMe_3$ [20]			
$Me_2Si \begin{array}{c} \diagup \diagdown \\ \diagdown \diagup \end{array} SiHMe_2$ [21]	$MeHSi \begin{array}{c} \diagup \diagdown \\ \diagdown \diagup \end{array} Si \begin{array}{c} \diagup \diagdown \\ \diagdown \diagup \end{array} SiHMe_3$ [22]			
$Me_2Si \begin{array}{c} \diagup \diagdown \\ \diagdown \diagup \end{array} SiHMe_2$ [23]	$Me_2Si \begin{array}{c} \diagup \diagdown \\ \diagdown \diagup \end{array} Si \begin{array}{c} \diagup \diagdown \\ \diagdown \diagup \end{array} SiHMe_2$ [24]			

\*see section (IV)-Q8/MS-Sealed tube experiments

### (ii) 2,3-dimethyl-1,3-butadiene/i-DMTS experiments

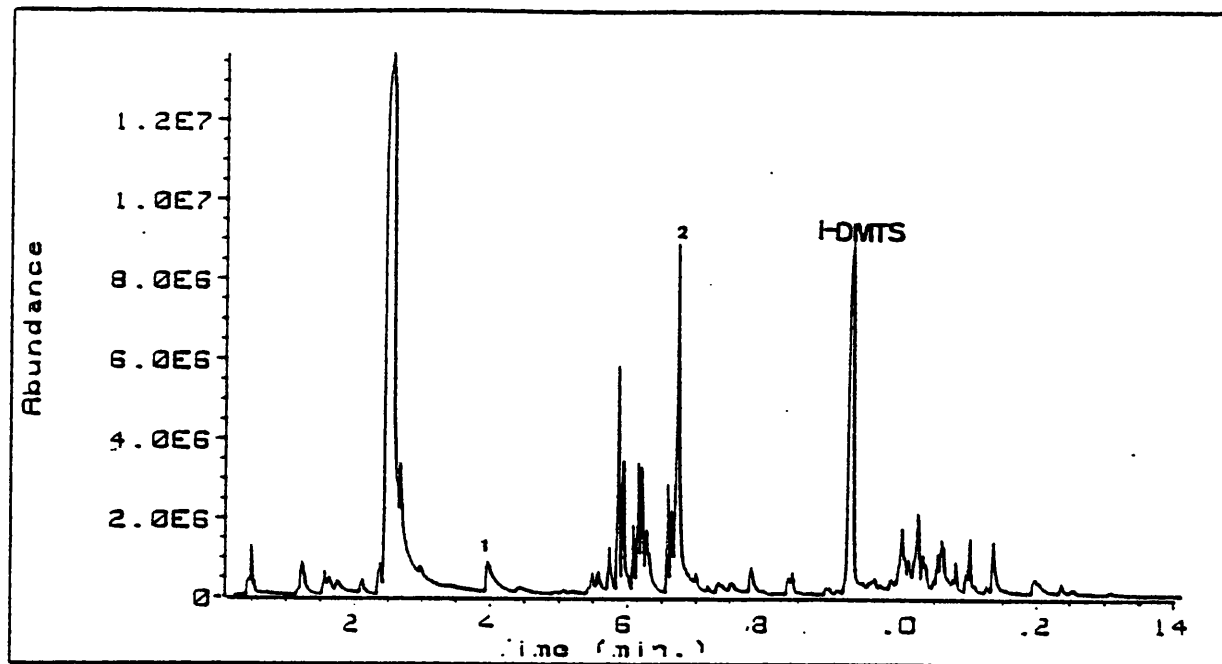
A 5:1 mixture of 2,3-dimethyl-1,3-butadiene and i-DMTS was pyrolysed between 570-650°C using the liquid injection technique. The yields of 3MS and high pressure products were reduced, but the yields of low pressure products were not affected. Products unique to this pyrolysis are shown in TIC 3:



The major intermediate trapped in this pyrolysis was dimethylsilylene ( $\text{Me}_2\text{Si}:$ ) with smaller amounts methylsilene, dimethylsilene and trimethyl(methyl)silylene. Other complex silylenes were also trapped ([5] & [6]).

### (iii) Toluene/i-DMTS experiments

A 10:1 mixture of toluene and i-DMTS was pyrolysed between 570-650°C using the liquid injection technique. Toluene had little effect on product composition but it did appear to slightly suppress 3MS and the products formed at high sample pressures. Products unique to this pyrolysis are shown in TIC 4:

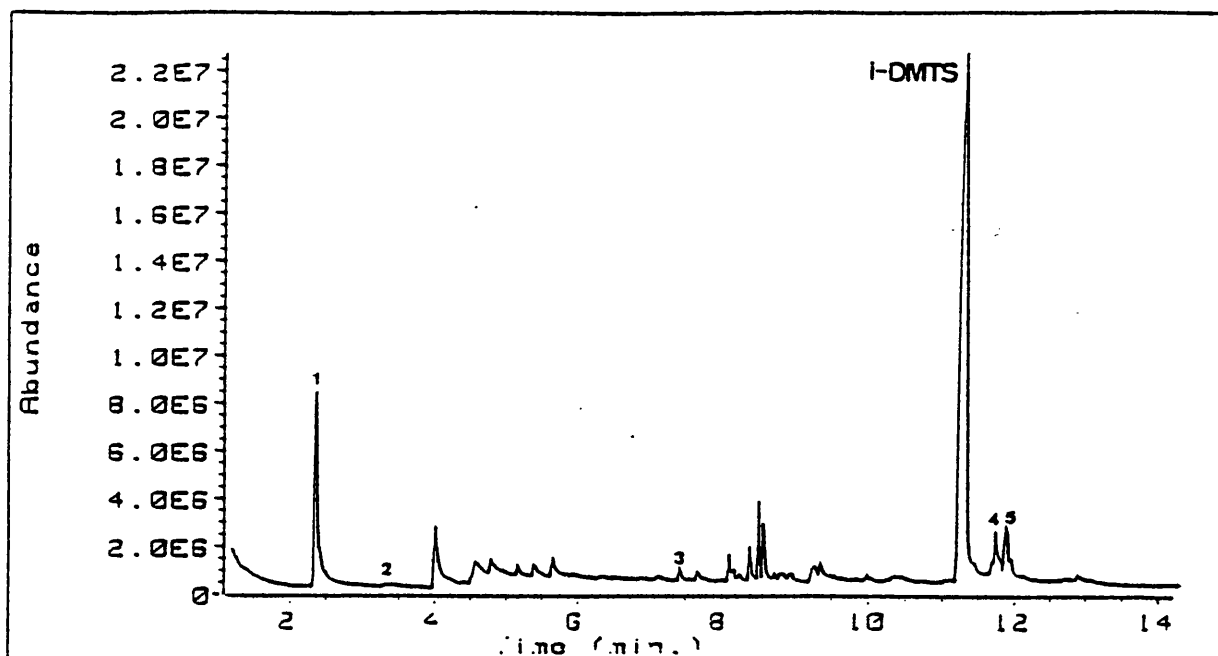


TIC 4: [1] ethylbenzene (ETHB), [2] benzyltrimethylsilane (TMSB).

The major trapping products of this pyrolysis were benzyltrimethylsilane (TMSB) and ethylbenzene (ETHB) arising from trimethylsilyl ( $\text{Me}_3\text{Si}\cdot$ ) and methyl radicals ( $\cdot\text{CH}_3$ ) respectively.

#### (iv) Methylchloride/i-DMTS experiments

i-DMTS was pyrolysed in an excess of methylchloride ( $\text{MeCl}$ ) between  $560\text{--}630^\circ\text{C}$ .  $\text{MeCl}$  was injected via the gas sample valve whilst i-DMTS was introduced using the liquid injection technique. Low pressure products were not affected but 3MS and high pressure products were suppressed. Products unique to this pyrolysis are shown in TIC 5:



TIC 5: [1]  $\text{Me}_3\text{SiCl}$ , [2]  $\text{Me}_2\text{SiCl}_2$ , [3]  $\text{Me}_3\text{Si}^{\text{H}}\text{SiMe}$   
 [4]  $\text{Me}_3\text{Si}-\text{Si}(\text{Me})_2-\text{SiMe}_2$ , [5]  $\text{Me}_3\text{Si}-\text{Si}(\text{Me})_2-\text{Si}(\text{Me})_2-\text{SiMe}_2$ .

The major product of this pyrolysis was trimethylchlorosilane formed by chlorine abstraction from  $\text{MeCl}$  by  $\text{Me}_3\text{Si}\cdot$  radicals. Two interesting products of this pyrolysis were [4] & [5]; these were non-chlorine containing cyclic carbosilanes not present in the i-DMTS pyrolyses.

### (III) Kinetic-SFR Results

#### (i) i-DMTS experiments

i-DMTS was pyrolysed between 570-650°C using the liquid injection technique. First order rate constants were measured for 3MS formation. The Arrhenius parameters for the formation of 3MS are given in table 5.2. Rate constants for methane, 2MS and 4MS were also measured but these gave scattered Arrhenius plots. A typical gas chromatogram for a kinetic experiment is shown in figure 5.1.

Table 5.2: Kinetic results for the formation of 3MS from i-DMTS.

Product	$\log (A/s^{-1})$	$E_a$ ( $\text{kJmol}^{-1}$ )	$k_{(620^\circ\text{C})}(s^{-1})$
$\text{Me}_3\text{SiH}$	$16.4 \pm 0.8$	$294.3 \pm 15$	0.153

The Arrhenius plot for the formation of 3MS is shown in figure 5.2. The Arrhenius plot is curved but if only the low temperature points are considered the Arrhenius parameters in table 5.2 result.

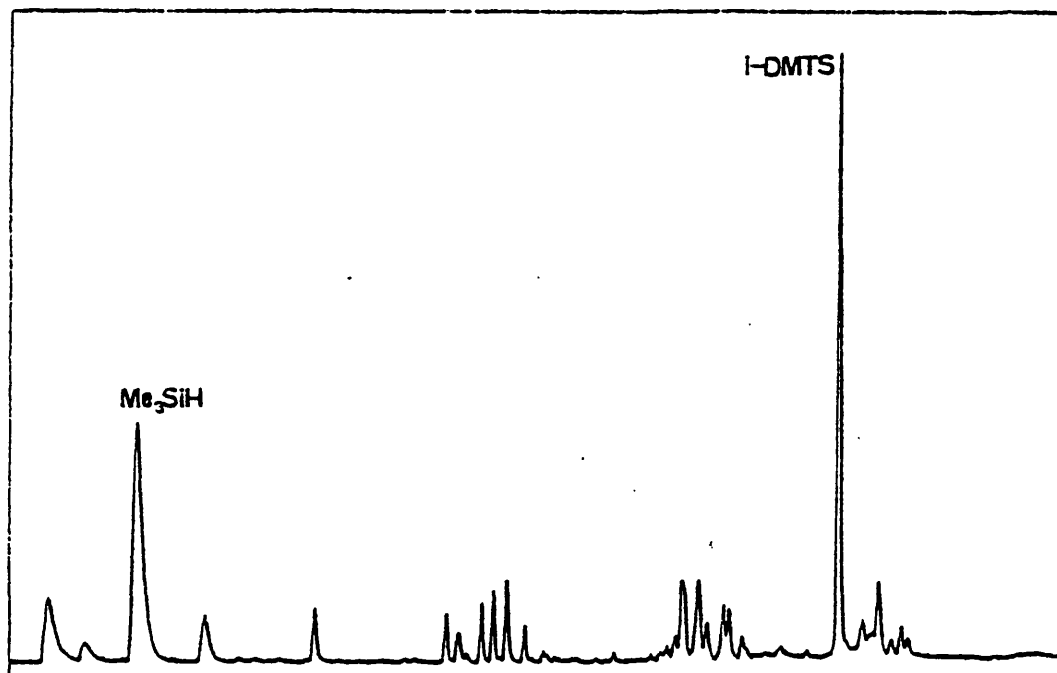


Figure 5.1: Gas chromatogram for the pyrolysis of i-DMTS at 607°C.

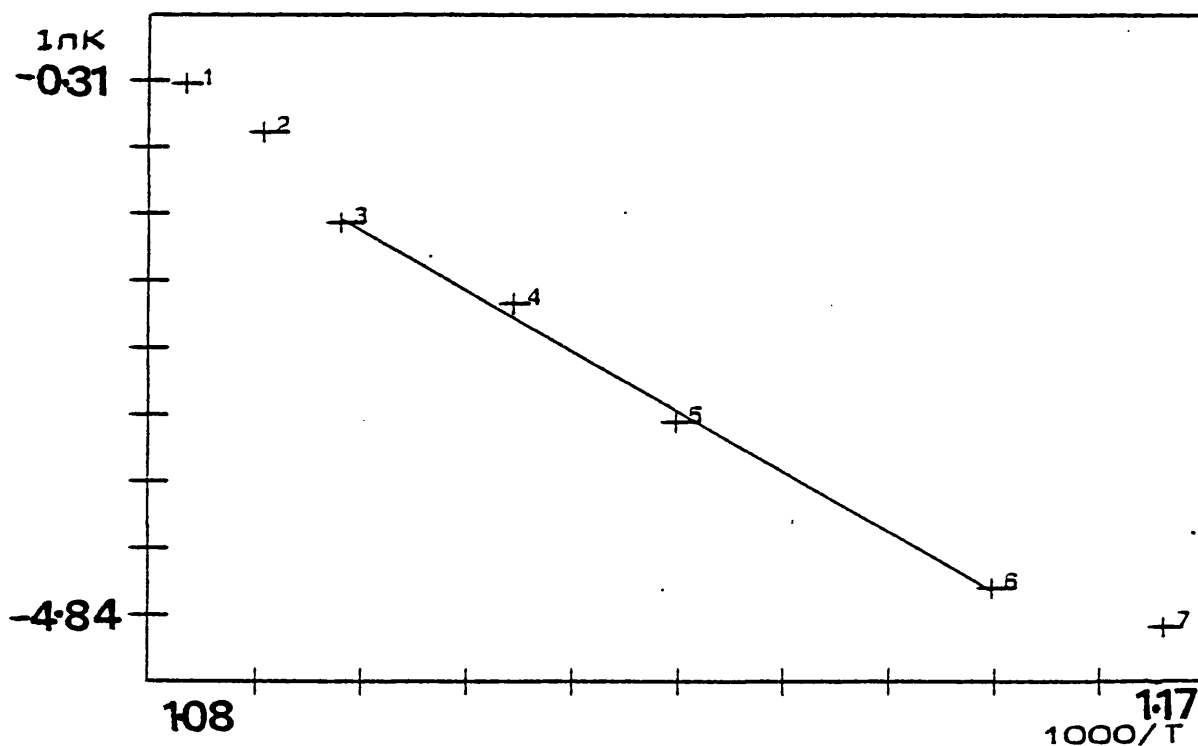


Figure 5.2: Arrhenius plot for the formation of 3MS

(ii) 2,3-dimethyl-1,3-butadiene/i-DMTS experiments

A 5:1 mixture of toluene and i-DMTS was pyrolysed between 570-650°C using the liquid injection technique. First order rate constants were measured for the formation of 1,1,3,4-tetramethyl-1-silacyclopent-3,4-ene (ADD 1) (fig. 5.3). The Arrhenius parameters for the formation of this product are given in table 5.3.

Table 5.3: Kinetic results for 2,3-dimethyl-1,3-butadiene/i-DMTS experiments.

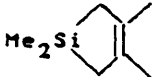
Product	$\log (A/s^{-1})$	$E_a (kJ\ mol^{-1})$	$k_{(620^\circ C)} (s^{-1})$
	$17.9 \pm 1.7$	$330 \pm 29$	0.039

Figure 5.4 shows the Arrhenius plot for the formation of ADD 1.

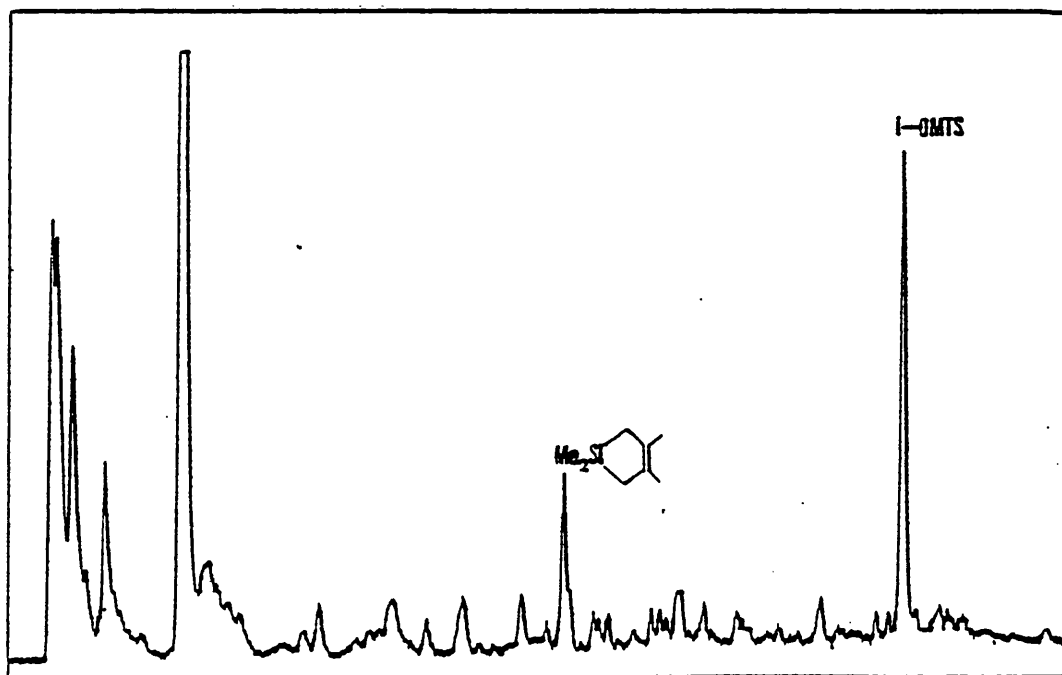
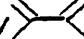


Figure 5.3: Gas chromatogram for the pyrolysis of i-DMTS/ at 626°C.

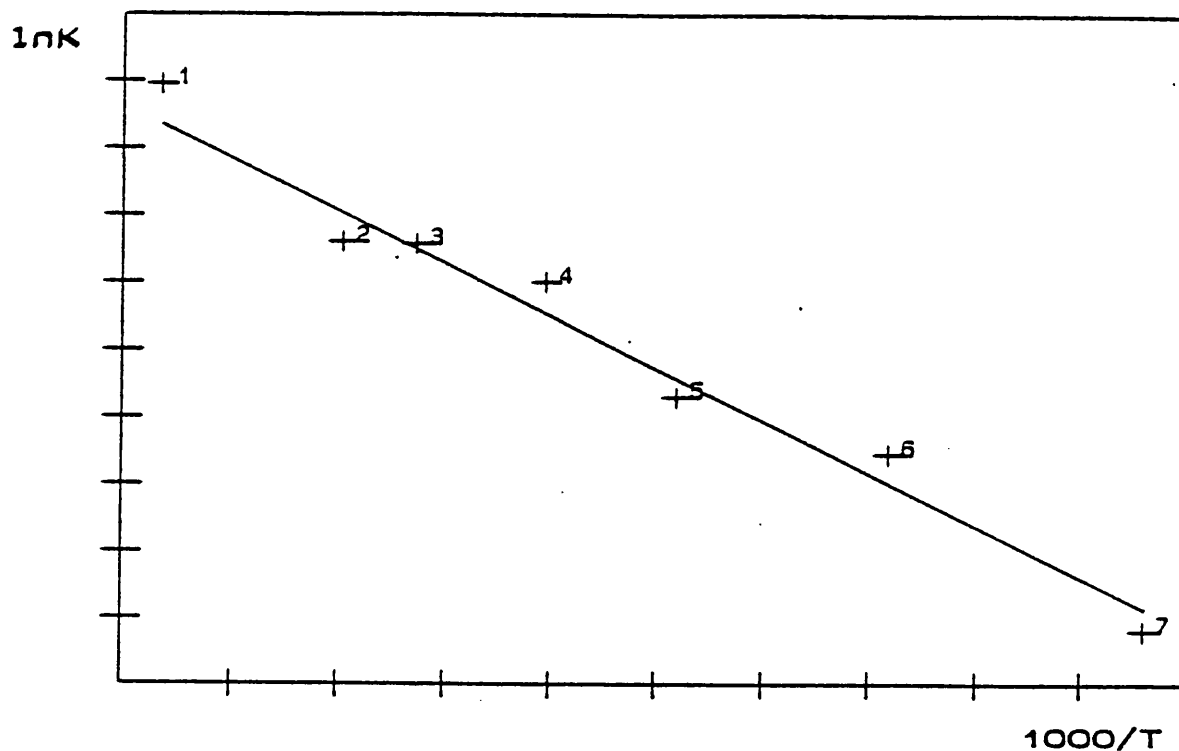


Figure 5.4: Arrhenius plot for the formation of ADD 1

Kinetic measurements were difficult to obtain due to the complexity of the reaction mixture, the secondary reactions of 2,3-dimethyl-1,3-butadiene interfering with the pyrolysis of *i*-DMTS.

### (iii) Toluene/*i*-DMTS experiments

A 5:1 mixture of toluene and *i*-DMTS was pyrolysed between 570-650°C using the liquid injection technique. First order rate constants were measured for the formation of the products shown in the gas chromatogram (fig. 5.5). Table 5.4 gives the Arrhenius parameters for the formation of these products.

Table 5.4: Kinetic results for the *i*-DMTS/toluene experiments.



Product	$\log A \text{ (s}^{-1}\text{)}$	$E_a \text{ (kJmol}^{-1}\text{)}$	$k_{(620^\circ\text{C})}$
$\text{Me}_3\text{SiH}$	$16.3 \pm 0.2$	$291.6 \pm 3$	0.175
$\text{Me}_3\text{Si-}$ 	$16.6 \pm 0.6$	$303.0 \pm 10$	0.075
$\text{CH}_4$	$17.9 \pm 0.4$	$326.0 \pm 7$	0.068
$\text{CH}_3$ 	$15.7 \pm 0.7$	$306.5 \pm 11$	$5.9 \times 10^{-3}$

Figure 6 shows the Arrhenius parameters for the formation



of 3MS.

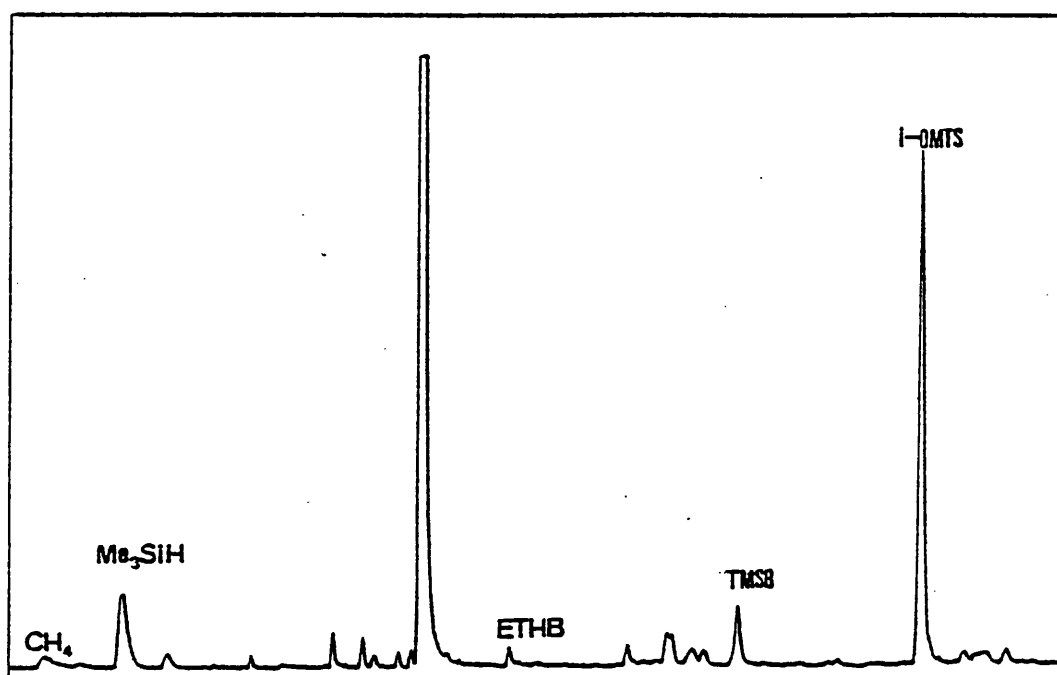


Figure 5.5: Gas chromatogram for the pyrolysis of i-DMTS/Toluene at 595°C.

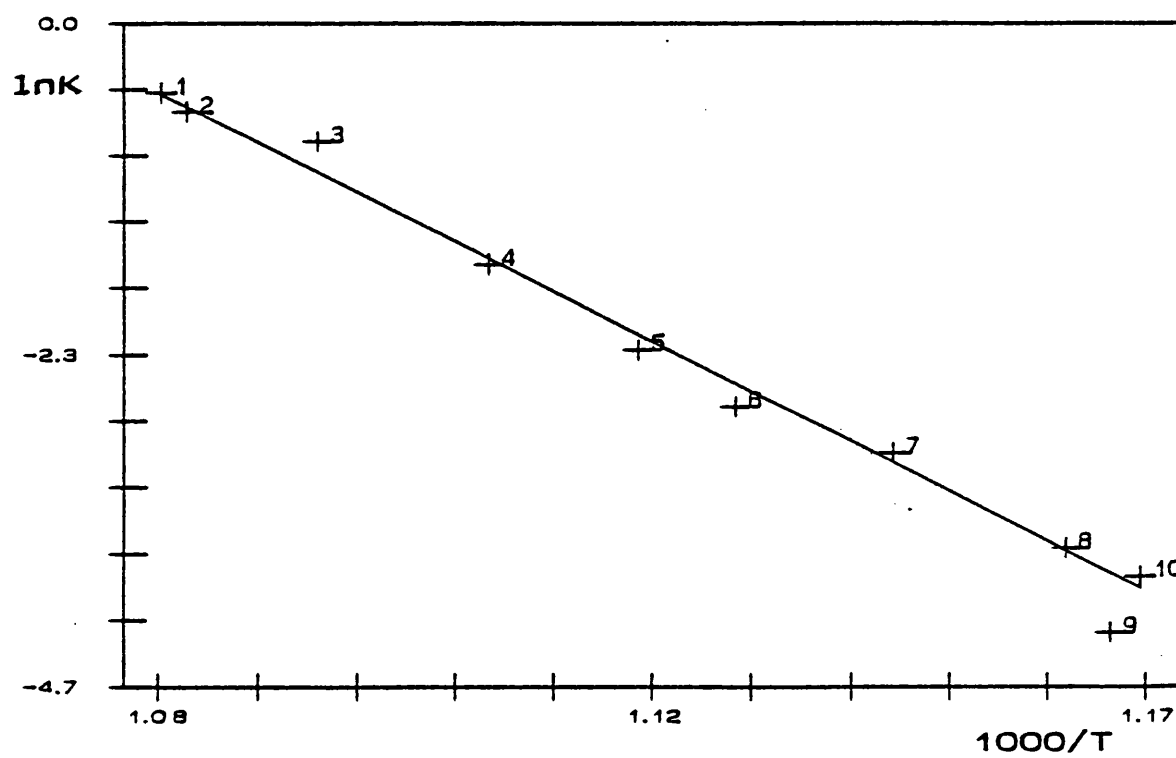


Figure 5.6: Arrhenius plot for the formation of 3MS in the presence of toluene.

#### (IV) Q8/MS-Sealed Tube Pyrolysis Results

i-DMTS was pyrolysed in a sealed tube at 550°C for 3.0 minutes. The time scale for the pyrolysis was calculated from the Arrhenius parameters for the formation of 3MS given by the kinetic-SFR experiments.

At 550°C:  $k = 5.25 \times 10^{-3} \text{ (s}^{-1}\text{)}$ ,  $t_{1/2} = 3.00 \text{ mins.}$

The Q8/MS revealed a large amount of hydrogen was produced in the pyrolysis. A smaller amount of methane is also formed.

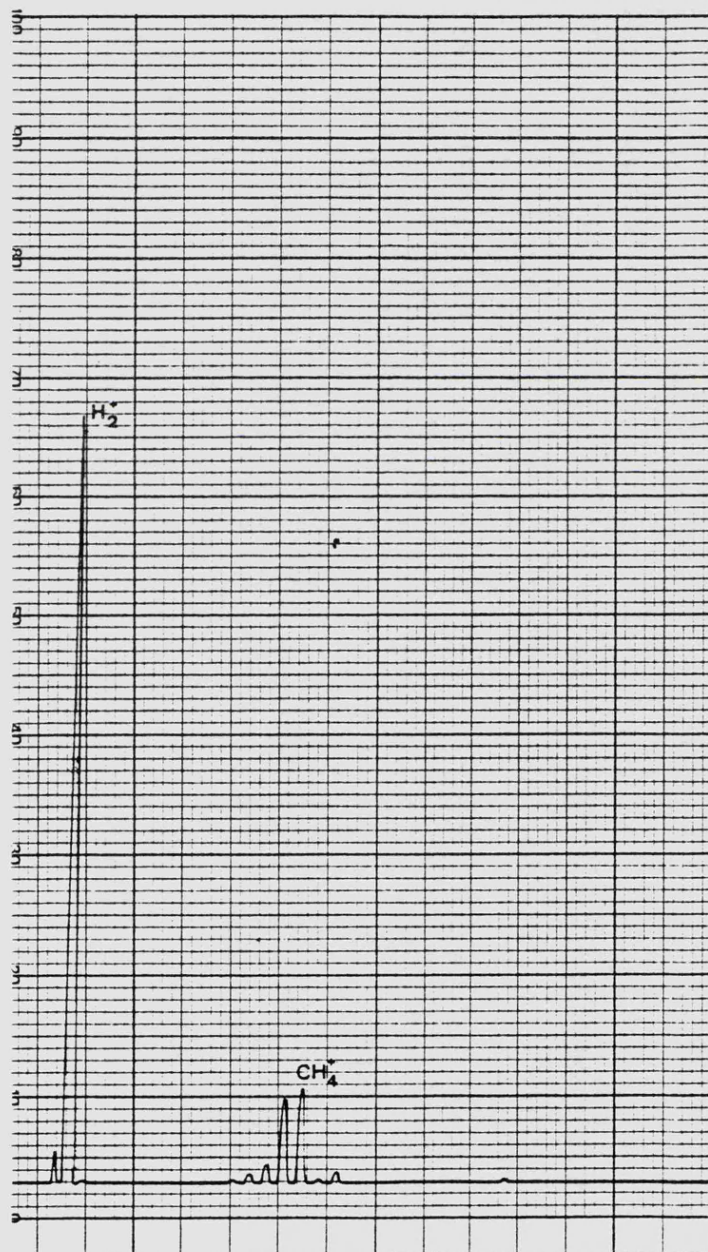


Figure 5.7: Mass Spectrum of  $\text{H}_2$  and  $\text{CH}_4$  from the sealed tube pyrolysis of i-DMTS at 550°C.

## (V) Discussion

It is believed that chemistry similar to that in the pyrolysis of n-DMTS is involved in the formation of the monosilanes, methane and major trapping products. The Arrhenius parameters for the formation of these products are of similar magnitude in both cases; the reactions leading to their formation are given in scheme 4.2, Chapter 4.

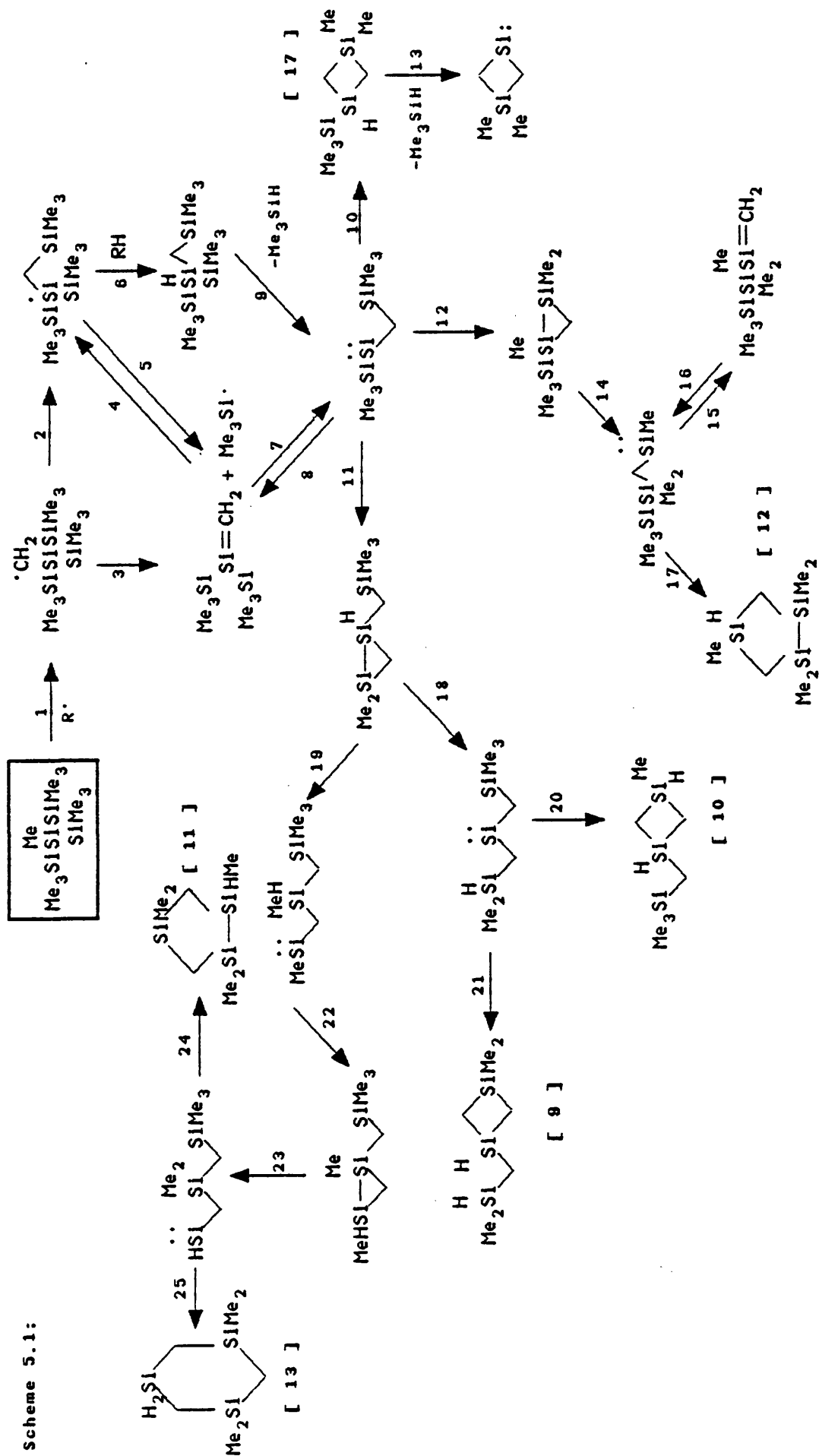
The major products containing more than one silicon atom in the low pressure pyrolyses were isomeric cyclic carbosilanes. Kinetic measurements were not performed on these products because they were:- (i) poorly resolved, (ii) formed by complex mechanisms that were probably not first order, (iii) susceptible to secondary decomposition reactions at these high temperatures<sup>6</sup>.

Scheme 5.1 shows the reactions leading to the formation of the major low pressure products.

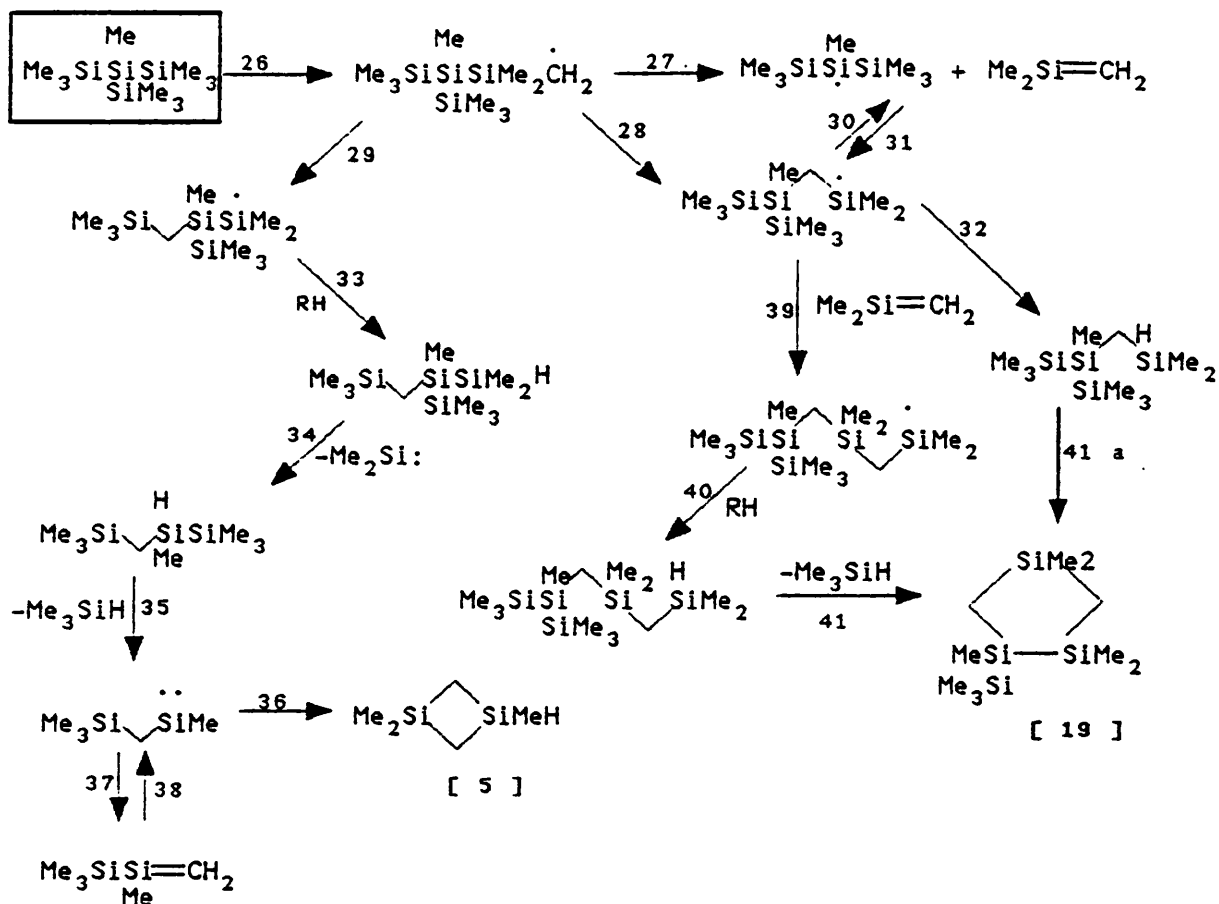
Initial Si-Si bond cleavage is followed by hydrogen abstraction from the methyl group on the central silicon atom (1). All the reactions in scheme 5.1 have precedents in organosilicon chemistry and can be summarised into general types:- (i) 1,2 Shifts (2)<sup>7</sup>, (ii) hydrogen abstractions (6), (iii) radical dissociations (3)<sup>1</sup>, (iv) silene-silylene interconversions via a 1,2-trimethylsilyl shifts (7, 8)<sup>4</sup>, (v) disilirane formation via internal Si-C (21), C-H (11), Si-H (22) insertions<sup>8</sup>, (vi) disilirane ring opening reactions to form silylenes via 1,2-H (18) and 1,2-Me (14, 23) shifts<sup>8</sup>, (vii) ring closure reactions via internal C-H (10, 17, 20, 21, 25) and Si-C (24) insertions<sup>8</sup>, (viii) silylene elimination via a 1,2 H-shifts (9, 13)<sup>9</sup>. Evidence for reaction (13) comes from the trapping of the silylene in the 2,3-dimethyl-1,3-butadiene experiments ([6] TIC 3).

Hydrogen abstraction from a terminal methyl group (35) will lead to the reactions in scheme 5.2.

Scheme 5.1:



Scheme 5.2:



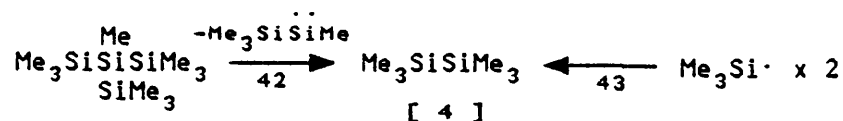
The carbon centred radical formed after initial hydrogen abstraction can either (i) dissociate into  $\text{Me}_2\text{Si}=\text{CH}_2$  and a bis-trimethylsilyl(methyl)silyl radical (27), (ii) undergo a 1,2-shift (28) or (iii) undergo a 1,3-shift (29).

The 1,3 shift is followed by hydrogen abstraction (33). A 1,2 H-shift on the resulting carbosilane will eliminate 3MS and yield a silylene (34). This silylene may isomerise to a silene via a 1,2-trimethylsilyl shift (37) or ring close via an internal C-H insertion (36) to yield product [5]. These reactions being unimolecular in nature will be favoured by low sample pressure pyrolyses<sup>4</sup>. Evidence for reaction (35) comes from the trapping of the silylene in the 2,3-dimethyl-1,3-butadiene experiments.

The radical formed via a 1,2-shift may dissociate to form  $\text{Me}_2\text{Si}=\text{CH}_2$  and a bis-trimethylsilyl(methyl)silyl radical (30). At higher sample pressures, however, it may undergo silene addition to yield a new silicon centred radical (39). This radical will then abstract hydrogen to yield a linear carbosilane (40) which can undergo cyclisation with elimination of 3MS (41) to yield product [19]<sup>2</sup>. The linear carbosilane formed by reaction (32) may also cyclise with the

elimination of hydrogen (41 a) to yield product [19].

HMDS could be formed via  $\text{Me}_3\text{Si}\cdot$  radical combination or the elimination of trimethylsilyl(methyl)silylene via a 1,2-trimethylsilyl shift:

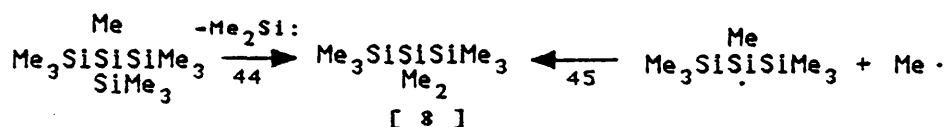


The major intermediate in the pyrolysis was  $\text{Me}_3\text{Si}\cdot$  and only a small quantity of trimethylsilyl(methyl)silylene was trapped in the 2,3-dimethyl-1,3-butadiene experiments, therefore it is thought that  $\text{Me}_3\text{Si}\cdot$  radical combination is the major source of HMDS.

The isomerisation of HMDS to ISO-HMDS will have an appreciable rate constant in the pyrolysis temperature range<sup>1</sup>. Therefore the source of ISO-HMDS is thought to be the decomposition of HMDS (see Chapter 1, scheme 1.2).

1,1,3,3-tetramethyl-1,3-disilacyclobutane is thought to be formed by the head to tail dimerisation of  $\text{Me}_2\text{Si}=\text{CH}_2$ <sup>10</sup> ( see reaction (46), Chapter 3). The major source of  $\text{Me}_2\text{Si}=\text{CH}_2$  reaction (27), other minor sources being reaction (30) and  $\text{Me}_3\text{Si}\cdot$  radical disproportionation<sup>11</sup> (see reaction (47), Chapter 3).

OMTS could be formed by  $\text{Me}_2\text{Si}:$  elimination from i-DMTS or from  $\cdot\text{CH}_3$  and bis-trimethylsilyl(methyl)silyl radical combination.



The abundance of  $\cdot\text{CH}_3$  and bis-trimethylsilyl(methyl)silyl radicals suggest that their combination is the major source of OMTS. This argument is supported by the Arrhenius parameters for the formation of ADD 1 which are not in the range expected for a unimolecular elimination of  $\text{Me}_2\text{Si}:$  from i-DMTS<sup>12</sup>.

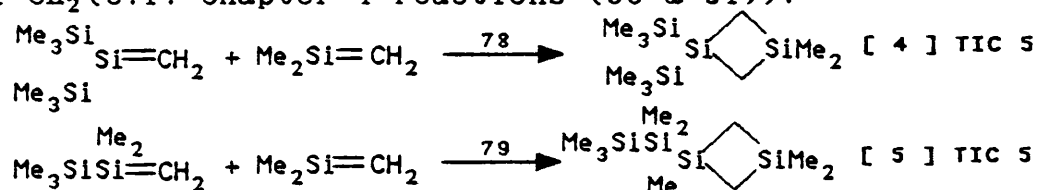
The formation of product [19] has already been rationalised by the high pressure reactions leading to the cyclisation elimination reaction, other high pressure reactions are thought to lead to the remainder of the products.

Scheme 3.8, Chapter 3, shows the series of reactions leading to the formation of [14]. The silene is formed in reaction (37) and the radical is formed during the isomerisation of HMDS.

The remainder of the products are multiple disilacyclobutane ring isomers. The mechanism for their formation is not immediately obvious but a simple solution could be the head to tail dimerisation of differently substituted silenes (scheme 3.9, Chapter 3)<sup>13</sup>. The silenes shown in scheme 3.9, Chapter 3 undoubtedly have complex mechanisms of formation explaining why they are not trapped in the presence of 2,3-dimethyl-1,3-butadiene. It is also known that the addition of silenes to butadienes is slow when compared to dimerisation. Scheme 3.9 Chapter 3 is only a suggestion as these complex products would be formed a long way down the reaction coordinate.

The MeCl/i-DMTS experiments revealed the nature of some of the radicals involved in the pyrolysis. The most abundant radical was Me<sub>3</sub>Si· with smaller amounts of the trimethylsilyl-(dimethylsilyl)methane radical ([3] TIC 5). Dimethyl-dichlorosilane ([2] TIC 5) is thought to be formed via the abstraction of chlorine from MeCl by Me<sub>2</sub>Si:<sup>14</sup>. The resulting radical would abstract another chlorine to yield Me<sub>2</sub>SiCl<sub>2</sub>.

Two interesting non-chlorine containing products in the MeCl pyrolysis were [4] & [5] (TIC 5). These disilacyclobutane compounds are thought to arise from the reaction of the silenes formed in reactions (3) and (15) to Me<sub>2</sub>Si=CH<sub>2</sub> (c.f. Chapter 4 reactions (90 & 91)):



These reactions are possible in the MeCl experiments as the reaction mixture is not as complex i.e. there are less radicals present. Low reaction pressure isomerisations were still possible yielding the characteristic carbosilanes in high yields (scheme 2). [4] and [5] (TIC 5) are not present in the i-DMTS pyrolyses as they would be rapidly consumed by radical addition<sup>15</sup>.

## (VI) Summary

The pyrolysis of i-DMTS has more features in common with the pyrolyses of OMTS and n-DMTS than HMDS as the major

products containing more than one silicon atom were cyclic carbosilanes. HMDS yielded a linear carbosilane as its major product.

Comparing the pyrolyses of OMTS, n-DMTS and i-DMTS it can be seen that the low pressure reactions of these compounds are very consistent. Although the low pressure products produced in the pyrolyses of n-DMTS and i-DMTS are the same, it is noticed that the relative yields of each is different. This result can be linked to the different silenes initially produced at low sample pressures (i-DMTS scheme 5.2; reaction (12), n-DMTS Chapter 4, scheme 4.3 reactions (18 & 20)).

The high sample pressure reactions of OMTS, n-DMTS and i-DMTS are significantly different. The high pressure pyrolyses of OMTS strongly favours the cyclisation/elimination reactions, the formation of multiple disilacyclobutane ring compounds being a relatively minor process. The high pressure reactions of n-DMTS strongly favour the formation of the multiple disilacyclobutane ring compounds, the cyclisation/elimination reactions do take place but are minor reaction pathways. The difference in the high pressure reactions is thought to arise from the difference in chain length of the linear carbosilane precursor for the cyclisation/elimination reactions. For n-DMTS the linear carbosilanes are too long for the ring closing reactions to be efficient. Therefore, the geometry of the transition state for the cyclisation/elimination reaction strongly affects the rate of this reaction.

From the product distribution for i-DMTS it is noticed that neither the cyclisation/elimination reactions nor the formation of multiple disilacyclobutane ring compounds is dominant. The cyclisation/elimination reactions should be feasible for i-DMTS as OMTS because the chain length of the linear carbosilane precursors is the same. However, in the case of i-DMTS there is a bulky trimethylsilyl group present on the terminal silicon atom of the carbosilane precursors, this may affect the geometry of the transition state thus lowering the probability of these reactions taking place. This obstacle to the cyclisation/elimination reaction could lead to the increase in formation of the multiple disilacyclobutane ring compounds.

Therefore the high pressure reactions of i-DMTS can be said



to be a hybrid of the OMTS and n-DMTS pyrolyses. the geometry of the transition states for the cyclisation/elimination reactions playing an important role in determining whether this reaction is favourable. The geometry of the transition state being dictated by the chain length and substituents on the linear carbosilane precursor.

The pyrolysis mechanisms of OMTS, n-DMTS and i-DMTS are very consistent. The major product (3MS) and trapped intermediates are the same in all three pyrolyses. The low pressure pyrolyses lead to similar reactions while the high pressure reactions are different, the cyclisation/elimination reactions appearing to be quite general for all three compounds but of different importance in each case.

#### (VII) Acknowledgements

I would like to thank Dr. R. Taylor of Dow Corning for preparing the iso-decamethyltetrasilane. Thanks also to Paul Gibbs, David Walmsley and Geraint Morgan their for help with the pyrolysis experiments.

#### (VIII) References

- (1) I.M.T. Davidson, A.V. Howard, *J. Chem. Soc., Faraday Trans. I*, 1975, 71, 69.
- (2) B.N. Bortolin, I.M.T. Davidson, D. Lancaster, T. Simpson, D.A. Wild, *Organometallics*, 1990, 9, 281.
- (3) I.M.T. Davidson, T. Simpson, R. Taylor in '*Frontiers of Organosilicon Chemistry*' Eds. A.R. Bassindale & P.P. Gaspar,, 1991, Section II, p 89.
- (4) T.J. Barton, G.T. Burns, S.A. Burns, *Organometallics*, 1982, 1, 210.
- (5) M.P. Clarke, I.M.T. Davidson, M.P. Dillon, *J. Chem. Soc., Chem. Commun.*, 1988, 1251.
- (6) I.M.T. Davidson, G. Fritz, F.T. Lawrence, A.E. Matern, *Organometallics*, 1982, 1, 1453; N. Auner, I.M.T. Davidson, S. Ijadi-Maghsoodi, F.T. Lawrence, *Organometallics*, 1986, 5, 431.
- (7) C. Eaborn, J.M. Simmie, *J. Chem. Soc., Chem. Commun.*,

- 1968, 1426.
- (8) T.J. Barton, S.A. Jacobi, *J. Am. Chem. Soc.*, 1980, 102, 7979; I.M.T. Davidson, *J. Organomet. Chem.*, 1988, 341, 255.
  - (9) I.M.T. Davidson, J.I. Matthews, *J. Chem. Soc., Faraday Trans. I*, 1976, 72, 1403.
  - (10) L.E. Gusel'nikov, M.C. Flowers, *J. Chem. Soc., Chem. Commun.*, 1967, 864.
  - (11) Th. Brix, U. Paul, P. Potzinger, B. Reimann, *J. Photochem. Photobiol., A: Chem.*, 1990, 54, 19.
  - (12) I.M.T. Davidson, K.J. Hughes, S. Ijadi-Maghsoodi, *Organometallics*, 1987, 6, 639.
  - (13) I.M.T. Davidson, R.J. Scampton, *J. Organomet. Chem.*, 1984, 271, 249.
  - (14) M.P. Clarke, M.R. Conqueror, I.M.T. Davidson, G.H. Morgan, unpublished results.
  - (15) E. Bastian, P. Potzinger, A. Ritter, H.-P. Schuchmann, C. von Sonntag, G. Weddle, *Ber. Bunsen. Phys. Chem.*, 1980, 84, 56.

## Chapter 6

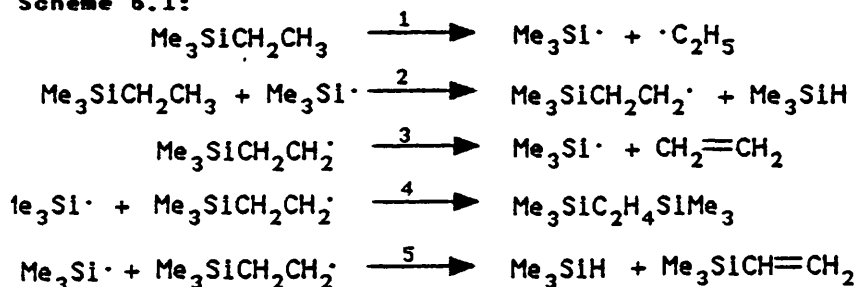
### The Pyrolysis of 2,2-Diethylhexamethyltrisilane

#### (I) Introduction

The pyrolysis of 2,2-diethylhexamethyltrisilane (DEHMTS) has not been previously studied. A knowledge of the pyrolysis mechanisms of octamethyltrisilane (OMTS)<sup>1</sup>, n-decamethyltetrasilane (n-DMTS) and iso-decamethyltetrasilane (i-DMTS)<sup>2</sup> should help elucidate the thermal breakdown mechanism of DEHMTS. The low sample pressure pyrolysis mechanisms of OMTS, n-DMTS and i-DMTS are very consistent, the major products arising via similar reactions. The high sample pressure reactions of OMTS, n-DMTS and i-DMTS are different, the importance of the cyclisation/elimination reactions being different for each compound studied. Therefore, the low pressure reactions of DEHMTS will be expected to be similar to those of OMTS, but it will be interesting to see how important the high sample pressure cyclisation/elimination reactions will be. The presence of bulky ethyl groups in DEHMTS may reduce the feasibility of the cyclisation/elimination reactions as the ethyl groups could cause steric hindrance in the transition state.

The presence of ethyl groups may open other reaction pathways not accessible to permethylated oligosilanes. The pyrolysis of trimethylethylsilane (TMES)<sup>3</sup> shows a different reaction course to that of tetramethylsilane (4MS)<sup>4</sup>. The major products of the pyrolysis of TMES are ethene, trimethylsilane (3MS) and vinyltrimethylsilane (VMTS). Scheme 6.1 shows reasonable reactions leading to their formation:

Scheme 6.1:



The main process of the thermolysis is formally the dehydrosilylation reaction  $\text{Me}_3\text{SiCH}_2\text{CH}_3 \rightarrow \text{Me}_3\text{SiH} + \text{CH}_2=\text{CH}_2$ . It

was concluded that the dehydrosilylation reaction involves a radical chain sequence (1-4). VMTS arises via the radical intermediate  $\cdot\text{C}_2\text{H}_4\text{SiMe}_3$  (5).

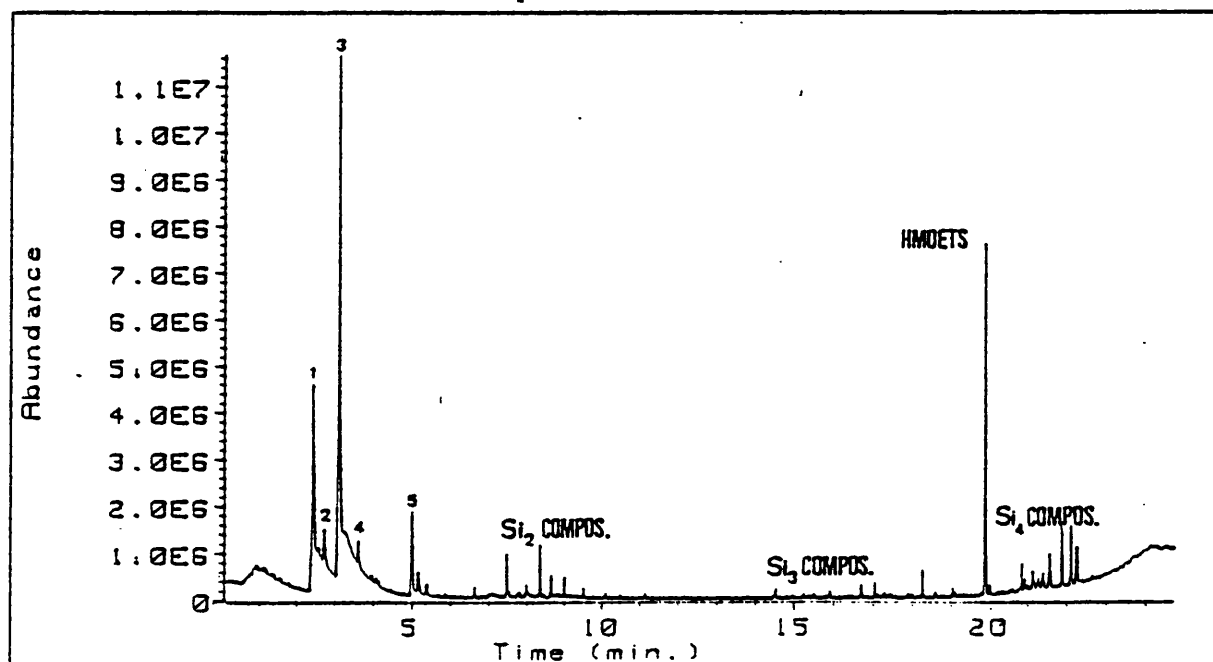
DEHMTS was pyrolysed on the GC/MS-SFR apparatus. Product identification was by mass spectral analysis and comparative retention time tests on known samples<sup>5</sup>.

Further mechanistic information was gained from kinetic measurements for major product formation. Experimental Arrhenius parameters were compared with those calculated by numerical integration using both the KINAL and ACUCHEM software packages<sup>6</sup>.

## (II) GC/MS-SFR Results

### (i) DEHMTS pyrolysis experiments

DEHMTS was pyrolysed between 580-633°C using the liquid injection technique. The volumes of DEHMTS injected were 0.06-0.10  $\mu\text{l}$ . The products of a typical high sample pressure/high temperature experiment are shown in TIC 1. The major products are numbered in TIC 1; the minor products were di-, tri- and tetra-silicon compounds:



TIC 1: [1]  $\text{CH}_2=\text{CH}_2$ , [2]  $\text{Me}_2\text{SiH}_2$ , [3]  $\text{Me}_3\text{SiH}$ , [4]  $\text{Me}_4\text{Si}$ , [5]  $\text{Me}_3\text{SiCH}=\text{CH}_2$   
vol = 0.1  $\mu\text{l}$ , temp = 633°C.

The major products of the pyrolysis were ethene [1], trimethylsilane (3MS) [3] and vinyltrimethylsilane (VTMS) [5].

Smaller amounts of dimethylsilane (2MS) [2] and tetramethylsilane (4MS) [4] were also formed.

The products identified from the pyrolysis of DEHMTS are shown in table 6.1:

Table 6.1:

Major Products				
$\text{CH}_2=\text{CH}_2$	$\text{Me}_2\text{SiH}_2$	$\text{Me}_3\text{SiH}$	$\text{Me}_4\text{Si}$	$\text{Me}_3\text{SiCH}=\text{CH}_2$
[1]	[2]	[3]	[4]	[5]
Minor products				
$\text{H}_2^*$	$\text{CH}_4^*$	$\text{Me}_3\text{SiSiMe}_3$	$\text{Me}_2\text{Si} \begin{array}{c} \diagup \diagdown \\ \diagdown \diagup \end{array} \text{SiMeH}$	$\text{Me}_3\text{Si} \begin{array}{c} \diagup \diagdown \\ \diagdown \diagup \end{array} \text{SiMe}_2$
		[6]	[7]	[8]
$\text{Me}_2\text{Si} \begin{array}{c} \diagup \diagdown \\ \diagdown \diagup \end{array} \text{SiMe}_2$	$\text{Me}_3\text{Si} \begin{array}{c} \text{Me} \\   \\ \text{SiSiEt}_2 \end{array}$			
[9]	[10]			
$\text{Me}_3\text{Si} \begin{array}{c} \text{Et}_2 \\   \\ \text{SiSi} \end{array} \text{SiMe}_2\text{H}$	$\text{Me}_2\text{Si} \begin{array}{c} \text{H} \text{ Et} \\   \quad   \\ \diagup \quad \diagdown \\ \diagdown \quad \diagup \end{array} \text{SiMe}_2$			
[11]	[12]			
$\text{MeHSi} \begin{array}{c} \diagup \diagdown \\ \diagdown \diagup \end{array} \text{Si} \begin{array}{c} \diagup \diagdown \\ \diagdown \diagup \end{array} \text{Si} \begin{array}{c} \diagup \diagdown \\ \diagdown \diagup \end{array} \text{SiMe}_3$	$\text{Me}_2\text{Si} \begin{array}{c} \diagup \diagdown \\ \diagdown \diagup \end{array} \text{Si} \begin{array}{c} \diagup \diagdown \\ \diagdown \diagup \end{array} \text{Si} \begin{array}{c} \diagup \diagdown \\ \diagdown \diagup \end{array} \text{SiMe}_3$			
[13]	[14]			
$\text{MeHSi} \begin{array}{c} \diagup \diagdown \\ \diagdown \diagup \end{array} \text{Si} \begin{array}{c} \diagup \diagdown \\ \diagdown \diagup \end{array} \text{Si} \begin{array}{c} \diagup \diagdown \\ \diagdown \diagup \end{array} \text{SiMeH}$	$\text{Me}_2\text{Si} \begin{array}{c} \diagup \diagdown \\ \diagdown \diagup \end{array} \text{Si} \begin{array}{c} \diagup \diagdown \\ \diagdown \diagup \end{array} \text{Si} \begin{array}{c} \diagup \diagdown \\ \diagdown \diagup \end{array} \text{SiMeH}$			
[15]	[16]			
$\text{Me}_2\text{Si} \begin{array}{c} \diagup \diagdown \\ \diagdown \diagup \end{array} \text{Si} \begin{array}{c} \diagup \diagdown \\ \diagdown \diagup \end{array} \text{Si} \begin{array}{c} \diagup \diagdown \\ \diagdown \diagup \end{array} \text{SiMe}_2$				
[17]				

\*see section (IV)-Q8/MS-Sealed tube experiments

The yields of the di-silicon compounds were minor in comparison with ethene and the monosilanes. Compounds identified from the di-silicon compound group include hexamethyldisilane (HMDS) [6], 1,1,3-trimethyl-1,3-disilacyclobutane [7], trimethylsilyl(dimethylsilyl)methane (ISO-HMDS) [8], 1,1,3,3-tetramethyl-1,3-disilacyclobutane [9] and 2,2-diethyl-1,1,1,2-tetramethyldisilane [10].

The yields of the tri-silicon compounds were less than those of the di-silicon compounds. This group contained small amounts of cyclic carbosilanes such as 1-ethyl-3,3,4,4-tetramethyl-1,3,4-trisilacyclopentane [12]. A trace amount of 1,1,1-trimethyl-2,2-diethyldisilyl(dimethylsilyl)methane (ISO-DEHMTS) [11] is also formed.

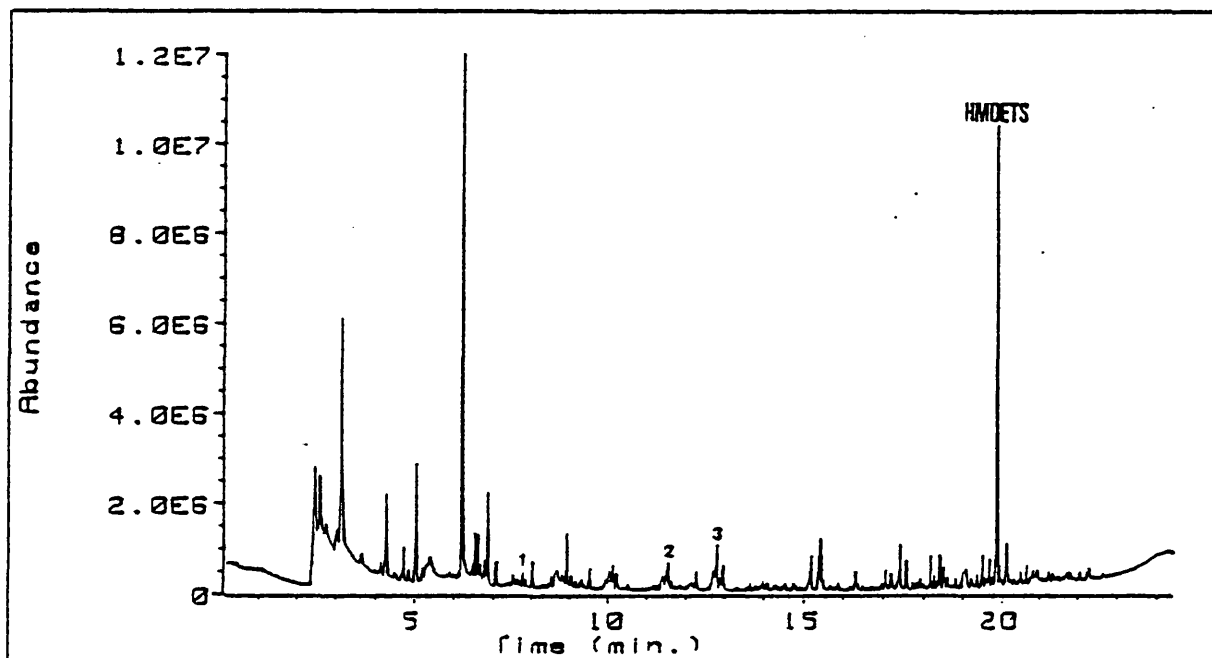
The tetra-silicon compounds were multiple disilacyclobutane

ring compounds ([13]-[17]). These products were minor in comparison to the monosilanes and ethene.

Low pressure experiments further reduced the yields of the di-, tri- and tetra-silicon compounds suggesting that these products arise from bi-molecular reactions. The yield of 2,2-diethyl-1,1,1,2-tetramethyldisilane [10], however, was not reduced. The yields of the major products were not affected by low sample pressure experiments.

#### (ii) 2,3-dimethyl-1,3-butadiene/DEHMTS experiments

A 5:1 mixture of 2,3-dimethyl-1,3-butadiene and DEHMTS was pyrolysed using the liquid injection technique. The pyrolysis temperature range was 600-630°C and the mixture volume range was 0.04-0.12  $\mu$ l. TIC 2 shows the products unique to this pyrolysis.



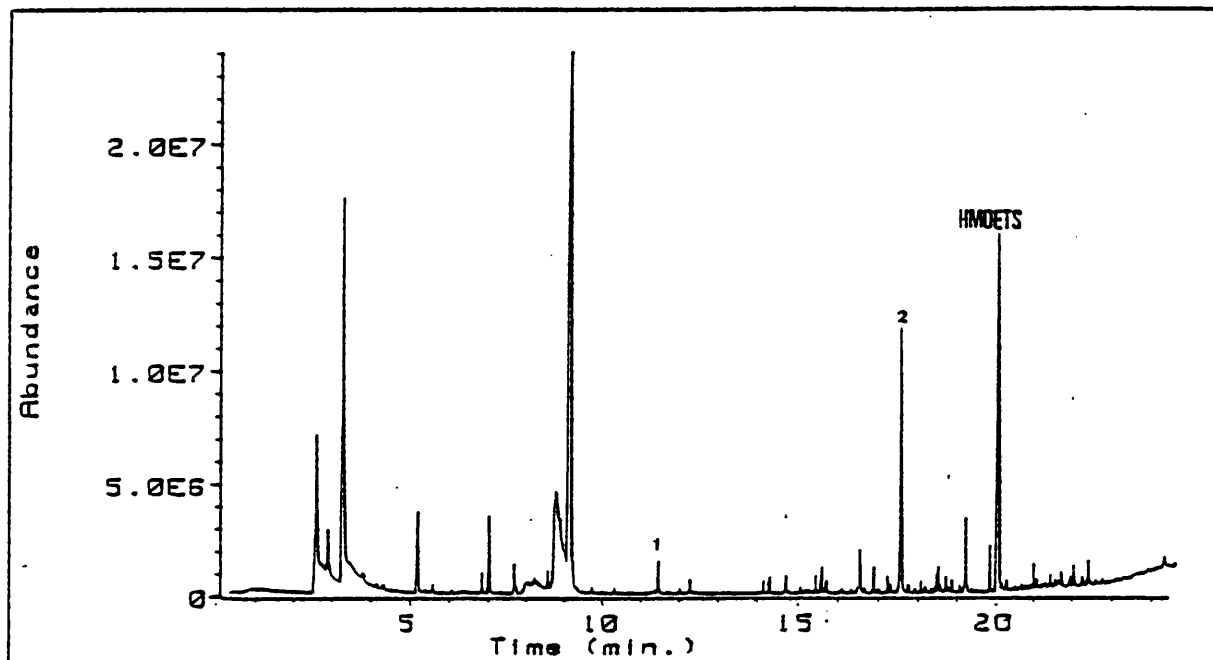
TIC 2: [1]  $\text{H}_2\text{Si}$  C=C, [2]  $\text{MeHSi}$  C=C, [3]  $\text{Me}_2\text{Si}$  C=C

vol = 0.04  $\mu$ l, temp = 625°C.

The yields of major and minor products were not affected by the presence of 2,3-dimethyl-1,3-butadiene. The trapping experiments revealed the presence of small amounts of dimethylsilylene ( $\text{Me}_2\text{Si}:$ ) and methylsilylene ( $\text{MeHSi}:$ ). Trace amounts of silylene ( $\text{H}_2\text{Si}:$ ) and ethylsilylene ( $\text{EtHSi}:$ ) were also noticed.

### (iii) Toluene/DEHMTS experiments

A 5:1 mixture of toluene and DEHMTS was pyrolysed using the liquid injection technique. The pyrolysis temperature range was 600-630°C and the mixture volume range was 0.20-0.24µl. Products unique to this pyrolysis are shown in TIC 3.

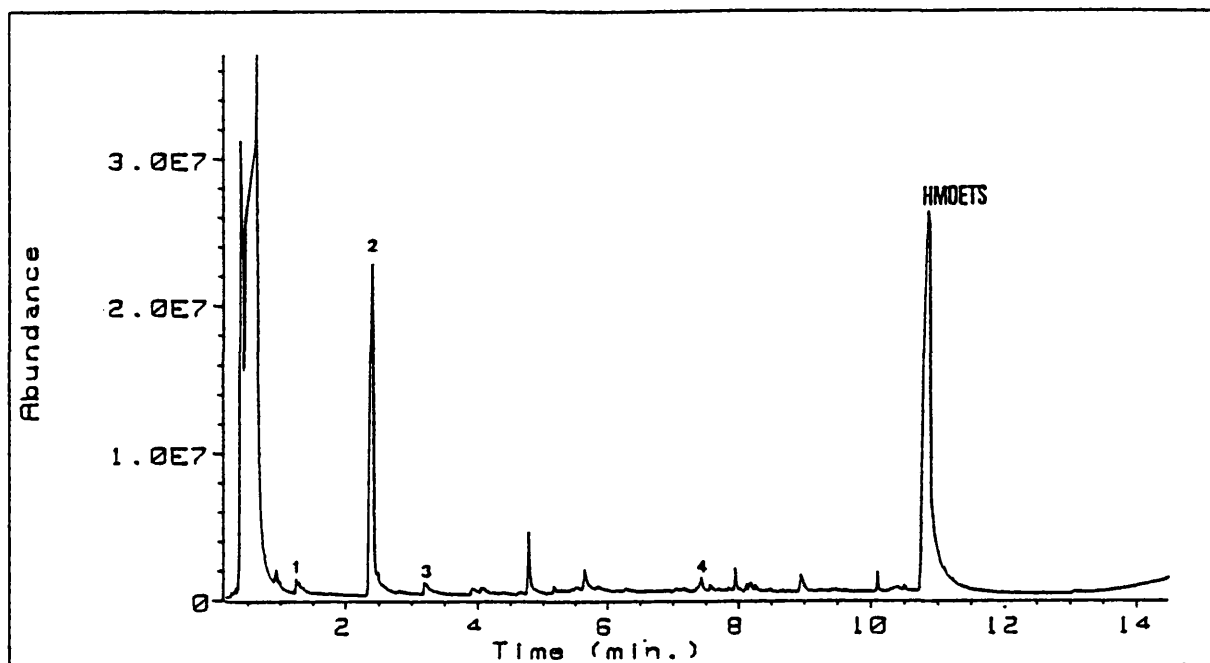


TIC 3: [1] ethylbenzene, [2] benzyltrimethylsilane.  
vol= 0.20µl, temp= 620°C.

No suppression of major or minor product formation was noticed. The major intermediates trapped were trimethylsilyl radicals ( $\text{Me}_3\text{Si}\cdot$ ) and methyl radicals ( $\cdot\text{CH}_3$ ) leading to the formation of benzyltrimethylsilane (TMSB) and ethylbenzene (ETHB) respectively.

### (iv) Methylchloride/DEHMTS experiments

DEHMTS was pyrolysed in an excess of methylchloride ( $\text{MeCl}$ ) between 565-575°C.  $\text{MeCl}$  was injected via the gas sample valve whilst DEHMTS was introduced using the liquid injection technique. Products unique to this pyrolysis are shown in TIC 4.



TIC 4: [1]  $\text{Me}_2\text{SiHCl}$ , [2]  $\text{Me}_3\text{SiCl}$ , [3]  $\text{Me}_2\text{SiCl}_2$ , [4]  $\text{Me}_3\text{Si-SiMe}_2\text{Cl}$ . Vol = 0.10  $\mu\text{l}$ , MeCl press. = 11.0 torr, temp = 565°C.

The yields of ethene and VMTS were not reduced, but the formation of 3MS was suppressed. The products containing more than one silicon atom were all suppressed (except 2,2-diethyl-1,1,1,2-tetramethyldisilane).

MeCl traps silyl radicals as chlorosilanes; the major radical trapped in this pyrolysis was  $\text{Me}_3\text{Si}\cdot$ , leading to the formation of trimethylchlorosilane [2].

### (III) Kinetic-SFR Results

#### (i) DEHMTS kinetic experiments

DEHMTS was pyrolysed using the liquid injection technique between 570-630°C. Kinetic measurements with initial concentrations of DEHMTS between  $10^{-5}$  and  $10^{-6}$  mol  $\text{dm}^{-3}$  gave an average order of formation of ethene, 3MS and VTMS of  $\approx 1.6$ . Figure 6.1 shows a typical order plot for the formation of ethene.



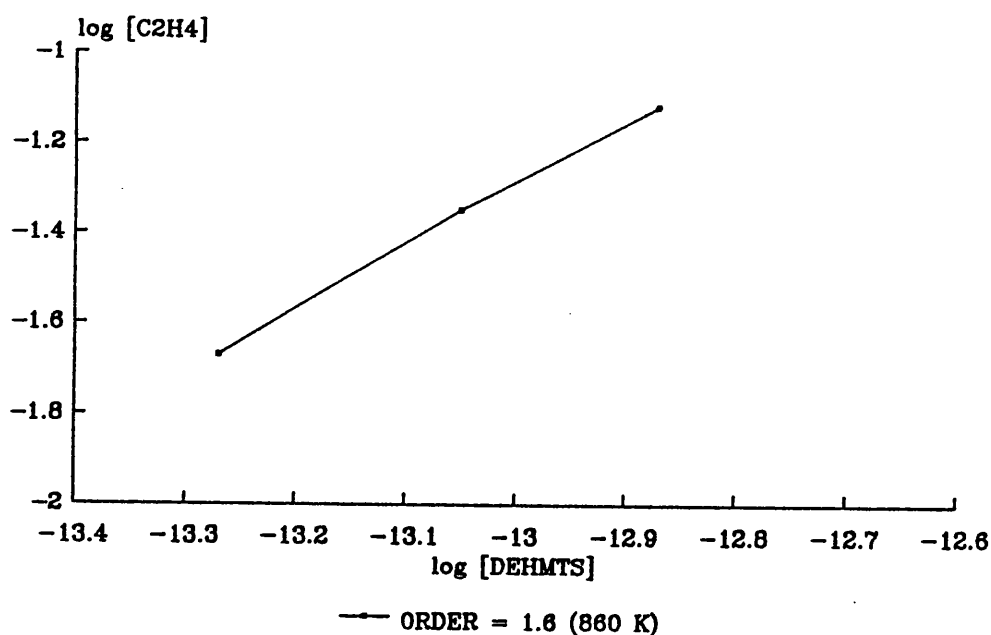


Figure 6.1: Order plot for the formation of ethene. Slope =  $1.7 \pm 0.1$ .

Rate constants based on an order of 1.6 were calculated for the formation of ethene, 3MS and VTMS. Table 6.2 gives the Arrhenius parameters calculated from these rate constants.

Table 6.2: Kinetic results for DEHMTS experiments.

Product	$\log (A/s^{-1})$	$E_a$ ( $\text{kJmol}^{-1}$ )
$\text{CH}_2=\text{CH}_2$	$20.8 \pm 0.5$	$308 \pm 9$
$\text{Me}_3\text{SiH}$	$20.8 \pm 0.6$	$310 \pm 9$
$\text{Me}_3\text{SiCH}=\text{CH}_2$	$18.0 \pm 0.6$	$274 \pm 10$

The percentage yields at  $580^\circ\text{C}$  for ethene, 3MS and VTMS were 46%, 36% and 9% respectively; at  $630^\circ\text{C}$  the yields were 56%, 30% and 5% respectively. The minor products accounted for approximately 5% of total product composition (demonstrated clearly in figure 6.2).

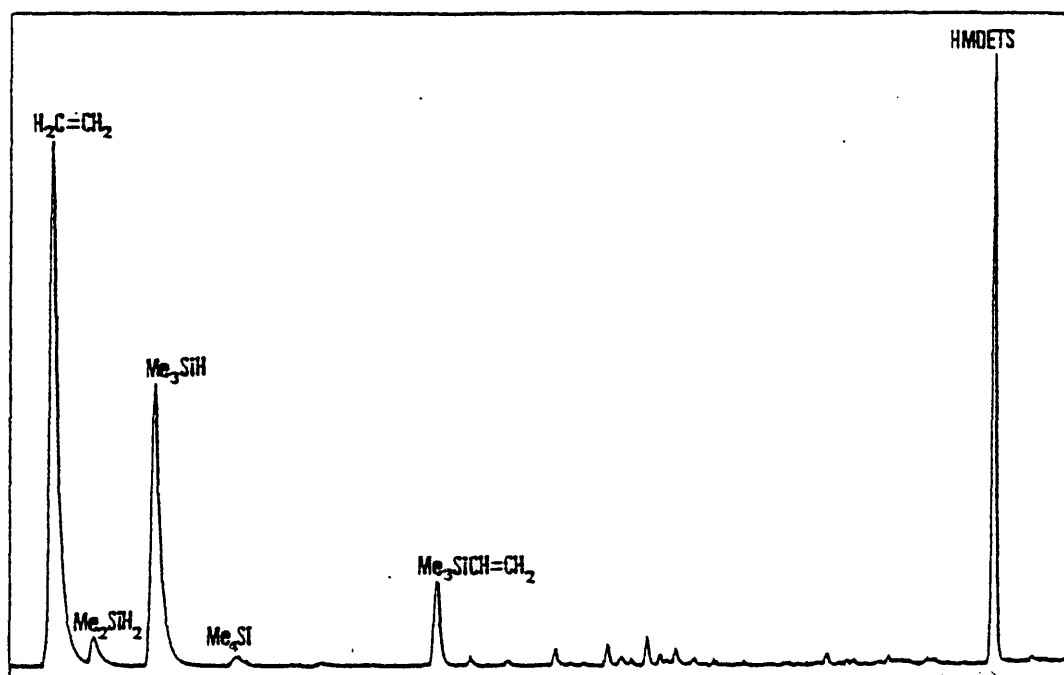


Figure 6.2: Gas chromatogram for the pyrolysis of DEHMTS at 616°C.

A typical Arrhenius plot for the formation of ethene is shown in figure 6.3.

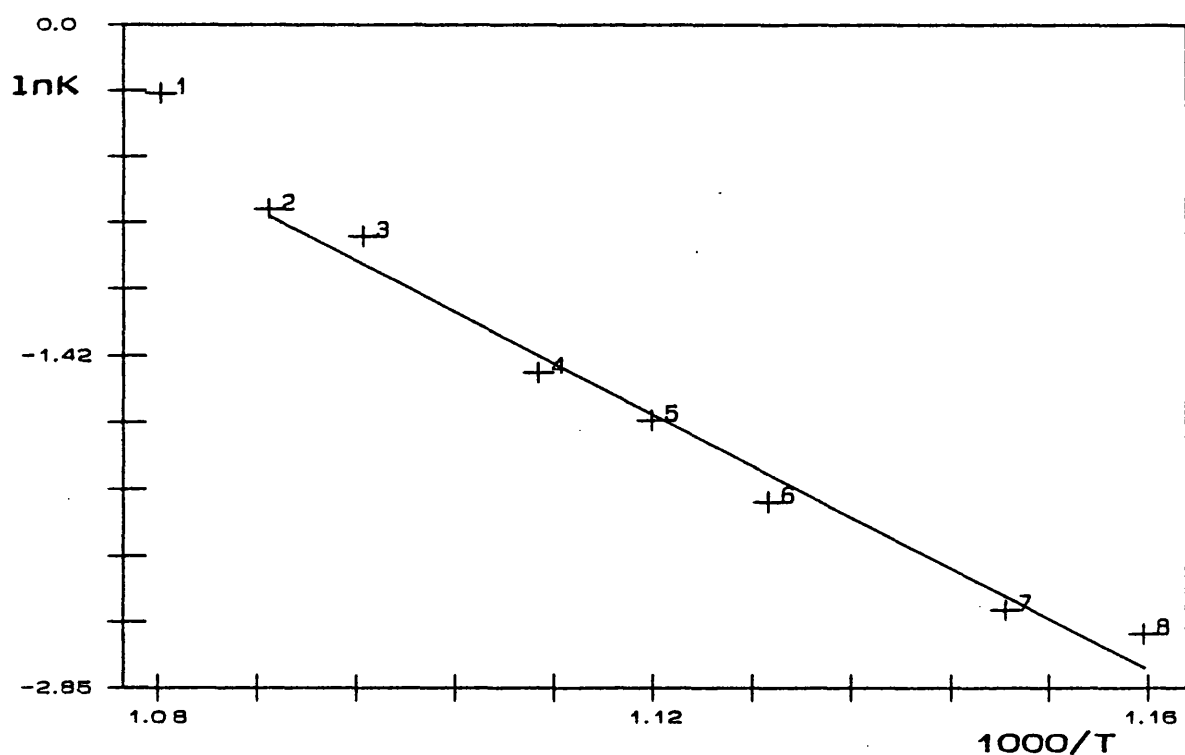


Figure 6.3: Arrhenius plot for the formation  $\text{CH}_2=\text{CH}_2$  from DEHMTS between 570-630°C.

The Arrhenius plot was curved over the experimental temperature range reflecting the kinetic complexity of the pyrolysis.

(ii) 2,3-dimethyl-1,3-butadiene/DEHMTS kinetic experiments

A 5:1 mixture of 2,3-dimethyl-1,3-butadiene and DEHMTS was pyrolysed using the liquid injection technique between 580-630°C. For simplicity, first order rate constants were measured for the products shown in figure 6.4. The Arrhenius parameters for the formation of these products are given in table 6.3.

Table 6.3: Kinetic results for DEHMTS/  
2,3-dimethyl-1,3-butadiene  
experiments.

Product	$\log (A/s^{-1})$	$E_a$ (kJmol <sup>-1</sup> )
CH <sub>2</sub> =CH <sub>2</sub>	17.5±0.9	304 ± 15
Me <sub>3</sub> SiH	17.5±1.4	312 ± 23
Me <sub>3</sub> SiCH=CH <sub>2</sub>	13.5±2.1	254 ± 35

Kinetic measurements were difficult due to the complexity of the reaction mixture, partly because of the radical induced secondary reactions of 2,3-dimethyl-1,3-butadiene.

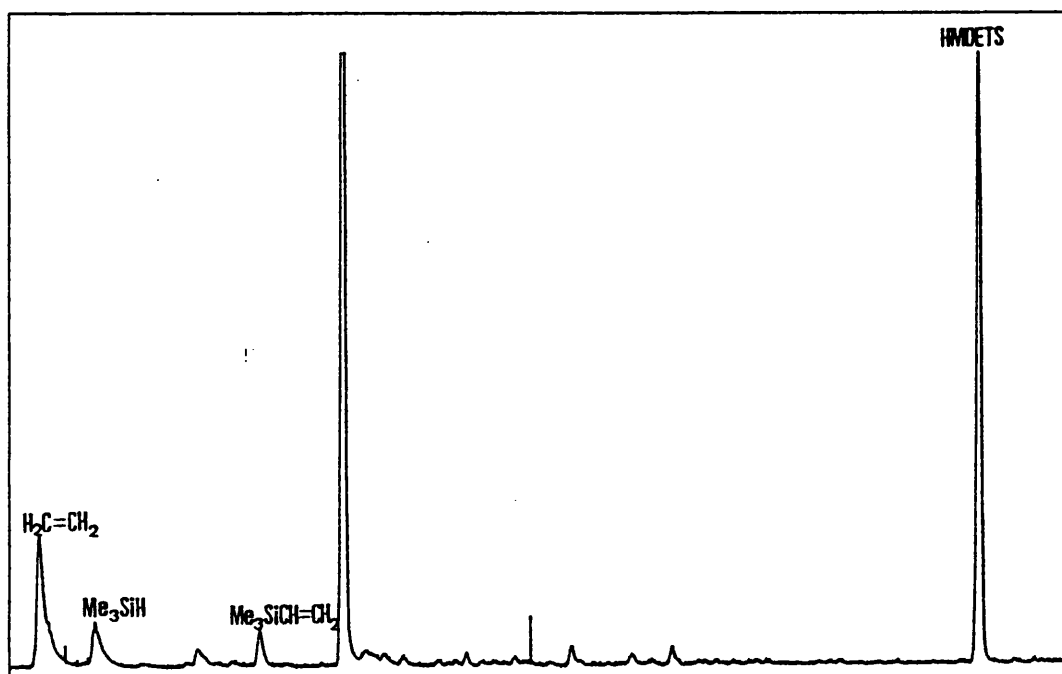


Figure 6.4: Gas chromatogram for the pyrolysis of DEHMTS/ at 579°C.

A typical Arrhenius plot for the formation of ethene is shown in figure 6.5. The Arrhenius plot is again curved over the whole temperature range.

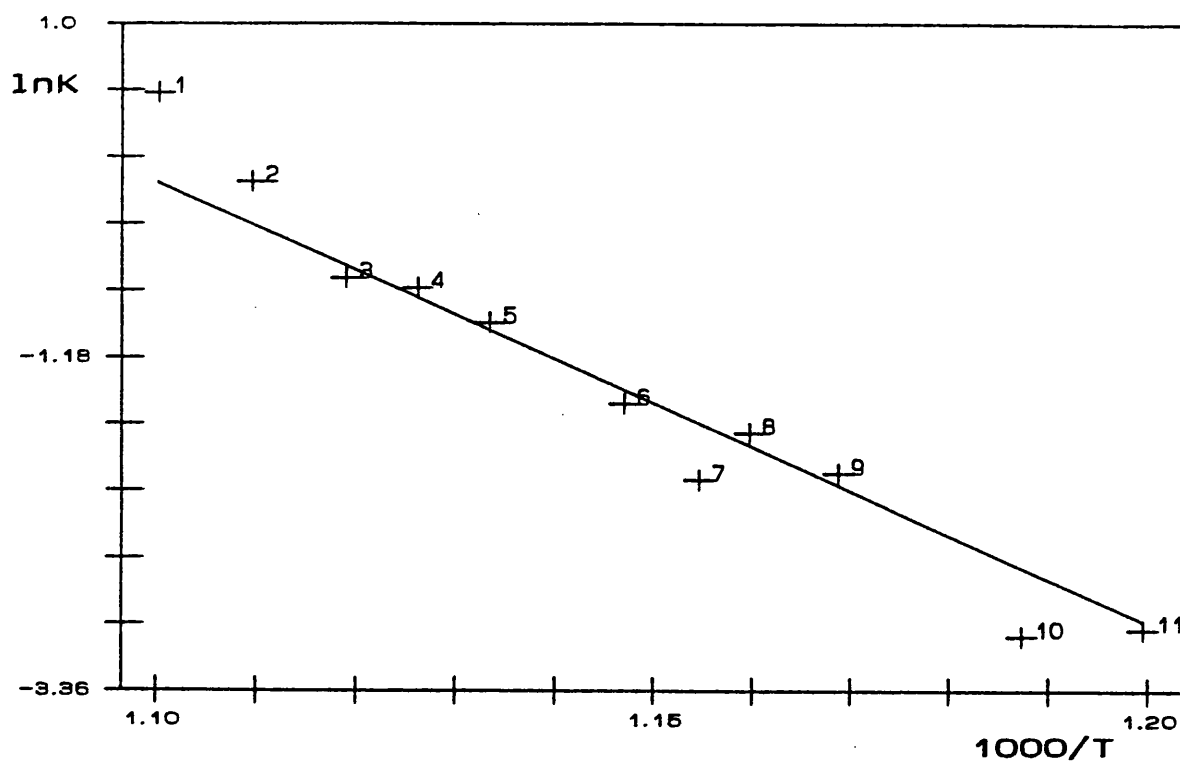


Figure 6.5: Arrhenius plot for the formation  $\text{CH}_2=\text{CH}_2$  from DEHMTS between 580–630°C in the presence of CC(C)C.

### (iii) Toluene/DEHMTS kinetic experiments

A 5:1 mixture of toluene and DEHMTS was pyrolysed using the liquid injection technique between 580–630°C. First order rate constants were measured for the products shown in figure 6.6. The Arrhenius parameters for the formation of these products are given in table 6.4.

Table 6.4: Kinetic results for DEHMTS/toluene experiments.

Product	$\log (A/s^{-1})$	$E_a$ ( $\text{kJmol}^{-1}$ )
$\text{CH}_2=\text{CH}_2$	$21.3 \pm 0.6$	$364 \pm 10$
$\text{Me}_3\text{SiH}$	$19.7 \pm 0.6$	$344 \pm 10$
$\text{Me}_3\text{SiCH}=\text{CH}_2$	$14.7 \pm 0.9$	$276 \pm 15$

A typical Arrhenius plot for the formation of ethene is shown in figure 6.7.

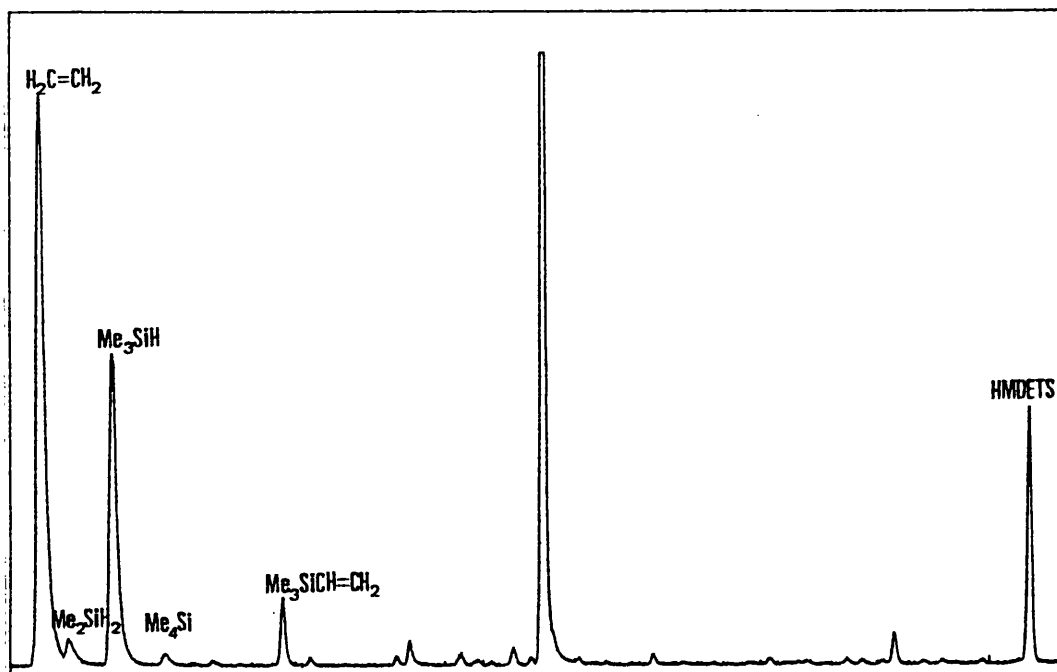


Figure 6.6: Gas chromatogram for the pyrolysis of DEHMTS/toluene at 630°C.

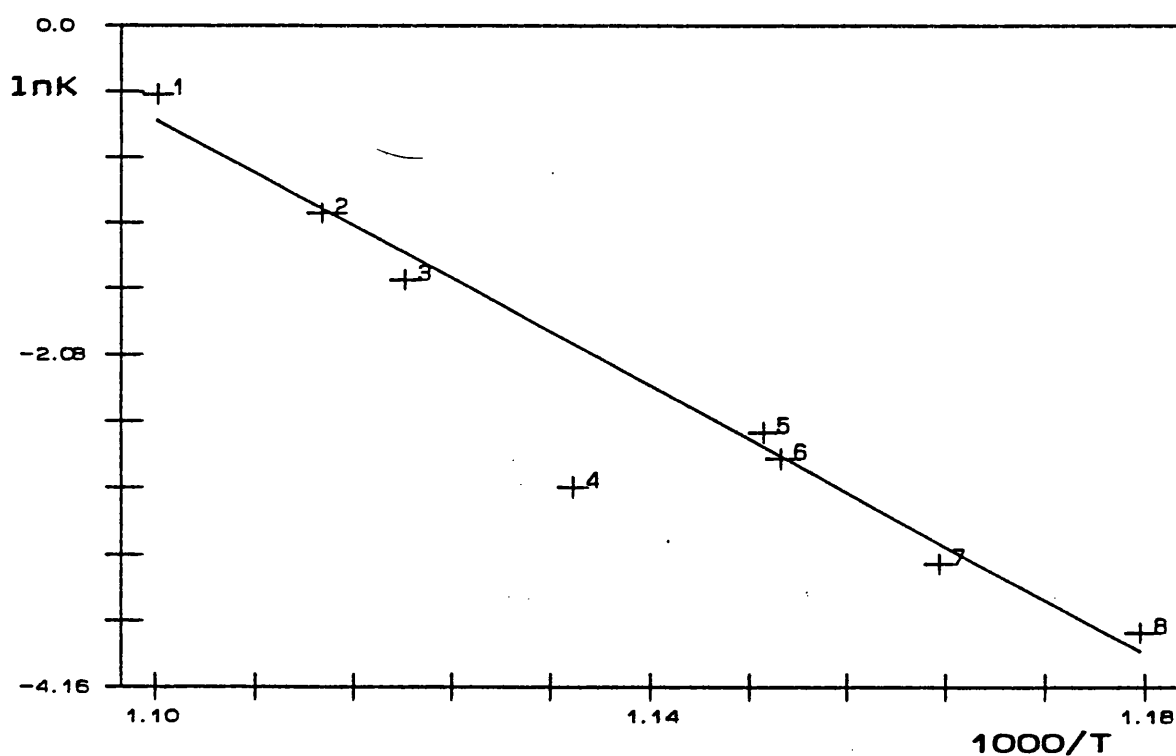


Figure 6.7: Arrhenius plot for the formation  $\text{CH}_2=\text{CH}_2$  from DEHMTS between 580-630°C in the presence of toluene.

#### (IV) Q8/MS-Sealed Tube Pyrolysis Results

DEHMTS was pyrolysed in a sealed sample vessel at 400°C for 5 minutes. The time scale of the pyrolysis was calculated from the Arrhenius parameters for ethene formation from the

kinetic-SFR experiments.

At 400°C:  $k = 7.83 \times 10^{-4} \text{ (s}^{-1}\text{)}$ ,  $t_{1/2} = 14 \text{ mins.}$

The Q8/MS showed the major volatile component at liquid nitrogen temperatures was hydrogen (fig 6.8). Smaller amounts of methane and ethene were also identified.

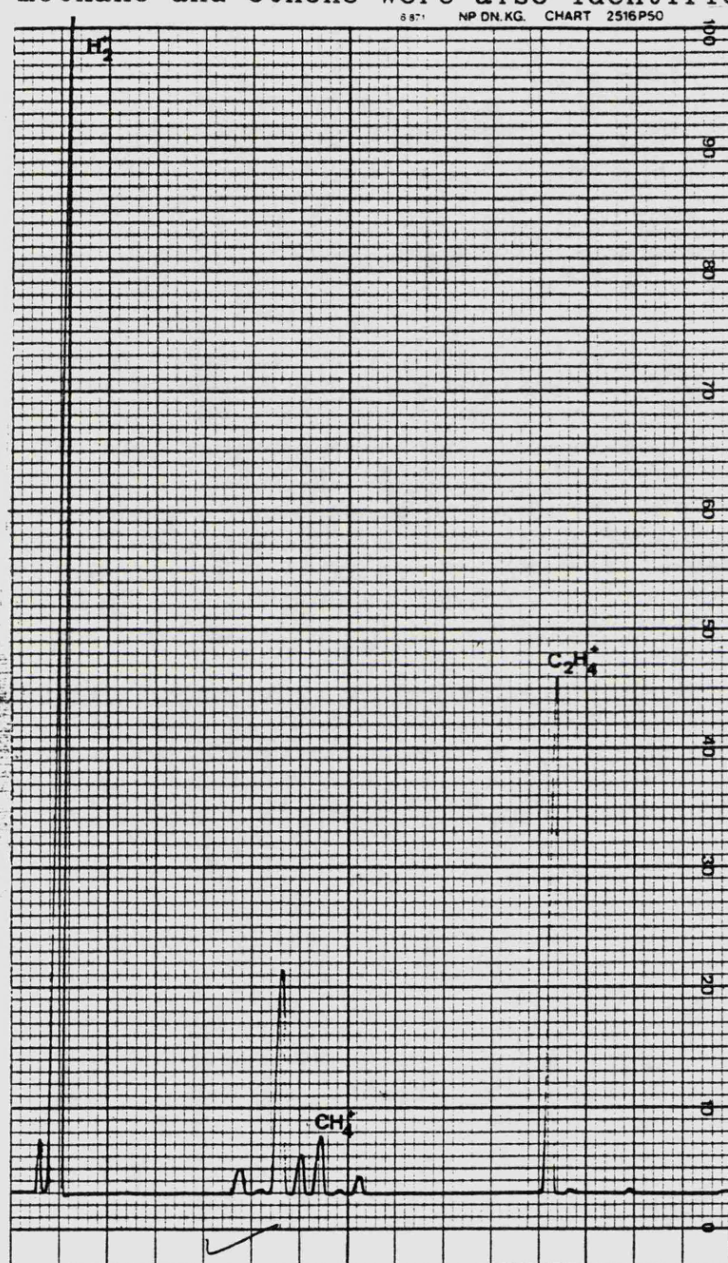
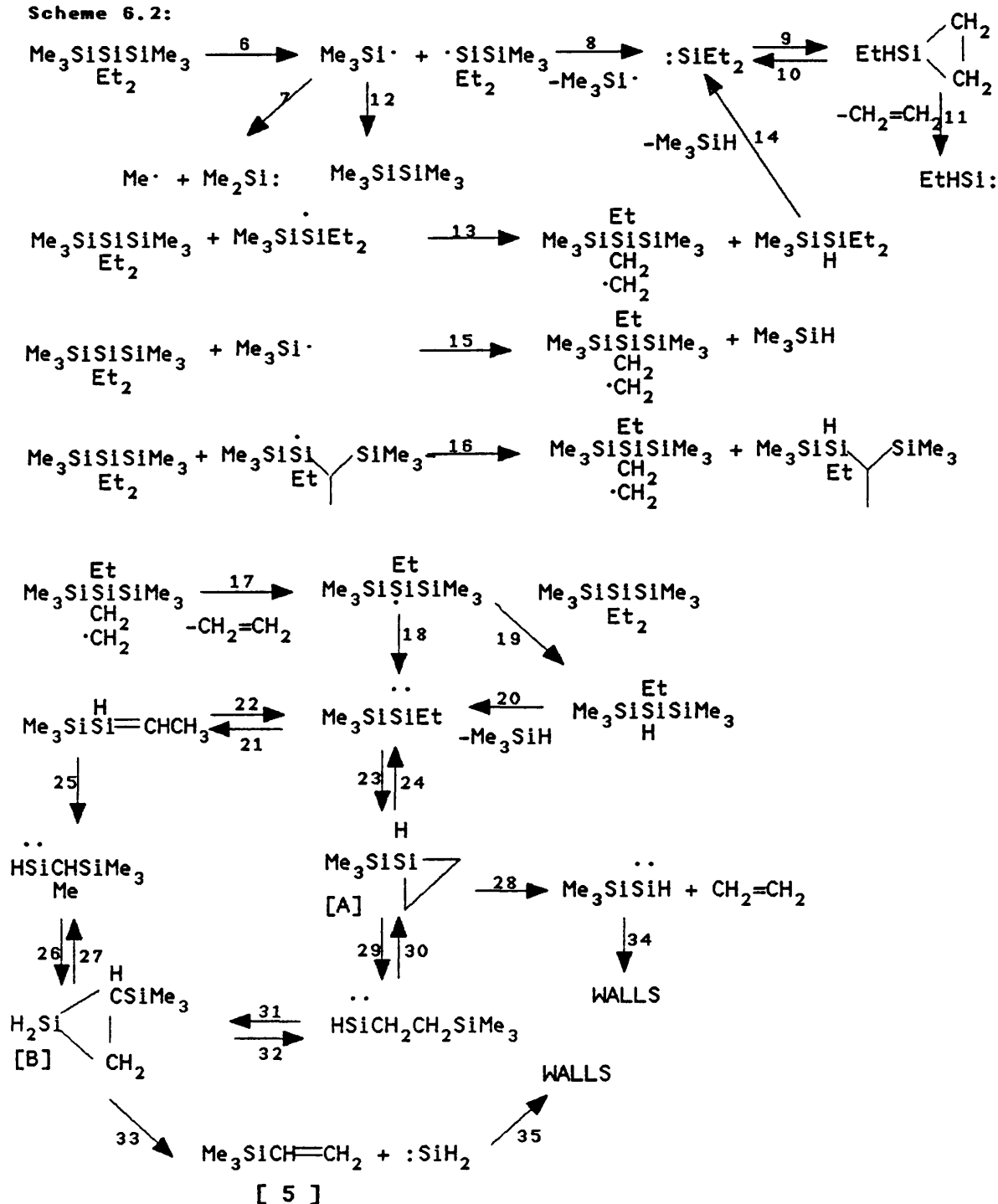


Figure 6.8: Mass Spectrum of  $\text{H}_2$ ,  $\text{CH}_4$  and  $\text{C}_2\text{H}_4$  from the sealed tube pyrolysis of DEHMTS at 400°C.

## (V) Discussion

DEHMTS gives only three major products, ethene, trimethylsilane (3MS) and vinyltrimethylsilane (VMTS) upon pyrolysis. Product yields revealed that the di-, tri and tetra-silicon compounds accounted for less than 5% of the product composition (see figure 6.1). Trapping experiments show the pyrolysis mechanism is primarily radical in nature, the first step being Si-Si bond homolysis leading to the formation of  $\text{Me}_3\text{Si}\cdot$  radicals and 1,1,1-trimethyl-2,2-diethydisilyl radicals.

Scheme 6.2:



Schemes 6.2 & 6.3 show reactions which could account for major product formation. Scheme 6.2,  $\text{Me}_3\text{Si}\cdot$  radicals can dissociate into a methyl radicals and  $\text{Me}_2\text{Si}\cdot$  (7); 1,1,1-trimethyl-2,2-diethydisilyl radicals can dissociate into  $\text{Me}_3\text{Si}\cdot$  radicals and diethylsilylene ( $\text{Et}_2\text{Si}:$ ) (8).

$\text{Et}_2\text{Si}:$  can undergo an internal  $\beta\text{-C-H}$  bond insertion leading to the formation of a silacyclopropane (9). This silacyclopropane can dissociate into ethene and ethylsilylene ( $\text{EtHSi}:$ ) (11).

The radicals produced by Si-Si bond cleavage can also abstract a  $\beta$ -hydrogen from an ethyl group on DEHMTS (13 & 14). The carbon centred radical formed can dissociate into ethene and a 2-ethyl-hexamethyltrisilyl radical (17). This new silicon centred radical can then abstract hydrogen to yield a hydridosilane (19) which would rapidly eliminate 3MS to yield trimethylsilyl(ethyl)silylene (20)<sup>7</sup>. Dissociation of the 2-ethyl-hexamethyltrisilyl radical also yields trimethylsilyl(ethyl)silylene (18).

Trimethylsilyl(ethylsilylene) can either isomerise via a 1,2 H-shift to a silene (21) or insert into a  $\beta\text{-C-H}$  bond to yield silacyclopropane [A] (23). The silene formed can isomerise to a silylene via a 1,2-silyl shift (25), the resulting silylene can insert into a  $\beta\text{-C-H}$  bond to yield silacyclopropane [B] (26).

Silacyclopropane [A] can either dissociate into ethene and trimethylsilylsilylene (28) or ring open via a 1,2 silyl shift to yield a silylene. The silylene formed can insert into a  $\beta\text{-C-H}$  bond to give silacyclopropane [B]. Silacyclopropane [B] can dissociate into silylene and VMTS ([5] TIC 1).

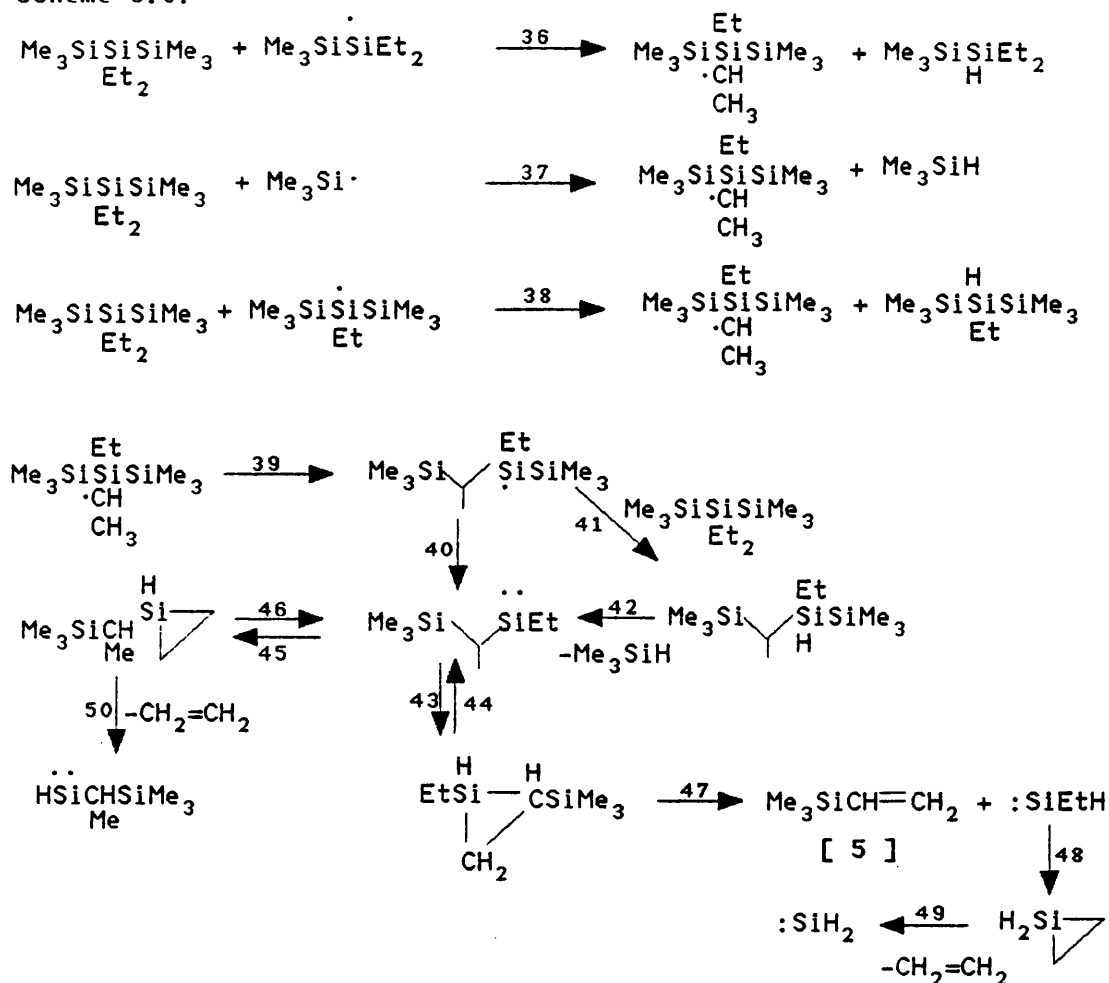
The trapping of methyl radicals as ETHB in the toluene co-pyrolysis experiments ([1] TIC 3) and  $\text{Me}_2\text{Si}\cdot$  as 1,1,3,4-tetramethyl-1-silacyclopent-3,4-ene (ADD 1) in the 2,3-dimethyl-1,3-butadiene experiments ([3] TIC 2) offers evidence for reaction (7). Evidence for reaction (11) comes from the trapping of  $\text{EtHSi}:$  in the 2,3-dimethyl-1,3-butadiene experiments. The trapping of silylene in the 2,3-dimethyl-1,3-butadiene experiments offers evidence for reaction (33).

$\alpha\text{-H}$  abstraction from an ethyl group on DEHMTS leads to the reactions in scheme 6.3.

The carbon centred radical formed by  $\alpha\text{-H}$  abstraction (36, 37 & 38) will rearrange via a 1,2-shift to yield a silicon



Scheme 6.3:

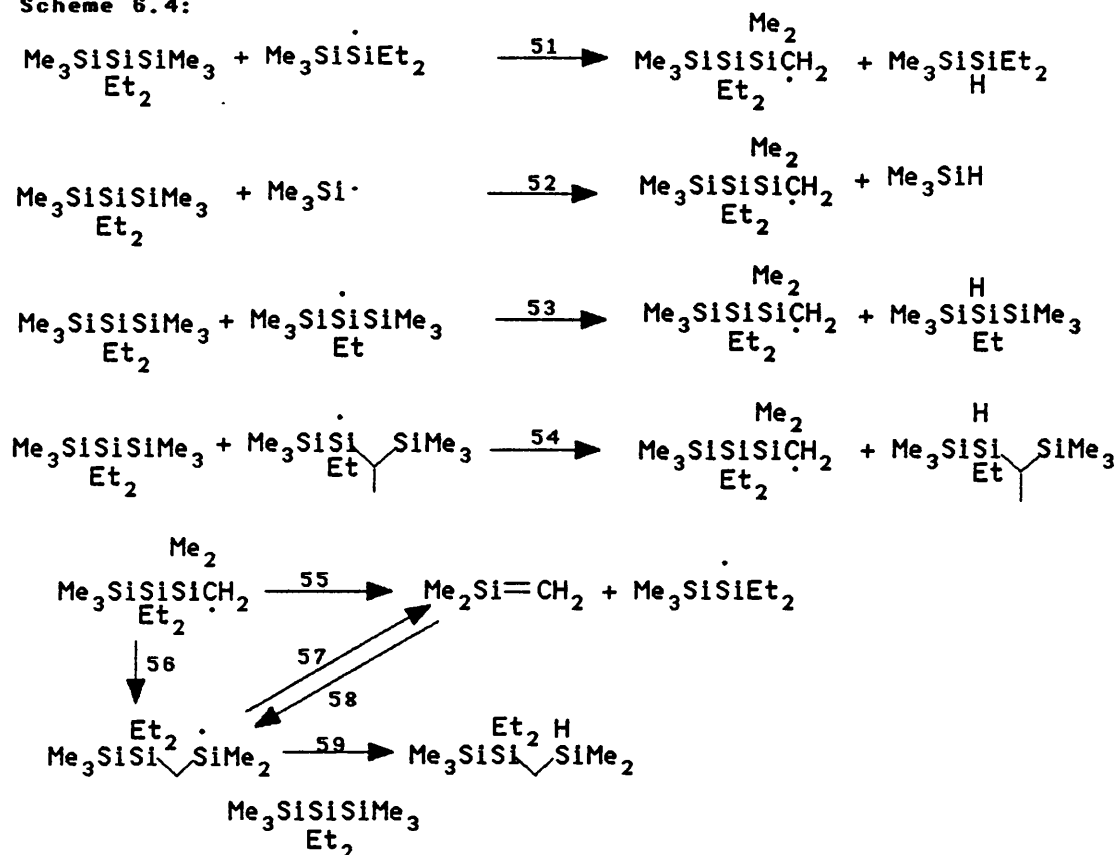


centred radical (39). This silicon centred radical can either dissociate into  $\text{Me}_3\text{Si}\cdot$  and a silylene (40) or abstract hydrogen to yield a hydridosilane (41) which would rapidly eliminate 3MS to yield the same silylene (42). This silylene can form two possible silacyclopropanes (45 & 43). The silacyclopropane formed in reaction (43) may eliminate  $\text{EtHSi:}$  to yield VMTS (47) ([5] TIC 1). The silacyclopropane formed by reaction (45) can eliminate ethene to yield a silylene (50) which in turn can form silacyclopropane [B] by  $\beta$ -C-H bond insertion (26) (scheme 6.2).

Terminal hydrogen abstraction leads to the reactions in scheme 6.4.

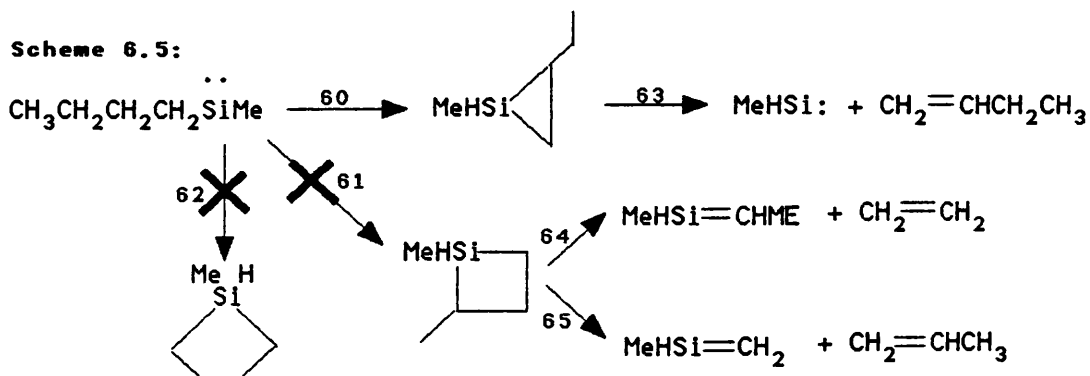
The carbon centred radical formed by terminal H-abstraction (51, 52, 53 & 54) can either dissociate into dimethylsilene and a 2,2-diethyl-1,1,1-trimethyldisilyl radical (55) or isomerise by a 1,2-shift to yield a new silicon centred radical. This silicon centred radical can either dissociate into dimethylsilene and a 2,2-diethyl-1,1,1-trimethyldisilyl radical or abstract hydrogen to yield ISO-DEHMTS ([12] TIC 1).

Scheme 6.4:



Product yields show that the reactions in scheme 4 are minor compared to those in scheme 6.2 & 6.3.

All the reactions in schemes 6.2, 6.3 and 6.4 have precedents in organosilicon chemistry e.g. the formation of silacyclopropanes via silylene insertion into  $\beta$ -C-H bonds has been shown to be a preferential reaction of n-butyl(methyl)silylene. Barton *et. al.* studied the reactions of n-butyl(methyl)silylene using flash vacuum pyrolysis<sup>8</sup>. Although a number of cyclic carbosilanes could be formed by C-H silylene insertion (scheme 6.5) silacyclopropane formation was found to be dominant (60). The silacyclopropane dissociates into methylsilylene and 1-butene.



Co-pyrolysis of DEHMTS in the presence of 2,3-dimethyl-1,3-butadiene or toluene did not reduce or suppress the formation

of ethene, 3MS and VMTS. These bimolecular trapping agent reactions cannot compete with the rapid unimolecular reactions leading to major product formation. MeCl did suppress the formation of 3MS by trapping  $\text{Me}_3\text{Si}\cdot$  radicals as trimethylchlorosilane, showing the major source of 3MS is  $\text{Me}_3\text{Si}\cdot$  radical H-abstraction. MeCl also suppressed the formation of the di-, tri- and tetra-silicon compounds; therefore, bimolecular reactions lead to the formation of these compounds e.g. HMDS is formed by the combination of  $\text{Me}_3\text{Si}\cdot$  radicals (12).

The formation of 2,2-diethyl-1,1,1,2-tetramethyldisilane is not suppressed by co-pyrolysis in the presence of any trapping agents, including MeCl. 2,2-diethyl-1,1,1,2-tetramethyldisilane is believed to be formed by the unimolecular elimination of  $\text{Me}_2\text{Si:}$  from DEHMTS:



Reaction (66) is minor in comparison to Si-Si bond cleavage (Chapter 1 (VIII)).

The Q8/MS-Sealed tube experiments showed that hydrogen is a major product of this pyrolysis. Hydrogen is formed by hydrogen radical abstraction reactions. These experiments also revealed the presence of methane, formed by either the abstraction of hydrogen by methyl radicals or hydrogen and methyl radical combination. Methyl radicals arise from the dissociation of  $\text{Me}_3\text{Si}\cdot$  radicals.

2MS is formed by the insertion of dimethylsilylene into the hydrogen  $\sigma$ -bond, a reaction that would be rapid at these temperatures<sup>9</sup>. 4MS is formed by the combination of  $\text{Me}_3\text{Si}\cdot$  and methyl radicals. The toluene pyrolysis experiments show that both these radicals are present, methyl radicals are trapped as ETHB ([1] TIC 3) and  $\text{Me}_3\text{Si}\cdot$  radicals are trapped as benzyltrimethylsilane (TMSB) ([2] TIC 3) (see Chapter 4, scheme 4.2).

Kinetic measurements showed first order processes did not lead to the formation of ethene, 3MS or VTMS. In the  $10^{-5}$ - $10^{-6}$  moldm<sup>-3</sup> concentration range their orders of formation were 1.6, suggesting complex mechanisms such as schemes 2 & 3 are in operation. Kinetic experiments performed in the presence of trapping agents did not reduce the rate of

formation of ethene, 3MS or VMTS by any large amount, the low pressure reactions (13 & 35) being dominant.

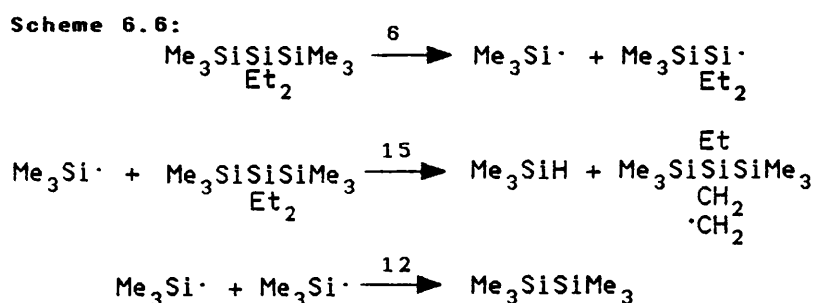
Reactions (5-60) were modelled by numerical integration (the Arrhenius parameters for the individual reactions are given in Appendix 2). The orders of formation of these products varied with temperature, but, over the experimental temperature range were found to be 1.6. Table 6.5 gives the experimental and calculated Arrhenius parameters calculated from rate constants based on an order of 1.6 for the formation of ethene, 3MS and VMTS. The model gave curved Arrhenius plots, in agreement with experiment. Numerical integration showed the amount of ISO-DEHMTS produced was very small in comparison to ethene, 3MS and VMTS, agreeing with the experimental results.

Table 6.5:

Product	Experimental		Calculated	
	log (A/s <sup>-1</sup> )	E <sub>a</sub> (kJmol <sup>-1</sup> )	log (A/s <sup>-1</sup> )	E <sub>a</sub> (kJmol <sup>-1</sup> )
CH <sub>2</sub> =CH <sub>2</sub>	20.8 ± 0.5	308 ± 9	20.7 ± 1.6	318 ± 22
Me <sub>3</sub> SiH	20.8 ± 0.6	310 ± 9	19.5 ± 1.4	303 ± 23
Me <sub>3</sub> SiCH=CH <sub>2</sub>	18.0 ± 0.6	374 ± 10	19.6 ± 1.4	312 ± 23

The calculated Arrhenius parameters appear to be in good agreement with those derived experimentally, giving further evidence that the reactions in schemes 1, 2 and 3 are valid for the pyrolysis of DEHMTS.

The orders of formation for the major products would be expected to be close to 1.5. Consider the simplified mechanism of formation for the radical formed by reaction (15), a major route to ethene (scheme 6.6 reaction (12) being the only termination step):



The rate of formation of this radical is given by equation {6.1}. To develop this rate equation the concentration of Me<sub>3</sub>Si· radicals must be found, which is done by using the

steady state approximation {6.2}. The solution to {6.2} is given by {6.3}. This leads to an overall rate equation {6.4} for the formation of this radical:

$$d[\text{Me}_3\text{SiSiSiMe}_3]_{\text{CH}_2\text{CH}_2}^{\text{Et}}/dt = k_{15} [\text{Me}_3\text{SiSiSiMe}_3]_{\text{Et}_2} [\text{Me}_3\text{Si}\cdot] \quad \text{---(6.1)}$$

$$d[\text{Me}_3\text{Si}\cdot]/dt = k_8 [\text{Me}_3\text{SiSiSiMe}_3]_{\text{Et}_2} - k_{12} [\text{Me}_3\text{Si}\cdot]^2 \approx 0 \quad \text{---(6.2)}$$

$$\Rightarrow [\text{Me}_3\text{Si}\cdot] = k_8/k_{12} [\text{Me}_3\text{SiSiSiMe}_3]_{\text{Et}_2}^{0.5} \quad \text{---(6.3)}$$

therefore

$$d[\text{Me}_3\text{SiSiSiMe}_3]_{\text{CH}_2\text{CH}_2}^{\text{Et}}/dt = k_{15} (k_8/k_{12})^{0.5} [\text{Me}_3\text{SiSiSiMe}_3]_{\text{Et}_2}^{1.5} \quad \text{---(6.4)}$$

The formation of the radical has an order of exactly 1.5.

#### (VI) Summary

There are many similarities in the pyrolysis mechanisms of OMTS, n-DMTS, i-DMTS and DEHMTS :- (i) the formation of the monosilanes 2MS, 3MS and 4MS are similar in all pyrolyses, (ii) the major trapping products are formed by the same mechanisms, (iii) the effect of trapping agents is small in all pyrolyses and (iv) the unimolecular elimination of  $\text{Me}_2\text{Si}$  from all of these oligosilanes is a minor process, Si-Si bond homolysis being dominant.

There is a balance between low pressure unimolecular reactions and high pressure bimolecular reactions in the pyrolyses of OMTS, n-DMTS and i-DMTS. This balance does not exist in the pyrolysis of DEHMTS, unimolecular reactions dominate.

The formation of silacyclopropanes is the favourable process in the pyrolysis of DEHMTS, a reaction pathway which is accessible because of the presence of ethyl groups. The high pressure bimolecular reactions of DEHMTS are not fast enough to compete with the rapid unimolecular reactions (including silacyclopropane formation).

The differences between the pyrolysis mechanisms of permethylated oligosilanes and those with partial substitution of ethyl groups may have some bearing on their possible use as

self-developing photoresists in laser photoablation.

### (VII) The Potential of Methylated versus Ethylated Polysilanes as Self-Developing Photoresists in Laser Photoablation

The aim of this project was to elucidate the thermal breakdown mechanisms of some oligosilanes by gas phase kinetics. It may be possible to use some of the results of this study in polysilane thermal chemistry and therefore help explain why some polysilanes are good self-developing photoresists.

The results reported here can be compared to the recent studies by Michl *et. al.* on the laser photoablation of polysilanes bearing methyl  $(\text{Me}_2\text{Si})_n$ , n-hexyl  $(\text{Hx}_2\text{Si})_n$ , n-butyl  $(\text{Bu}_2\text{Si})_n$  and propyl  $(\text{Pr}_2\text{Si})_n$  groups<sup>10</sup>. There are many similarities in the results from the two studies and some clarification of Michl's study may be offered from the results reported here.

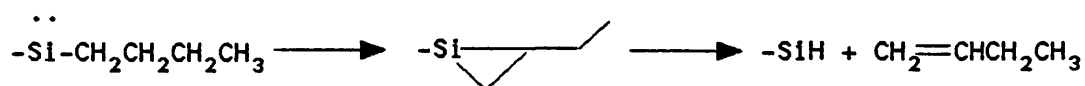
Michl confirmed that laser photoablation is a thermal rather than photochemical process. Identification of the ablated materials by mass spectroscopy proved difficult due to the complexity of the thermal breakdown mechanism of these high molecular weight polysilanes. Some general results were reported.

In the case of  $(\text{Me}_2\text{Si})_n$  the ablated materials contained  $\text{Me}_3\text{Si}^+$  radical cations and large amounts of cyclic carbosilanes containing two or three silicon atoms. The formation of higher molecular weight cyclic carbosilanes were also reported. Full characterisation of high molecular weight carbosilanes was not possible but they were believed to be either multiple ring carbosilanes or carbosilanes containing carbon-carbon double bonds. Linear carbosilanes were not formed. Silylenes, silenes and disilenes were not major intermediates in the pyrolysis. The major intermediates were postulated as being either radical or ionic.

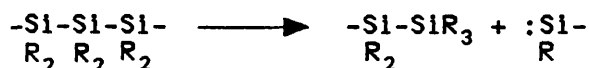
The results of the pyrolysis of  $(\text{Me}_2\text{Si})_n$  are similar to those reported here on OMTS, n-DMTS and i-DMTS. The higher molecular weight carbosilanes are probably similar to the multiple disilacyclobutane ring compounds found in our experiments. The di- and tri-silicon cyclic carbosilanes

could be envisaged as being formed by the low pressure reactions reported in Chapters 3, 4 and 5.

The polysilanes containing Hx, Bu and Pr groups showed a deviation from the thermolysis mechanism to the permethylated polysilanes. The major products were 1-alkenes,  $\text{Me}_3\text{Si}\cdot$  and small amounts cyclic carbosilanes. 1-alkenes are thought to arise via silacyclopropane formation, the silacyclopropanes being formed by internal silylene  $\beta$ -C-H insertion. Michl quotes Barton's work as a precedent for this mechanism<sup>7</sup>.



Michl favours silylene formation by via a 1,2 alkyl group shift (analogous to the unimolecular elimination of  $\text{Me}_2\text{Si}$ : from OMTS, n-DMTS, i-DMTS and DEHMTS):



The results reported here show that the silylene formation by unimolecular elimination is a very minor process. A more reasonable route to silylene formation is silyl radical dissociation (a source also postulated by Michl).

It is probable that permethylated polysilanes would not make the most efficient self-developing photoresists as the studies reported here and in Michl's experiments show that there is a tendency for these oligo/polysilanes to form high molecular weight carbosilanes. The formation of these carbosilanes may affect the line widths of the image left on the photoresist by leaving a carbosilane residue after ablation.

Polysilanes containing longer alkyl groups would make ideal self-developing photoresists as the major products of ablation are volatile 1-alkenes and monosilanes (as in the pyrolysis of DEHMTS). These polysilanes will leave little carbosilane residue to affect the line widths of the ablated area.

#### (VIII) Acknowledgements

I would like to thank Dr. Richard Taylor of Dow Corning for preparing the 2,2-diethylhexamethyltrisilane. I am also grateful to Geraint Morgan for his help with the pyrolysis experiments.

## (IX) References

- (1) B.N. Bortolin, I.M.T. Davidson, D. Lancaster, T. Simpson, D.A. Wild, *Organometallics*, 1990, 9, 281
- (2) I.M.T. Davidson, T. Simpson, R. Taylor in '*Frontiers of Organosilicon Chemistry*' Eds. A.R. Bassindale & P.P. Gaspar, section II, page 89.
- (3) I.M.T. Davidson, C. Eaborn, J.M. Simmie, *J. Organomet. Chem.*, 1973, 47, 45.
- (4) A.C. Baldwin, I.M.T. Davidson, M.D. Reed, *J. Chem. Soc. Faraday Trans. I*, 1978, 74, 2171.
- (5) M. Ahmed, I.M.T. Davidson, G.H. Morgan, T. Simpson, *Organometallics*, accepted for publication.
- (6) T. Turanyi, V.S. Berces, S. Vajada, *Int. J. Chem. Kinetics*, 1989, 21, 83; T. Turanyi, *J. Mathematical Chem.*, 1990, 5, 203; W. Braun, J.T. Herron, D.K. Kahaner, *Int. J. Chem. Kinetics*, 1988, 20, 51.
- (7) I.M.T. Davidson, K.J. Hughes, S. Ijadi-Maghsoodi, *Organometallics*, 1987, 6, 639.
- (8) T.J. Barton, G.T. Burns, *Organometallics*, 1983, 2, 1.
- (9) P. John, J.H. Purnell, *J. Chem. Soc., Faraday Trans. I*, 1973, 69, 1455.
- (10) T.F. Magnera, V. Balaji, J. Michl, R.D. Miller, R. Sooriyakumaran, *Macromolecules*, 1989, 22, 1624.



## Chapter 7

### The Photochemistry of Some Permethyloligosilanes

#### (I) Introduction

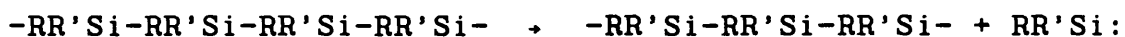
Permethylated oligosilanes have long been known to absorb light in the near-UV region of the electromagnetic spectrum<sup>1</sup>. The photochemistry of branched<sup>2</sup> and straight chained<sup>3</sup> permethyloligosilanes was first studied by Ishikawa and Kumada<sup>4</sup>. Their study involved the irradiation of n-hexane solutions of oligosilanes at 254 nm. The major reaction was silylene extrusion with simultaneous cleavage of a silicon-silicon (Si-Si) bond e.g. n-decamethyltetrasilane gave 84% silylene extrusion and 11% Si-Si bond homolysis.

Photochemical studies on polysilanes revealed that three simultaneous primary processes occur:

A Chain scission by homolytic Si-Si bond cleavage<sup>5</sup>:



B Silylene extrusion<sup>5</sup>:



C Chain scission with formation of a silylene on the polysilyl chain<sup>6</sup>:



Process A (Si-Si bond homolysis) was found to be the major photochemical breakdown route (Chapter 1, part VII). It has been proved that the silyl radicals produced by process A abstract hydrogen from the  $\alpha$ -position on pendant substituent groups<sup>7</sup>.

Pathway C has no counterpart in oligosilane photochemistry, although C does occur in the gas phase irradiation of hexamethyldisilane at low pressures<sup>8</sup>. The photochemical breakdown mechanisms of the following branched and straight chained oligosilanes were studied<sup>9</sup>.

(i) 2,3-bis-trimethylsilyl-octamethyltetrasilane (BTMS-OMTS),

(ii) iso-decamethyltetrasilane (i-DMTS),

(iii) n-decamethyltetrasilane (n-DMTS),

(iv) 2,2-diethylhexamethyltrisilane (DEHMTS),

(v) octamethyltrisilane (OMTS).

The UV absorption characteristics of oligosilanes (i)-(v) are listed in table 1; the absorption maxima for the branched oligosilanes (BTMS-OMTS and i-DMTS) were in the vacuum UV region of the electromagnetic spectrum and therefore outside the range of UV/VIS spectrophotometer used in these measurements. The values  $\lambda_{init}$  and  $\epsilon_{init}$  are used to characterise these compounds, these values were recorded at the highest wavelength of absorbance for these compounds.

Table 7.1: UV absorption characteristics of oligosilanes (i)-(v).

COMPOUND	$\lambda_{max}(\lambda_{init}^*)$ (nm)	$\epsilon_{max}(\epsilon_{init}^*)$ (mol dm <sup>-3</sup> cm <sup>-1</sup> )
BTMS-OMTS	260 *	1090 *
i-DMTS	245 *	515 *
n-DMTS	235	14700
DEHMTS	214	9000
OMTS	215	9020

Oligosilanes (i)-(v) were dissolved in highly purified n-hexane or n-pentane with concentrations ranging from 0.02-0.99 mol dm<sup>-3</sup>. The oligosilane solutions were degassed and irradiated at either 254 nm (low pressure mercury lamp) or 228 nm (cadmium spectral lamp). Product identification was by GC/MS, supplemented by comparative retention time tests and mass spectral analysis on known samples. Where some doubt remained over product identification preparative photolysis experiments were performed and the relevant products were isolated by GC/PREP. The isolated products were then identified by <sup>1</sup>H and <sup>13</sup>C NMR.

Experiments were performed in 1:1 n-hexane:triethylsilane (TES) solutions to ascertain the intermediates involved in the photolysis; silylenes readily insert into the TES Si-H bond to form photochemically stable hydridosilanes, while characteristic products were identified from radicals formed by hydrogen abstraction from the TES Si-H bond.

Product identification was followed by the construction of progress curves. GC peak areas were measured for products at timed intervals of irradiation, the peak areas were normalised by an internal standard (n-decane). Products formed by

primary photochemical pathways can be distinguished from those formed via secondary routes using this method.

Samples of products were isolated by preparative scale photolyses, enabling GC calibration for each product. The yield of each product could then be calculated and the relative importance of each photochemical process ascertained. The error involved in product yield calculations was typically  $\pm 5\%$  e.g. for i-DMTS + HMDS

Error for i-DMTS = Error in vol. injected into GC + Error in making up i-DMTS solution =  $1\% + 2\% = \pm 3\%$

Error for sensitivity measurement =  $\pm 1\%$

Error in Area measurement =  $\pm 1\%$

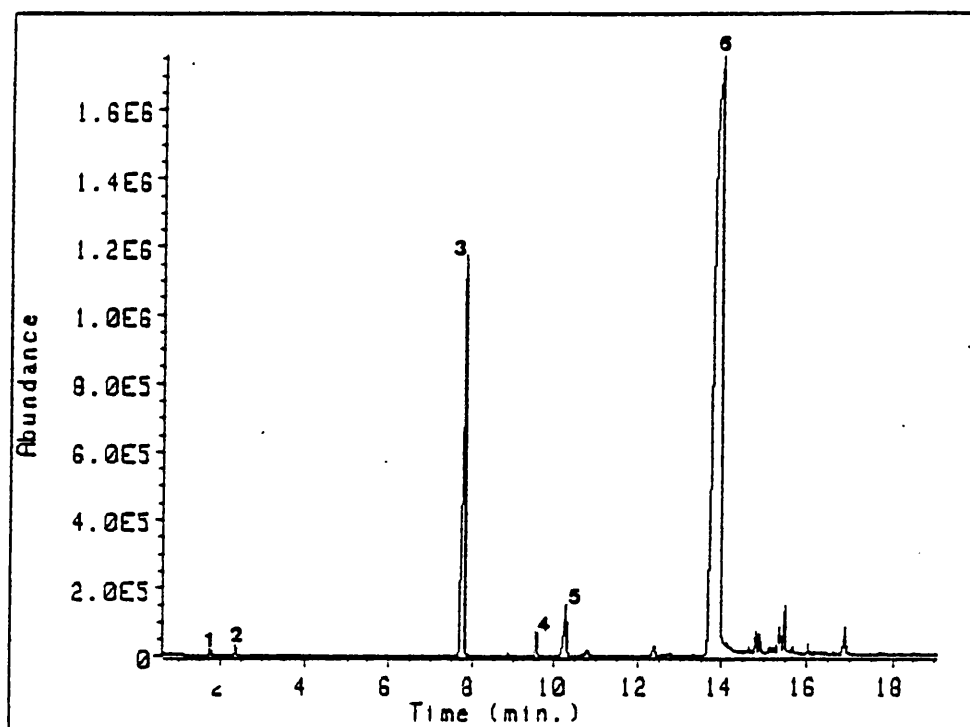
Therefore, Total Error in converting peak area into mol unit area<sup>-1</sup> =  $\pm 2\%$

Total relative yield error =  $3\% + 2\% = \pm 5\%$ .

## (II) Results

### (i) BTMS-OMTS

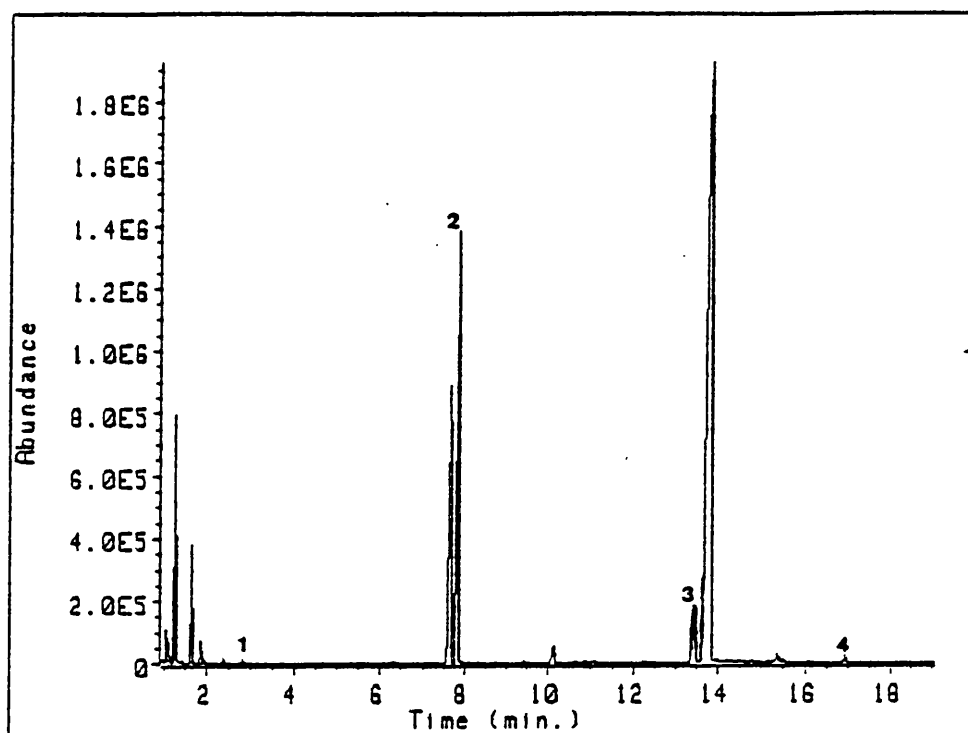
A solution of BTMS-OMTS in n-hexane ( $0.052 \text{ mol dm}^{-3}$ ) was irradiated at 254 nm. TIC 1 shows a sample taken after 10 minutes irradiation (approximately 20% photolysis):



TIC 1: [1]  $\text{Me}_3\text{SiSiSiMe}_3$ , [2]  $\text{Me}_3\text{SiSiSiMe}_3$ ,  
 [3]  $\text{Me}_3\text{SiSiSiMe}_3$ , [4]  $\text{Me}_3\text{SiSiSiH}$ , [5]  $\text{Me}_3\text{SiSiSiMe}_3$ ,  
 [6]  $\text{Me}_3\text{SiSiSiSiMe}_3$  (BTMS-OMTS).

The major product was i-DMTS [3] with smaller amounts of 1,1,1,2,3,3,3-heptamethyltrisilane [1] (2-HMTS), OMTS [2], 2,3-bistrimethylsilyl-1,1,1,2,3-pentamethyltrisilane [4] and 2,3-bistrimethylsilyl-1,1,1,2,3,3-hexamethyltrisilane [5]. Some trimethylsilane (3MS) is also produced but the GC temperature program used did not allow its separation.

A 1:1 n-hexane:TES solution of BTMS-OMTS ( $0.026 \text{ mol dm}^{-3}$ ) was irradiated at 254 nm. TIC 2 shows a sample taken after 5 minutes irradiation, identifying the unique trapping products:



TIC 2: [1]  $\text{Et}_3\text{SiSiH}$ , [2]  $\text{Et}_3\text{SiSiH}$ , [3]  $\text{Et}_3\text{SiSiSiH}$ ,  
 $\text{Me}_3\text{Si}$   $\text{Me}_2$   $\text{SiMe}_3$   $\text{MeMe}$   
 [4]  $\text{Et}_3\text{SiSiH}$ .  
 $\text{Me}_3\text{Si}$

The major intermediate trapped was trimethylsilyl(methyl)silylene ( $\text{Me}_3\text{Si}(\text{Me})\text{Si:}$ ) [2], smaller amounts of dimethylsilylene ( $\text{Me}_2\text{Si:}$ ) [1] and bis-trimethylsilylsilylene [4] were also trapped. Product [3] was derived from the insertion of  $\text{Me}_3\text{Si}(\text{Me})\text{Si:}$  into the Si-H bond of [2].

BTMS-OMTS was irradiated in n-hexane solutions containing different concentrations of TES to ensure all the silylenes produced upon irradiation were trapped. This was necessary before any quantitative experiments could be carried out. Figure 7.1 shows that above approximately  $4 \text{ mol dm}^{-3}$  TES concentration all silylenes are trapped.

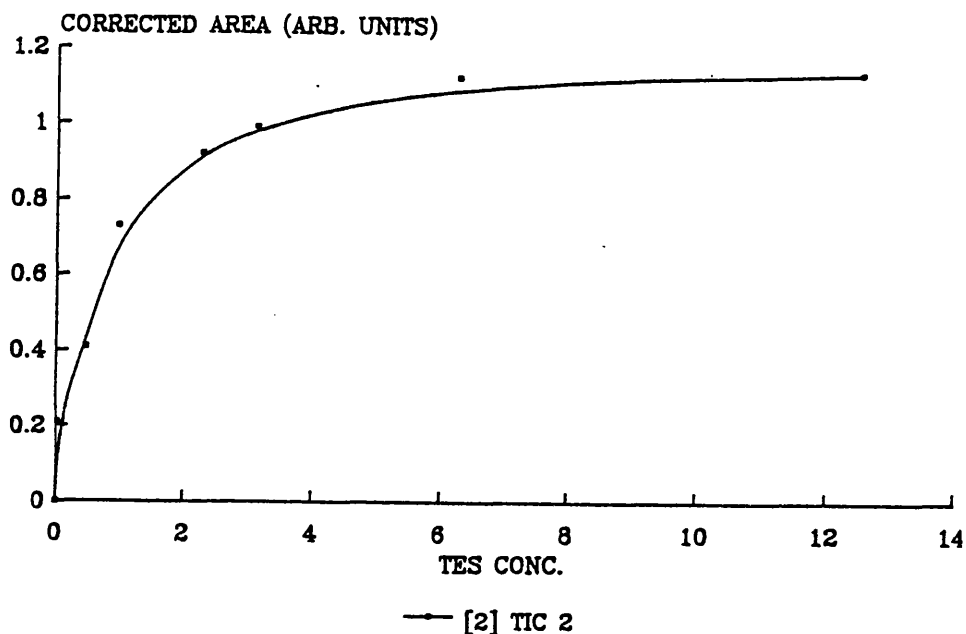


Figure 7.1: Graph showing the increase in trapping product ([2] TIC 2) formation with increasing TES concentration. TES concentration in  $\text{mol dm}^{-3}$ .

A progress curve for the photolysis of BTMS-OMTS (in the presence and absence of TES) showed that all products were produced via primary photochemical pathways (fig. 7.2):

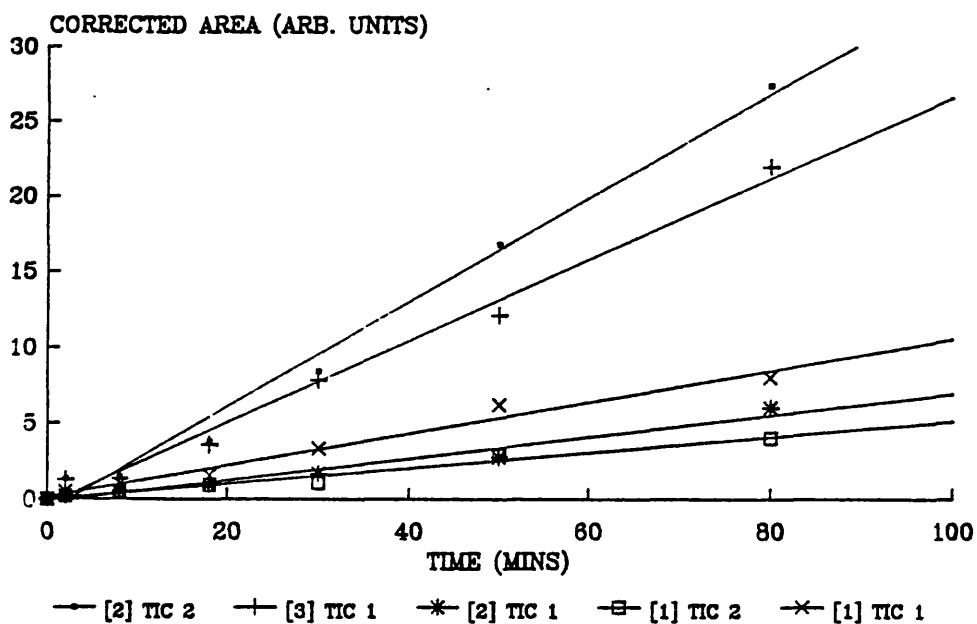


Figure 7.2: Progress curve for the irradiation of BTMS-OMTS at 254 nm.

The relative yields of products formed by photolysis at 254 nm are shown in table 7.2.

Table 7.2: Relative Yields for Products of BTMS-OMTS irradiation.

Product	% Yield
$\text{Me}_3\text{SiSiSiMe}_3$ [1] TIC 1 H Me	4
$\text{Me}_3\text{SiSiSiMe}_3$ [2] TIC 1 Me <sub>2</sub>	3
$\text{Me}_3\text{SiSiSiMe}_3$ [3] TIC 1 Me SiMe <sub>3</sub>	87
$\text{Me}_3\text{SiSiSiH}$ [4] TIC 1 MeMe Me <sub>3</sub> SiSiMe <sub>3</sub>	2
$\text{Me}_3\text{SiSiSiMe}$ [5] TIC 1 MeMe Me <sub>3</sub> SiSiMe <sub>3</sub>	3
$\text{Et}_3\text{SiSiH}$ [1] TIC 2 Me <sub>2</sub>	3
$\text{Et}_3\text{SiSiH}$ [2] TIC 2 Me SiMe <sub>3</sub>	87
$\text{Et}_3\text{SiSiH}$ [4] TIC 2 (SiMe <sub>3</sub> ) <sub>2</sub>	3

A 1:1 n-hexane:TES solution of BTMS-OMTS ( $0.052 \text{ mol dm}^{-3}$ ) was irradiated at 228 nm; the resulting progress curve shows a maximum for i-DMTS formation, revealing some product decomposition at this wavelength of irradiation (fig. 7.3):

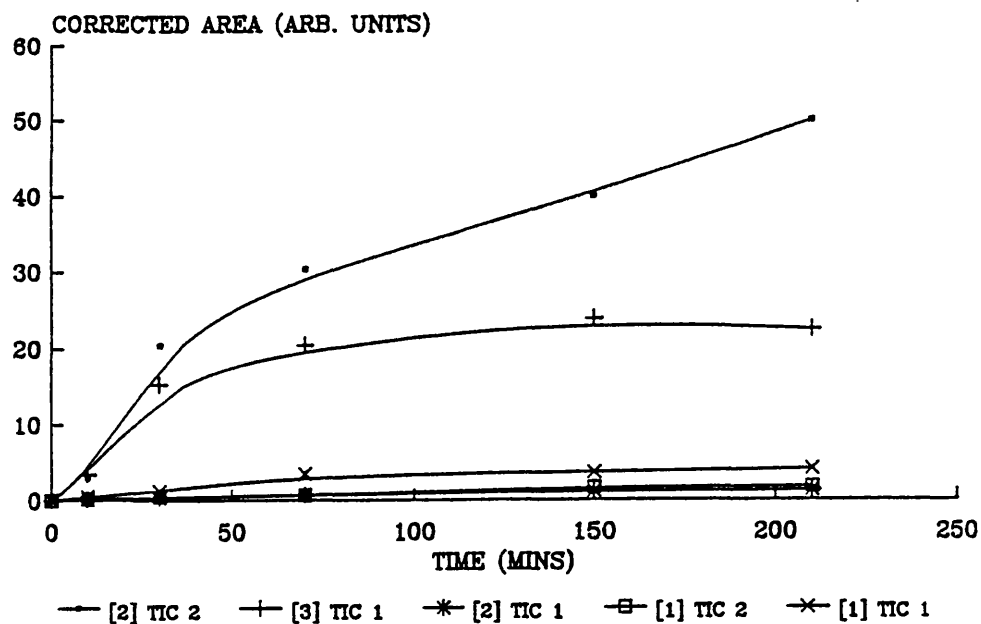
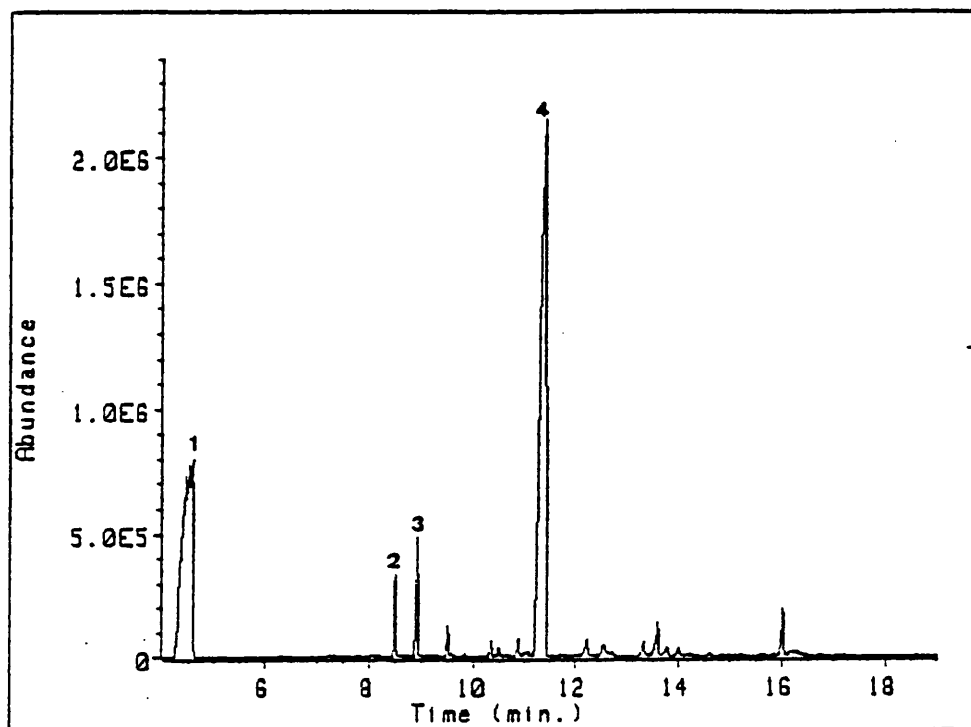


Figure 7.3: Progress curve for the irradiation of BTMS-OMTS at 228 nm.

(ii) i-DMTS

A solution of i-DMTS in n-hexane ( $0.045 \text{ mol dm}^{-3}$ ) was irradiated at 254 nm. TIC 3 shows a sample taken after 3 hours photolysis (approximately 30% decomposition).

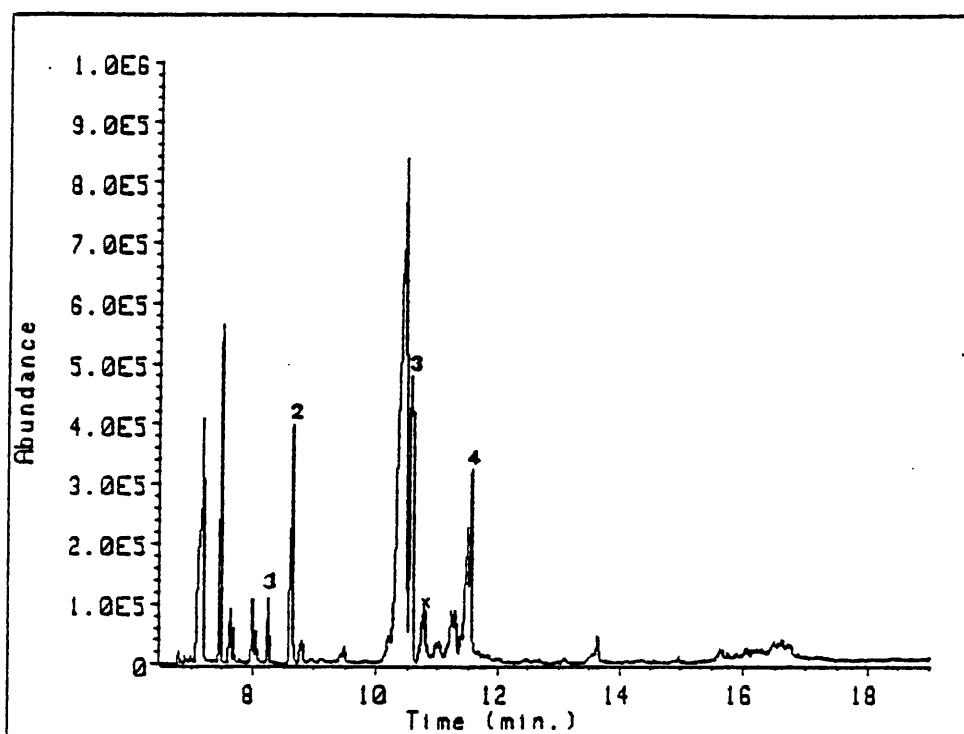


TIC 3: [1]  $\text{Me}_3\text{SiSiMe}_3$ , [2]  $\text{Me}_3\text{Si}\overset{\text{H}}{\underset{\text{Me}}{\text{Si}}}\text{SiMe}_3$ ,  
[3]  $\text{Me}_3\text{Si}\overset{\text{Me}}{\underset{\text{Me}_2}{\text{Si}}}\text{SiMe}_3$ , [4]  $\text{Me}_3\text{Si}\overset{\text{Me}}{\underset{\text{SiMe}_3}{\text{Si}}}\text{SiMe}_3$  (i-DMTS).

The major product was hexamethyldisilane (HMDS), smaller amounts of 2-HMTS and OMTS were also observed. 3MS is also a minor product of this photolysis (*vide supra*).

A 1:1 n-hexane:TES solution of i-DMTS ( $0.0225 \text{ mol dm}^{-3}$ ) was irradiated at 254 nm. TIC 4 shows a sample taken after 3 hours irradiation.





TIC 4: [1]  $\text{Et}_3\text{SiSiH}$ , [2]  $\text{Et}_3\text{Si}-\text{SiH}$ , [3]  $\text{Et}_3\text{SiSiH}$ ,  
 $\text{Me}_2$   $\text{Me}_2$   $\text{SiMe}_3$   
 [4]  $\text{Et}_3\text{SiSiEt}_3$ .

The major intermediate trapped was  $\text{Me}_3\text{Si}(\text{Me})\text{Si}$ : [3], a small amount of  $\text{Me}_2\text{Si}$ : [1] was also trapped.

A progress curve for the photolysis of i-DMTS (with and without TES) showed that all products were formed via primary photochemical pathways (fig 7.4).

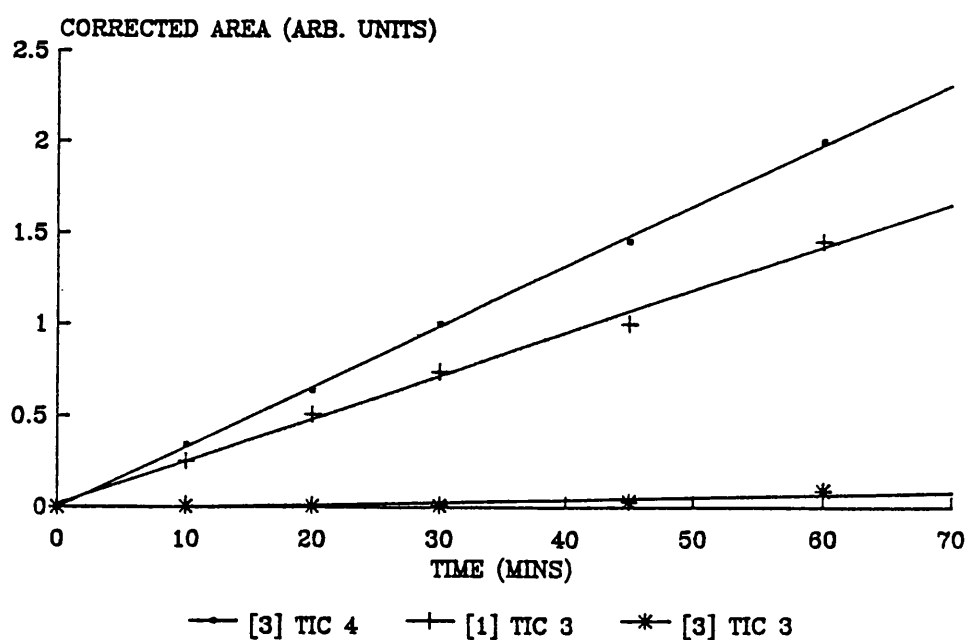


Figure 7.4: Progress curve for the irradiation of i-DMTS at 254 nm.

Table 7.3 lists the relative yields of the products

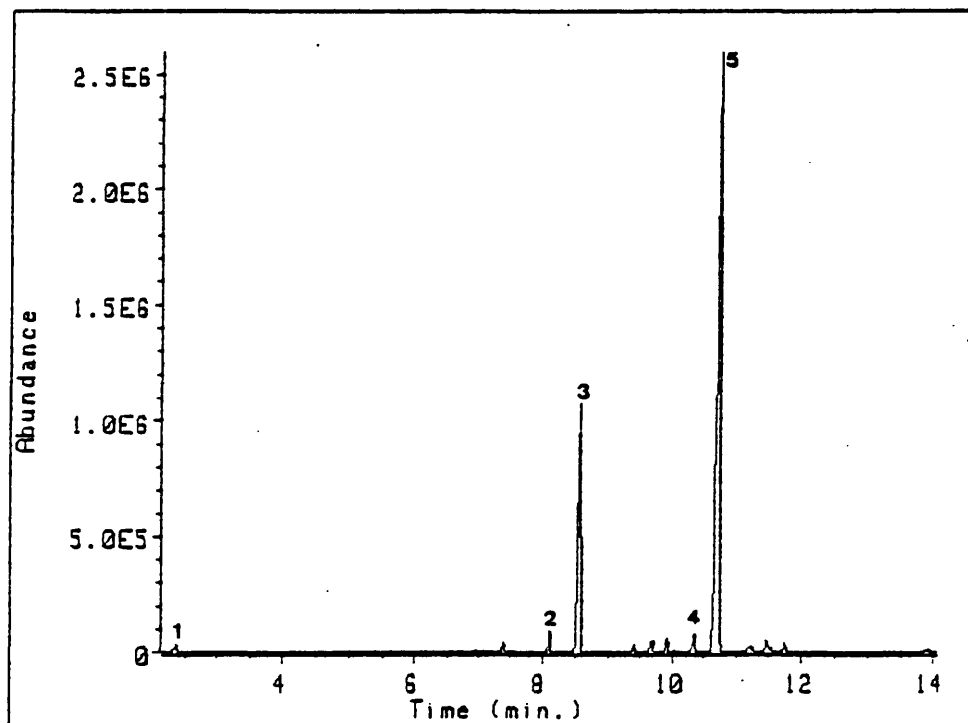
identified in TIC's 3 & 4.

Table 7.3: Relative Yields for Products of i-DMTS irradiation.

Product	% Yield
$\text{Me}_3\text{SiSiMe}_3$ [1] TIC 3	76
$\text{Me}_3\text{SiSiSiMe}_3$ [2] TIC 3	9
$\text{Me}_3\text{SiSiSiMe}_3$ [3] TIC 3	4
$\text{Et}_3\text{SiSiH}$ [1] TIC 4	5
$\text{Et}_3\text{SiSiH}$ [3] TIC 4	80

### (iii) n-DMTS

A solution of n-DMTS in n-hexane ( $0.025 \text{ mol dm}^{-3}$ ) was irradiated at 254 nm. TIC 5 shows a sample taken after 5 minutes photolysis.

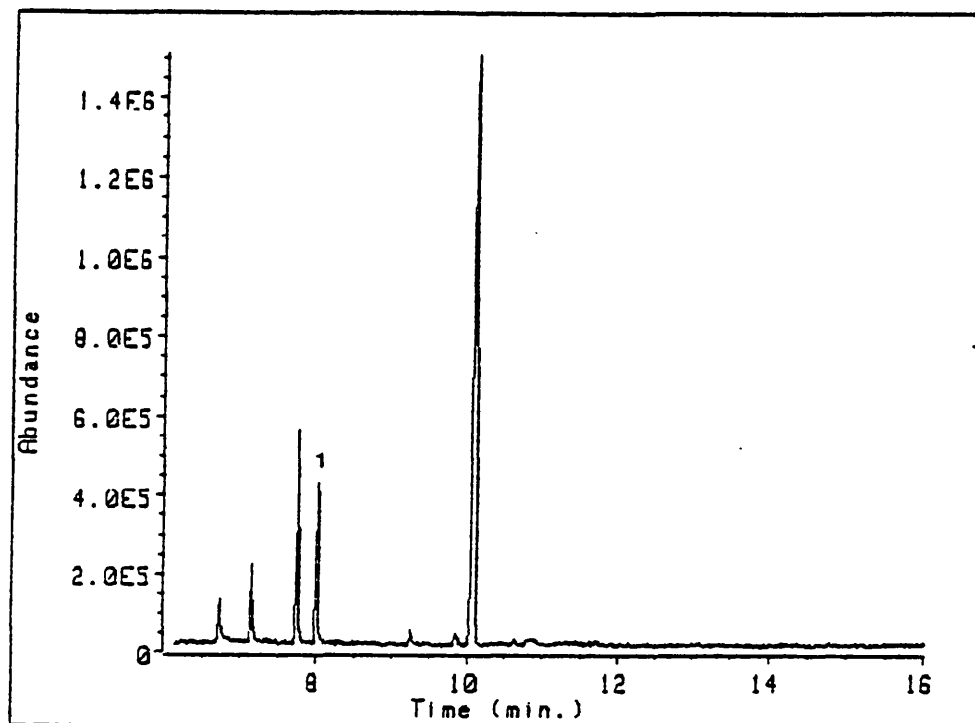


TIC 5: [1]  $\text{Me}_3\text{SiSiMe}_2\text{H}$ , [2]  $\text{Me}_3\text{SiSiSiMe}_2\text{H}$ , [3]  $\text{Me}_3\text{SiSiSiMe}_3$ ,  
 [4]  $\text{Me}_3\text{SiSiSiMe}_2\text{H}$ , [5]  $\text{Me}_3\text{SiSiSiMe}_3$  (n-DMTS).

The major product was OMTS [3], with smaller amounts of pentamethyldisilane [1] (PMDS), 1,1,1,2,2,3,3-heptamethyl-

trisilane [2] (3-HMTS) and 1,1,1,2,2,3,3,4,4-nonamethyl-tetrasilane [4] (NMTS). 3MS was also a product of this photolysis (*vide supra*).

A 1:1 n-hexane:TES solution of n-DMTS ( $0.0125 \text{ mol dm}^{-3}$ ) was irradiated at 254 nm. TIC 6 shows a sample taken after 5 minutes photolysis.



TIC 6: [1]  $\text{Et}_3\text{SiSiHMe}_2$ .

Product [1] is formed by the insertion of  $\text{Me}_2\text{Si:}$  into the Si-H bond of TES.

A progress curve for the photolysis of n-DMTS (with and without TES) revealed that all products are produced via primary photochemical pathways.

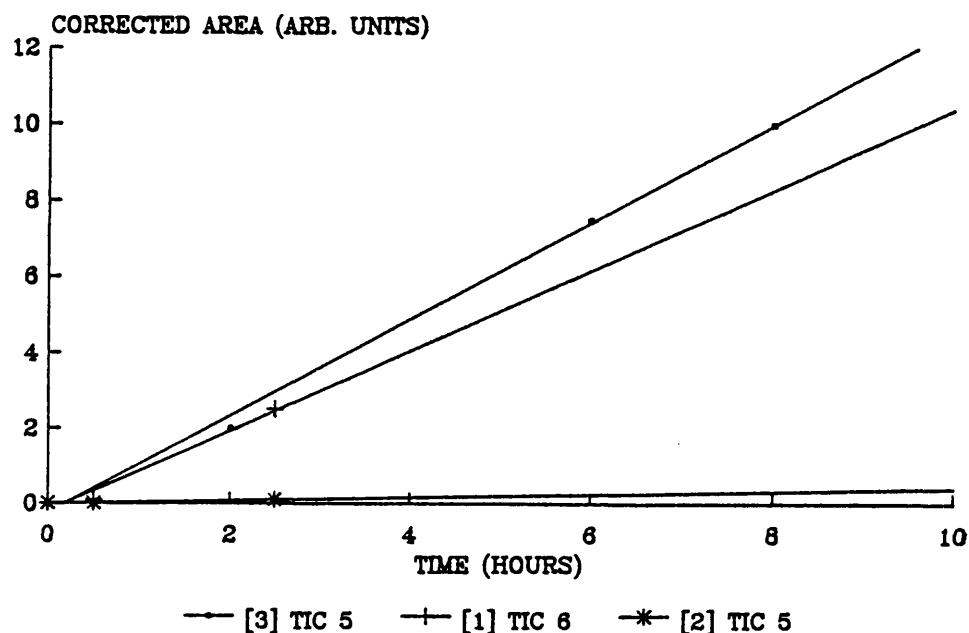


Figure 7.5: Progress curve for the irradiation of n-DMTS at 254 nm.

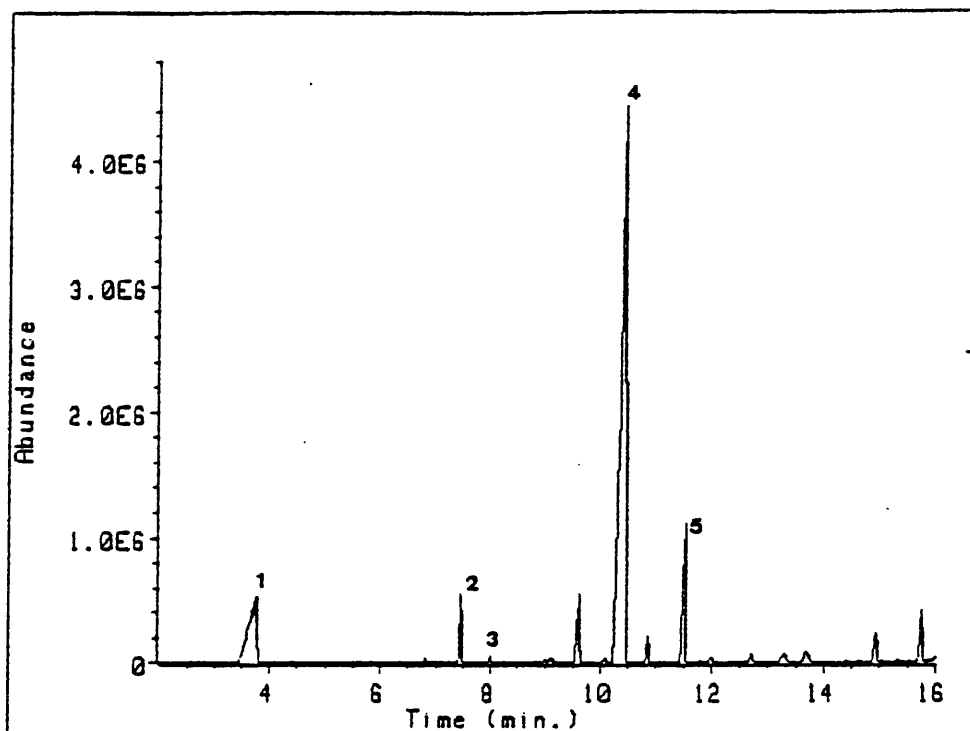
The relative yields of the products shown in TIC's 5 & 6 are given in table 7.4.

Table 7.4: Relative Yields for Products of n-DMTS irradiation

Product	% Yield
$\text{Me}_3\text{SiSiMe}_2\text{H}$ [1] TIC 5	15
$\text{Me}_3\text{SiSiSiMe}_2\text{H}$ [2] TIC 5 $\text{Me}_2$	6
$\text{Me}_3\text{SiSiSiMe}_3$ [3] TIC 5 $\text{Me}_2$	78
$\text{Et}_3\text{SiSiH}$ [1] TIC 6 $\text{Me}_2$	78

#### (iv) DEHMTS

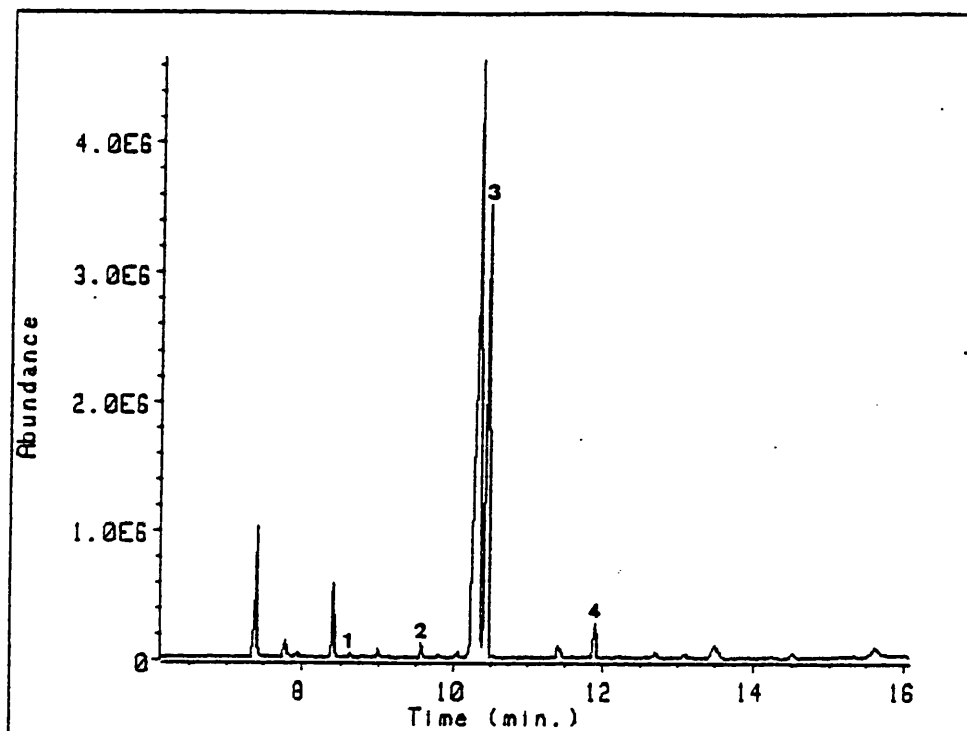
A solution of DEHMTS in n-pentane ( $0.154 \text{ mol dm}^{-3}$ ) was irradiated at 228 nm. TIC 7 shows a sample taken after 8 hours photolysis.



TIC 7: [1]  $\text{Me}_3\text{SiSiMe}_3$ , [2]  $\text{Me}_3\text{SiSiEt}_2\text{H}$ , [3]  $\text{Me}_3\text{SiSiEt}_2\text{Me}$ ,  
 [4]  $\text{Me}_3\text{SiSiEt}_2\text{SiMe}_3$  (DEHMTS), [5]  $\text{Me}_3\text{SiSiEt}_2\text{SiEt}_2\text{H}$ .

The major product was HMDS [1] with smaller amounts of 2,2-diethyl-1,1,1-trimethyldisilane and 2,2-diethyl,1,1,1,2-tetramethyldisilane. 3MS is also a minor product of this photolysis (*vide supra*).

A 1:1 n-pentane:TES solution of DEHMTS ( $0.077 \text{ mol dm}^{-3}$ ) was irradiated at 228 nm. TIC 8 shows a sample taken after 4 hours photolysis.



TIC 8: [1]  $\text{Et}_3\text{SiSiH}$ , [2]  $\text{Et}_3\text{Si}\text{---}\text{SiMe}_2\text{H}$ , [3]  $\text{Et}_3\text{SiSiH}$ ,  
 [4]  $\text{Et}_3\text{SiSiEt}_3$   $\text{Me}_2$   $\text{Et}_2$

The major intermediate trapped was diethylsilylene ( $\text{Et}_2\text{Si:}$ ) [3]; a small amount of  $\text{Me}_2\text{Si:}$  [1] was also trapped.

A progress curve for the photolysis of DEHMTS (in the absence and presence of TES) showed that products were formed via primary photochemical pathways (fig. 7.6).

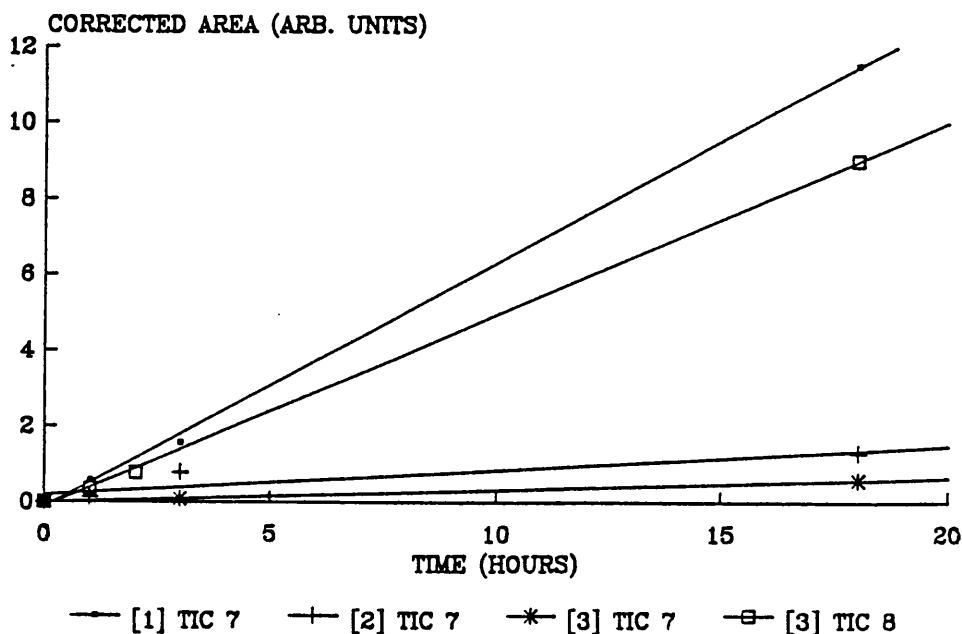


Figure 7.6: Progress curve for the irradiation of HMDETS at 228 nm.

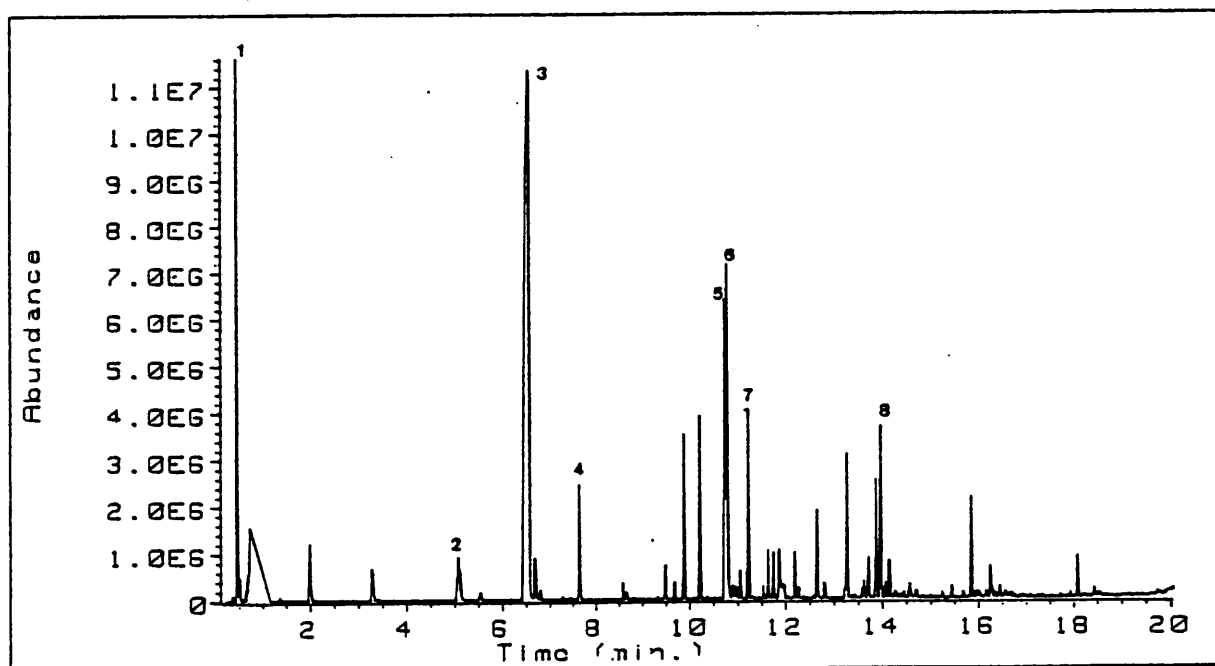
Table 7.5 gives the relative yields of the products identified in TIC's 7 & 8.

Table 7.5: Relative Yields for Products of DEHMTS irradiation.

Product	% Yield
$\text{Me}_3\text{SiSiMe}_3$ [1] TIC 7	80
$\text{Me}_3\text{SiSiEt}_2\text{H}$ [2] TIC 7	15
$\text{Me}_3\text{SiSiSiMeEt}_2$ [3] TIC 7	1
$\text{Et}_3\text{SiSiHMe}_2$ [1] TIC 8	1
$\text{Et}_3\text{SiSiHEt}_2$ [2] TIC 8	80

#### (v) OMTS

A solution of OMTS ( $0.99 \text{ mol dm}^{-3}$ ) in n-pentane was irradiated at 228 nm. TIC 9 shows a sample taken after 6 hours photolysis.



TIC 9: [1]  $\text{Me}_3\text{SiH}$ , [2]  $\text{Me}_3\text{SiSiMe}_2\text{H}$ , [3]  $\text{Me}_3\text{SiSiMe}_3$ ,

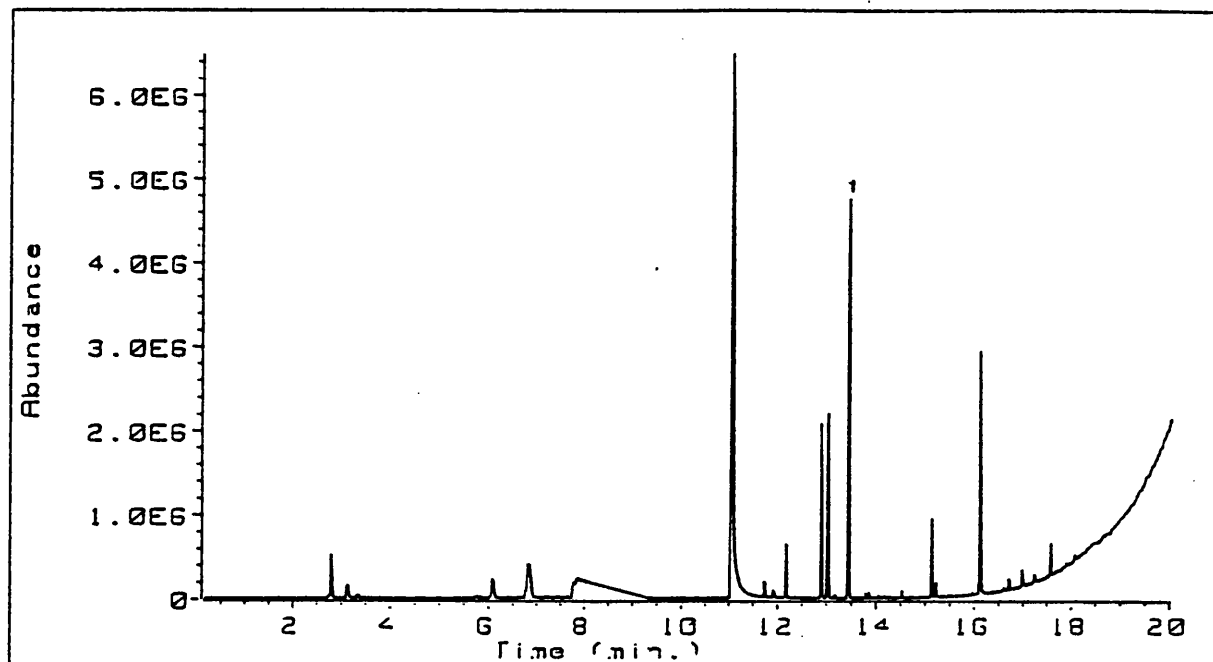
[4]  $\text{Me}_2\text{Si} \diamond \text{SiMe}_2$ , [5] n-decane, [6]  $\text{Me}_3\text{SiSiSiMe}_3$ ,  
 $\text{Me}_2$

[7]  $\text{Me}_2\text{Si} \diamond \text{Si(Me)SiMe}_3$ , [8]  $\text{Me}_3\text{Si(Me)Si} \diamond \text{Si(Me)SiMe}_3$

The major product was HMDS with smaller amounts of 3MS and PMDS. Three interesting products were the disilacyclobutanes [4], [7] and [8].

A 1:1 n-pentane:TES solution of OMTS ( $0.50 \text{ mol dm}^{-3}$ ) was

irradiated at 228 nm. TIC 10 shows a sample taken after 6 hours photolysis.



TIC 10: [1]  $\text{Et}_3\text{SiSiH}_2\text{Me}_2$

The only intermediate trapped was  $\text{Me}_2\text{Si}^{\cdot\cdot}$ .

A progress curve for the photolysis of OMTS (with and without TES) showed that all products arose via primary photochemical pathways (fig. 7.7).

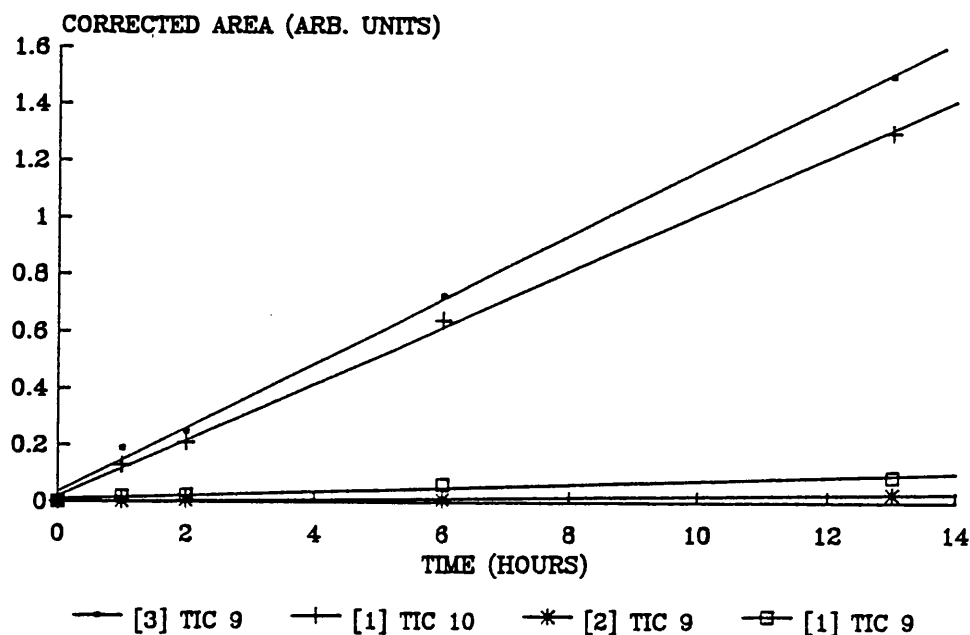


Figure 7.7: Progress curve for the irradiation of OMTS at 228 nm.

Relative yields for the major products shown TIC's 9 & 10 are given in table 7.6.



**Table 7.6: Relative Yields of Products for irradiation of OMTS**

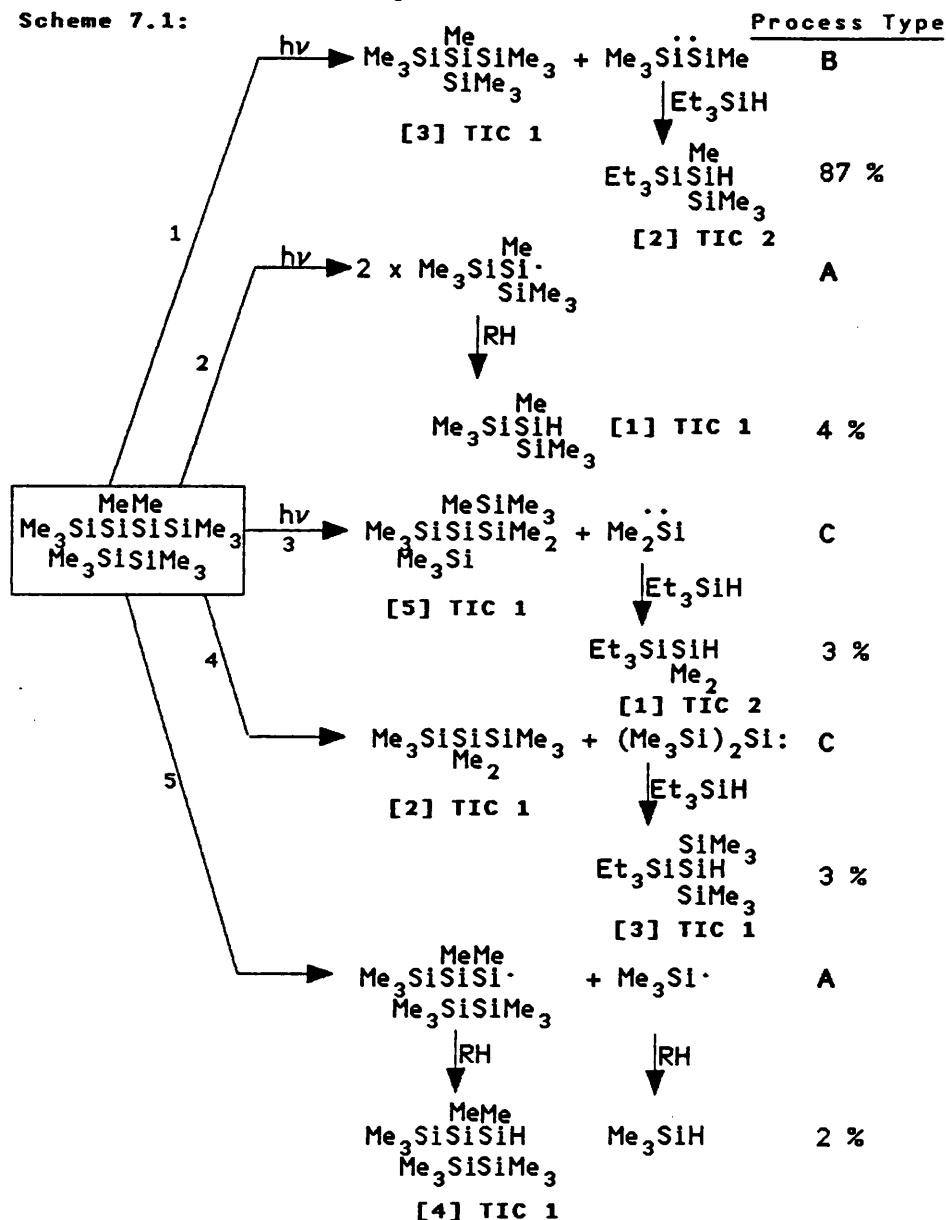
Product	% Yield
$\text{Me}_3\text{SiH}$	2
$\text{Me}_3\text{SiSiMe}_2\text{H}$	2
$\text{Me}_3\text{SiSiMe}_3$	75
$\text{Et}_3\text{SiSiHMe}_2$	75

### (III) Discussion

#### (i) BTMS-OMTS

Scheme 7.1 shows the primary processes which lead to the formation of the products of the photolysis of BTMS-OMTS. Unique products from TES experiments are also shown.

Scheme 7.1:



Process B is the major photochemical breakdown route (87%) leading to the formation of i-DMTS and  $\text{Me}_3\text{Si}(\text{Me})\text{Si:}$ .  $\text{Me}_3\text{Si}(\text{Me})\text{Si:}$  is trapped by TES to yield [2] TIC 2.

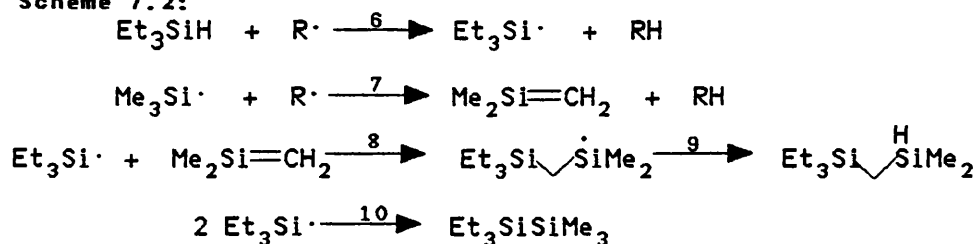
Two separate reactions are classified as process C, observed for the first time in oligosilane photochemistry as a minor photochemical pathway.

Silyl radicals are formed in reactions (2 & 5) by process A. These silyl radicals abstract hydrogen to yield

hydridosilanes.

Silyl radical hydrogen abstraction is thought to lead to the formation of two minor products which are general to all TES photolyses,  $\text{Et}_3\text{SiCH}_2\text{Si}(\text{H})\text{Me}_2$  and  $\text{Et}_6\text{Si}_2$ . Hydrogen abstraction from either trimethylsilyl radicals ( $\text{Me}_3\text{Si}\cdot$ ) or TES leads to the reactions in scheme 7.2.

Scheme 7.2:

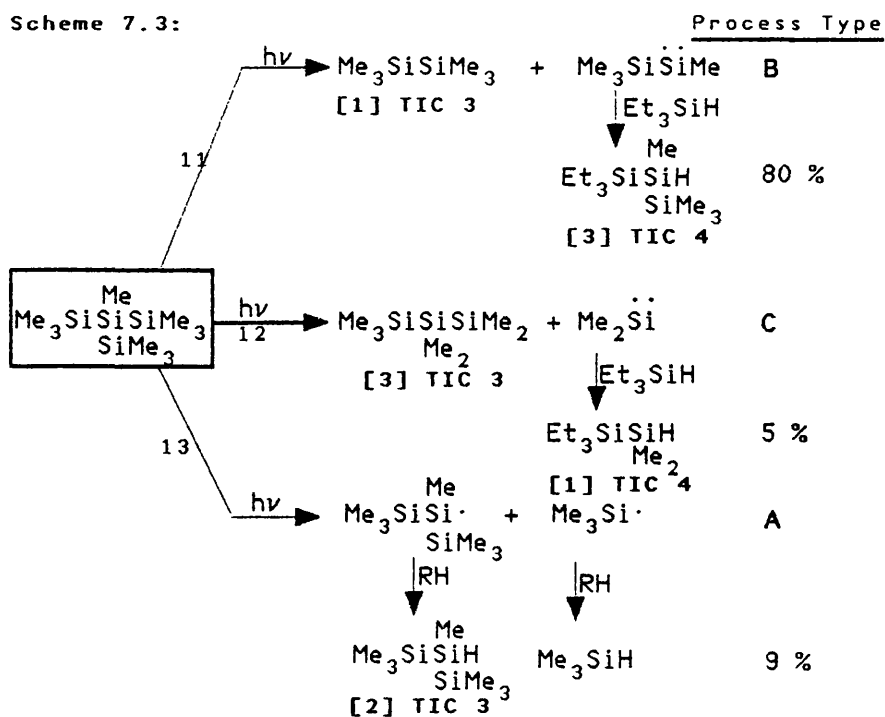


Hydrogen abstraction from  $\text{Me}_3\text{Si}\cdot$  radicals yields a hydridosilane and dimethylsilene ( $\text{Me}_2\text{Si}=\text{CH}_2$ ) (7). Hydrogen abstraction from TES yields a triethylsilyl radical ( $\text{Et}_3\text{Si}\cdot$ ) and a hydridosilane (6). Addition of  $\text{Et}_3\text{Si}\cdot$  radicals to  $\text{Me}_2\text{Si}=\text{CH}_2$  generates a new silicon centred radical (8) which can abstract hydrogen to yield  $\text{Et}_3\text{SiCH}_2\text{SiMe}_2\text{H}$  (9). The combination of  $\text{Et}_3\text{Si}\cdot$  radicals leads to the formation of hexaethyldisilane (10). In the absence of TES the silyl radicals are thought to abstract hydrogen from  $\text{Me}_3\text{Si}\cdot$  radicals, although no characteristic products from the dimerisation of the resulting  $\text{Me}_2\text{Si}=\text{CH}_2$  were observed.

## (ii) i-DMTS

The processes leading to the formation of products from the photolysis of i-DMTS are shown in scheme 7.3. Unique products from the TES are also rationalised.

Scheme 7.3:



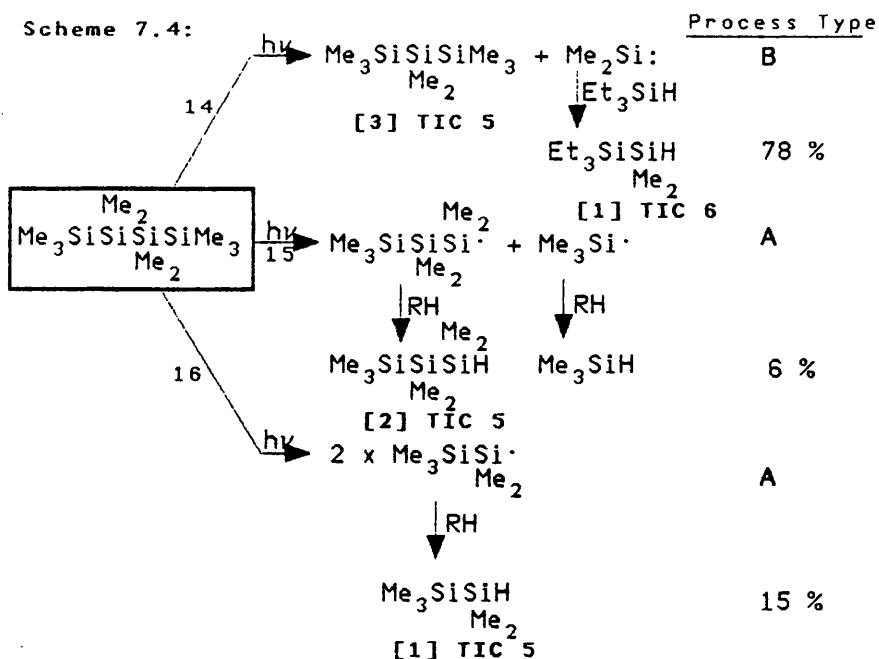
The major photochemical pathway is B (85 %), leading to the formation of HMDS and  $\text{Me}_3\text{Si}(\text{Me})\text{Si}^\cdot$ , the silylene being trapped in the presence of TES to yield [3] TIC 4.

Process C leads to the formation of OMTS and  $\text{Me}_2\text{Si}^\cdot$ ,  $\text{Me}_2\text{Si}^\cdot$  being trapped in the presence of TES ([1] TIC 4).

Process A leads to the formation of two silyl radicals which abstract hydrogen (see scheme 7.2) to yield two hydrosilanes.

### (iii) n-DMTS

Scheme 7.4 shows the processes leading to the formation of the major products of the photolysis of n-DMTS (including TES trapping products).

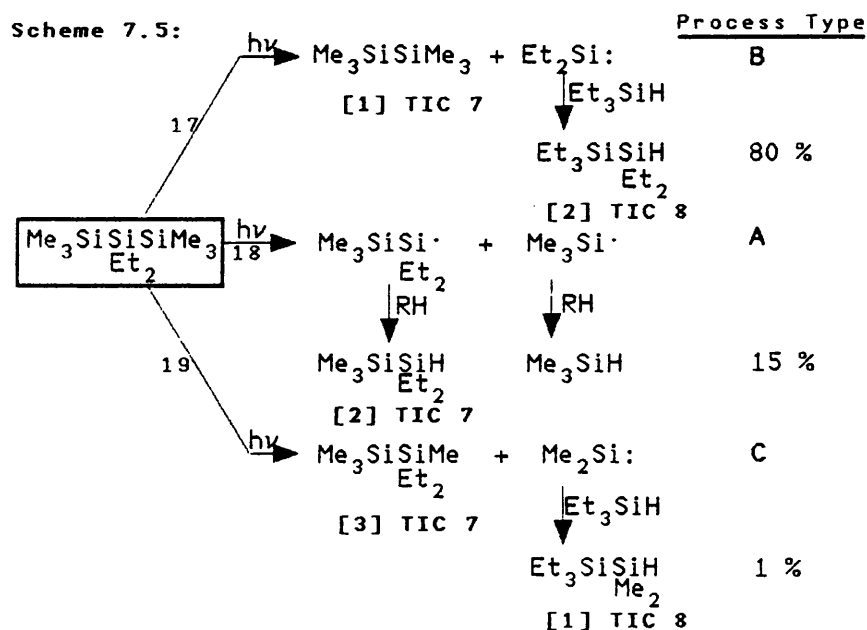


The major photochemical process is B, leading to the formation of OMTS and  $\text{Me}_2\text{Si:}$ .  $\text{Me}_2\text{Si:}$  is trapped by TES to yield [1] TIC 6.

Process A yields three silyl radicals (15 & 16) which can abstract hydrogen to give hydridosilanes (scheme 7.2).

#### (iv) DEHMTS

The primary photochemical processes occurring in DEHMTS are summarised in scheme 7.5.



Process B (80 %) leads to the formation of HMDS and  $\text{Et}_2\text{Si:}$

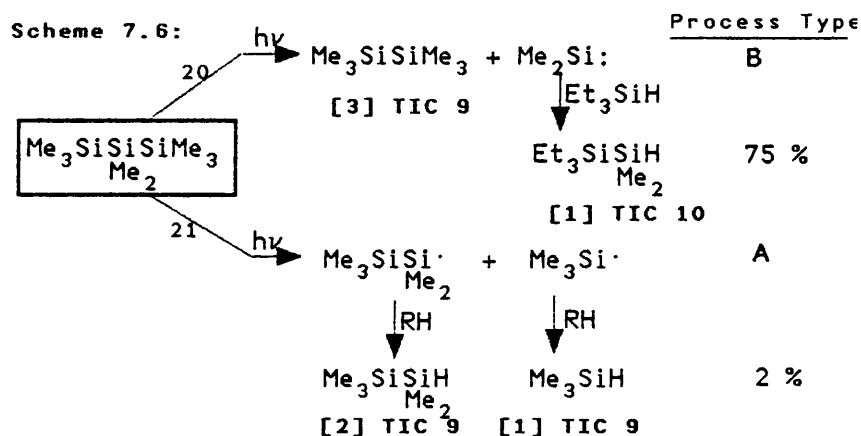
which is trapped in the presence of TES to yield [2] TIC 8.

For the first time in a straight chained oligosilane process C is observed (19), leading to the formation of 2,2-diethyl-1,1,1,2-tetramethyldisilane and  $\text{Me}_2\text{Si:}$ , the silylene being trapped in the presence of TES ([1] TIC 8)

The silyl radicals produced via process A (18) abstract hydrogen (Scheme 7.2) to yield hydridosilanes.

#### (v) OMTS

The primary photochemical processes occurring in OMTS are shown in scheme 7.6.

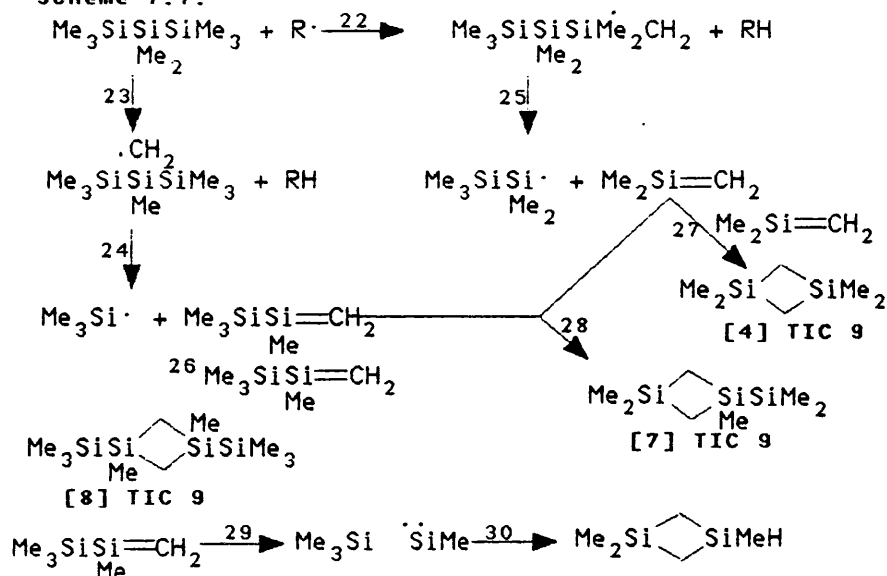


The major process is again B, leading to the formation of HMDS and  $\text{Me}_2\text{Si:}$ .

The hydridosilanes [1] & [2] (TIC 9) are formed via silyl radical hydrogen abstraction, the silyl radicals being formed via process A.

Scheme 7.2 offers one explanation for the source of hydrogen for these silyl radicals. Another source of hydrogen could be OMTS. Characteristic products of hydrogen abstraction from terminal and central methyl groups are observed ([4], [7] & [8] TIC 1). Scheme 7.7 shows possible reactions leading to these products.

Scheme 7.7:



Hydrogen abstraction from a central methyl group yields a carbon centred radical (23). This radical can dissociate to form a  $\text{Me}_3\text{Si}\cdot$  radical and trimethylsilyl(methyl)silene (24). Trimethylsilyl(methyl)silene can dimerise to form 1,3-bis-trimethylsilyl-1,3-dimethyl-1,3-disilacyclobutane ([8] TIC 1) (26).

Trimethylsilyl(methyl)silene can also isomerise to a silylene (29) which ring closes via an internal C-H insertion to form 1,1,3-trimethyl-1,3-disilacyclobutane (30), a product detected in trace amounts.

Hydrogen abstraction from a terminal methyl group yields a carbon centred radical (22) which dissociates to form a pentamethyldisilyl radical and dimethylsilene (25).  $\text{Me}_2\text{Si}=\text{CH}_2$  can dimerise to yield 1,1,3,3-tetramethyl-1,3-disilacyclobutane ([4] TIC 1) or it may add to trimethylsilyl(methyl)silene to yield 1-trimethylsilyl-1,3,3-trimethyl-1,3-disilacyclobutane ([7] TIC 1).

#### (IV) Summary

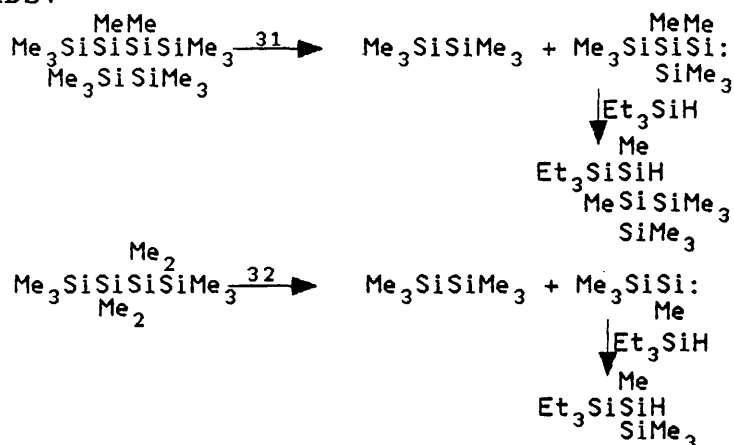
For all the oligosilanes studied, process B is the major photochemical breakdown route. The photochemistry of the branched oligosilanes (BTMS-OMTS & i-DMTS) reveal that process C is a general reaction for these compounds.

Evidence for process C in the photochemistry of straight chained oligosilanes comes from DEHMTS. Process C probably

occurs in the photochemistry of n-DMTS and OMTS but it is not detected because the same products as process B result. Therefore, the production of Me<sub>2</sub>Si: from n-DMTS and OMTS is more complicated than previously assumed, the majority is formed by B where an internal silicon atom is lost, while some will be formed by C where a terminal silicon atom is lost.

Processes A, B and C in polysilane photochemistry have counterparts in oligosilane photochemistry. Process A is dominant in polysilane photochemistry while process B is dominant in oligosilane photochemistry (Chapter 1, part VII).

Not all possible process C reactions take place e.g. one possible product of the irradiation of both BTMS-OMTS and n-DMTS is HMDS.



Neither HMDS nor the corresponding hydridosilanes of the trapped silylenes in TES experiments were noticed in either case, the reason for this is unknown.

The photolysis study gives three suggestions for the source of hydrogen for silyl radical H-abstraction:-

- (i) Me<sub>3</sub>Si· radicals (scheme 2),
- (ii) Oligosilane starting material (scheme 7),
- (iii) TES (if present) (scheme 2).

Suggestion (ii) could be a general source of hydrogen in all cases studied, the characteristic products being noticed only in the case of OMTS because this solution was the most concentrated photolysed.

The difference between the photo and thermal chemistry of the oligosilanes studied is clear. In the photolysis studies silylene formation dominates while thermal decomposition is predominantly silyl radical in nature.



#### (V) Acknowledgements

I would like to thank Dr. Alan Mckinley of the University of Texas at Austin for help with the photochemical techniques. I am particularly grateful to Dr. Richard Taylor of Dow Corning for the synthesis of the oligosilanes. Thanks also to Richard Weaver and Matthew Eaves for their help with some of the photolysis experiments.

#### (VI) References

- (1) H. Gilman, W.H. Atwell, G.G. Schweke, *J. Organomet. Chem.*, 1964, 2, 369.
- (2) M. Ishikawa, M. Kumada, *J. Chem. Soc., Chem. Commun.*, 1971, 489.
- (3) M. Ishikawa, T. Takaoka, M. Kumada, *J. Organomet. chem.*, 1972, 42, 333.
- (4) M. Ishikawa, M. Kumada, *Adv. Organomet. Chem.*, 1986, 6, 19.
- (5) P. Trefonas, R. West, R.D. Miller, *J. Am. Chem. Soc.*, 1985, 107, 2737.
- (6) A.J. McKinley, T. Karatsu, G.M. Wallraff, R.D. Miller, R. Sooriyakumaran, J. Michl, *Organometallics*, 1988, 7, 2567.
- (7) T. Karatsu, R.D. Miller, R. Sooriyakumaran, J. Michl, *J. Am. Chem. Soc.*, 1989, 111, 1140.
- (8) Th. Brix, E. Bastian, P. Potzinger, *J. Photochem. Photobiol., A*, 1989, 49, 287.
- (9) I.M.T. Davidson, J. Michl, T. Simpson, *Organometallics*, 1991, 10, 842.

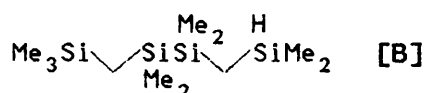
## Appendix 1

### The Pyrolysis of Carbosilanes [A]\* & [B]\*

\*Where [A] = 1,1,1,2,2,4,4,6,6-nonamethyl-1,2,4,6-n-tetrasilahexane:

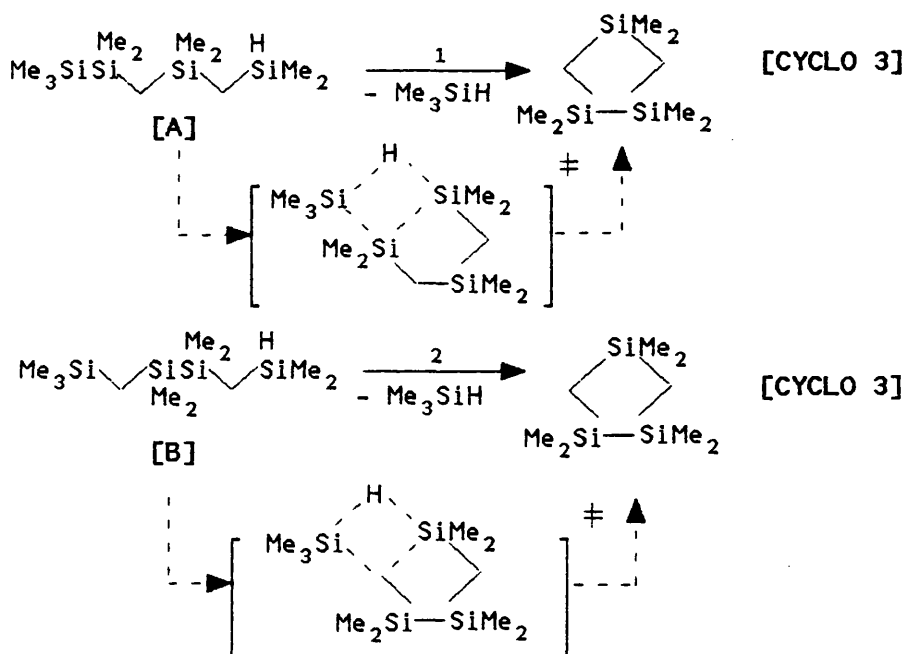


and [B] = 1,1,1,3,3,4,4,6,6-nonamethyl-1,3,4,6-n-tetrasilahexane:



#### (I) Introduction

1,1,3,3,4,4-hexamethyl-1,3,4-trisilacyclopentane (Chapter 3 TIC 1c- product [16] CYCLO 3) is a prominent product of the high sample pressure pyrolysis of octamethyltrisilane (OMTS). Carbosilanes [A] and [B] were believed to be precursors to the formation of CYCLO 3 (Chapter 3, Schemes 3.3 & 3.4), undergoing a novel ring closure reaction with the elimination of trimethylsilane (3MS):



To test these mechanistic suggestions, carbosilanes [A] and [B] were synthesised.

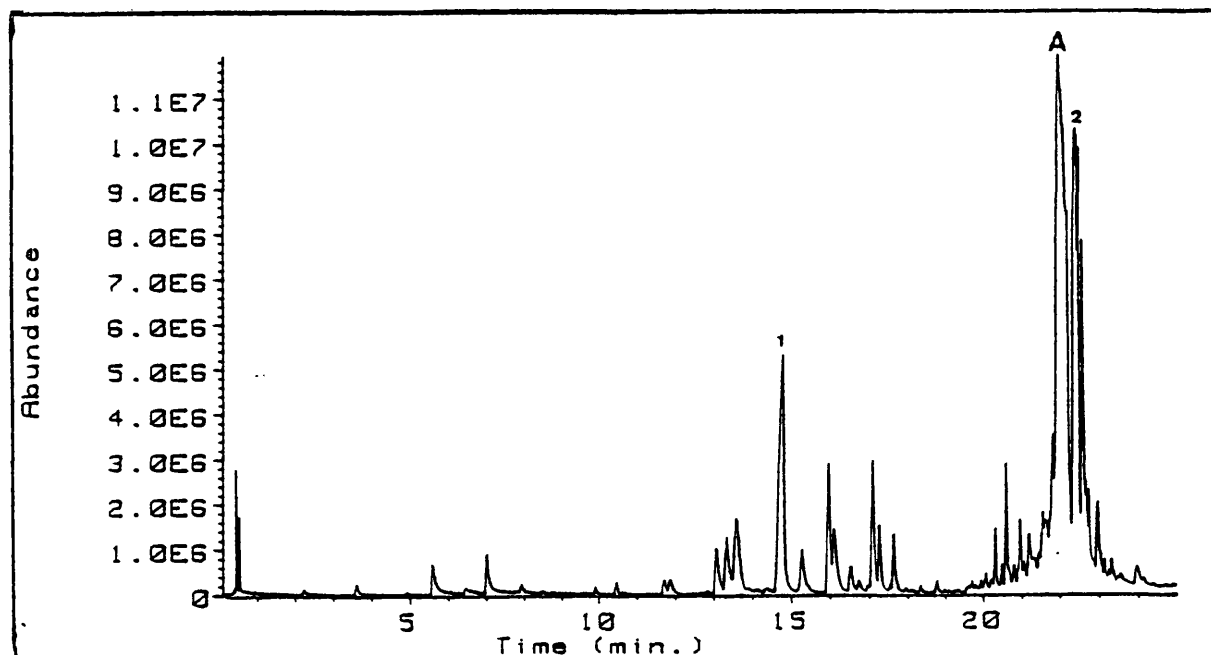
[A] and [B] were pyrolysed in the same temperature range as OMTS (570-650°C). Product identification was by GC/MS, supplemented by comparative retention time tests and mass

spectral analysis on known samples.

Kinetic experiments were performed to further elucidate the thermal breakdown mechanisms of [A] and [B]. First order rate constants were calculated for major product formation.

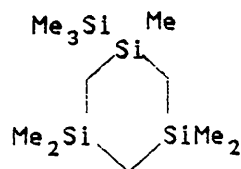
## (II) GC/MS-SFR Results for [A]

[A] was pyrolysed by the liquid injection technique between 600-650°C. Prominent products included 3MS and CYCLO 3. Another major product was a cyclic carbosilane of molecular weight 274 (mw [A] = 276). This cyclic carbosilane [CYCLO A] gave a mass spectrum corresponding to the structure given below TIC 1:



TIC 1: [1] CYCLO 3, [2] CYCLO [A]; vol [A] = 0.1  $\mu$ l,  
temp = 618°C.

where CYCLO [A] corresponds to:-

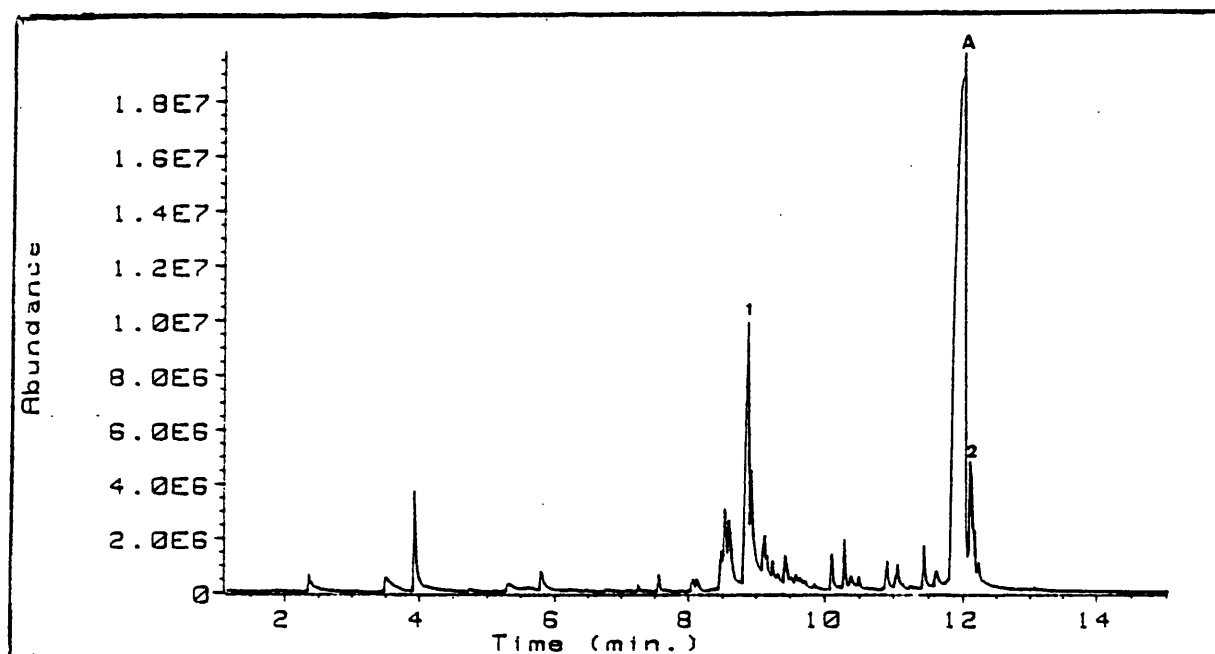


The minor products were cyclic carbosilanes in common with those found in the pyrolysis of OMTS. CYCLO 3 and CYCLO [A] were the prominent products in low sample pressure pyrolyses, the other cyclic carbosilanes being suppressed.

Co-pyrolysis in the presence of butadiene or toluene did not affect product composition or yield. The butadiene experiments revealed the presence of a small amount of dimethylsilylene. The toluene experiments showed that methyl

and trimethylsilyl radicals were also present.

Pyrolysis in the presence of methylchloride (MeCl) suppressed the formation of the minor cyclic carbosilanes, however, CYCLO 3 and CYCLO [A] remain unaffected (TIC 2). Minor products in this pyrolysis were chlorosilanes, including trimethylchlorosilane, derived from silyl radical chlorine abstraction reactions:



TIC 2: [1] CYCLO 3, [2] CYCLO [A]; vol [A] = 1.0  $\mu$ l, sample pres. MeCl = 15.0 torr, temp = 606°C

### (III) Kinetic-SFR Results for [A]

[A] was pyrolysed using the liquid injection technique between 600-650°C. Rate constants for the formation of the 3MS, CYCLO 3 and CYCLO [A] were calculated (fig A1.1). Table A1.1 gives the Arrhenius parameters for the formation of these products.

Table A1.1: Arrhenius parameters for the formation of 3MS, CYCLO 3 & CYCLO [A].

Product	$\log(A/s^{-1})$	$E_a(kJmol^{-1})$	$k(620^\circ C)$
3MS	$11.7 \pm 1.3$	$220 \pm 23$	0.060
CYCLO 3	$11.5 \pm 0.7$	$215 \pm 13$	0.076
CYCLO [A]	$9.4 \pm 0.4$	$192 \pm 6$	0.013

The rate constants of formation for both 3MS and CYCLO 3 are greater than those for the formation of CYCLO [A]. The

Arrhenius plot for the formation of CYCLO 3 is shown in figure A1.2.

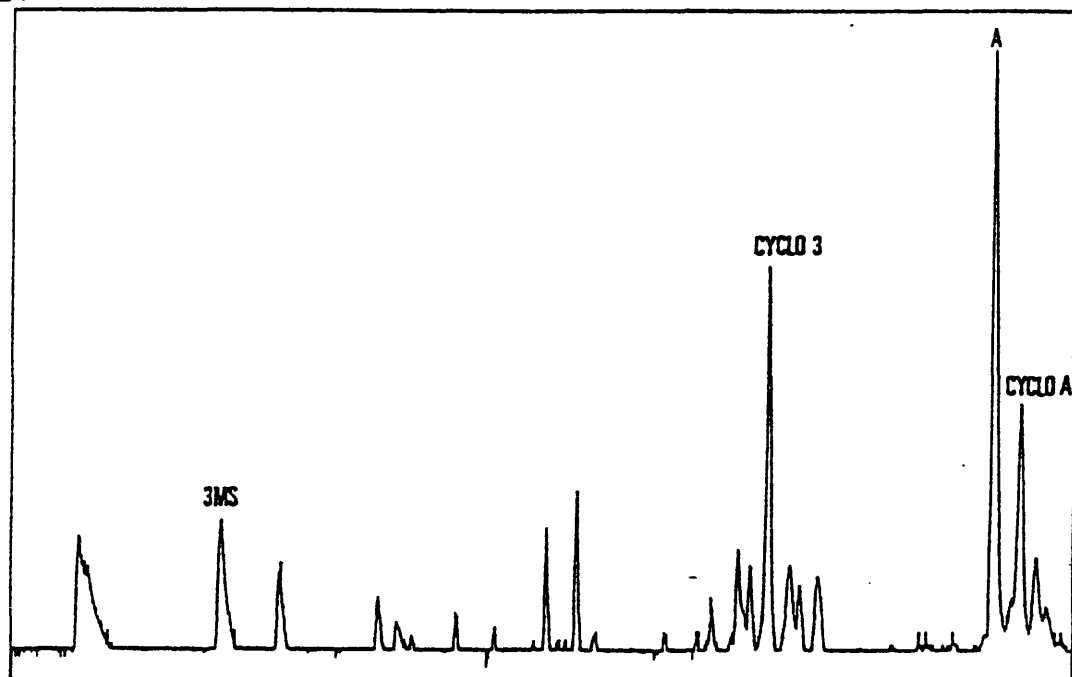


Figure A1.1: Gas chromatogram for the pyrolysis of [A] at 530°C.

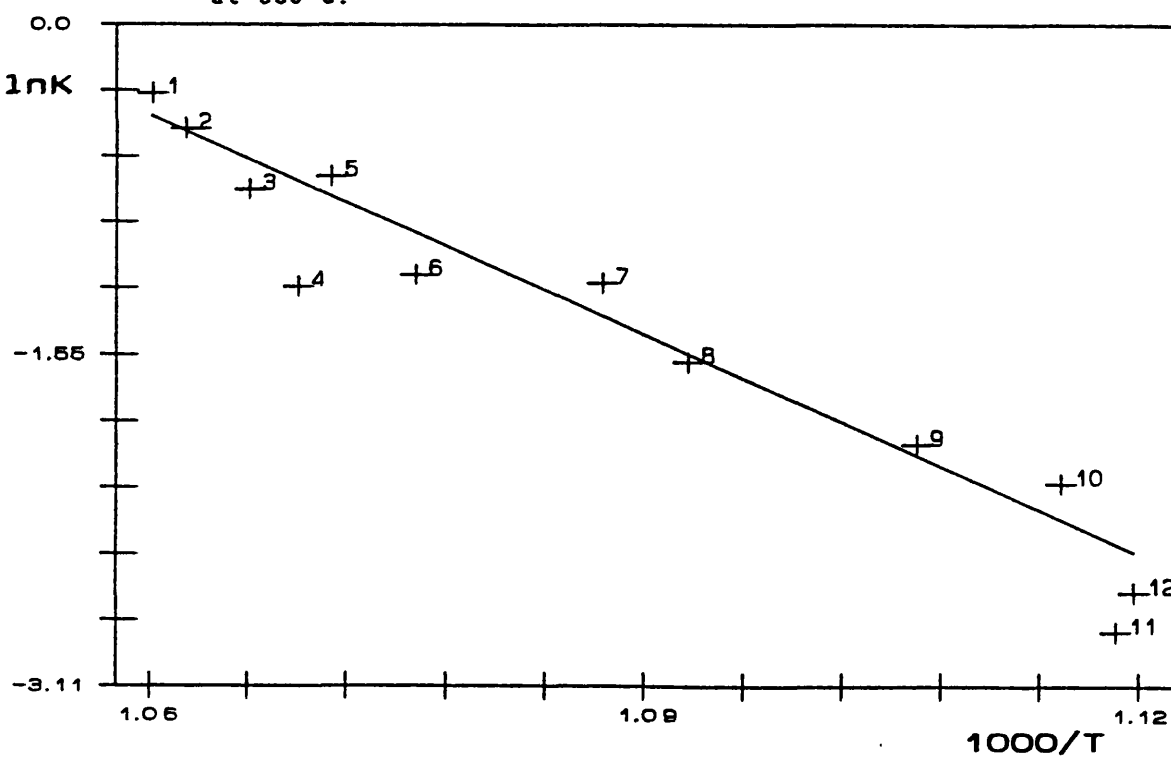


Figure A1.2: Arrhenius plot for the formation of CYCLO 3

A Q8/MS-sealed tube pyrolysis experiment on [A] showed that hydrogen was a prominent product. Some methane was also identified. The time scale for this pyrolysis was calculated from the Arrhenius parameters for the formation of 3MS:

At 550°C  $k = 5.5 \times 10^{-3} \text{ (s}^{-1}\text{)}$ ,  $t_{1/2} = 2.1 \text{ mins.}$

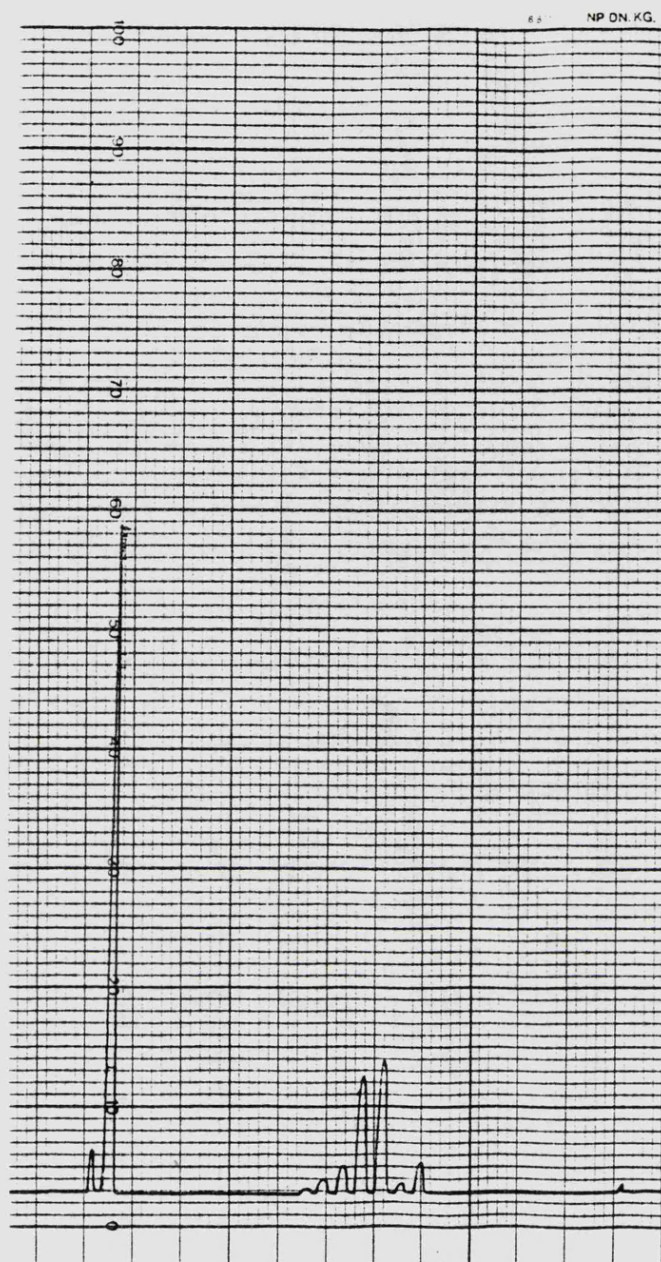
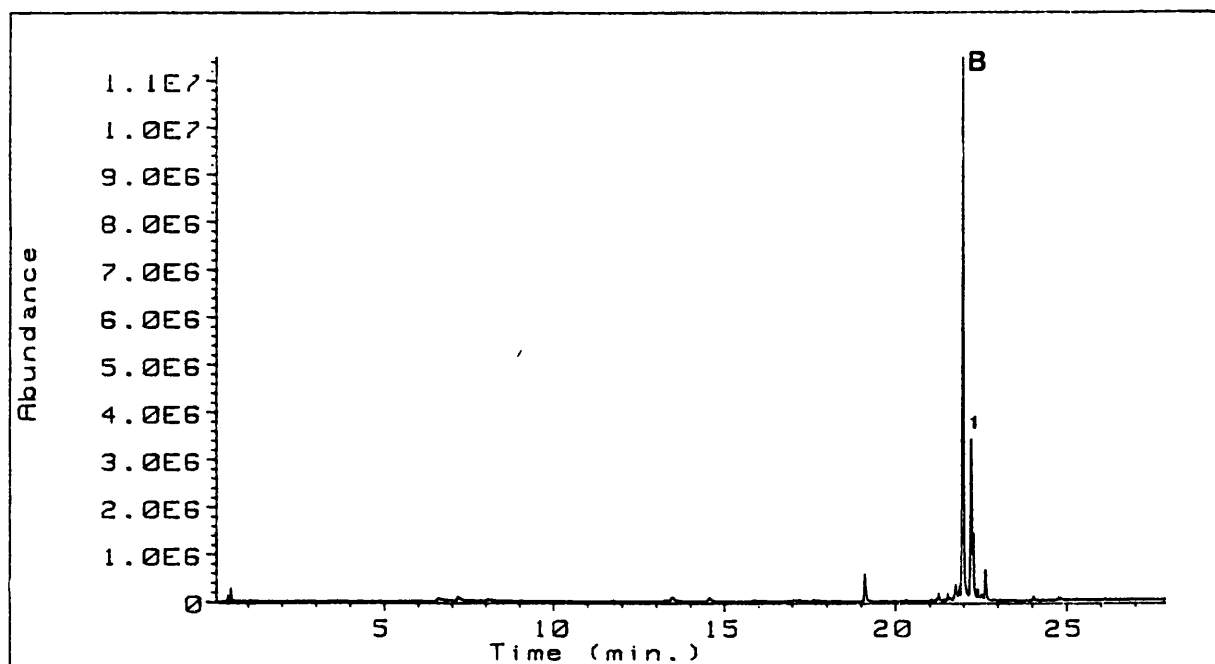


Figure A1.3: Mass Spectrum of  $H_2$  and  $CH_4$  from the sealed tube pyrolysis of [A] at  $550^\circ C$ .

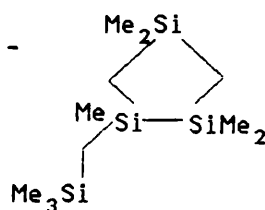
### (III) GC/MS-SFR Results for [B]

[B] was pyrolysed between  $600-650^\circ C$  using the liquid injection technique. The major product was a cyclic carbosilane (CYCLO [B]) with molecular weight 274 (mw [B] = 276). The structure of [B] is shown below TIC 3:



TIC 3: [1] CYCLO [B]; vol [B] = 0.04  $\mu$ l, temp = 612°C

where CYCLO [B] corresponds to:-



Co-pyrolysis in the presence of butadiene, toluene or MeCl had no affect on the production of CYCLO [B].

Kinetic experiments were performed between 600-650°C and rate constants measured for the formation of [B]. The Arrhenius parameters for the formation of this product are given in table A1.2:

Table A1.2: Arrhenius parameters for the formation of CYCLO [B].

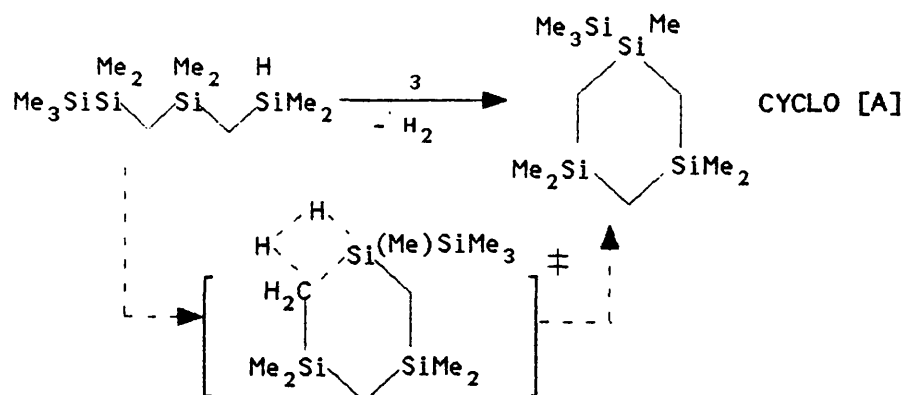
Product	$\log(A/s^{-1})$	$E_a(kJmol^{-1})$	$k(620^\circ C)$
CYCLO [B]	$10.6 \pm 1.2$	$214 \pm 21$	0.012

A Q8/MS-Sealed tube experiment on [B] showed there was a substantial amount of hydrogen produced in the pyrolysis.

#### (IV) Conclusion

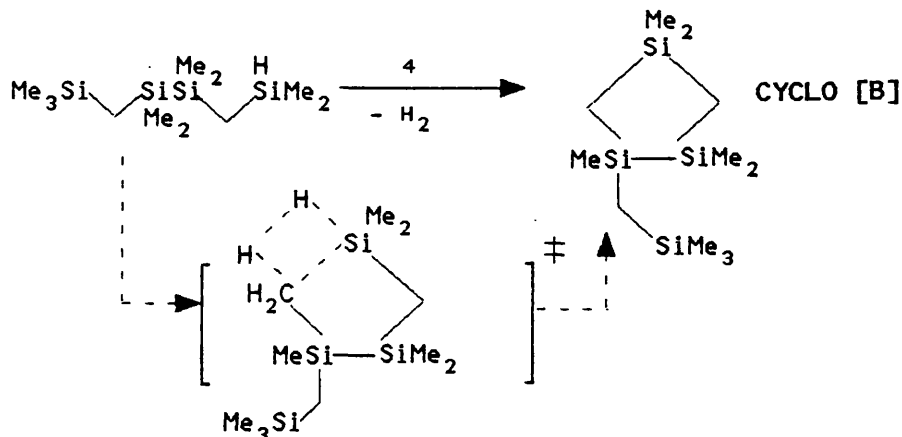
The pyrolysis of carbosilane [A] showed that the formation of CYCLO 3 by the elimination of 3MS is indeed the major thermal breakdown mechanism. CYCLO [A] is thought to be formed by cyclisation with the elimination of hydrogen. Hydrogen has been shown to be a prominent product in the

pyrolysis [A]:



The Arrhenius parameters for the formation of 3MS, CYCLO 3 and CYCLO [A] support these related cyclisation/elimination mechanisms, the A-factors and activation energies being low.

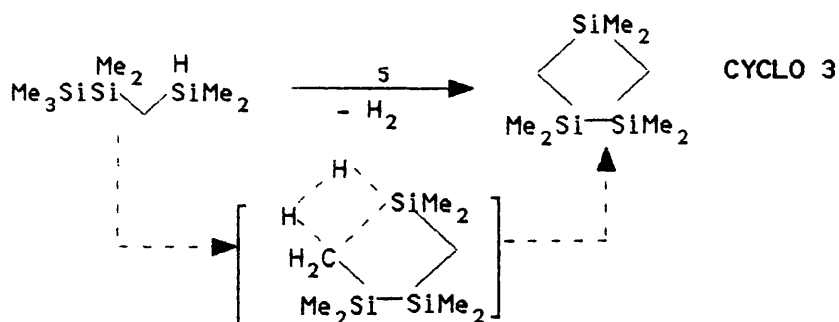
Carbosilane [B] does not undergo the cyclisation with elimination of 3MS reaction. All the centres involved in the transition state are silicon in the cyclisation with elimination of 3MS for [A] (1). In CYCLO [B] not all the centres in the transition state are silicon, offering an explanation why reaction (2) does not take place. [B] is able to undergo cyclisation with elimination of hydrogen to yield CYCLO [B]:



Therefore, the elimination 3MS is a general reaction as long as the constituents of 3MS to be eliminated are attached to silicon. The elimination of hydrogen also appears to be a general reaction, taking place in both carbosilanes [A] and [B]. It is believed that carbosilane [A] offers a reasonable route to the formation of CYCLO 3 in the pyrolysis of OMTS.

Cyclisation with elimination of hydrogen can offer another route to the formation of CYCLO 3:





The high sample pressure pyrolysis of OMTS yields only a small quantity of the isomer of OMTS undergoing reaction (5) (unlike the high sample pressure pyrolysis of hexamethyldi-silane Ch 1, part VII). Reaction (5) may offer some explanation to why this isomer of OMTS is being formed in such a low yield (the isomer of OMTS should be stable at these temperatures).

The isomer of OMTS was not isolated in the preparative pyrolysis experiments and therefore this mechanistic suggestion remains to be substantiated, but the cyclisation with elimination of hydrogen does appear to be a general reaction for linear carbosilanes.

#### (V) Acknowledgement

I am most grateful to Dr. B.N. Bortolin of Dow Corning for preparing the carbosilanes [A] and [B].

## Appendix 2: Numerical Integration

### (I) Introduction

Computer modelling has become a useful tool in the investigation of complex pyrolysis mechanisms. The thermolysis of octamethyltrisilane (OMTS) and 2,2-diethyl-hexamethyltrisilane (DEHMTS) were studied using the KINAL and ACUCHEM numerical integration packages<sup>1</sup>. Numerical integration requires a proposed mechanism to be broken down into single step reactions, each reaction having its own set of Arrhenius parameters. At a specific temperature, these Arrhenius parameters were used to calculate rate constants for each reaction. The computer simulation uses the basic differential equation for each reaction:

$$\frac{dc}{dt} = f(c, k) ; c(0) = 0 \quad \text{---(A2.)}$$

The calculations take place within a given time interval (usually the same as  $\tau$  in the SFR). The calculated rate constants allow an initial concentration of reactant to be converted into the final concentrations of reactant, intermediates and products (at time  $\tau$ ).

The order of product formation can be ascertained by varying the reactant concentration at constant temperature. A plot of  $\log [\text{product}]$  against  $\log [\text{reactant}]$  yields a straight line with a slope equal to the order. The calculated order of the formation for a product can then be compared to the experimental value. Overall rate constants for major product formation can then be calculated based upon the orders of their formation. Experimental rate constants and Arrhenius parameters can be compared with those given by the model.

An important function of computer modelling is concentration sensitivity analysis. This test perturbs individual rate constants for each reaction. The effect this perturbation has on product formation is measured, thus examining the importance of each reaction. Redundant reactions are therefore ruled out by a concentration sensitivity analysis.

## (II) The Pyrolysis of OMTS

The pyrolysis mechanism of OMTS (schemes 3.2, 3.3 and 3.4 in chapter 3) was modelled by numerical integration. Scheme A2.1 shows the proposed individual reactions with their corresponding Arrhenius parameters. The Arrhenius parameters for the individual reactions were either adapted from literature values or measured experimentally (see references).

At 580°C the model gave relative product yields of 14:3:4:1.6:1 for trimethylsilane (3MS); 1,1,3,3,4,4-hexamethyl-1,3,4-trisilacyclopentane (CYCLO 3); 1,1,3-trimethyl-1,3-disilacyclobutane (CYCLO 1); hexamethyldisilane (HMDS) and 1,1,3,3-tetramethyl-1,3-disilacyclobutane (CYCLO 2) (in the same range as the experimental values).

Scheme 1 was modelled over the experimental temperature (570-650°C) and concentration ( $10^{-5}$  -  $10^{-6}$  mol dm<sup>-3</sup>) ranges. Orders for major product formation were between 1.0 and 1.3 at low temperatures and between 1.0 to 1.5 at high temperatures (c.f. experimental values). Figure A2.1 shows a typical plot for determining the order of formation for CYCLO 2 at two different temperatures (i.e. a plot of log [CYCLO 2] against log [OMTS]).

For simplicity, first order rate constants were calculated from the final calculated concentrations. Table 1 shows the Arrhenius parameters for major product formation derived from experimental and calculated rate constants.

The calculated and experimental Arrhenius parameters are in good agreement, supporting the mechanism suggested. Figures A2.2 and A3.3 show experimental and calculated Arrhenius plots for the formation of HMDS respectively; both plots show a degree of scattering and give similar Arrhenius parameters (Table A2.1).

Scheme A2.1:		$\log A^*$	$E_a^*$
(1)	$\text{Me}_3\text{SiSiSiMe}_3 \xrightarrow{\text{(RH)}} \text{Me}_3\text{Si}^\cdot + \text{Me}_3\text{SiSi}^\cdot_{\text{Me}_2}$	17.2	337 <sup>2</sup>
(2)	$\text{RH} + \text{Me}_3\text{Si}^\cdot \xrightarrow{\text{Me}} \text{Me}_3\text{SiSiSiMe}_3 + \text{Me}_3\text{SiH}$	10.4	65 <sup>3</sup>
(3)	$\text{RH} + \text{Me}_3\text{SiSi}^\cdot_{\text{Me}_2} \xrightarrow{\text{Me}} \text{Me}_3\text{SiSiSiMe}_3 + \text{Me}_3\text{SiSiH}_{\text{Me}_2}$	10.4	80 <sup>3</sup>
(4)	$\text{Me}_3\text{SiSiSiMe}_3 \xrightarrow{\text{Me}} \text{Me}_3\text{SiSi}^\cdot_{\text{Me}}\text{SiMe}_3$	12.3	90 <sup>3</sup>
(5)	$\text{Me}_3\text{SiSiSiMe}_3 \xrightarrow{\text{Me}} \text{Me}_3\text{Si}^\cdot + \text{Me}_3\text{SiSi}^\cdot_{\text{Me}}=\text{CH}_2$	16	165 <sup>3</sup>
(6)	$\text{Me}_3\text{SiSi}^\cdot_{\text{Me}}\text{SiMe}_3 \xrightarrow{\text{Me}} \text{Me}_3\text{Si}^\cdot + \text{Me}_3\text{SiSi}^\cdot_{\text{Me}}=\text{CH}_2$	16	203 <sup>3</sup>
(7)	$\text{RH} + \text{Me}_3\text{SiSi}^\cdot_{\text{Me}}\text{SiMe}_3 \xrightarrow{\text{Me}} \text{Me}_3\text{SiSiSiMe}_3 + \text{Me}_3\text{SiSi}^\cdot_{\text{Me}}\text{SiMe}_3$	10.4	75 <sup>3</sup>
(8)	$\text{Me}_3\text{SiSi}^\cdot_{\text{Me}}\text{SiMe}_3 \xrightarrow{\text{H}} \text{Me}_3\text{SiH} + \text{Me}_3\text{SiSi}^\cdot_{\text{Me}}\text{SiMe}_3$	13.3	203 <sup>4</sup>
(9)	$\text{Me}_3\text{SiSi}^\cdot_{\text{Me}}=\text{CH}_2 \xrightarrow{\text{Me}} \text{Me}_3\text{SiSi}^\cdot_{\text{Me}}$	14.2	110 <sup>5</sup>
(10)	$\text{Me}_3\text{SiSi}^\cdot_{\text{Me}}\text{SiMe}_3 \xrightarrow{\text{Me}} \text{Me}_2\text{Si}^\cdot\text{SiMe}_3$	12	145 <sup>6</sup>
(11)	$\text{RH} + \text{Me}_3\text{Si}^\cdot \xrightarrow{\text{CH}_2} \text{Me}_3\text{SiSiSiMe}_2 + \text{Me}_3\text{SiH}$	10.4	65 <sup>3</sup>
(12)	$\text{RH} + \text{Me}_3\text{SiSi}^\cdot_{\text{Me}_2} \xrightarrow{\text{CH}_2} \text{Me}_3\text{SiSiSiMe}_2 + \text{Me}_3\text{SiSiH}_{\text{Me}_2}$	10.4	80 <sup>3</sup>
(13)	$\text{Me}_3\text{SiSiSiMe}_2 \xrightarrow{\text{CH}_2} \text{Me}_3\text{SiSiMe}_2 + \text{Me}_2\text{Si}^\cdot=\text{CH}_2$	16	165 <sup>3</sup>
(14)	$\text{Me}_3\text{SiSiSiMe}_2 \xrightarrow{\text{CH}_2} \text{Me}_3\text{SiSi}^\cdot_{\text{Me}_2}\text{SiMe}_2$	13.3	90 <sup>3</sup>
(15)	$\text{Me}_3\text{SiSi}^\cdot_{\text{Me}_2}\text{SiMe}_2 \xrightarrow{\text{CH}_2} \text{Me}_3\text{SiSi}^\cdot_{\text{Me}_2} + \text{Me}_2\text{Si}^\cdot=\text{CH}_2$	15	203 <sup>3</sup>
(16)	$\text{Me}_3\text{SiSi}^\cdot_{\text{Me}_2} + \text{Me}_2\text{Si}^\cdot=\text{CH}_2 \xrightarrow{\text{CH}_2} \text{Me}_3\text{SiSi}^\cdot_{\text{Me}_2}\text{SiMe}_2$	8.4	0 <sup>3</sup>
(17)	$\text{RH} + \text{Me}_3\text{SiSi}^\cdot_{\text{Me}_2}\text{SiMe}_2 \xrightarrow{\text{CH}_2} \text{Me}_3\text{SiSiSiMe}_2 + \text{Me}_3\text{SiSi}^\cdot_{\text{Me}_2}\text{SiMe}_2$	10.4	80 <sup>3</sup>
(18)	$\text{Me}_3\text{SiSi}^\cdot_{\text{Me}_2}\text{SiMe}_2 + \text{Me}_2\text{Si}^\cdot=\text{CH}_2 \xrightarrow{\text{CH}_2} \text{Me}_3\text{SiSi}^\cdot_{\text{Me}_2}\text{SiMe}_2$	8.4	0 <sup>3</sup>
(19)	$\text{Me}_3\text{SiSi}^\cdot_{\text{Me}_2}\text{SiMe}_2 + \text{RH} \xrightarrow{\text{CH}_2} \text{Me}_3\text{SiSi}^\cdot_{\text{Me}_2}\text{SiMe}_2 + \text{Me}_3\text{SiSiSiMe}_2$	10.4	75 <sup>3</sup>

(20)	$\text{Me}_3\text{SiSi}(\text{Me}_2)\text{Si}(\text{Me}_2)\text{H} \longrightarrow \text{Me}_2\text{Si}(\text{SiMe}_2)_2 + \text{Me}_3\text{SiH}$	11.5	214	7
(21)	$\text{Me}_3\text{Si}^\bullet \longrightarrow \text{Me}_2\text{Si:} + \text{Me}^\bullet$	14.5	265	8
(22)	$2 \times \text{Me}_3\text{Si}^\bullet \longrightarrow \text{Me}_3\text{SiSiMe}_3$	10.0	0	3
(23)	$\text{Me}^\bullet + \text{Me}_3\text{Si}^\bullet \longrightarrow \text{Me}_4\text{Si}$	11.0	0	3
(24)	$2 \times \text{Me}_2\text{Si}=\text{CH}_2 \longrightarrow \text{Me}_2\text{Si}(\text{SiMe}_2)_2$	6.8	0	3
(25)	$\text{Me}_3\text{SiSi}(\text{Me}_2)^\bullet \longrightarrow \text{Me}_2\text{Si:} + \text{Me}_3\text{Si}^\bullet$	16.0	236	8
(26)	$\text{Me}^\bullet + \text{Me}_2\text{Si}=\text{CH}_2 \longrightarrow \text{Me}_2\text{Si}^\bullet\text{CH}_2\text{CH}_3$	8.68	0	3
(27)	$\text{Me}_3\text{Si}^\bullet + \text{Me}_2\text{Si}=\text{CH}_2 \longrightarrow \text{Me}_3\text{Si}(\text{SiMe}_2)^\bullet$	8.38	0	3
(28)	$\text{Me}_3\text{SiSi}(\text{Me}_2)\text{H} \longrightarrow \text{Me}_2\text{Si:} + \text{Me}_3\text{SiH}$	12.9	199	4
(29)	$\text{Me}_3\text{SiSiMe}_3 \longrightarrow 2 \times \text{Me}_3\text{Si}^\bullet$	17.2	337	2
(30)	$\text{Me}_3\text{Si}(\text{SiMe}_2)^\bullet \longrightarrow \text{Me}_2\text{Si}=\text{CH}_2 + \text{Me}_3\text{Si}^\bullet$	15.0	192	3
(31)	$\text{Me}_3\text{Si}(\text{SiMe}_2)^\bullet + \text{RH} \longrightarrow \text{Me}_3\text{Si}(\text{SiMe}_3)\text{CH}_2^\bullet + \text{Me}_3\text{Si}(\text{SiMe}_2)\text{H}$	10.4	75	3
(32)	$\text{Me}_3\text{Si}(\text{SiMe}_2)^\bullet + \text{RH} \longrightarrow \text{Me}_3\text{Si}(\text{SiMe}_2)\text{CH}_2^\bullet + \text{Me}_3\text{Si}(\text{SiMe}_2)\text{H}$	10.4	75	3
(33)	$\text{Me}_8\text{Si}_3 \longrightarrow \text{Me}_2\text{Si:} + \text{Me}_3\text{SiSiMe}_3$	13.7	282	2

\*log (A/s<sup>-1</sup>) for unimolecular reactions and dm<sup>3</sup> mol<sup>-1</sup> s<sup>-1</sup> for bimolecular reactions; Ea in kJ mol<sup>-1</sup>.

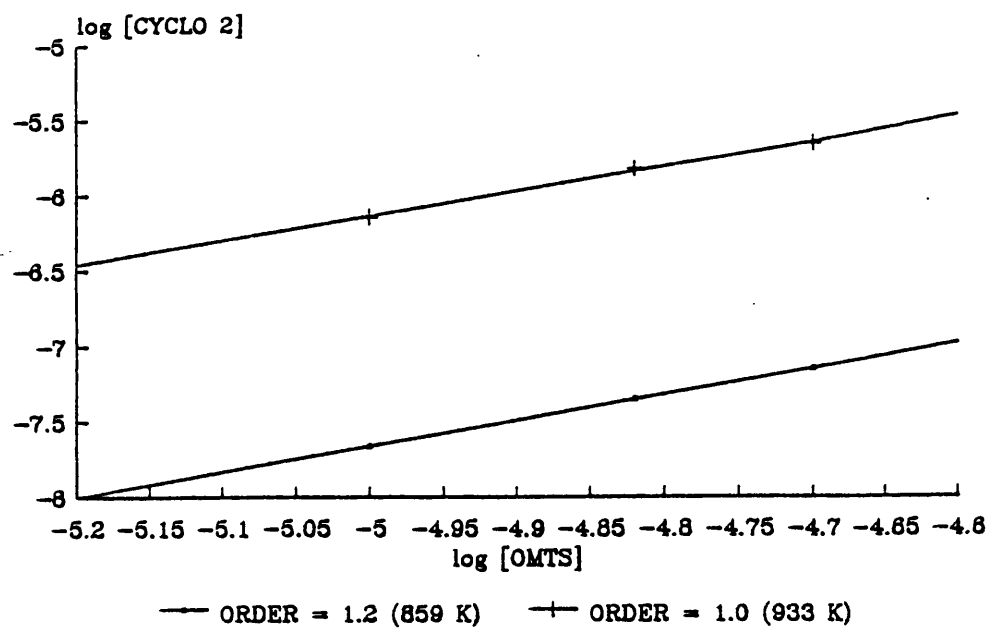


Figure A2.1: Plot of  $\log[\text{CYCLO 2}]$  against  $\log[\text{OMTS}]$ .  
 Slope =  $1.2 \pm 0.1$  at 859 k and  $1.0 \pm 0.1$  at 933 k.

Table A2.1:

Product	Experimental		Calculated	
	$\log(A/s^{-1})$	$E_a$ (kJmol $^{-1}$ )	$\log(A/s^{-1})$	$E_a$ (kJmol $^{-1}$ )
$\text{Me}_3\text{SiH}$	$14.6 \pm 0.6$	$268 \pm 11$	$12.1 \pm 0.9$	$216 \pm 13$
$\text{Me}_2\text{Si} \begin{array}{c} \diagup \text{Me} \\ \diagdown \text{H} \end{array} \text{Si} \begin{array}{c} \diagup \\ \diagdown \end{array}$	$10.0 \pm 0.6$	$198 \pm 10$	$10.6 \pm 0.9$	$204 \pm 17$
$\text{Me}_2\text{Si} \begin{array}{c} \diagup \\ \diagdown \end{array} \text{Si} \begin{array}{c} \diagup \\ \diagdown \end{array} \text{Me}_2$	$5.2 \pm 0.3$	$123 \pm 6$	$7.1 \pm 0.2$	$138 \pm 4$
$\text{Me}_3\text{SiSiMe}_3$	$8.9 \pm 0.2$	$186 \pm 4$	$9.1 \pm 0.9$	$188 \pm 15$
$\text{Me}_2\text{Si} \begin{array}{c} \diagup \\ \diagdown \end{array} \text{Si} \begin{array}{c} \diagup \\ \diagdown \end{array} \text{Me}_2$	$13.6 \pm 0.4$	$269 \pm 5$	$13.8 \pm 1.1$	$264 \pm 18$

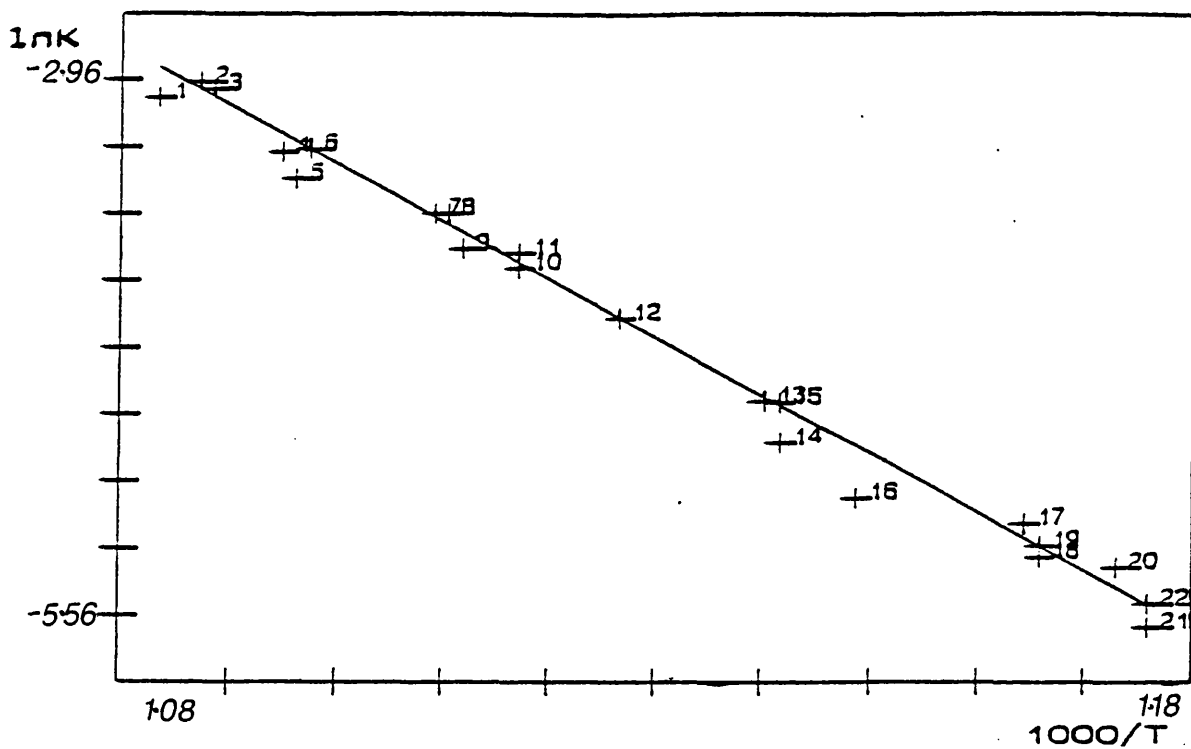


Figure A2.2: Experimental Arrhenius plot for the formation of HMDS between 570-650°C.

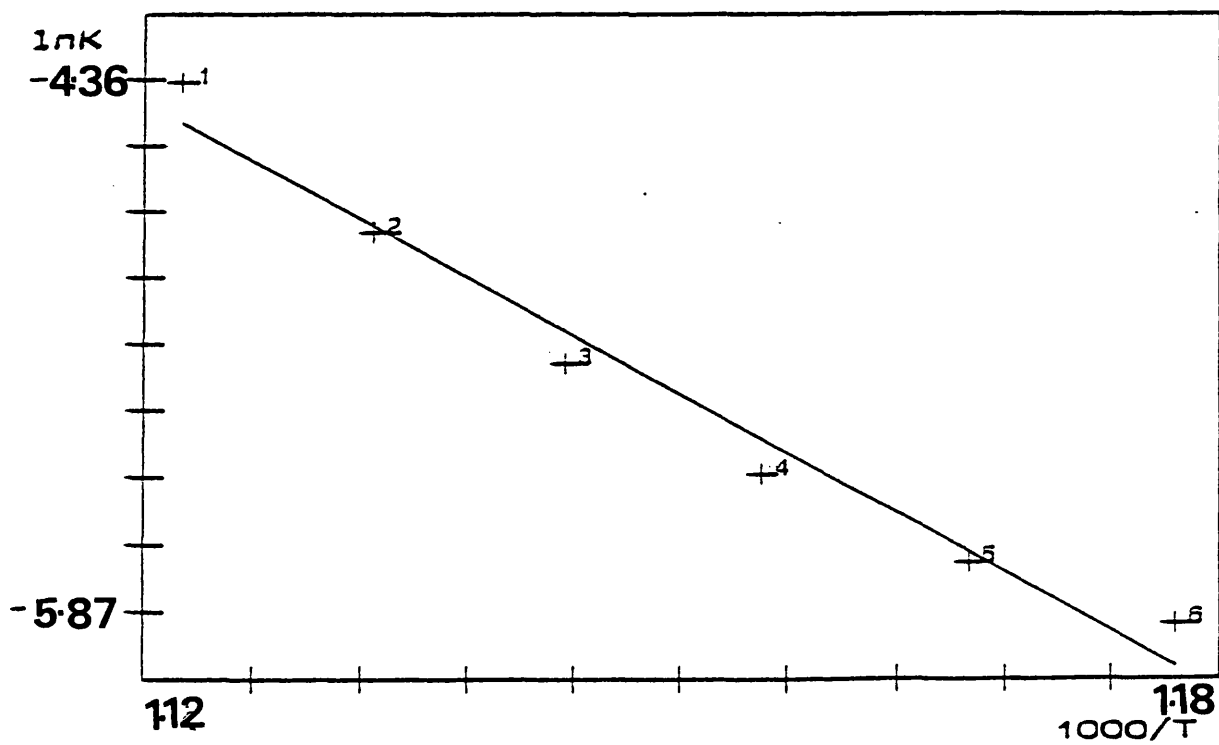


Figure A2.3: Calculated Arrhenius plot for the formation of HMDS between 570-620°C.

### (III) The pyrolysis of DEHMTS

The pyrolysis mechanism of DEHMTS (schemes 6.2, 6.3 and 6.4 Chapter 6) was modelled by numerical integration. Scheme A2.2 shows the individual reactions with their corresponding Arrhenius parameters. The Arrhenius parameters used in scheme A2.2 were either adapted from literature values or estimated from thermochemical values.

The model gave ethene, 3MS and vinyltrimethylsilane (VMTS) as the major products, in agreement with experiment. The system was modelled over the experimental concentration ( $10^{-5}$ – $10^{-6}$  mol dm $^{-3}$ ) and temperature ranges (570–630°C). The orders of formation for ethene, 3MS and VTMS were 1.6, again in agreement with experiment. Figure A2.4 shows a typical plot for determining the order of formation for ethene ( $\log[C_2H_4]$  against  $\log[DEHMTS]$ ).

Rate constants based upon an order of 1.6 were calculated. Table A2.2 shows the Arrhenius parameters derived from experimental and calculated rate constants.

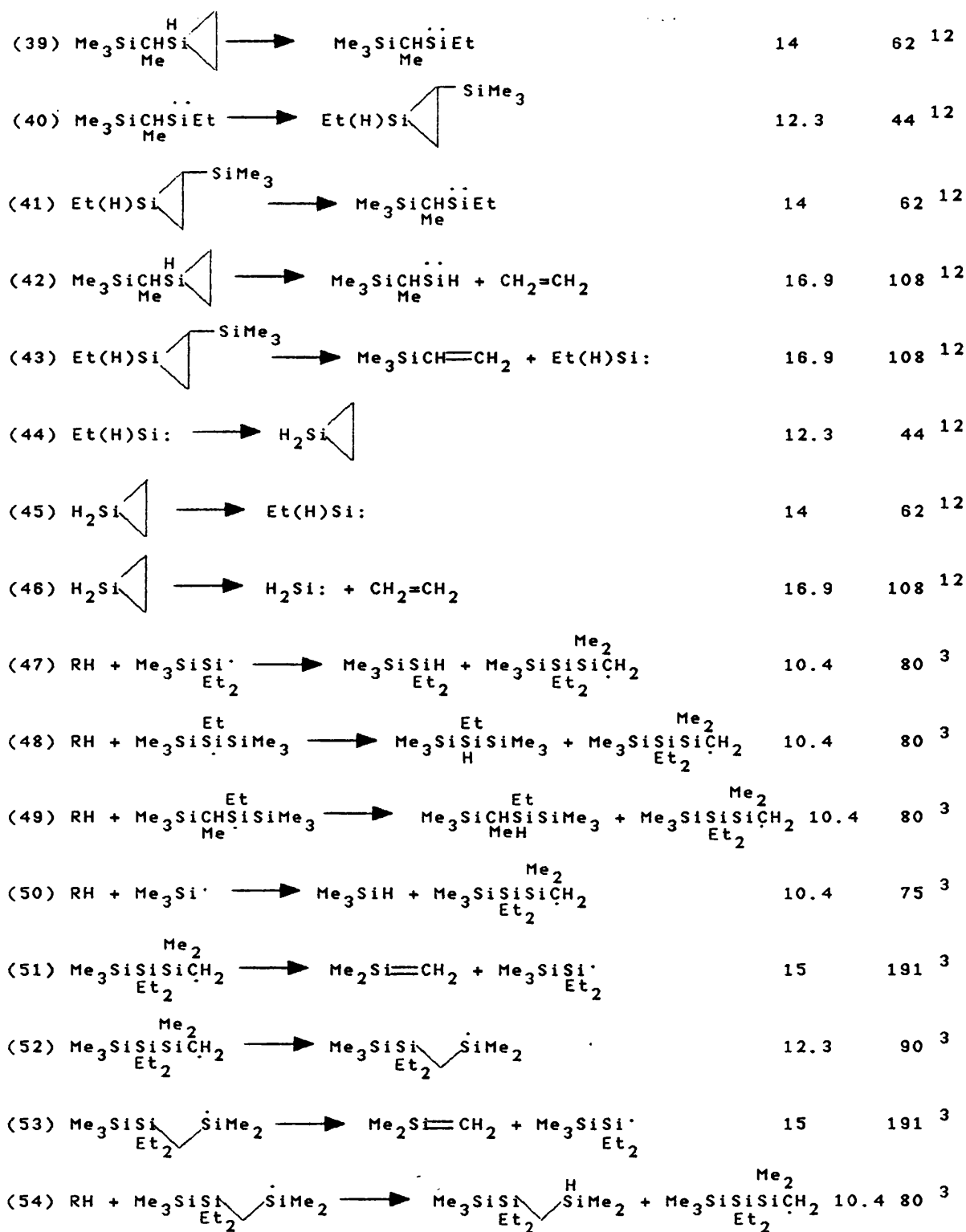
The Arrhenius parameters given by the model are in agreement with those derived experimentally. Figures A2.5 and A2.6 show experimental and calculated Arrhenius plots for the formation of ethene respectively; both plots show a degree of scattering and curvature which would be expected in this kinetically complex system.



Scheme A2.2:

		$\log A^*$	$E_a^*$
(1)	$\text{Me}_3\text{SiSiSiMe}_3 \xrightarrow{\text{Et}_2} \text{Me}_3\text{Si}^\cdot + \text{Me}_3\text{SiSi}^\cdot\text{Et}_2$ (RH)	17.2	320 <sup>2</sup>
(2)	$\text{Me}_3\text{Si}^\cdot \longrightarrow \text{Me}^\cdot + \text{Me}_2\text{Si}^\cdot$	14.5	255 <sup>8</sup>
(3)	$\text{Me}_3\text{SiSi}^\cdot\text{Et}_2 \longrightarrow \text{Me}_3\text{Si}^\cdot + \text{Et}_2\text{Si}^\cdot$	16.0	235 <sup>9</sup>
(4)	$2 \times \text{Me}_3\text{Si}^\cdot \longrightarrow \text{Me}_3\text{SiSiMe}_3$	9.0	0 <sup>3</sup>
(5)	$\text{Me}_3\text{SiSi}^\cdot\text{Et}_2 + \text{RH} \longrightarrow \text{Me}_3\text{SiSiH}\text{Et}_2 + \text{Me}_3\text{SiSiSiMe}_3$ Et CH <sub>2</sub> ·CH <sub>2</sub>	10.4	75 <sup>3</sup>
(6)	$\text{Me}_3\text{SiSiH}\text{Et}_2 \longrightarrow \text{Me}_3\text{SiH} + \text{Et}_2\text{Si}^\cdot$	13.3	203 <sup>4</sup>
(7)	$\text{Et}_2\text{Si}^\cdot \longrightarrow \text{EtHSi} \triangleleft$	12.3	44 <sup>10</sup>
(8)	$\text{EtHSi} \triangleleft \longrightarrow \text{Et}_2\text{Si}^\cdot$	14	62 <sup>10</sup>
(9)	$\text{EtHSi} \triangleleft \longrightarrow \text{CH}_2=\text{CH}_2 + \text{EtHSi}^\cdot$	16.9	108 <sup>10</sup>
(10)	$\text{Me}_3\text{Si}^\cdot + \text{RH} \longrightarrow \text{Me}_3\text{SiH} + \text{Me}_3\text{SiSiSiMe}_3$ Et CH <sub>2</sub> ·CH <sub>2</sub>	10.4	65 <sup>3</sup>
(11)	$\text{Me}_3\text{Si}^\cdot\text{CSiSiMe}_3 + \text{RH} \longrightarrow \text{Me}_3\text{SiHCSiSiMe}_3 + \text{Me}_3\text{SiSiSiMe}_3$ Me· HEt Et Et Et CH <sub>2</sub> ·CH <sub>2</sub>	10.4	80 <sup>3</sup>
(12)	$\text{Me}_3\text{SiSiSiMe}_3 \xrightarrow{\text{Et}_2} \text{CH}_2=\text{CH}_2 + \text{Me}_3\text{SiSiSiMe}_3$ Et CH <sub>2</sub> ·CH <sub>2</sub>	16	154 <sup>11</sup>
(13)	$\text{Me}_3\text{SiSiSiMe}_3 \xrightarrow{\text{Et}_2} \text{Me}_3\text{Si}^\cdot + \text{Me}_3\text{SiSi}^\cdot\text{Et}$	16	235 <sup>9</sup>
(14)	$\text{Me}_3\text{SiSiSiMe}_3 + \text{RH} \longrightarrow \text{Me}_3\text{SiSiSiMe}_3 + \text{Me}_3\text{SiSiSiMe}_3$ Et Et Et H CH <sub>2</sub> ·CH <sub>2</sub>	10.4	80 <sup>3</sup>
(15)	$\text{Me}_3\text{SiSiSiMe}_3 \xrightarrow{\text{H}} \text{Me}_3\text{SiH} + \text{Me}_3\text{SiSi}^\cdot\text{Et}$	13.3	203 <sup>4</sup>
(16)	$\text{Me}_3\text{SiSi}^\cdot\text{Et} \longrightarrow \text{Me}_3\text{SiSi}^\cdot\text{H}=\text{CHCH}_3$	13.3	182 <sup>5</sup>
(17)	$\text{Me}_3\text{SiSi}^\cdot\text{H}=\text{CHCH}_3 \longrightarrow \text{Me}_3\text{SiSi}^\cdot\text{Et}$	13.9	179 <sup>5</sup>
(18)	$\text{Me}_3\text{SiSi}^\cdot\text{H}=\text{CHCH}_3 \longrightarrow \text{H}^\cdot\text{SiCHSiMe}_3$ Me	14.2	110 <sup>5</sup>
(19)	$\text{Me}_3\text{SiSi}^\cdot\text{Et} \longrightarrow \text{Me}_3\text{Si(H)Si} \triangleleft$	12.3	44 <sup>12</sup>

(20)	$\text{Me}_3\text{Si}(\text{H})\text{Si} \begin{array}{c} \diagup \\ \diagdown \end{array}$	$\longrightarrow$	$\text{Me}_3\text{SiSi} \begin{array}{c} \diagup \\ \diagdown \\ \text{Et} \end{array}$	14	62	12
(21)	$\text{Me}_3\text{Si}(\text{H})\text{Si} \begin{array}{c} \diagup \\ \diagdown \end{array}$	$\longrightarrow$	$\text{Me}_3\text{SiSiH} + \text{CH}_2=\text{CH}_2$	16.9	108	12
(22)	$\text{H} \begin{array}{c} \diagup \\ \diagdown \end{array} \text{SiCHSiMe}_3 \begin{array}{c} \diagup \\ \diagdown \end{array}$	$\longrightarrow$	$\text{H}_2\text{Si} \begin{array}{c} \diagup \\ \diagdown \end{array} \text{SiMe}_3$	12.3	44	12
(23)	$\text{H}_2\text{Si} \begin{array}{c} \diagup \\ \diagdown \end{array} \text{SiMe}_3$	$\longrightarrow$	$\text{H} \begin{array}{c} \diagup \\ \diagdown \end{array} \text{SiCHSiMe}_3 \begin{array}{c} \diagup \\ \diagdown \end{array}$	14	62	12
(24)	$\text{Me}_3\text{Si}(\text{H})\text{Si} \begin{array}{c} \diagup \\ \diagdown \end{array}$	$\longrightarrow$	$\text{H} \begin{array}{c} \diagup \\ \diagdown \end{array} \text{SiCH}_2\text{CH}_2\text{SiMe}_3$	14	62	12
(25)	$\text{H} \begin{array}{c} \diagup \\ \diagdown \end{array} \text{SiCH}_2\text{CH}_2\text{SiMe}_3$	$\longrightarrow$	$\text{Me}_3\text{Si}(\text{H})\text{Si} \begin{array}{c} \diagup \\ \diagdown \end{array}$	12.3	44	12
(26)	$\text{Me}_3\text{SiSiH}$	$\longrightarrow$	WALL	4.0	0	
(27)	$\text{H} \begin{array}{c} \diagup \\ \diagdown \end{array} \text{SiCH}_2\text{CH}_2\text{SiMe}_3$	$\longrightarrow$	$\text{H}_2\text{Si} \begin{array}{c} \diagup \\ \diagdown \end{array} \text{SiMe}_3$	12.3	44	12
(28)	$\text{H}_2\text{Si} \begin{array}{c} \diagup \\ \diagdown \end{array} \text{SiMe}_3$	$\longrightarrow$	$\text{H} \begin{array}{c} \diagup \\ \diagdown \end{array} \text{SiCH}_2\text{CH}_2\text{SiMe}_3$	14	62	12
(29)	$\text{H}_2\text{Si} \begin{array}{c} \diagup \\ \diagdown \end{array} \text{SiMe}_3$	$\longrightarrow$	$\text{Me}_3\text{SiCH}=\text{CH}_2 + \text{H}_2\text{Si}:$	16.9	108	12
(30)	$\text{H}_2\text{Si}:$	$\longrightarrow$	WALL	4.0	0	
(31)	$\text{RH} + \text{Me}_3\text{Si} \cdot$	$\longrightarrow$	$\text{Me}_3\text{SiH} + \text{Me}_3\text{Si} \begin{array}{c} \text{Et} \\ \diagup \\ \text{CH} \\ \diagdown \\ \text{CH}_3 \end{array} \text{SiMe}_3$	10.4	65	3
(32)	$\text{RH} + \text{Me}_3\text{SiSi} \begin{array}{c} \text{Et} \\ \diagup \\ \text{Et}_2 \end{array} \cdot$	$\longrightarrow$	$\text{Me}_3\text{SiSiH} + \text{Me}_3\text{Si} \begin{array}{c} \text{Et} \\ \diagup \\ \text{CH} \\ \diagdown \\ \text{CH}_3 \end{array} \text{SiMe}_3$	10.4	65	3
(33)	$\text{RH} + \text{Me}_3\text{Si} \begin{array}{c} \text{Et} \\ \diagup \\ \text{Si} \\ \diagdown \\ \text{Si} \end{array} \text{SiMe}_3$	$\longrightarrow$	$\text{Me}_3\text{Si} \begin{array}{c} \text{Et} \\ \diagup \\ \text{Si} \\ \diagdown \\ \text{H} \end{array} \text{SiMe}_3 + \text{Me}_3\text{Si} \begin{array}{c} \text{Et} \\ \diagup \\ \text{CH} \\ \diagdown \\ \text{CH}_3 \end{array} \text{SiMe}_3$	10.4	80	3
(34)	$\text{Me}_3\text{Si} \begin{array}{c} \text{Et} \\ \diagup \\ \text{CH} \\ \diagdown \\ \text{CH}_3 \end{array} \text{SiMe}_3$	$\longrightarrow$	$\text{Me}_3\text{Si} \begin{array}{c} \text{Me} \cdot \\ \diagup \\ \text{CH} \\ \diagdown \\ \text{Et} \end{array} \text{SiMe}_3$	12.3	90	3
(35)	$\text{Me}_3\text{Si} \begin{array}{c} \text{Me} \cdot \\ \diagup \\ \text{CH} \\ \diagdown \\ \text{Et} \end{array} \text{SiMe}_3$	$\longrightarrow$	$\text{Me}_3\text{Si} \cdot + \text{Me}_3\text{Si} \begin{array}{c} \cdot \\ \diagup \\ \text{CH} \\ \diagdown \\ \text{Me} \end{array} \text{SiEt}$	16	235	9
(36)	$\text{RH} + \text{Me}_3\text{Si} \begin{array}{c} \text{Me} \cdot \\ \diagup \\ \text{CH} \\ \diagdown \\ \text{Et} \end{array} \text{SiMe}_3$	$\longrightarrow$	$\text{Me}_3\text{Si} \begin{array}{c} \text{MeH} \\ \diagup \\ \text{CH} \\ \diagdown \\ \text{Et} \end{array} \text{SiMe}_3 + \text{Me}_3\text{Si} \begin{array}{c} \text{Et} \\ \diagup \\ \text{CH} \\ \diagdown \\ \text{CH}_3 \end{array} \text{SiMe}_3$	10.4	80	3
(37)	$\text{Me}_3\text{Si} \begin{array}{c} \text{MeH} \\ \diagup \\ \text{CH} \\ \diagdown \\ \text{Et} \end{array} \text{SiMe}_3$	$\longrightarrow$	$\text{Me}_3\text{SiH} + \text{Me}_3\text{Si} \begin{array}{c} \cdot \\ \diagup \\ \text{CH} \\ \diagdown \\ \text{Me} \end{array} \text{SiEt}$	13.3	203	4
(38)	$\text{Me}_3\text{Si} \begin{array}{c} \cdot \\ \diagup \\ \text{CH} \\ \diagdown \\ \text{Me} \end{array} \text{SiEt}$	$\longrightarrow$	$\text{Me}_3\text{Si} \begin{array}{c} \text{H} \\ \diagup \\ \text{CH} \\ \diagdown \\ \text{Me} \end{array} \text{Si} \begin{array}{c} \diagup \\ \diagdown \end{array}$	12.3	44	12



\*Log (A/s<sup>-1</sup>) for unimolecular reactions and (A/dm<sup>3</sup> mol<sup>-1</sup> s<sup>-1</sup>) for bimolecular reactions; Ea in kJ mol<sup>-1</sup>

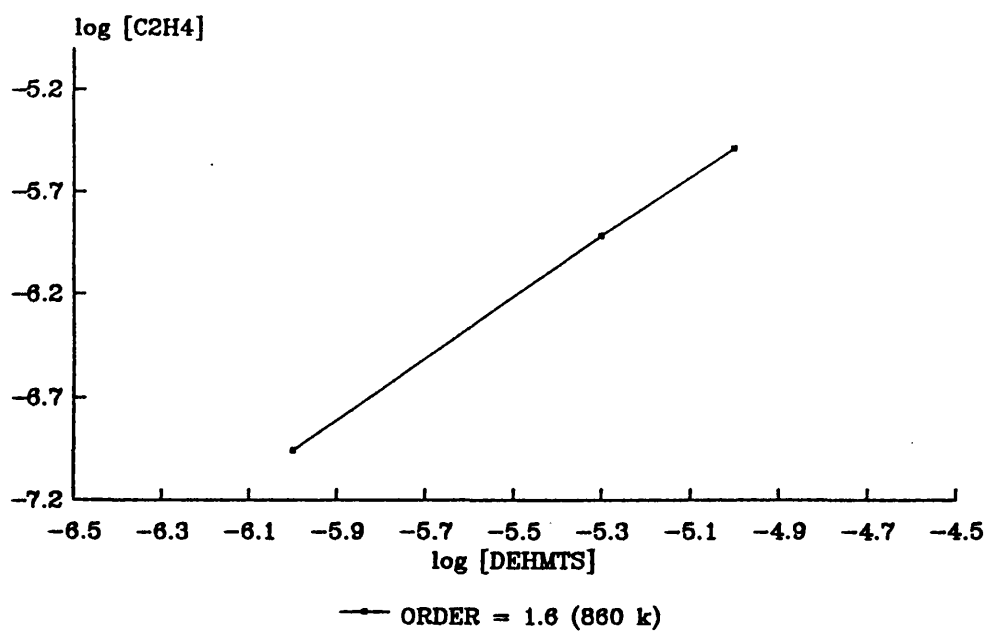


Figure A2.4: Plot of  $\log[C_2H_4]$  against  $\log[DEHMTS]$ .  
Slope =  $1.57 \pm 0.05$ .

Table A2.2:

Product	Experimental		Calculated	
	$\log (A/s^{-1})$	$E_a (kJmol^{-1})$	$\log (A/s^{-1})$	$E_a (kJmol^{-1})$
$CH_2=CH_2$	$20.8 \pm 0.5$	$308 \pm 9$	$20.7 \pm 1.6$	$318 \pm 22$
$Me_3SiH$	$20.8 \pm 0.6$	$310 \pm 9$	$19.5 \pm 1.4$	$303 \pm 23$
$Me_3SiCH=CH_2$	$18.0 \pm 0.6$	$374 \pm 10$	$19.6 \pm 1.4$	$312 \pm 23$

[A factors calculated using  $mol dm^{-3}$  as the unit of concentration]

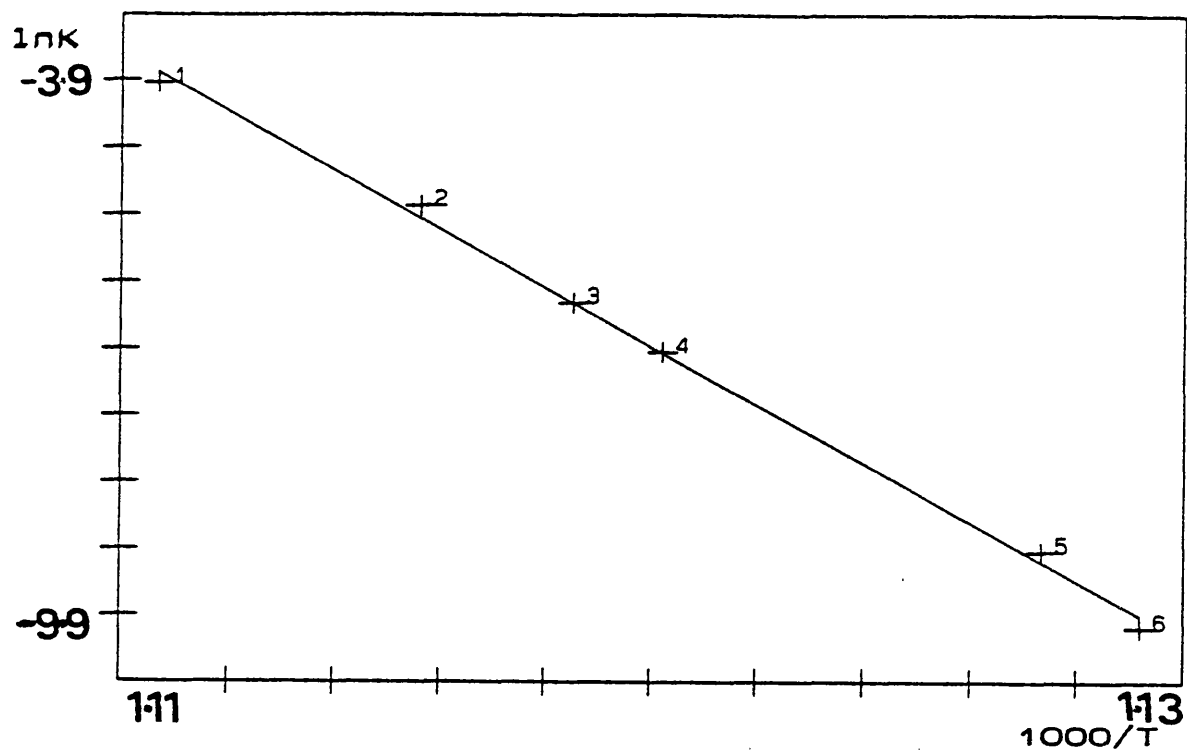


Figure A2.5: Experimental Arrhenius plot for the formation of ethene between 570-630°C.

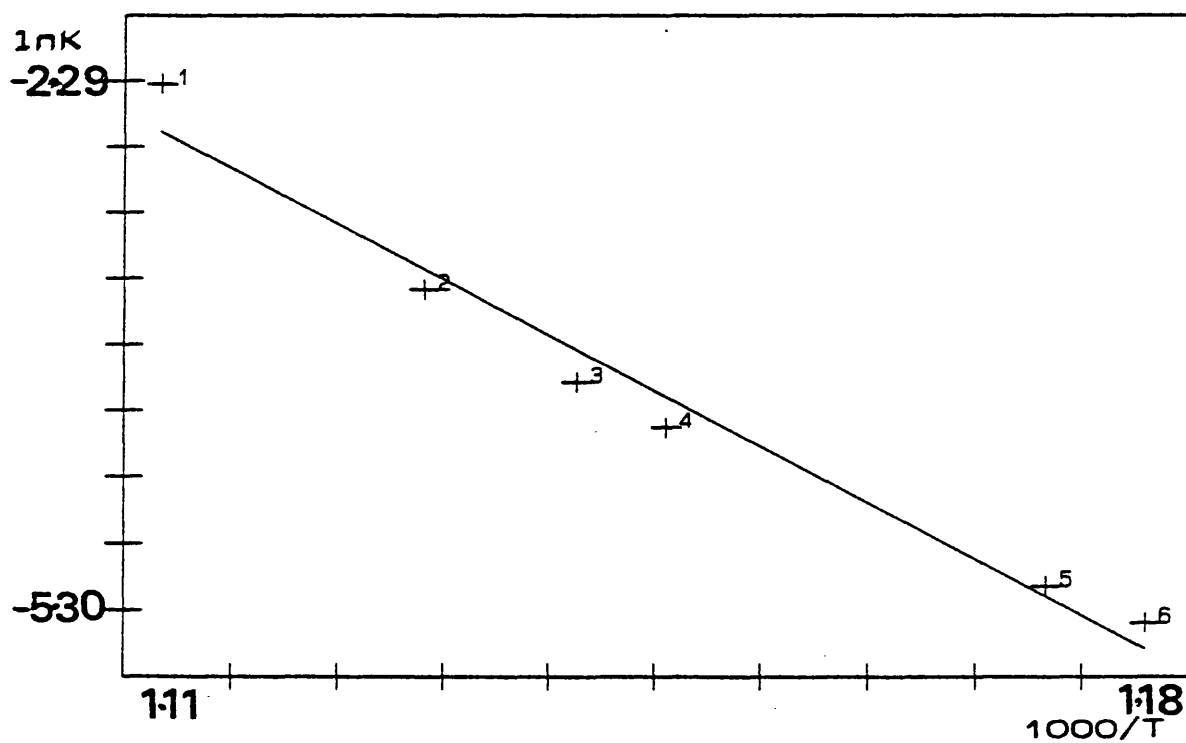


Figure A2.6: Calculated Arrhenius plot for the formation of ethene between 570-630°C.

#### (IV) Acknowledgement

I would like to thank Dr. Musahid Ahmed for the modelling of DEHMTS and for his help with the modelling of OMTS.

#### (V) References

- (1) T. Turanyi, V.S. Berces, S. Vajada, *Int. J. Chem. Kinetics*, 1989, 21, 83; T. Turanyi, *J. Mathematical Chem.*, 1990, 5, 203; W. Braun, J.T. Herron, D.K. Kahaner, *Int. J. Chem. Kinetics*, 1988, 20, 51.
- (2) I.M.T. Davidson, A.V. Howard, *J. Chem. Soc., Faraday Trans. I*, 1975, 71, 69
- (3) I.M.T. Davidson, P. Potzinger, B. Reimann, *Ber. Bunsen. Phys. Chem.*, 1982, 86, 13.
- (4) I.M.T. Davidson, K.J. Hughes, S. Ijadi-Maghsoodi, *Organometallics*, 1987, 6, 639.
- (5) I.M.T. Davidson, H.E. O'Neal, unpublished results.
- (6) I.M.T. Davidson, R.J. Scampton, *J. Organomet. Chem.*, 1984, 271, 249.
- (7) Experiment (see Ch. 3).
- (8) I.M.T. Davidson, C.E. Dean, *Organometallics*, 1987, 6, 966.
- (9) R. Walsh, in *The Chemistry of Organosilicon Compounds*, Eds. S. Patai, Z. Rappoport, John Wiley, New York, 1989 p. 371.
- (10) G.T. Burns, T.J. Barton, *J. Am. Chem. Soc.*, 1983, 105, 2006.
- (11) Estimated from thermochemistry.
- (12) H.E. O'Neal, personnel communication; A.P. Dickinson, H.E. O'Neal, M.A. Ring, presented at Organosilicon meeting, El Paso, 1991.